

The Ministry of Education and
Science of the Russian
Federation

**Kemerovo Institute of Food
Science and Technology**

**Foods and
Raw Materials**

Vol.1, (No. 1), 2013

ISSN 2308-4057

Published twice a year.

Established by the Kemerovo
Institute of Food Science and
Technology (KemIFST), bul'v.
Stroitelei 47, Kemerovo, 650056
Russia

Editorial Office:

650056, Russia, Kemerovo, bul'v.
Stroitelei 47, office 1212,
tel.: +7(3842)39-68-45
http: frm-kemtipp.ru
e-mail: fjournal@mail.ru

Publishing Office:

650056, Russia, Kemerovo,
ul. Institutskaya 7, office 2006,
tel.: +7(3842)39-09-81

Mass Media Registration
Certificate
PI no. FS77-52352
(December 28, 2012).

Opinions of the authors of
published materials do not always
coincide with the editorial staff's
viewpoint. Authors are responsible
for the scientific content of their
papers.

Signet for publishing 06.12.2013
Date of publishing 09.12.2013
Circulation 300 ex.
Open price.

Kemerovo Institute of Food
Science and Technology
(KemIFST), bul'v. Stroitelei 47,
Kemerovo, 650056 Russia
© 2013, KemIFST. All rights
reserved.

ISSN 2308-4057

Editor-in-Chief

Aleksandr Yu. Prosekov, Dr. Sci. (Eng.), Kemerovo Institute of Food
Science and Technology, Kemerovo, Russia

Deputy Editor-in-Chief

Olga V. Koroleva, Dr. Sci. (Biol.), Bach Institute of Biochemistry,
Moscow, Russia;

Zheng Xi-Qun, Dr., Prof., Vice President, Qiqihar University
Heilongjiang Province, Qiqihar, P.R. China.

Editorial Board

Gosta Winberg, M.D., Ph.D. Assoc. Prof., Karolinska Institutet,
Stockholm, Sweden;

Aleksandr N. Avstrieviskikh, Dr. Sci. (Eng.), OOO ArtLaif , Tomsk,
Russia;

Berdan A. Rskeldiev, Dr. Sci. (Eng.), Shakarim Semipalatinsk State
University, Semei, Kazakhstan;

Aram G. Galstyan, Dr. Sci. (Eng.), All-Russian Research Institute of
Dairy Industry, Moscow, Russia;

Tamara A. Krasnova, Dr. Sci. (Eng.), Kemerovo Institute of Food
Science and Technology, Kemerovo, Russia;

Olga A. Neverova, Dr. Sci. (Biol.), Institute of Human Ecology,
Siberian Branch, Russian Academy of Sciences, Kemerovo, Russia;

Aleksei M. Osintsev, Dr. Sci. (Eng.), Prof., Kemerovo Institute of
Food Science and Technology, Kemerovo, Russia;

Viktor A. Panfilov, Dr. Sci. (Eng.), Prof., Moscow State University of
Food Production, Moscow, Russia;

Sergei L. Tikhonov, Dr. Sci. (Eng.), Ural State Academy of
Veterinary Medicine, Troitsk, Russia;

Irina S. Khamagaeva, Dr. Sci. (Eng.), East-Siberian State University
of Technology and Management, Ulan-Ude, Russia;

Lidiya V. Shulgina, Dr. Sci. (Biol.), Pacific Research Fishery Center,
Vladivostok, Russia.

Secretary of Editorial Office

Anna I. Loseva, Cand. Sci. (Eng.), Kemerovo Institute of food
Science and Technology, Kemerovo, Russia.

CONTENTS

FOOD PRODUCTION TECHNOLOGY

<i>G. V. Gurinovich and I. S. Patrakova</i> Effect of Wheat Germ on the Functional Properties and Oxidation Stability of Ground Meat Systems	3
<i>A. M. Osintsev, E. S. Gromov, and V. I. Braginsky</i> A Phenomenological Model of Milk Coagulation	11
<i>T. V. Renzyaeva</i> On the Role of Fats in Baked Flour Goods	19
<i>I.A. Smirnova, I.V. Romanovskaya, V.K. Shtrigul</i> Method of Obtaining Microparticulated Casein and the Possibility of Its Application in the Production of Nonfat Fermented Milk Products	26
<i>I.S. Khamagaeva</i> Effect of Iron Sulfate on Biosynthesis of Extracellular Metabolites of Propionic Acid Bacteria	33
<i>L. V. Shul'gina, N. V. Dolbnina, L. Yu. Lazhentseva, and Yu. P. Shul'gin</i> New Technological Approaches to Canning Cephalopod Mollusks	40

BIOTECHNOLOGY

<i>O. O. Babich, L.S. Dyshlyuk, and I. S. Milent'eva</i> Expression of Recombinant L-Phenylalanine Ammonia-Lyase in <i>Escherichia Coli</i>	48
--	----

PROCESSES, EQUIPMENT, AND APPARATUSES OF FOOD INDUSTRY

<i>V. N. Ivanets, and D. M. Borodulin</i> Development of Mathematical Models of Centrifugal Mixing Units of New Design for the Production of Dry Combined Food Units of New Design for the Production of Dry Combined Food Products	54
<i>A. E. Rjabova, V. V. Kirsanov, M. N. Strizhko, A. S. Bredikhin, V. K. Semipyatnyi, V. V. Chervetsov, and A. G. Galstyan</i> Lactose Crystallization: Current Issues and Promising Engineering Solutions	66
<i>B. A. Lobasenko and A. G. Semenov</i> Intensification of Ultrafiltration Concentrating by the Separation of the Concentration Boundary Layer	74

FOOD HYGIENE

<i>T. K. Kalenik, M. V. Kravchenko, V. V. Grishchenko, Yu. E. Bubnov, and V. A. Lyakh</i> Enriched Protein Products of Marine Origin. New Components of the Diet for People with Physical Load	82
<i>E. I. Reshetnik and E. A. Utochkina</i> Healthy Food Products with Probiotic and Prebiotic Properties	88

STANDARDIZATION, CERTIFICATION, QUALITY, AND SAFETY

<i>T. A. Krasnova and I. V. Timoshchuk</i> The Impact of Priority Water Contaminants on the Stability of the Main Components of Nectars	95
--	----

CHEMISTRY AND ECOLOGY

<i>S. N. Khabarov, A. L. Vereshchagin, Yu. G. Gur'yanov, N. V. Goremykina, and N. V. Bychin</i> Identification of the Origin of Sea Buckthorn Oil of the Altai Krai by Differential Scanning Calorimetry	108
---	-----

ECONOMY OF THE AGROINDUSTRIAL COMPLEX

<i>V.P. Zotov, E.A. Zhidkova, and N.S. Alekseeva</i> A Methodology for Implementing a Current Cost Management System at Processing Companies of the Distilling Industry: The Case of the Mariinsk Distilling Plant	114
---	-----

UDC 637.514:664.765

DOI 10.12737/1439

EFFECT OF WHEAT GERM ON THE FUNCTIONAL PROPERTIES AND OXIDATION STABILITY OF GROUND MEAT SYSTEMS

G. V. Gurinovich and I. S. Patrakova

Kemerovo Institute of Food Science and Technology,
bul'v. Stroitelei 47, Kemerovo, 650056 Russia
phone:/Fax: +7 (3842) 39-68-57, e-mail: meat@kemtipp.ru

(Received January 11, 2013; Accepted in revised form February 26, 2013)

Abstract: The results of a study of the chemical composition and functional properties of the plant raw material in the form of wheat germ flakes (WGFs) with a view to combining it with a meat feedstock are represented. WGFs subjected to preliminary heat treatment in various modes (toasted) are studied. It is found that water-soluble and salt-soluble proteins of WGFs exhibit high solubility, which achieves maximum values of $45 \pm 2\%$ at a pH of 7.0–8.0 and a sodium chloride concentration of 2.0%. The functional properties of WGFs and dependences of the functional and technological properties of combined ground meat systems prepared of meat feedstocks of different types and nature of autolysis are determined. A preliminary heat treatment of WGFs does not decrease their functional properties, which are particularly shown in feedstock with anomalies in the development of autolysis, and contributes to a decrease in the oxidative transformation of lipids. In combined ground meat systems, toasted WGFs should be used in conjunction with 0.3% of a Delikaroma smoking flavor; this inhibits the oxidation of the lipid fraction of both raw and heat-treated ground meat systems.

Key words: meat, wheat germ, lipid fraction, toasting, oxidation inhibition

INTRODUCTION

Meat products are traditional gastronomically valuable foods that have a long history of consumption. This is the main source of proteins with a high nutritional value, which have a significant effect on the protein metabolism of the human body. According to the modern concepts of nutritional science, the fraction of proteins should be 10–15% of dietary calories and animal proteins should be 50–60% of daily protein requirements. According to the data of the Institute of Nutrition of the Russian Academy of Medical Sciences (RAMS), the recommended intake of meat products depending on the age group of the population is 143 g/day (18–29 and 30–44 years old), 124 g/day (45–59 years old), and 85 g/day for people aged 60 years and over.

Analysis of the actual diet of Russians in recent years has revealed a number of positive tendencies in changing its structure and qualitative composition. The per capita consumption of biologically valuable foods, such as meat and meat products, milk and dairy products, eggs, and fish, has significantly increased, although it is still below the standard. A consequence of this is the lack of an animal protein (33%) at a total protein deficiency in human nutrition (at a level of 26%). These data provide a significant ground for the development of scientifically based ways of correcting the diet of the population. However, it should be remembered that an increase in the consumption of

animal food is associated with an increased consumption of animal fats, which contain high amounts of saturated fatty acids.

Therefore, the modern concept of formulation of meat products involves not only an expansion of the product range and an increase in the volume of their production, but also the solution of a number of important problems, among which a particular position is held by the development of a technology for products meant for improving the nation's health and furthering the safety of products.

Scientists and experts in the implementation of this direction should pay particular attention to plant raw materials because the possibilities and prospects for the use of these materials are extremely broad. Cultivated and wild plant raw materials may be used as a basic ingredient or flavoring and aromatic components in the manufacture of general-purpose products, custom-designed food stuff, dietary supplements, and supplements exhibiting antioxidant and antimicrobial activity. Plant raw materials can be used to solve the problem of reducing the calorie intake with the compensation for the reduction of fat intake by carbohydrates, including complex carbohydrates, and replacing saturated fats with polyunsaturated fatty acids of plant raw materials.

Plant raw materials with a high content of proteins are of great importance in the meat product technology; the significance of proteins is determined not only by

their nutritional value, but also by the involvement in the formation of the basic functional and technological characteristics of the feedstock and, consequently, the consumer properties of the products.

Analysis of scientific and engineering information shows an expansion of research into various types of plant raw materials as an alternative to traditionally used soybeans. Fairly well-known promising plants for producing flour and isolated and concentrated forms of proteins are lentils, chickpeas, peas, beans [1–4]. By-products of grain processing, in particular, wheat and rice bran, have a high technological potential [5, 6]. A high-protein feedstock for producing isolates and concentrates are nuts, such as peanuts, which contain 21% to 36% protein [7, 8], almonds containing about 33% protein [9, 10], and walnut [11]. Along with nuts, the researchers study seeds, extraction cakes, and press cakes of other oil-bearing crops, such as rape and flax; the protein content in press cakes of the last-mentioned plants is up to 54% [12, 13]. It should be noted that there is a keen interest in some plant species, in particular amaranth, a commercial use of which is possible in the near future [14]. These data suggest that the use of plant raw materials in food technology have broad possibilities; the combining of these materials with an animal feedstock for manufacturing products with a complex feedstock composition is a common practice in the world.

Wheat germ is of obvious interest in terms of nutritional value and the possibility of using it in the meat product technology. Despite small sizes of the germ (2.0–3.0% with respect to the mass of the grain), it is the most important part of the grain because it contains the primary organs of development of the plant, and this is responsible for its unique chemical composition. Wheat germ contains a large number of biologically active components; its protein is close to the physiologically active proteins of animal tissues and more fully-featured and balanced with respect to amino acid composition than the grain protein in general. This is attributed to the fact that gluten proteins, which are classified as reserve proteins, are mostly contained in whole grains, while biologically active proteins are dominant in the germ [15–18].

Wheat germ remains insufficiently demanded in the meat product technology because of scarce data on its technological capabilities and the pattern of interaction with components of the feedstock to be enriched in it.

A study of the fractional composition of the protein complex of wheat germ will make it possible to determine its affinity to muscle salt- and water-soluble proteins that are involved in the formation of stable meat systems and find the fraction of gluten proteins that can form a complex that stabilizes the product structure directly in meat systems.

Of great importance from the standpoint of safety and nutritional value of food products is the stability of their lipid component. According to the best available data, wheat germ contains phenolic components exhibiting antioxidant activity, including ubiquinone coenzymes and vitamins E [19]; at the same time, it contains prooxidant factors against the background of a high content of polyunsaturated fatty acids [20, 21]. It

should be taken into account that the oxidation of lipids in the composition of meat products takes place under special conditions, which are primarily associated with the presence of heme pigments. Research into the redox potential of heme components has proved that coordinated iron of heme pigments is ideally suited for the role of an oxidation catalyst for fatty acids owing to the presence of unpaired electrons in their structure. Heme pigments are oxidized by hydroperoxides; this process is accompanied by a change in the valence of iron from Fe^{2+} to Fe^{3+} ; the resulting free radicals are involved in a variety of oxidation chain branching reactions [22].

Thermal action methods are efficient for the stabilization of wheat germ lipids; according to the best available data, these methods do not cause a significant change in the fatty acid profile and a decrease in the activity of phenolic antioxidants [23]. In addition, it is possible to improve their hygienic quality, particularly owing to a decrease in the activity of anti-nutritional factors, such as trypsin inhibitors [24, 25] and microbial contamination. Therefore, in this study, along with native wheat germ flakes (WGFs), previously toasted WGFs were analyzed. Heat pretreatment is also aimed at imparting improved organoleptic properties, particularly flavor and smell, to the germ. At the same time, heat pretreatment can also result in a change in the functional properties of wheat germ owing to a change in the protein and carbohydrate components and initiate the oxidation of labile lipids under complicated conditions of meat systems.

The aim of this study was to examine the chemical composition and functional and technological properties of wheat germ depending on the pretreatment method and its effect on the technological properties of ground meat systems prepared of feedstocks of different types and nature of autolysis and the stability of the lipid fraction of the systems in order to substantiate its use in the cooked sausage technology.

RESEARCH OBJECTS AND METHODS

The object of study is edible wheat germ isolated during grain milling; it has the form of flat dry golden yellow petals, which are easily destroyed under mechanical action; it contains crushed shells, which do not change the color, and has a characteristic odor (Mel'korm flour mill, Kemerovo, Russia). The exterior features are responsible for the brand name of this raw material: WGFs.

The following samples were studied: WGFs unexposed to a pretreatment (native) WGFs_{nat}; WGFs subjected to conductive heating in two modes: 70°C with duration of exposure of 30 min (WGFs_{70°C, 30}) and 140°C with duration of exposure of 15 min (WGFs_{140°C, 15}); and WGFs subjected to dielectric heating at a frequency of 2450 MHz for 1.5 min (WGFs_{microwave}). The treatment was conducted in a thin layer with a thickness of no more than 1 cm. The treated WGFs were cooled at room temperature.

Taking into account a high specific weight of feedstocks with anomalies in the development of the autolysis, the following types of ground meat systems were used to study pH and water-binding capacity

(WBC): ground meat with normal autolysis (NOR beef, NOR pork, pH_{24} of less than 6.2), exudative meat (PSE pork, pH_{24} of 5.3), feedstock of a transient quality (PSE–NOR pork, pH_{24} of 5.3–5.5), and dark, firm, and dry meat (DFD beef, pH_{24} of more than 6.4). Wheat germ was introduced into the system in a hydrated form in a ratio with water of 1 : 2; the duration of hydration was 10 min; the temperature of water for hydration was 16–18°C, the level of introduction of hydrated WGFs was 5–20%.

In studying the stability of ground meat systems during heat treatment, ground meat models based on a feedstock with normal autolysis were used: refrigerated semifat pork or a mixture of semifat pork and first-grade trimmed beef taken in equal proportions. The meat feedstock was ground and admixed with 2.0% of sodium chloride; the mixture was stirred until a uniform distribution of the salt and kept in the salted state for 24 h. In each of the systems, 5.0, 10, and 15.0% of meat was replaced with WGFs hydrated during homogenization of the feedstock; the amount of process water was 20.0% with respect to the weight of the meat feedstock. The ground meat systems were placed in metal weighing bottles with tight-fitting lids and heated in water at a temperature of $85 \pm 2^\circ\text{C}$; the temperature was controlled in an automatic mode with a chromel–copel thermocouple. The record of the thermocouple suggests that all the test samples were heated at an equal rate during a heat-treatment cycle of 15 min. Immediately after the treatment, the samples were cooled in an ice–water mixture and then re-cooled in the air in a cooling chamber at $6 \pm 2^\circ\text{C}$.

To study the stability of the lipid fraction, a ground meat system based on semifat pork with the addition of 10% of toasted and native WGFs was used. Biotone Fos K-144 nutritional supplements (Budenheim, Germany), sodium ascorbate, and a Zhidkii Dym Delikaroma smoking flavor (SF) (AO Virteks, Novosibirsk, Russia) containing 3.0–4.0% of phenolic compounds in terms of guaiacol and 8.0–9.0% of organic acids in terms of acetic acid were used as antioxidants.

MEASURING TECHNIQUES

The *chemical composition*—the weight fraction of proteins, fats, and ashes—was determined using conventional reference methods.

The *fractional composition of proteins of WGFs* was found using the Ermakov's method based on the sequential extraction of proteins with ice water, a 5.0% K_2SO_4 solution, a 70.0% ethanol solution, and a 0.2% NaOH solution. At each stage, a weighed portion of 2.5 g was exposed to the solvent two times [26]. At each of the stages, the liquid portion was separated by centrifugation at 5000 rpm for 10 min. The amount of proteins in the solution was determined by the Kjeldahl method. To specify the amount of glutelins after the extraction of albumins and globulins, a joint extraction of prolamins and glutelins with a 0.2% NaOH solution was conducted with the subsequent precipitation of glutelin at a pH of 10.0 in the presence of NaCl [27].

The *solubility of proteins of WGFs* was determined by a modified Betschart method [28]. To this end, a

weighed portion of 1 g was mixed with distilled water and the pH of the suspension was adjusted to a value of 2.0–9.0 by adding 1.0, 0.1, or 0.01 N NaOH or HCl. The suspension was thoroughly mixed for 30 min, centrifuged at 5000 rpm for 15 min, and filtered through a paper filter. The amount of dissolved nitrogen was determined by the Kjeldahl method. The solubility of proteins of WGFs was calculated as the ratio of the dissolved nitrogen to the total amount. The *reduced glutathione content* was found by a method based on the oxidation of glutathione with iodine.

The *total content of pentosans* was determined by the colorimetric method after the prehydrolysis of a weighed portion of 0.2 N HCL at 100°C for 150 min and a yeast suspension. The absorbance at a wavelength of 580 and 670 nm was measured using an SF PE-5400UF spectrophotometer [29]. The active acidity (pH) was found by a potentiometric method using a 150-M digital pH meter or an ELWRO 5170 pH meter in the case of the aqueous extract and an ELWRO 5123 portable pH meter equipped with a combined electrode in the case of the meat feedstock. The WBC of the ground meat was determined by centrifugation according to the technique of Wierbicki et al. [30].

The *oxidative deterioration of lipids* in the model systems was found through the determination of peroxide number (PN) according to a standard technique [31] using a chloroform extract prepared by the Piulskaya's method [32] and the determination of thiobarbituric acid number (TBN) by a modified distillation method of Tarladgis using a sulfanilic reagent [33].

RESULTS AND DISCUSSION

Chemical Composition and Properties of WGFs

The study of the chemical composition of wheat germ included the determination of the main components and their fractional composition. According to the findings, the average protein content in the test germ was $32.8 \pm 0.3\%$. Highly functional albumins and globulins comprise 52.9–63.4% of this amount; albumins compose a major protein fraction, which accounts for an average value of 39.8% of the total number of proteins. The average amount of proteins extracted by 70% ethanol (prolamins) and alkali (glutelins) is 10.2 and 17.8%, respectively. The amount of proteins in the insoluble precipitate that cannot be extracted by the adopted system of solvents was 13.8%.

One of the most important nonprotein nitrogen-containing compounds of plant cells is glutathione; it is a biological reducing agent capable of participating in enzymatic and nonenzymatic reactions that reduce the toxicity of free radicals and peroxides and in metmyoglobin reduction reactions. These properties are very important in terms of stability of the lipid fraction and the color intensity and stability in products during storage. According to the findings, the content of reduced glutathione in WGFs is $0.52 \pm 0.03\%$. These data characterize WGFs as a raw material with a high content of the reducing agent.

Some carbohydrates are technologically significant in the manufacture of meat products; their concentration in WGFs was experimentally determined. Thus, the

content of mono- and disugars is 14.1–18.8% in terms of glucose, including the amount of reducing sugars that contribute to a more complete involvement of heme pigments into the color formation reaction, a decrease in the amount of metpigments and nonheme iron from 0.8 to 0.3%. The amount of polysaccharides that, along with muscle proteins, can participate in the formation and stabilization of the structure of meat products has been found. These polysaccharides include cellular tissue (celluloses), which gets into the germ with bran components, nonstarch polysaccharides pentosans, and starches. According to the findings, the weight fraction of cellulose is $2.40 \pm 0.04\%$; insoluble pentosans, 3.9–4.2%; and starch, $6.2 \pm 0.3\%$.

For the studied WGFs, in the case of using diethyl ether as a solvent, the average amount of extractable lipids was $11.72 \pm 0.14\%$, which is equal to their concentration in semi-skimmed soy flour. The average weight fraction of mineral components is $3.95 \pm 0.37\%$. It was experimentally found that the weight fraction of moisture in wheat germ varies from 9.7 to 10.5% with an average value of 10.1%.

According to the findings, wheat germ can be classified as a protein–carbohydrate feedstock with a high content of technologically significant components and lipids.

The dependence of solubility of proteins of WGFs in a pH range of 2.0–9.0 has been determined. The minimum solubility is found in a pH range of 2.0–5.0 (18–36%) with an extremum at a pH of 3.0 (16%). As the acidity of the medium decreases, the amount of extractable proteins gradually increases and achieves a maximum value at a pH of 7.0–8.0 (43–45%). The dependence of protein solubility in a sodium chloride (NaCl) concentration range of 0–12% is as follows. The maximum solubility (42–48%) is observed as the sodium chloride concentration increases from the minimal value to 2.0%. At a reagent concentration of 2.0–8.0%, the solubility of proteins continuously decreases and achieves a value of 31.0%. An increase in the NaCl concentration from 8.0 to 12.0% leads to an increase in the solubility to 37.0%.

These data suggest that the proteins of WGFs will exhibit high functional properties in meat systems.

Functional and Technological Properties of WGFs

The moisture-retaining ability (MRA) and fat-retaining ability (FRA) of WGFs, including hydrated WGFs subjected to heat treatment to a temperature of cooking doneness of meat products (MRA_t , FRA_t), have been studied.

According to the findings, the water absorbing ability (WAA) of the wheat germ subjected to a high-temperature heating (140°C, 15 min) is 315–340%, while the average WAA of the native germ is 303%; this can be primarily attributed to an increase in the porosity of the structure with increasing internal specific surface area of the capillaries. This assumption is supported by the results of determination of MRA, which increases by 12% relative to the estimate for the native germ. A possible cause of an increase in the WAA can be a thermal modification of the starch.

These data are consistent with the results of determination of WAA and MRA for the flakes subjected to microwave heating and heating at 70°C in which, owing to gentle treatment, the carbohydrate component does not change; at the same time, proteins do not undergo significant denaturation after the microwave treatment either. Therefore, the MRA remains at a level of untoasted flakes, while the WAA slightly increases, which can be attributed to an increase in the rate of diffusion of moisture owing to a decrease in the water content in the flakes.

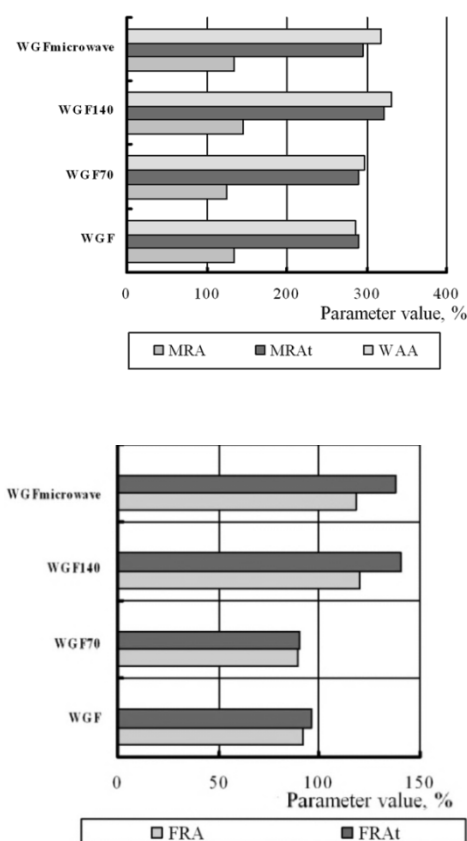


Fig. 1. Functional and technological properties of WGFs as a function of pretreatment method.

The MRA of WGFs increases during heat treatment, which should be attributed to the gelatinization of the compactly arranged starch and the dissolution of carbohydrates of the intercellular space, which stimulate osmotic processes through cell walls.

The method of heat pretreatment of WGFs does not have a significant effect on the value of fat absorbing ability (FAA), which remains in a range of $130 \pm 5\%$.

Effect of WGFs on the Functional Properties of Ground Meat Systems

Figures 2 and 3 show results of studying the effect of the level of introduction of native WGFs on the pH and WBC of combined ground meat systems prepared of meat feedstock with the different nature of autolysis.

The data suggest that the introduction of wheat germ into ground meat systems based on the feedstock of any of the quality groups leads to an increase in pH. In addition, the maximum effect is revealed for the ground meat system based on PSE pork: the addition of 5.0% of

WGFs to this system leads to an increase in pH by 0.14 units; with a further increase in the level of introduction of wheat germ, the pH value increases by 0.08 and 0.06 units, respectively.

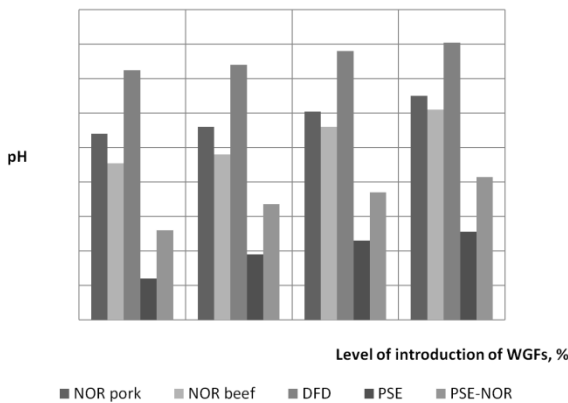


Fig. 2. Effect of the level of introduction of WGFs on the pH of systems prepared of meat feedstocks of the different quality groups.

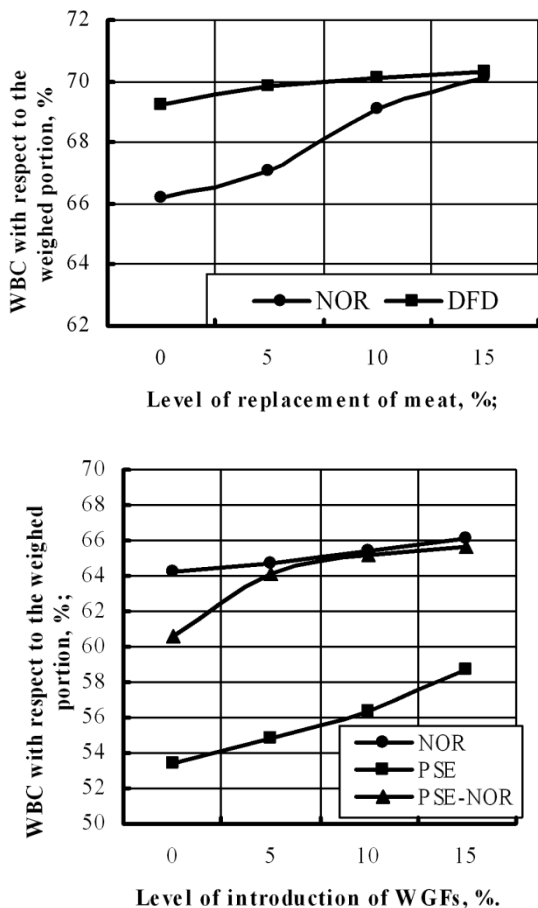


Fig. 3. Effect of the level of introduction of WGFs on the WBC of the combined systems.

Changes in the pH of the combined systems have a positive effect on their WBC value, which increases with increasing level of introduction of WGFs regardless of the type and quality group of feedstock,

particularly for systems prepared of an exudative PSE material. At the same time, the ground meat systems based on the feedstock with a normal autolysis (NOR beef, NOR pork) and dark, firm, and dry meat (DFD beef) exhibit a tendency to increase the parameter rather than a significant gain in WBC.

The total effect of concentration and state of the functional proteins of the muscle portion of the ground meat system and technologically active components of WGFs can lead to a greater or lesser effect of retaining the moisture and fat during the heating of the system to the temperature of cooking doneness.

Results of determination of the functional and technological properties that characterize the resistance of systems to heating depending on the studied factors are shown in Table 1. According to the findings, combined systems with native WGFs are more stable during heat treatment than pure ground meat systems; a reliable increase in the stability of the ground meat systems is observed in the case of replacement of 10.0% of meat with wheat germ.

Table 1. Effect of the level of replacement of meat with native WGFs on the functional and technological properties of systems subjected to heat treatment

Weight fraction of components	Weight fraction of moisture, %	MRA with respect to moisture, %	Weight fraction of fat, %	FRA with respect to fat, %	Stability of systems, %
ground meat system based on semifat pork					
100 : 0	60.32	75.46	23.71	54.98	75.10
95 : 5	61.65	76.85	22.57	55.44	76.42
90 : 10	62.46	81.64	21.22	62.73	82.04
85 : 15	62.87	85.92	20.02	68.47	85.99
ground meat system based on semifat pork and first-grade beef					
50 : 50 : 0	66.52	79.84	12.35	72.69	76.49
50 : 45 : 5	67.19	81.07	10.47	78.24	79.05
50 : 40 : 10	67.28	84.76	10.22	80.74	84.34
50 : 35 : 15	68.03	86.32	9.64	93.89	91.17

The stability of a ground meat system is achieved owing to the retention of both moisture and fat in the system, as evidenced by the results of determination of MRA and FRA. In particular, in the case of replacement of 10.0% of semifat pork with WGFs, MRA and FRA of the system increase by 8.19 and 14.10%, respectively. These data suggest that the protein and carbohydrate fractions of wheat germ are involved in the stabilization of the functional and technological properties of the systems. At the same time, it should be noted that the stability of combined systems decreases with increasing weight fraction of fat.

Stability of the Lipid Fraction of Combined Systems

The dynamics of primary and secondary oxidation products in the ground meat systems with toasted WGFs and the effect of various food supplements on the stability of the lipid component of the combined systems have been studied.

Results of determination of the PN of the combined ground meat systems with toasted WGFs are shown in Fig. 4. It is found that the heating pretreatment of WGFs is a fairly efficient method for inhibiting the oxidation of lipids of raw ground meat. However, in the absence of antioxidants, oxidation in the systems with WGFs occurs faster than in a pure ground meat system (reference system), which suggests that it is necessary to use supplements exhibiting antioxidant activity.

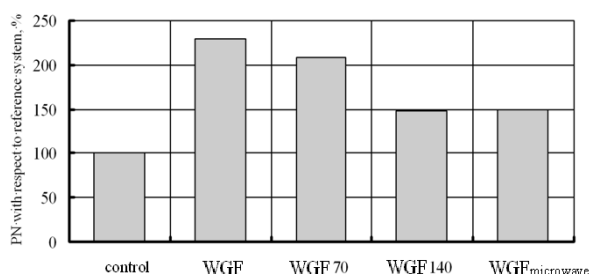


Fig. 4. PN ratio between the reference system and the combined systems with WGFs.

The supplements used in this study were a phosphate compound based on trisodium polyphosphate, sodium ascorbate, and an SF.

Table 2 Effect of Bioton Fos K-144 on the stability of the combined systems

Model system composition	PN with respect to reference system, %	570 nm/650 nm absorbance ratio
Reference system (without WGFs and phosphate)	100	1.92
Combined system with native WGFs	225	1.65
Combined system with native WGFs and 0.3% phosphate	229	1.62
Combined system with native WGFs, 0.3% phosphate, and 0.05 % sodium ascorbate	218	1.68
Combined system with WGFs _{140°C, 15}	148	1.74
Combined system with WGFs _{140°C, 15} and 0.3% phosphate	145	1.63
Combined system with WGFs _{140°C, 15} , 0.3% phosphate, and 0.05 % sodium ascorbate	140	1.81

The experimental data (Table 2) show that the introduction of 0.3% of a Bioton Fos K-144 phosphate supplement into the combined system has not led to the inhibition of oxidation. Moreover, the PN of the system with native WGFs in the presence of the phosphate has increased by a factor of 2.3 compared to the reference system, while in the system with native WGFs without phosphates, it has increased by a factor of 2.25, which can be attributed to the catalyzing action of the alkali phosphate on the wheat germ lipoxigenase. This is

consistent with the results of determination of the level of oxidation in the combined system with toasted WGFs containing partially inactivated lipoxigenase. According to the findings, the PN has increased by a factor of 1.48 and 1.45 for the combined systems with WGFs_{140°C, 15} without and with phosphate, respectively.

A possible cause of the process acceleration can be the formation of meat metpigments (Fe^{3+}) exhibiting high prooxidant action, which can have an additional initiating effect against the background of accumulation of hydroperoxides as active oxidants.

To verify this assumption, we experimentally studied model systems admixed, along with WGFs and phosphate, with sodium ascorbate as a reducing agent of pigments. In this case, the 570 nm/650 nm absorbance ratio of acetone extracts of heme pigments, as a ratio of the reduced and oxidized forms of the pigments, was determined for all the systems.

The research results suggest that the use of tripolyphosphate in combined systems with native WGFs is inappropriate because of its prooxidant action. The use of this compound in combined systems with toasted WGFs in conjunction with sodium ascorbate contributes to the inhibition of the process; at the same time, this does not provide a reliable stabilization of the lipid fraction.

Inhibition of the accumulation of primary and secondary oxidation products is achieved through the introduction of a Delikaroma SF into the system with WGFs (Fig. 5).

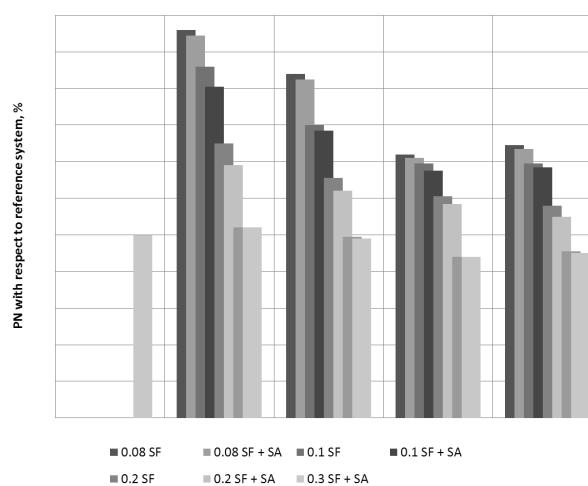


Fig. 5. Effect of the Delikaroma SF concentration on the oxidation of the lipid fraction of the combined systems.

Based on the findings, we can state that the mechanism of action of the SF on the oxidation of fats does not change upon the introduction of the SF into systems with different concentrations of primary oxidation products as oxidation catalysts. Inhibition of the process occurs owing to the oxidation chain termination and the binding of free radicals with phenolic compounds having a more mobile proton to form stable products incapable of continuing the free radical oxidation process. Since the oxidation process is developing, a high concentration of inhibitors as free radical traps is required; therefore, the efficiency of

action of the SF increases with increasing concentration. In the case of a joint use of the SF and ascorbic acid, a synergetic effect is observed. The SF concentration of 0.3% with respect to the weight of the feedstock is sufficient for effective inhibition of oxidation.

Results of determination of the amount of primary and secondary oxidation products and free fatty acids in cooked systems with SF and differently processed WGFs during refrigerated storage are shown in Table 3.

Table 3. Parameters of storage stability (at $4 \pm 2^\circ\text{C}$) of the fat phase of combined systems with WGFs subjected to heat treatment to a temperature of cooking doneness

Research object	Storage time, days														
	0			1			2			3			4		
	PN	TBN	AN	PN	TBN	AN	PN	TBN	AN	PN	TBN	AN	PN	TBN	AN
Reference system	6.08	-	2.1	6.08	1.12	2.4	7.02	2.12	3.8	7.02	2.75	3.9	7.56	3.53	4.1
Combined systems with: native WGFs	6.47	-	2.7	7.18	1.25	3.1	9.28	2.37	3.8	9.12	2.92	3.8	10.61	3.60	4.1
WGFs _{70°C, 30}	6.55	-	2.1	6.24	1.09	2.2	6.40	2.01	3.1	6.63	2.54	3.4	7.49	3.26	3.4
WGFs _{140°C, 15}	5.85		2.2	6.00	0.97	2.4	6.00	1.75	2.8	6.24	2.45	3.2	7.02	3.04	3.7
WGFs _{microwave}	5.69		2.2	5.85	1.86	2.2	6.24	1.64	2.6	6.32	2.34	3.1	6.94	2.90	3.5

Note: PN, mmol of active oxygen per kilogram of fat; TBN, mg/1000 g of product; and AN, mg KOH.

The data suggest that the SF has an inhibiting effect on the systems with toasted WGFs under conditions of refrigerated storage for a time corresponding to the shelf life of cooked sausages and prevents the development of a typical defect that is referred to as "the smell of excessively overcooked meat."

Results of the study allow us to recommend the use of WGFs in the technology of cooked sausage products.

The flakes should be preheated at 140°C for 15 min. The use of 10% of pretoasted WGFs provides a reliable improvement of the functional and technological properties of combined systems. The stabilization of the lipid fraction is achieved through the simultaneous introduction of 0.3% of a Delikaroma SF into the systems.

REFERENCES

- Krylova, V.B., Chechevitsa - istochnik pishchevogo rastitel'nogo syr'ya (Lentils as a source of edible plant raw material), *Vestnik Rossiiskoi Akademii Sel'skokhozyaistvennykh Nauk (Bulletin of the Russian Academy of Agricultural Sciences)*, 1994, no. 2, pp. 21–22.
- Suhaila, M., Jamilah, B., Norhashima, H., and Abd, H., Differences in functional properties of mungbean protein concentrate and the effect of incorporation into fish sausages, *Pertanika Journal of Tropical Agricultural Science*, 1996, vol. 19, no. 1, pp. 69–75.
- Gorlov, I.F., Shindyalova, E.V., and Sapozhnikova, L.G., Novaya vysoko-belkovaya dobavka iz nuta (A new high-protein supplement of chickpeas), *Myasnaya Industriya (Meat Industry)*, 1999, no. 6, pp. 24–25.
- Mizubuti, I.Y., Biondo, O., Jr. Souza, L.W.O., da Silva, R.S.S.F., and Ida, E.I., Functional properties and protein concentrate of Pigeon pea (*Cajanus cajan* (L.) Millsp) flour, *Archivos Latinoamericanos de Nutricion*, 2000, vol. 50, no. 3, pp. 274–280.
- Kolpakova, V.V., Martynova, I.V., Severinenko, S.M., Nechaev, A.P., and Berman, Yu.K., Belok iz pshenichnykh otrubei: Proektirovanie sbalansirovannogo sostava pishchevykh kompozitov belkovo-zhirovoy prirody (Wheat bran protein: Formulation of a balanced composition of protein–fatty food composites), *Khranenie i Pererabotka Sel'khozsyrya (Storage and Processing of Agricultural Raw Materials)*, 2001, no. 11, pp. 42–47.
- Chandi, G.K. and Sogi, D.S., Functional properties of rice bran protein concentrates, *Journal of Food Engineering*, 2007, vol. 79, pp. 592–597.
- Venkatachalam, M. and Sathe, S.K., Chemical composition of selected edible nut seeds, *Journal of Agricultural and Food Chemistry*, 2006, vol. 54, no. 13, pp. 4705–4714.
- Ahmedna, Yu. J. and Goktepe, I., Peanut protein concentrate: Production and functional properties as affected by processing, *Food Chemistry*, 2007, vol. 103, pp. 121–129.
- Sze-Tao, K. and Sathe, S., Functional properties and in vitro digestibility of almond (*Prunus dulcis* L.) protein isolate, *Food Chemistry*, 2000, vol. 69, pp. 153–160.
- Olatidoye, O.P., Sobowale, S.S., Akinlotan, J.V., and Olorode, O.O., Chemical composition and physicochemical characteristics of tropical almond nuts (*terminalia catappia* l) cultivated in South West Nigeria, *Journal of Medical and Applied Biosciences*, 2011, vol. 2.
- Mao, X. and Hua, Y., Composition, structure and functional properties of protein concentrates and isolates produced from walnut (*Juglans regia* L.), *International Journal of Molecular Sciences*, 2012, vol. 13, no. 2, pp. 1561–1581.

12. Pankrushina, A.N., Grigor'eva, A.L., Pakhomov, P.M., and Steblinin, A.N., Izuchenie sodержaniya belka v l'nyanykh zhmykhakh i produktakh ikh pererabotki (A study of the protein content in linseed cakes and their derivatives), *Biomeditsinskie Tekhnologii i Radioelektronika (Biomedical Technology and Radioelectronics)*, 2005, no. 10, pp. 7–10.
13. Yoshie-Stark, Y., Wada, Y., and Wäsche, A., Chemical composition, functional properties, and bioactivities of rapeseed protein isolates, *Food Chemistry*, 2008, vol. 107, pp. 32–39.
14. Mahajan, A. and Dua, S., Salts and pH induced changes in functional properties of amaranth (*Amaranthus tricolor* L.) seed meal, *Cereal Chemistry*, 2002, vol. 79, no. 6, pp. 834–837.
15. Koz'mina, N.P., *Biokhimiya zerna i produktov ego pererabotki (Biochemistry of Grain and Its Derivatives)*, Moscow: Kolos, 1976.
16. Lasztity, R., *The Chemistry of Cereal Proteins*, Boca Raton, FL: CRC Press, 1984, p. 3.
17. Safronova, A.M., Vysotskii, B.G., Narodetskaya, R.V., Trushina, E.N., et al., Pishchevaya tsennost' khlop'ev pshenichnogo zarodysha (Nutritional value of wheat germ flakes), *Voprosy Pitaniya (Nutritional Issues)*, 1990, no. 3, pp. 54–58.
18. Vishnyakov, A.B., Vlasov, V.N., Novitskii, O.A., and Babenko, I.P., Kompleksnaya pererabotka pshenitsy s polucheniem biologicheskii aktivnykh produktov (Integrated processing of wheat to produce biologically active products), *Khranenie i Pererabotka Zerna (Grain Storage and Processing)*, 2000, no. 12, pp. 52–58.
19. Oufnac, D.S., Determination of antioxidant capacity in corn germ, wheat germ and wheat bran using solvent and microwave-assisted solvent extraction, *B.S. Culinary Arts Thesis*, Thibodaux: Nicholls State University, 2006.
20. Zherebtov, N.A., Zyablova, T.V., and Cheremushkina, I.V., Vliyanie pH i temperatury na aktivnost' i ustoychivost' lipoksigenazy zarodyshei zerna pshenitsy (Effect of pH and temperature on the activity and stability of wheat germ lipoxygenase), *Khranenie i Pererabotka Sel'khozsyrya (Storage and Processing of Agricultural Raw Materials)*, 2000, no. 1, pp. 53–55.
21. Sudha, M.L., Srivastava, A.K., and Leelavathi, K., Studies on pasting and structural characteristics of thermally treated wheat germ, *European Food Research and Technology*, 2007, vol. 225, pp. 351–357.
22. Tarladgis, B.G., An hypothesis for the mechanism of heme catalyzed lipid oxidation in animal tissues, *Journal of the American Oil Chemists Society*, 1961, vol. 38, pp. 479–483.
23. Ramadan, M.F., Showky, H.E.S., and Sulieman, A.E.R.M., Comparison between the effect of γ -irradiation and roasting on the profile and antioxidant activity of wheat germ lipids, *Grasas y Aceites*, 2008, vol. 59, no. 2, pp. 166–173.
24. Pitebskaya, V.S., Shabalta, O.M., Kochegura, A.V., and Zelentsov, S.V., Povyshenie biologicheskoi tsennosti semyan soi pishchevogo naznacheniya (Improvement of the biological value of edible soybean seeds), *Izvestiya Vysshikh Uchebnykh Zavedenii, Pishchevaya Tekhnologiya (Transactions of Higher Educational Institutions, Food Technology)*, 1997, nos. 2–3, pp. 19–22.
25. Lisitsyn, A.N., Klyuchkin, V.V., and Grigor'ev, V.N., Izuchenie vliyaniya SVCh-nagreva na aktivnost' nekotorykh fermentov (A study of the effect of microwave heating on the activity of some enzymes), *Izvestiya Vysshikh Uchebnykh Zavedenii, Pishchevaya Tekhnologiya (Transactions of Higher Educational Institutions, Food Technology)*, 1998, no. 3, pp. 12–17.
26. Mineev, V.G., Sychev, V.G., Amel'yanchik, O.A., Bolysheva, T.N., Gomonova, N.F., et al., *Praktikum po agrokhemii: Uchebnoe posobie (Handbook of Agricultural Chemistry)*, Moscow: Mosk. Gos. Univ., 2001, 2nd ed.
27. Savai, H. and Morita, V., Studies of rise glutelin: 1. Isolation and purification of glutelin from rise endosperm, *Agricultural and Biological Chemistry*, 1968, vol. 32, pp. 76–80.
28. Betshart, A.A., Nitrogen solubility of alfalfa protein concentrate as influenced by various factors, *Journal of Food Science*, 1974, vol. 39, pp. 1110–1115.
29. Delcour, J.A., Vanhamel, S., and De Geest, C., Physico-chemical and functional properties of rye nonstarch polysaccharides: 1. Colorimetric analysis of pentosans and their relative monosaccharide compositions in fractionated (milled) rye products, *Cereal Chemistry*, 1989, vol. 66, no. 2, pp. 107–111.
30. Wierbicki, E. and Deatherage, F.E., Determination of waterholding capacity of fresh meats, *Journal of Agricultural and Food Chemistry*, 1958, vol. 6, no. 5, pp. 397–392.
31. GOST (State Standard) R 51 487: *Masla rastitel'nye i zhiry zhiivotnye. Metod opredeleniya perekisnogo chisla (Vegetable oils and animal fats: A method for the determination of peroxide number)*.
32. Piul'skaya, V., Ekspress-metod ekstragirovaniya zhira iz zhirovoi tkani (A rapid method for the extraction of fat from adipose tissues), *Myasnaya Industriya SSSR (Meat Industry of the Soviet Union)*, 1958, no. 1, p. 9.
33. Tarladgis, B.G., Watts, B.M., Yonathan, M., and Dugan, L.R., Jr., A distillation method for the quantitative determination of malonaldehyde in rancid foods, *Journal of the American Oil Chemists Society*, 1960, vol. 37, no. 1, pp. 44–48.

UDC 637.1:66.065.2
DOI 10.12737/1512

A PHENOMENOLOGICAL MODEL OF MILK COAGULATION

A. M. Osintsev, E. S. Gromov, and V. I. Braginsky

Kemerovo Institute of Food Science and Technology,
bul'v. Stroitelei 47, Kemerovo, 650056 Russia
phone/Fax: +7 (3842) 39-00-98, e-mail: olex1@mail.ru

(Received March 07, 2013; Accepted in revised form July 23, 2013)

Abstract: A model of additional stabilization for the milk colloid system by means of the micelle electric charge arising owing to dissociation of micellar calcium caseinate is offered. The model allows comprehending the unique role of calcium in milk clotting and describing some features of coagulation temperature dependence, as well as explaining the nature of rennet, acid, heat-acid and heat-calcium coagulation within uniform concepts.

Key words: milk coagulation, sticky hard spheres, calcium caseinate, colloid calcium phosphate, ionized calcium.

INTRODUCTION

Milk clotting is one of important technological processes in the manufacturing of many foodstuffs, in particular, cheeses. This process is based on the coagulation of casein micelles, which may be caused by various factors, such as enzymes, acids, spirits, salts, or high temperature [1].

It is recognized now that the colloid stability of casein micelles in milk is ensured, basically, by the presence of the κ -casein macropeptide hairy layer on the casein micelle surface, sterically restricting the possible clinging together of micelles [2--5]. In essence, this layer represents a quasielastic polyelectric brush formed by negatively charged macropeptide residues [6, 7].

The loss of colloid stability by the casein micellar system may be attributed to different ways of the destruction of the hairy layer. Therefore, under rennet conditions, κ -casein macropeptide hairs are split off by chymosin, which leads to the destruction of the protective layer. During acid coagulation, additional hydrogen ions easily get into the polyelectric brush and shift ion equilibrium to the recombination of dissociated κ -casein macropeptide acid groups, thus reducing the electric charge of macropeptide hairs and finally collapsing the protective layer [8].

Certain distinctions in mechanisms of the destruction of the casein micelle protective layer, as well as a number of factors affecting the micellar casein system's colloid stability, make it very difficult to describe various kinds of milk coagulation with a uniform approach. For example, it is known that the lack of calcium in milk has no significant effect on acid milk coagulation, while it is impossible to coagulate this milk by adding chymosin even after it has completely cut off the protective hairy layer [9, 10].

This research is an attempt to work out a universal model of milk coagulation, which would correctly describe, at least qualitatively, observable features of the milk coagulation phenomenon under various conditions of casein colloid system destabilization.

The background of our model is represented by both well-known experimentally confirmed facts and somehow substantiated but still hypothetical assumptions. In particular, the basic hypothesis rests on the analysis of the outstanding role of calcium ions in the stabilization of the micellar colloid systems in milk.

We hope that this paper will become a stimulus for the direct experimental check of our hypotheses by interested experimentalists.

MATERIALS AND METHODS

Skim milk was reconstituted by mixing up 90 g of low-fat milk powder (Milk Factory, Kemerovo, Russia) with 910 ml of distilled water and 4 cm³ of 10% solution of calcium chloride. Then, after complete dissolution, the reconstituted milk was left for about 12 hours at $6 \pm 2^\circ\text{C}$.

Milk coagulation was carried out in a thermostatted 200 ml cell.

The chymosin under the trademark of Maxiren[®] (DSM, Netherlands) was used for rennet coagulation. To prepare the enzyme solution, 0.1 g of dry Maxiren[®] powder was dissolved in 100 cm³ of distilled water.

For simulating acid coagulation, a 10% lactic acid solution (Univerkhim, Chelyabinsk, Russia) was slowly brought to milk under careful mixing.

To increase the pH of some milk samples, a 0.5-mM sodium hydroxide solution (NaOH) (Univerkhim, Chelyabinsk, Russia) was used.

Soluble calcium was added to milk in the form of 10% CaCl₂ medical solution (Shenlu Pharm, China).

To decrease calcium ion concentration in milk, in a number of experiments Trilon B[®] (Na₂EDTA) (Khimservis, Ufa, Russia) was used as a chelating agent.

Calcium ion concentration and pH in milk were measured with ELIT (Niko-Analit, Moscow, Russia) ion selective electrodes.

The casein micelles ζ -potential was measured by means of Zetasizer Nano Z - ZEN2600 (Malvern Instruments, Malvern, UK).

Milk coagulation was monitored with a computer-driven "thermometric" gauge of our own design [11]. This device measures temperature difference between two thermocouple junctions immersed in milk at a distance of about 3 cm from each other. One of the junctions is attached directly to a small resistor dissipating permanently about 0.5 W of heat. An increase in milk viscosity during coagulation leads to an increase in temperature difference. It is more correct to say that the temperature increase near the warmed-up junction is due not only to the viscosity increase but also to the formation of a gel net structure, which also restricts convection in milk. In a sense, our method is similar to the hot wire method [12]. Hereinafter, the curves obtained by means of the thermometric gauge are called thermograms (by analogy with rheograms).

RESULTS AND DISCUSSION

Figure 1 demonstrates the dependence of rennet coagulation kinetics on ionized calcium concentration. Various doses of the 10% solution of calcium chloride were brought to milk at its reconstitution.

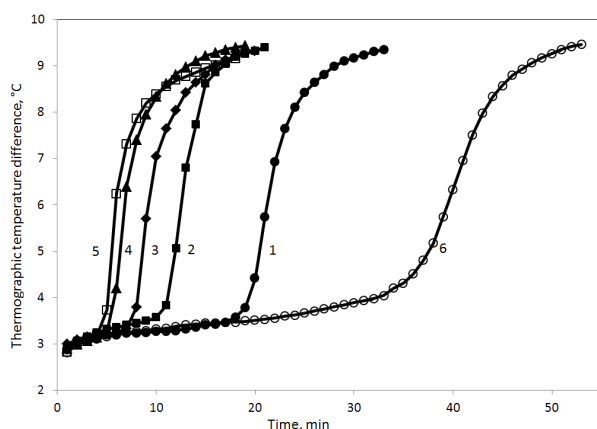


Fig. 1. Thermograms of reconstituted skim milk coagulation by chymosin (25 mg/L) at 30°C.

Curves: 1 – reference sample;

2 – 0.8 g/L of CaCl_2 added to reconstituted milk;

3 – 1.2 g/L of CaCl_2 added to reconstituted milk;

4 – 1.6 g/L of CaCl_2 added to reconstituted milk;

5 – 2.0 g/L of CaCl_2 added to reconstituted milk;

6 – no CaCl_2 added to milk at its reconstitution.

The reference sample, represented with the curve 1 in Fig. 1, was prepared as specified in the previous section (4 cm³ of 10% CaCl_2 solution was added to 1 L of reconstituted milk). The concentration of calcium ions in the reference sample, measured directly before coagulation, was 3.2 ± 0.3 mM.

Enhanced doses of calcium chloride were added to the samples, represented by curves 2--5, as specified in Fig. 1.

The sample represented by curve 6 was reconstituted without adding calcium chloride. Immediately before coagulation, calcium ion concentration in this sample was 1.8 ± 0.3 mM.

All samples were coagulated at $30 \pm 1^\circ\text{C}$ by adding 5 ml of the enzyme solution to 200 ml of reconstituted milk.

Predictably, the increase in the concentration of soluble calcium in reconstituted milk considerably reduces the duration of rennet coagulation. However, the increase in the concentration of calcium ions above approximately 10 mM leads to the saturation effect. Thus, for samples 4 and 5, for which the concentration of calcium ions was 9.5 ± 0.4 mM and 11.7 ± 0.4 mM, respectively, the coagulation time was almost the same.

Figure 2 shows thermograms for the coagulation of reconstituted skim milk with a reduced calcium ion concentration by adding Trilon B (Na_2EDTA). The reference sample (curve 1) is the same as in Fig. 1.

The samples represented by curves 2 and 3 in Fig. 2 are prepared as specified in Fig. 2. The calcium ion concentration for these samples was 1.2 ± 0.2 mM. All samples were coagulated at $30 \pm 1^\circ\text{C}$ by adding 5 ml of the enzyme solution to 200 ml of reconstituted milk.

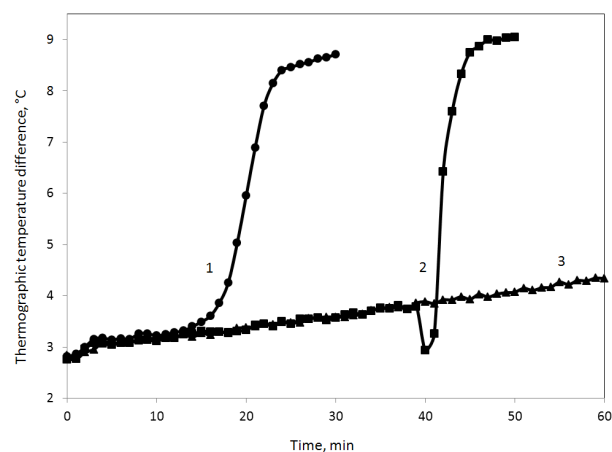


Fig. 2. Thermograms of reconstituted skim milk clotting by chymosin (25 mg/L) at 30°C.

Curves: 1 – reference sample (addition of 0.4 g/L of CaCl_2 to milk);

2 – 1.5 g/L of Na_2EDTA and no CaCl_2 added to milk at reconstitution, 0.8 g/L of CaCl_2 added after 40 minutes of renneting;

3 – 1.5 g/L of Na_2EDTA and no CaCl_2 added to milk at reconstitution.

The samples represented by curves 2 and 3 are identical, but 1.6 cm³ of the 10% calcium chloride solution was brought to sample 2 40 minutes after the addition of the enzyme solution. It is clear from Fig. 2 that coagulation started immediately after the addition of calcium. Note that the sample to which calcium had not been added (curve 3) did not coagulate within 2 hours after the addition of the enzyme solution.

A similar rennet coagulation behavior can be observed if calcium ion concentration in milk decreases one way or another to values less than approximately 1.5 mM: milk can undergo no coagulation for hours after the addition of chymosin (if pH is not decreasing), but, if ionized calcium is brought to milk after κ -casein cleavage by chymosin is over, coagulation begins immediately.

The most common ways to explain the role of calcium in the rennet coagulation of milk are to consider calcium as an agent bridging micelles together or as an

agent affecting the ionic strength of milk and, consequently, the density of the protective electrolytic brush.

However, if bridging is the case, it is difficult to explain why the decrease in calcium ion concentration from 3.2 mM (Fig. 1, curve 1) to 1.8 mM (Fig. 1, curve 6) almost doubles the coagulation time, while the decrease in calcium ion concentration from 3.2 mM (Fig. 2, curve 1) to 1.2 mM (Fig. 2, curve 3) stops coagulation.

Note also that, if, in the case of sample 2 in Fig. 2, one brings to milk solutions of sodium chloride or potassium chloride instead of calcium chloride (with the same ionic strength), it does not lead to coagulation.

We introduce a hypothesis of colloid stabilization for the milk micellar system, based on a simple phenomenological square-potential model. Let micelles be “hairy spheres” with a hard sticky surface and an elastic nonsticky hairy layer attached to the surface and protecting the spheres from sticking together [8]. The potential of interaction between two micelles for this system is shown in Fig. 3.

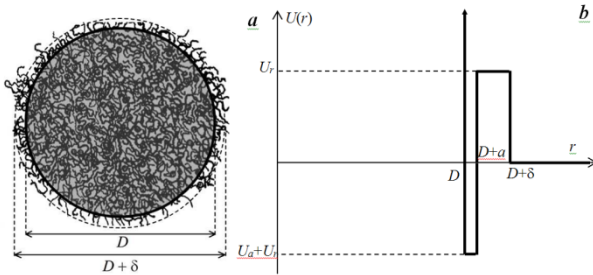


Fig. 3. Schematic micelle image (a) and (b) the interaction potential depending on distance r between the centers of two micelles.

It consists of an infinite hard sphere “wall” at distance D , a deep narrow adhesive “well” of width a , and a repulsive “step” of width δ :

$$U(r) = U_w(r) + U_a(r) + U_r(r), \quad (1)$$

where

$$U_w(r) = \begin{cases} +\infty, & r \leq D \\ 0, & r > D \end{cases}$$

$$U_a(r) = \begin{cases} -U_0 + U_{add}, & r \leq D + a \\ 0, & r > D + a \end{cases}$$

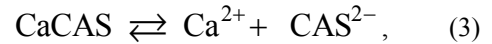
$$U_r(r) = \begin{cases} U_r, & r \leq D + \delta \\ 0, & r > D + \delta \end{cases} \quad (2)$$

The main idea of our model is an additional micellar potential, U_{add} , resulting from the dissociation of micellar calcium caseinate [13]. In spite of the fact that we are inclined to consider this additional potential as sufficiently screened by Debye layer electrostatic repulsion, it is placed into the “adhesive” part of the whole potential. This is mostly to simplify the

coordinate dependence of the whole potential. In this way, the additional potential just varies the adhesive well depth. It is not even forbidden to transform the “well” into “step.”

It is known that calcium is able to bind chemically with phosphoserine groups of α - and β -caseins [10, 14–16], forming compounds, so to speak, of an ambiguous chemical structure, which are usually called calcium caseinates.

If one assumes the binding of calcium to phosphoserine groups as a chemically reversible process, it is possible to present formally the reaction of calcium caseinate dissociation--recombination as follows:



where symbol “CAS” is chosen to represent a “casein molecule.”

The equilibrium constant for reaction (3) is

$$K_{CAS} = \frac{[\text{Ca}^{2+}][\text{CAS}^{2-}]}{[\text{Ca CAS}]}, \quad (4)$$

Thus, the decrease in calcium ion concentration $[\text{Ca}^{2+}]$ leads to the emergence of an additional micellar negative electric charge, q_{CAS} , proportional to the concentration of dissociated caseinates $[\text{CAS}^{2-}]$, which, in turn, is inversely proportional to $[\text{Ca}^{2+}]$

$$q_{CAS} \propto -[\text{CAS}^{2-}] = -\frac{K_{CAS}[\text{Ca CAS}]}{[\text{Ca}^{2+}]}, \quad (5)$$

Expression (5) may be directly verified by micelle ζ -potential measurement. Figure 4 demonstrates a possible verification. The decrease in calcium ion concentration in our case was attained by adding Trilon B® to milk, and its increase, by adding the calcium chloride solution to reconstituted skim milk. In both cases, the pH of milk was adjusted to 6.7 with a sodium hydroxide solution.

To fit experimental data, the following function for the negative micellar ζ -potential absolute value was used

$$\zeta = \frac{a}{[\text{Ca}^{2+}]} + b, \quad (6)$$

The solid line in Fig. 4 was calculated according to formula (6) with $a = 45.7 \text{ mV}\cdot\text{mM}$ and $b = 10.4 \text{ mV}$.

The constant term b , in our opinion, is basically attributed to the electric charge arising as a result of the dissociation of κ -casein macropeptide residues and, probably, some other functional groups of casein molecules.

The results shown in Fig. 3 are in quite a reasonable accordance with earlier experimental data [17, 18]. For example, the article [17] states that the negative casein micelle ζ -potential of skimmed bulk milk in absolute value was 24.4 mV, and after the removal of 51% of

calcium from milk through ionic exchange, it became 30.6 mV (in absolute value).

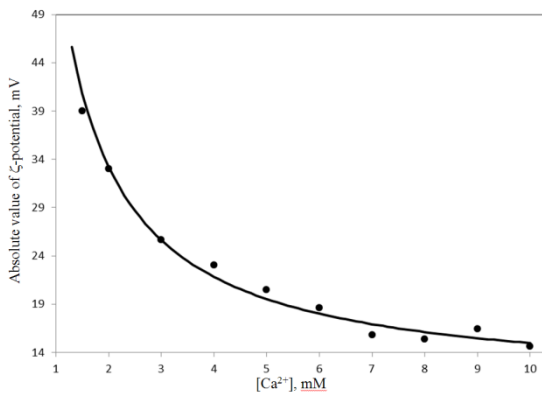


Fig. 4. Dependence of the micellar ζ -potential on calcium ion concentration in reconstituted skim milk at pH = 6.7.

Thus, we can conclude that the lack of calcium ions in milk causes an essential increase in the micelle electric charge as a result of micellar calcium caseinate dissociation. This leads to additional short-ranged (because of Debye screening) electrostatic repulsion. In our square-potential model, it counts as the increase in U_{add} in (2) and, hence, the decrease in the adhesive well depth. Therefore, when calcium ion concentration in milk is decreased by any possible way, micelle “hard spheres” become unstuck and coagulation is impossible even when the “repulsive step” is completely destroyed by chymosin.

It is useful to note that the “chemical” nature of the role of calcium in the stabilization of the milk casein colloid system can be proved by the fact that magnesium acts very similarly when added to milk, while sodium or potassium act differently.

It is known that κ -casein cleavage by chymosin does not depend essentially on the concentration of calcium ions in milk. This may be justified by the conclusions in [19, 20]. In this case, the destruction of the protective hairy layer on the micelle surface for the sample whose thermogram is presented by curve 6 in Fig. 1 occurs practically simultaneously with that for the samples represented by curves 4 or 5. However, coagulation for sample 6 does not occur at this time. It occurs much later.

According to our square-potential model, coagulation is a process of “all-or-nothing” type. Therefore, if the depth of U_a is enough and U_r is not very high, coagulation occurs. However, if the depth of U_a is not enough (whatever U_r is), coagulation does not occur. Then why do both milk samples with calcium ion concentrations of 2 mM and 10 mM coagulate, although in the latter case much faster?

Apparently, there should be a process that is able to decrease the additional negative charge of casein micelles, raised in the way described above. Judging by the form of thermograms recorded at different calcium ion concentrations, this process may be similar to the proteolytic cleavage of κ -casein by chymosin.

Let us now introduce another hypothesis to our model. We assume that the additional negative charge

of casein micelles can be decreased due to the nonspecific proteolytic activity of chymosin, directed to the charged functional groups of α - and β -caseins. Researchers are aware of such nonspecific activity [21--23]. In principle, α - and β -caseins located mainly inside micelles can be accessible to chymosin during the primary stage of coagulation. According to modern ideas, the micelle is a porous structure penetrable for small protein molecules [24--27].

To substantiate the hypothesis of chymosin additional proteolytic activity, we performed experiments on renneting calcium-depleted milk with different amounts of chymosin (Fig. 5). One can see that the increase in enzyme concentration leads to an almost proportional reduction of coagulation time. Such dependence is characteristic of enzymatic reactions. Thus, we may suppose that κ -casein proteolysis on the micellar surface and the proteolysis of α - and β -caseins inside micelles are similar processes, although in the latter case the rate of proteolysis is much slower (by about ten times according to our estimates) apparently due to the lower availability of the internal micelle area for chymosin molecules.

Now we can explain the role of calcium ions in milk renneting in the following way. The rennet coagulation time is determined by the rate of κ -casein cleavage by chymosin on the micelle surface only in the case of a sufficient concentration of calcium ions in milk. According to our estimates, this concentration is about 10 mM. As a rule, the concentration of ionized calcium in milk is below this value and chymosin needs some time to cut off the functional groups of α - and β -caseins, negatively charged due to calcium caseinate dissociation, inside casein micelles. Since the additional electric charge of micelles strongly depends on calcium ion concentration, the rennet coagulation time is usually affected dramatically by the quantity of calcium ions added to milk.

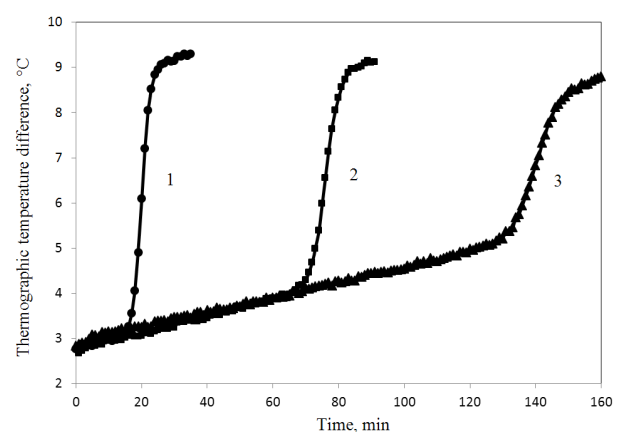


Fig. 5. Thermograms of reconstituted skim milk clotting by different amount of chymosin at 30°C.

Curves: 1 – reference sample (0.4 g/L of CaCl_2 added to milk, clotting with 25 mg/L of chymosin);
2 – no CaCl_2 added to milk, clotting with 100 mg/L of chymosin;
3 – no CaCl_2 added to milk, clotting with 50 mg/L of chymosin.

It is usually believed that acid milk coagulation does not depend on calcium ion concentration and is determined only by the milk pH value. Nevertheless, this is not obvious. It is known that, under acid conditions, casein flocculation in milk begins at a pH value of about 5.2. On the other hand, at such pH values, micellar calcium phosphate is practically entirely ionized. Thus, the mechanism of casein colloid system destabilization during acid milk coagulation is perhaps similar to that described above.

On the one hand, additional hydrogen ions under acid conditions reduce the macropeptide hair charge and make the polyelectric brush collapse (U_r is destroyed in our model). On the other hand, the increase in calcium ion concentration owing to the dissolution of colloid calcium phosphate leads to a decrease in the additional micelle charge (U_a becomes adhesive).

We tried a simple experiment to substantiate this idea. The point is that Na_2EDTA exhibits acid properties under dissolution. Thus, we were able to decrease the milk pH by adding either lactic acid or Trilon B[®]. In both cases, we decreased it to 4.8.

In both cases, an increase in milk viscosity was observed. However, in case of coagulation with lactic acid, the increase in viscosity was more intensive and a classic acid clot was observed as a result. In case of coagulation with Trilon B[®], despite a slow increase in viscosity, clot formation in milk does not occur.

Perhaps, despite the decrease in EDTA's chelating ability at a low pH, the competition between this process and reversible calcium caseinate dissociation leads to the retention of part of the additional charge of casein micelles and, as a consequence, to the reduction of the micelle coagulation ability. Thus, it is quite possible that casein colloid stability in milk is controlled by the same mechanism for both rennet and acid coagulation.

To include acid milk coagulation in our model, we add a couple of highly simplified schemes (similar to scheme (3)) to our phenomenological chemistry. First, we will consider the negative charge of κ -casein macropeptide hairs q_{CMP} as a result of dehydrogenation



with the equilibrium constant

$$K_{CMP} = \frac{[\text{CMP}^-][\text{H}^+]}{[\text{CMP}]}, \quad (8)$$

Then

$$q_{CMP} \propto -[\text{CMP}^-] = -\frac{K_{CMP}[\text{CMP}]}{[\text{H}^+]}, \quad (9)$$

The CMP symbol is chosen to represent κ -casein macropeptide hydrophilic groups. We may assume that basically this charge ensures micelle steric stability by means of the elastic polyelectrolyte brush.

Second, because of the complexity of the colloid calcium phosphate (CCP) structure, its hydrogenation is considered within the extremely simplified one-step scheme:



Here CCP^* is the hydrogenated form of CPP. We hope that this "averaged" scheme of CPP hydrogenation is qualitatively correct at least for describing the basic features of the process (for example, dependence on pH).

The mechanism of acid milk coagulation can now be described as follows. A decrease in milk pH or, respectively, an increase in $[\text{H}^+]$ shifts, on the one hand, the equilibrium of reaction (7) to the left and, consequently, decreases (in absolute value) the polyelectric brush's negative charge q_{CMP} (according to (9)). On the other hand, the increase in $[\text{H}^+]$ leads to the hydrogenation of the micellar colloid calcium phosphate complex according to scheme (10) and, hence, to an increase in calcium ion concentration. As a result of $[\text{Ca}^{2+}]$ growth, balance in scheme (3) is shifted to the left, decreasing the absolute value of the additional negative charge of casein micelles q_{CAS} (according to (5)). Eventually, micelles lose both steric stabilization by means of the κ -casein macropeptide hairy layer and stabilization by means of the additional electric charge. Thus, colloid stability is lost, and an acid gel starts to form.

We are of the opinion that our model, including schemes (3), (7), and (10), makes it possible to explain the results discussed in [28], where the authors tried to understand the role of soluble and insoluble calcium in milk coagulation. As is shown above, only ionized (active) calcium is of primary importance for milk colloid stability. In this sense, only calcium hydrogenated from colloid calcium phosphate with lactic acid may be considered as "active." Meanwhile, the authors of [28] consider calcium chelated by EDTA soluble as well (Na_4EDTA could be used in [28], because it seems that it does not change milk pH).

Now we declare that the potential in our model is a function of two charges:

$$U_r = U_r(q_{CMP}) \text{ and } U_{add} = U_{add}(q_{CAS}).$$

The explicit form of these two functions is a problem for a special study. However, for semiquantitative analysis, it would perhaps be enough to put

$$\begin{aligned} U_r &\propto q_{CMP}^2, \\ U_{add} &\propto q_{CAS}^2. \end{aligned} \quad (11)$$

Probably, it is also useful to add the rennet way of q_{CMP} reduction in (9). Taking into account the exponential decrease in CMP brush density under rennet conditions (see, for example, [8]) and the fact that

$[\text{CMP}^-] + [\text{CMP}] = [\text{CMP}]_0$ is the maximum concentration of CMP hairs, one can easily get from (9):

$$q_{\text{CMP}} \propto -\frac{K_{\text{CMP}}[\text{CMP}]_0}{K_{\text{CMP}} + [\text{H}^+]} \exp(-k_{\text{CMP}} \cdot t), \quad (11)$$

Here k_{CMP} is the reaction constant for CMP proteolysis by chymosin.

Walking through similar procedure one can get from (5):

$$q_{\text{CAS}} \propto -\frac{K_{\text{CAS}}[\text{CaCAS}]_0}{K_{\text{CAS}} + [\text{Ca}^{2+}]} \exp(-k_{\text{CAS}} \cdot t), \quad (12)$$

Here $[\text{CaCAS}]_0 = [\text{CAS}^{2-}] + [\text{CaCAS}]$ is the full concentration of α - and β -casein phosphoserine groups available for calcium binding and k_{CAS} is the reaction constant for additional nonspecific proteolysis of α - and β -caseins by chymosin.

One more hypothesis in addition to the scheme described above allows explaining some features of temperature dependence for acid and rennet coagulation, as well as the similarity of heat-acid and heat-calcium milk coagulation.

Let us assume that the equilibrium of reactions (3) and (10) is shifted to the left when temperature increases. In other words, at higher temperatures, calcium forms less soluble compounds with both phosphates and caseins. Note that for reaction (10) such dependence is an established fact, while for reaction (3) this assumption is just a working hypothesis. It is based on the possible similarity of the chemical interaction of calcium with phosphate groups and phosphoserine residues of proteins.

Then, if temperature decreases, reaction (3) shifts to dissociation (i.e., K_{CAS} becomes greater) and, as a consequence, to an increase in an additional micellar charge according to expression (5). Indeed, we understand that the temperature dependence of hydrophobic interactions is the main contributor to milk colloid stability at low temperatures. In our model, it counts as the maximal depth of the adhesive well U_0 . Apparently, when temperature becomes as low as approximately 6°C , U_0 becomes so low that, even at zero U_{add} , the micelle surface remains unstuck. For this reason, rennet [29] and acid [30] coagulation of milk is impossible at low temperatures.

Temperature increase leads to a decrease in K_{CAS} and, as a consequence, to a decrease in the additional micellar charge, q_{CAS} . Therefore, the rennet coagulation time becomes shorter, and it decreases as temperature grows up to the point of enzyme inactivation. For acid coagulation, temperature growth leads to higher pH values at which coagulation begins.

Figure 6 demonstrates the results of the experiment examining the dependence of temperature at which acid milk coagulation begins on the milk pH value.

The experiment was carried out as follows. The samples of milk were adjusted to a desirable pH value

with a lactic acid solution at room temperature and then put into a warmed-up cell equipped with a thermometric viscosity gauge. As one can see in Fig. 6, the coagulation of samples with a lower pH value begins at lower temperatures. These results correspond well to the conclusions made above on the basis of our hypothesis.

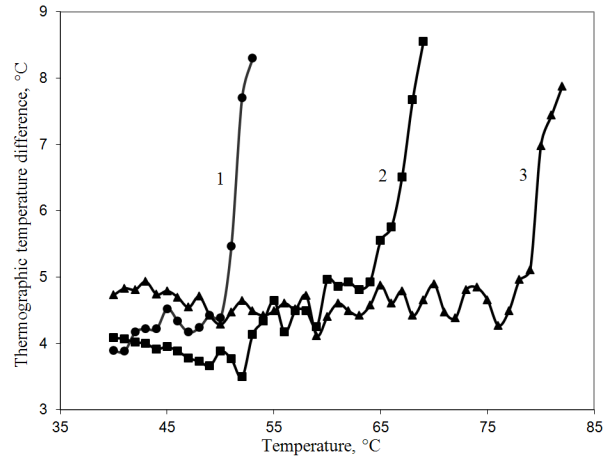


Fig. 6. Thermograms of reconstituted skim milk samples subjected to heating after acidification.

Curves: 1 – sample pH = 5.6;
2 – sample pH = 5.9;
3 – sample pH = 6.2.

Apparently, calcium hysteresis in milk, discussed, for example, in [31], may also be explained within the framework of our scheme, assuming that both the direct and reverse reaction constants in scheme (1) are essentially higher than the similar constants for reaction (10).

In addition, it is noteworthy that the developed approach, based on the analysis of the outstanding role of calcium ions in milk coagulation, can explain the amazing similarity of heat-acid and heat-calcium milk coagulation. It is well known that the addition of acid solutions or calcium chloride to milk heated up to 90 – 95°C leads to immediate coagulation. Such technologies are used for manufacturing both fresh cheeses and technical casein.

Within the described model, heat-acid and heat-calcium milk coagulation proceeds as follows. As milk is heated, the reverse reaction in (10) leads to an increase in hydrogen ion concentration and, as a consequence, to the shift of reaction (7) to the left. As a result, the charge of the κ -casein macropeptide hairy layer on the micelle surface decreases and the colloid stability of milk is determined only by the additional stabilization due to dissociated calcium caseinate. The reverse reaction in scheme (1) leads to the reduction of the additional negative charge of casein molecules, but the concentration of ionized calcium is usually insufficient for its full neutralization. Adding soluble calcium to heated milk quickly decreases the additional charge. Adding an acid solution to milk leads to the shift of reaction (5) to the right and, hence, to a quick increase in calcium ion concentration, reducing the additional casein charge. Thus, in both cases colloid

stability is completely destroyed and coagulation quickly begins.

CONCLUSION

Making use of the hypothesis of the additional electric micelle charge arising owing to the dissociation of micellar calcium caseinate, we managed to describe the outstanding role of calcium in the coagulation of milk and, moreover, to show that various kinds of milk coagulation may be represented as fundamentally very similar processes. In all cases of milk coagulation, two major factors contribute to casein colloid stability:

- steric limitation for the approach of micelles by means of a polyelectrolyte brush consisting of hydrophilic κ -casein macropeptide residues on micelle surfaces; and

- electrostatic (in the sense of the Debye layer) limitation for the approach of micelles owing to the additional electric charge arising as a result of micellar calcium caseinate dissociation.

The destruction of the polyelectrolyte brush can be made either “mechanically,” using the proteolytic cleavage of macropeptide hairs with chymosin or

“chemically,” by neutralizing the negative charge of macropeptide hairs with acid hydrogen ions and thus collapsing the polyelectrolyte brush. In the first case, one has rennet milk coagulation and in the second, acid milk coagulation.

The other stabilizing factor associated with the additional electric micelle charge operates equally under any type of milk coagulation. To decrease the additional charge, it is necessary to bring additional calcium ions to milk (that is why milk coagulation is very sensitive to calcium ion concentration in milk). Hypothetically, the additional charge may also be decreased in the way similar to renneting, i.e., due to nonspecific (or specific in another sense) proteolytic activity of chymosin directed to charged functional groups of α - and β -caseins.

Taking into account the hypothesis of the temperature dependence of calcium caseinate dissociation, we can describe the coagulation of milk and heat-acid coagulation as a high-temperature kind of acid coagulation. In addition, our model shows that heat-acid and heat-calcium milk coagulations are similar because they are based on the same principle: a quick decrease in the additional micelle charge.

REFERENCES

- 1.Fox, P.F., Guinee, T.P., Cogan, T.M., and McSweeney, P.L.H., *Fundamentals of Cheese Science*, Aspen, 2000.
- 2.Dalgleish, D.G., Casein micelles as colloids: Surface structure and stabilities, *Journal of Dairy Science*, 1998, vol. 81, pp. 3013--3017.
- 3.Horne, D.S., Casein structure, self-assembly, and gelation, *Current Opinion in Colloid and Interface Science*, 2002, vol. 7, pp. 456--461.
- 4.Dalgleish, D.G., On the structural models of bovine casein micelles – review and possible improvements, *Soft Matter*, 2011, vol. 7, pp. 2265--2272.
- 5.De Kruif, C.G., Huppertz, T., Urban, V.S., and Petukhov, A.V., Casein micelles and their internal structure, *Advances in Colloid and Interface Science*, 2012, vols. 171–172, pp. 36–52.
- 6.De Kruif, C.G. and Zhulina, E.B., κ -Casein as a polyelectrolyte brush on the surface of casein micelles, *Colloids Surfaces A*, 1996, vol. 117, pp. 151–159.
- 7.Tuinier, R. and De Kruif, C.G., Stability of casein micelles in milk, *Journal of Chemical Physics*, 2002, vol. 117, pp. 1290–1295.
- 8.De Kruif, C.G., Supra-aggregates of casein micelles as a prelude to coagulation, *Journal of Dairy Science*, 1998, vol. 81, pp. 3019--3028.
- 9.Udabage, P., McKinnon, I.R., and Augustin, M.A., Effects of mineral salts and calcium chelating agents on the gelation of renneted skim milk, *Journal of Dairy Science*, 2001, vol. 84, pp. 1569–1575.
- 10.Tsioulpas, A., Michael, J.L., and Grandison, A.S., Effect of Minerals on Casein Micelle Stability of Cows' Milk, *Journal of Dairy Research*, 2007, vol. 74, pp. 167–173.
- 11.Osintsev, A.M., Bakhtin, N.A., Braginsky, V.I., and Ivanenko, O.V., Termograficheskiy metod issledovaniya koagulyatsii moloka (Thermographic method of investigation of milk coagulation), *Syrodelie i maslodolie (Cheese making and butter making)*, 2005, no. 5, pp. 20--21.
- 12.Hori, T., Objective measurements of the process of curd formation during rennet treatment of milks by the hot wire method, *Journal of Food Science*, 1985, vol. 50, pp. 911--917.
- 13.Osintsev, A.M., Braginsky, V.I., Lapshakova, O.Yu., and Chebotarev, A.L., Rol' ionov kaltsiya v kolloidnoi stabil'nosti mitsell kazeina (The role of calcium ions in the colloid stability of casein micelles), *Tekhnika i tekhnologiya pishchevykh proizvodstv (Technique and technology of food production)*, 2009, no. 1, pp. 63--67.
- 14.Dalgleish, D.G. and Parker, T.G., Binding of calcium ions to bovine α_{s1} -casein and precipitability of the protein-calcium ion complexes, *Journal of Dairy Research*, 1980, vol. 47, pp. 113--122.
- 15.Parker, T.G. and Dalgleish, D.G., Binding of calcium ions to bovine β -casein, *Journal of Dairy Research*, 1981, vol. 48, pp. 71--76.
- 16.Wahlgren, N.M., Dejmek, P., and Drakenberg, T., Binding of Mg^{2+} and Ca^{2+} to β -casein A¹: a multi-nuclear magnetic resonance study, *Journal of Dairy Research*, 1993, vol. 60, pp. 65--78.
- 17.Grimley, H.J., Grandison, A.S., and Lewis, M.J., The effect of calcium removal from milk on casein micelle stability and structure, *Milchwissenschaft*, 2010, vol. 65, pp. 151--154.

18. Philippe, M., Gaucheron, F., Le Graet, Y., Michel, F., and Garem, A., Physicochemical characterization of calcium-supplemented skim milk, *Lait*, 2003, vol. 83, pp. 45--59.
19. Vasbinder, A.J., Rollema, H.S., and De Kruif, C.G., Impaired rennetability of heated milk; study of enzymatic hydrolysis and gelation kinetics, *Journal of Dairy Science*, 2003, vol. 86, pp. 1548--1555.
20. Sandra, S., Ho, M., Alexander, M., and Corredig, M., Effect of soluble calcium on the renneting properties of casein micelles as measured by rheology and diffusing wave spectroscopy, *Journal of Dairy Science*, 2012, vol. 95, pp. 75--82.
21. McSweeney, P.L., Olson, N.F., Fox, P.F., Healy, A., and Hojrup, P., Proteolytic specificity of chymosin on bovine alpha s1-casein, *Journal of Dairy Research*, 1993, vol. 60, pp. 401--412.
22. McSweeney, P.L.H., Fox, P.F., and Olson, N.F., Proteolysis of bovine caseins by cathepsin D: Preliminary observations and comparison with chymosin, *International Dairy Journal*, 1995, vol. 5, pp. 321--336.
23. Hynes, E.R., Aparo, L., and Candiotti, M.C., Influence of residual milk-clotting enzyme on κ_{s1} casein hydrolysis during ripening of Reggianito Argentino cheese, *Journal of Dairy Science*, 2004, vol. 87, pp. 565--573.
24. Holt, C. and Horne, D.S., The hairy casein micelle: Evolution of the concept and its implications for dairy technology, *Netherlands Milk and Dairy Journal*, 1996, vol. 50, pp. 85--111.
25. McMahon, D.J. and McManus, W.R., Rethinking casein micelle structure using electron microscopy, *Journal of Dairy Science*, 1998, vol. 81, pp. 2985--2993.
26. Dalglish, D.G., Spagnuolo, P.A., and Goff, H.D., A possible structure of the casein micelle based on high-resolution field-emission scanning electron microscopy, *International Dairy Journal*, 2004, vol. 14, pp. 1025--1031.
27. Lencki, R.W., Evidence for fibril-like structure in bovine casein micelles, *Journal of Dairy Science*, 2007, vol. 90, pp. 75--89.
28. Choi, J., Horne, D.S. and Lucey, J.A., Effect of insoluble calcium concentration on rennet coagulation properties of milk, *Journal of Dairy Science*, 2007, vol. 90, pp. 2612--2623.
29. O'Sullivan, M.M., Kelly, A.L., and Fox, P.F., Influence of transglutaminase treatment on some physico-chemical properties of milk, *Journal of Dairy Research*, 2002, vol. 69, pp. 433--442.
30. Vasbinder, A.J., Rollema, H.S., Bot, A., and De Kruif, C.G., Gelation mechanism of milk as influenced by temperature and pH; studied by the use of transglutaminase cross-linked casein micelles, *Journal of Dairy Science*, 2000, vol. 86, pp. 1556--1563.
31. Canabady-Rochelle, L.S., Sanchez, C., Mellema, M., Bot, A., Desobry, S., and Banon, S., Influence of calcium salt supplementation on calcium equilibrium in skim milk during pH cycle, *Journal of Dairy Science*, 2007, vol. 90, pp. 2155--2162.



UDC 664.68/664.6: 665.1
DOI 10.12737/1513

ON THE ROLE OF FATS IN BAKED FLOUR GOODS

T. V. Renzyaeva

Kemerovo Institute of Food Science and Technology,
bul'v. Stroitelei 47, Kemerovo, 650056 Russia
phone:/Fax: +7 (3842) 39-68-59, e-mail: ren-tamara@mail.ru

(Received February 11, 2013; Accepted in revised form April 25, 2013)

Abstract: The role of fats in developing the structure of dough and baked bread goods and pastries is considered. Criteria of choosing fatty materials by their nutritional value and physical state for obtaining safe and quality products are presented. A method of producing pastries with liquid vegetable oils and natural biopolymer-based stabilizing food additives is proposed.

Key words: fats, oils, dough, baked flour goods, food additives.

Flour goods are a wide-range group of flour-based products, different in their recipe composition, production technology, and consumer attributes. Baked bread goods are bread, buns, pies, and doughnuts. Pastries include cookies, hardtacks, crackers, gingerbread goods, wafers, fruitcakes, jelly and cream rolls, small cakes, cakes, Oriental sweets, etc. They are characterized by high gustatory qualities, a pleasing appearance, and convenience in consumption and storage.

Pastries and baked bread goods are a weighty group of mass consumption foods, which enjoy persistent and stable demand. Their variety is ensured by variations in the quality and relation of recipe components, as well as by the diversity of technological methods, regimes, and equipment. At the same time, there are common features characteristic of flour baked goods, such as the use of the same raw materials (flour, sugar, fats, etc.), analogous semiprepared goods (emulsion, dough, baked semiprepared products, etc.), and similar technological operations (kneading, baking, etc.).

The raw components that form a complex system during the preparation and structure development of flour baked goods play the decisive role in the formation of their consumer attributes. Their relation is determined by the recipe—the aggregate of critical and additional raw materials. The critical raw materials in the production of pastries are flour, sugar, and fats, while those used in the production of bread goods are flour, yeast, salt, and water. In addition, the recipes include a large list of other raw materials, such as dairy products, egg products, fruit and berry products, leavening agents, flavorings, and so on.

Depending on the formula, the quality of the critical and additional raw materials, and technological methods and regimes, one gets dough with various structural and mechanical properties, which, after baking, yield products with different textures. In other words, the diversity of baked flour goods is mainly determined by the development of different types of dough. Each

dough type is prepared under strictly established relations of recipe components and the observance of the technology that ensures obtaining a product with specified properties.

The majority of baked flour goods and their semiprepared products are multicomponent disperse systems, in which particles of the disperse phase are distributed in a dispersion medium of a complex composition. They are characterized by a high concentration of the disperse phase in dispersion media and a strongly developed interphase surface. The properties of such disperse systems are determined primarily by surface phenomena at interphase boundaries, such as processes occurring at interfaces: moistening, adsorption, adhesion, and others. Spatial structures emerge in the systems, whose type is determined by the type of contacts between particles of the disperse phase and the composition of the dispersion medium.

A large number of works study how dough is formed from wheat flour [1--5]. The best studied is the development of bread-baking dough. Mechanisms of developing different types of pastry dough are less studied. This is due both to the diversity of dough types and raw components and to different conditions of their interaction. Fats, along with flour and sugar, are important ingredients of pastry dough, which affect its structural and mechanical properties and the texture of products. The properties of fats are very complicated and diverse.

This paper gives an analysis of hypotheses about the role of fats in developing the structure of dough and baked flour goods, aimed at elaborating a pastry production technology involving liquid vegetable oils for obtaining safe and competitive goods.

Fats in pastry production are critical raw materials. Fat is quantitatively the third component in recipes after flour and sugar and is the most expensive one. Despite the fact that pastries are not essential foods, they are traditionally in high demand. Pastries are

characterized by high food energy and low nutritional value. This is determined by the fact that their composition includes many lipids and carbohydrates and few vitamins, macro- and microelements, proteins, food fibers, and so on.

Today's healthy diet vogue affects the development of the pastry market. Buyers are becoming fastidious and pay increasingly more attention to the quality composition of the foods that they consume. At present, the assortment of pastries is widening due to the creation of new low-calorie and high-nutrition products. This problem can be solved through the development of innovative technologies and the use of nontraditional types of raw materials, which make it possible to decrease the weight fraction of sugar and fat, to increase their nutritional value, and to enrich the products with physiologically functional food ingredients.

At present, much attention is paid to the choice of fats for baked goods. The criteria for choosing fatty products are their physicochemical and organoleptic properties, resistance to oxidative spoilage, nutritional value, and safety, especially with regard to the content of saturated fatty acids and transisomers of fatty acids.

The nutritional value of fats is determined by their fatty-acid composition and the presence of accompanying compounds. The recipe formulas of baked goods usually employ margarines and specialized fats that include solid fats obtained through the hydrogenation of vegetable oils. However, such fats contain considerable amounts of saturated fatty acids and fatty acid transisomers. In addition, food additives with a limited acceptable consumption level, such as preservation agents, stabilizers, emulsifiers, and flavorings, are often introduced in the composition of fats for baking.

The World Health Organization has established that eating foods containing many saturated fatty acids and fatty acid transisomers has an adverse effect on the human organism. There exists the opinion that transisomers, as well as saturated fatty acids, are digested by the human organism worse than unsaturated ones, decrease its resistance to oncological diseases, increase the risk of diabetes, and lead to cardiovascular disorders [6, 7].

At present, we witness the trend toward decreasing the content of saturated fatty acids and fatty acid transisomers in all foods. For example, the US Institute of Health stated the necessity to achieve the zero consumption of transisomers with a simultaneous decrease in the dose of saturated fatty acids in developing healthy diets [7, 8]. In Russia, the level of transisomers (no more than 8%) is limited only in the production of spreads and margarines for retailing.

Many researchers have studied the technological role of fatty products in pastry production [3--5, 9--15]. It is shown that not only the chemical composition of fat but also its physical state is significant in the development of the necessary structure of dough and baked goods. To prepare pastry dough, it is recommended using solid fats (butter, margarine, specialized fats, palm oil, and others), which are introduced into dough in a melted and plasticized state.

Flour plays the leading role in dough development. Pastry production uses wheat flour, from which cohesive dough is obtained due to the ability of its proteins to form gluten. Other types of flour are rarely used, but today increasingly more attention is paid to improving the nutritional value of flour goods; in this context, the assortment of goods made of various types of flour from cereals, legumes, and oilseeds is widening.

Rheological properties of dough are primarily determined by the ability of flour hydrophilic colloids to bind water under definite moistening. Water molecules not only interact with such colloids on the surface but also penetrate deep into them, which makes them swell. The formation of a desired dough structure is connected with the directed effect on the mechanism of interaction between recipe components, which form a complicated system, where each of them plays a definite role. The most important point for the formation of desired dough properties and consumer attributes of flour goods is to forecast the behavior of flour under its interaction with water, fats, and sugar solutions at temperatures and pH values corresponding to the conditions of making dough and baked products.

During dough kneading, water and fat compete in their interaction with flour particles and other components. The structural and mechanical properties of dough are ultimately determined by the relation and properties of high-molecular hydrophilic polymers (proteins, starch, gluten, pectins, etc.) and low-molecular hydrophilic and hydrophobic compounds (sugars, fats, and amino acids). The structure of dough is influenced by the chemical composition and the strength of contact interaction between its ingredients. The recipe formula of each type of flour products should represent an optimal set of components able to form desired structural and mechanical dough properties because any deviations affect the texture and quality of baked semiprepared and fully prepared products.

Water interacts with the flour protein, forming gluten as a bound extensible structure. If flour is covered with fat, this chain is interrupted, and, after baking, the product turns to be crisper and less hard. If the content of fat is high, little water is needed to obtain the desired consistency, gluten formation, swelling, and starch gelatinization being limited. Such dough is easily torn under stretching, weakly bound, and plastic. In addition, with a high content of sugar, fat hinders the transformation of sugar syrups into a hard amorphous mass under cooling. Fatty products make flour products soft and add delicate flavor to them owing to better dough aeration and the lubricating effect in the mouth [3, 4, 15].

During the development of the desired dough properties and structure of baked products, not only the chemical composition of fat but also its physical state is important. Important technological characteristics of fats used for baking are the content of dry substances, melting and congelation temperatures, firmness, and the number and size of solid-phase crystals at different stages of the process of making and storing flour products.

The content of the solid phase in fatty products is determined by the fat's melting and congelation

temperatures and by the ambient temperature, and the conditions under which fat transforms from the liquid state into the solid one affect the size of its crystals. If fats are cooled in the static state, a firm mass consisting of large crystals is formed. Large fat crystals can gather into conglomerates; as a result, the mass is perceived as more solid than that with fine crystals. Under the subsequent mixing, large crystals are destroyed and the mass becomes much softer and more plastic. A fat with fine crystals is called plasticized and is a mixture of solid and liquid phases in a definite relation.

Fats are mixtures rather than pure compounds and, hence, have no clear melting characteristics. The melting and congelation temperatures of different fat triglycerides do not coincide, which is determined by the presence of several crystal modifications. The more diverse the set of fatty acids in a fatty product, the wider the melting temperature range is. Melting characteristics of fatty products can be established through determining the amount of the solid fat fraction (solid fat index) at different temperatures. In this context, there is the notion of the slip melting point--the temperature range in which fat is liquid with a certain amount of the solid phase.

In choosing fatty products for flour goods, it is necessary to account for their solid indices at the following temperatures: ambient temperature (it affects the firmness of ready products), the temperature of technological operations with the use of fat (it affects the consistency of fat when it binds with other dough ingredients), semiprepared product temperature (it determines the state of fat under the formation of dough pieces and baked semiprepared products), and human body temperature (it determines how much fat will melt in the mouth during eating and, respectively, how much solid fat can give a waxy flavor to the product).

Despite the wide diversity of fats, dough types, flour products, and technological methods of making them, there are few hypotheses on the role of fats in the development of the properties of different dough types and the structure of flour products, which, basically, supplement one another and are applicable to different types of flour products.

The traditional view on the role of fats in the kneading of pastry dough is that they are distributed in the form of films among flour particles; are adsorbed by the surface of protein molecules and starch grains; block hydrophilic groups, hindering their interaction with water; prevent the swelling of flour colloids; and increase the content of the dough liquid phase. Fats tear secondary protein bindings, penetrate between macromolecules, and block active centers. As a result, the binding between flour particles becomes weaker, the continuity of gluten and starch is violated, and dough acquires plastic properties. The thinner the fat films and the larger their number in dough, the more porous and crisper the structure of ready products is [3, 4, 14, 15].

Obviously, fats in the liquid state are better distributed over the dough volume. Hence, in a number of technologies of pastry preparation, it is recommended introducing fats in dough in the melted state in the form of a well-dispersed emulsion. In this state, during dough kneading, fat particles are more uniformly distributed

between flour particles and, during dough piece baking, favor the formation of the laminated structure of the products. In the technology of making sugar and dry cookies and crackers, it is recommended adding fat in the melted state. However, adverse effects are possible in this case due to overheating during the melting of solid fat. This can increase the temperature of the dough, affect its structure, and cause a premature reaction of the leavening agent.

Interaction of fats with dough components largely depends on the chemical composition and properties of a fat in question. For example, glycolipids play the role of structural lipids: they participate in the construction of cellular membranes and in the formation of gluten, which determines the baking quality of flour. As is known, fats can change the structure of protein particles by interacting with different chemical groups of protein macromolecules or through adsorption on the surface of protein molecules. Under dough kneading, fats change the properties of starch as a result of the formation of complexes with an amylase fraction. Some lipid molecules turn to be closed in the amylase helix, while others form a film on the surface of starch particles. An important role in this respect is played by saturated and unsaturated fatty acids in fat composition. It is noted that unsaturated fatty acids interact with flour biopolymers to a greater extent than saturated ones [1, 2].

In studying the influence of fats on baking dough properties and dough quality, it has been established that fat substantially affects the rheological properties of gluten and dough and the quality of bread. As is established, the more unsaturated fatty acids in a fat, the more complex compounds with proteins it forms, which makes gluten more elastic, decreases dough viscosity and adhesiveness, increases dough gas retaining ability, improves the structure of the crumb, and increases the specific weight of bread [2, 11, 16]. This action of fat is more expressed in bread-baking and pastry dough with a low fat content.

Under a long maturation of bread semiprepared products, fat is subjected to hydrolytic splitting, which leads to the accumulation of free fatty acids, di- and monoglycerides, polar lipids, peroxides, and hydroperoxides, which interact with structural components of flour. This improves the rheological properties of dough and the quality of baked goods [17].

During baking, fats participate in the formation of the leavening structure and texture of the goods. The composition and properties of fat affect the aeration level and rise of dough pieces during baking. For example, S.P. Cauvain [5] stresses the importance of adding fat or an emulsifier to dough to reach the desired porosity of baked products. It is noted that fat ensures a high gas retaining ability, affecting positively the size and stability of gas bubbles. It is stated that the stabilizing action on gas bubbles can be produced by the solid part of fat. The crystals of the solid part of fat align at the boundary of a gas bubble and the liquid phase of the dough and affect both the size and stability of gas bubbles. As dough temperature rises, some fat crystals melt and lose their ability to stabilize gas bubbles. Ultimately, all fat is melted, and the stability of

the gas bubbles is maintained by other components, namely, gelatinized starch and gluten denatured protein.

Therefore, the role of fat at the initial stages of baking is retaining gas bubbles in dough and preventing their coalescence. As dough is heated in the oven, its structure cannot restrict the dilatation of gas bubbles, and individual bubbles increase, coalesce, and get destroyed. All this makes dough settle down. As the dough temperature in the oven grows, solid fat becomes liquid and air bubbles tend to emerge from the dough and to come to the top. The longer the bubbles are retained in the dough, the larger the volume of the products. The author concludes that fat should have a high melting point. However, to ensure the effectiveness of solid fats, it is important to ensure their uniform distribution in dough, which is difficult to attain if at least a part of the fat is not liquid.

Other works [9, 10, 15, 18, 20] also note that fats restrict gas diffusion through pore walls at the initial stage of baking at temperatures of 38--58°C, when the dough becomes softer before the stage of absorbing water by starch grains. The stabilization of pores leads to a more stable volume and a thinner texture of baked products. The necessity to use solid fats in dough is substantiated as follows: during baking, solid fat crystals are separated from the liquid phase and are covered with a protein membrane. This membrane allows a large amount of solid phase crystals of a fatty product to attach to air bubbles. In the course of baking, fat crystals melt, and the protein membrane unites with the surface of the bubbles as they extend, increasing extension resistance. It is assumed that the greater the number of fine crystals in fat, the higher is the efficiency of this process under baking. This mechanism can explain the formation of a dough texture containing a plasticized fat with hard crystals.

Fat also affects the size and stability of air bubbles in beaten pastry dough before baking and at initial baking stages [14, 15, 19]. The main function of fat in baking products from beaten dough is to aerate dough during kneading. Beaten dough is foam in which air bubbles are retained in the liquid phase and are separated from each other by a thin film of a stabilizing agent. This stabilization is especially important at initial baking stages, when the rise in temperature increases the tendency to the rise of air bubbles. Later, in the course of baking, as proteins denature, starch gelatinizes, and moisture evaporates, the walls of the bubbles gradually become stronger, the foam begins to harden, and the gas bubbles burst and come out of the cavities, forming a spongy structure, in which individual cells are interconnected, allowing gases and liquids to pass through it.

The moment when the liquid dough foam transforms into a "sponge" is largely determined by the recipe, while the stability of air bubbles under a temperature increase significantly affects the porosity and volume of the product. Protective films that are formed around the gas bubbles can be of different origin, including the participation of fat in their formation. To maintain the stability of air bubbles during baking, it is recommended, prior to the transformation of foam into a biscuit, adding emulsifiers in amounts sufficient for this.

The mobility of fats in products depends on the content of the liquid fraction at a given temperature because, under the action of gravity, liquid fat can go down. The dripping of fat can also depend on the product's storage temperature. The higher the storage temperature, the larger the liquid phase in this fat is and, hence, the higher is the risk of fat dripping and oiling the packing.

In baking laminated dough products [5, 15, 19], dough layers are affected by forces that spread them, which considerably increases the volume of the products. Pressure is created by bubbles of steam or gas exhaling under the use of baking powder or yeast. When gas bubbles enlarge, fat acts as a barrier for their movement and the dough layers are spread. To obtain a maximal volume, it is important to preserve fatty layers as long as possible; hence, it is recommended cooling the fat to 12--13°C before lamination to increase the share of its solid phase. The rise of laminated dough products depends on the following characteristics of fat: the amount of fat added (the larger the amount, the higher the rise is), the content of solid fat (the higher the content, the higher the rise is), the solidity of fat (the higher the solidity, the higher the rise is), and the size of crystals (the smaller the size, the higher the rise is).

Despite the better rise of baked products under a high content of solid fats, their organoleptic properties can worsen because fats with a low melting temperature create the impression of "greasiness" and an unpleasant feeling of an envelope in the mouth. Hence, importantly, the content of solid fat should not be too high.

The importance of the uniform distribution of recipe components in pastes for improving the quality of semiprepared and prepared products is stressed in many works [3, 4, 18]. When using fat in the solid form, one can have problems associated with its uniform distribution in dough. For example, to improve the organoleptic properties of biscuits, it is recommended using melted fats heated up to transition to the liquid state. It is emphasized that adding solid fat is an option, but the volume and texture of products will be worse.

The aforementioned statements concerning the role, composition, and physical state of fat during dough preparation and dough piece baking are applicable only to some types of flour products. For example, the supposition that it is advisable to introduce fats in the plasticized fine-crystalline state is applicable to pastry dough with a high fat content. The opinion that it is recommended introducing fats in the melted form together with a well-dispersed emulsion is more applicable to plastic dough with a lower content of fat.

Hypotheses about the role of fat in the production of baked flour goods mainly come down to the following. Liquid fats, as a result of their better distribution and interaction with recipe components, favor the formation of the necessary structural--mechanical properties of dough and the texture of the organoleptic properties of products. Solid fats play the role of a stabilizing structure primarily at the initial stage of baking and during storage.

However, the above hypotheses cannot embrace the entire diversity of dough types and explain the role of fats in the formation of ready products' properties. For

example, melted fats are used to knead dough for sugar and dry cookies, crackers, and gingerbreads. The temperature and duration of the stages preceding baking cannot create conditions for the crystallization of fats. Obviously, fat in a dough piece at the baking stage is liquid. Fat crystals can form only after cooling during storage, which makes the products harder.

Noteworthy is also the hypothesis about the role of unsaturated fatty acids in forming bread dough [2, 11, 16]. It is stressed that they can form complex compounds with proteins, which increases the ability of gluten films to spread without tearing under the pressure of the growing gas bubbles. The elasticity of gluten and the retaining ability of dough increase, the crumb structure improves, and the bread specific volume grows. Evidently, this action of fat is more expressed in bread and pastry dough with a low fat content.

Ultimately, the structural--mechanical properties of any dough are determined by the relation and properties of high-molecular hydrophilic polymers (proteins, starch, dietary fiber, and pectins) and low-molecular hydrophilic and hydrophobic compounds (sugars, fats, and amino acids). In other words, the structure of dough is determined by its chemical structure, the strength of contact interaction between its components, and process parameters. An optimum of these indicators should exist for each product, because both their decrease and increase will affect the ability of dough to form and the quality of baked products.

Note that many studies are dedicated to the elaboration of fatty products for flour goods. These developments are mainly aimed at creating specialized fats for baking (shortenings). Such fats are obtained by mixing fats with oils, flavorings, emulsifiers, stabilizers, and preservation agents with the subsequent cooling and packing. The necessary hardness is reached through a definite relation of solid and liquid fractions of fats. Many shortenings have specific properties that make them fit for individual products, for example, for baking cakes, cookies, or crackers.

The need for the use of specialized fatty products is determined by the fact that they make it possible to increase the production performance and ensure the stable quality of products. However, the problem of using fats is associated with their high cost, and their positive effect is often brought to naught due to an increase in price. In addition, little attention is paid to the nutritional and biological value of such fats.

In the mid-1990s, increasingly more palm oil began to appear in the Russian market. Taking into account its low cost, many fabricators began to use it for kneading dough. However, the use of palm oil in the dough composition has elucidated a number of its drawbacks. Palm oil contains a large quantity of solid triglycerides and saturated fatty acids, which make cookies harder during storage as the oil is crystallized. During storage, on the surface of cookies with palm oil, fat bloom can appear as a result of the formation of large crystals under temperature fluctuation. In addition, since recently, palm oil prices have been growing, and fabricators have to look for an alternative [7].

A universally available type of fatty products is liquid vegetable oils. Owing to the presence of a large

amount of unsaturated fatty acids, including the essential polyunsaturated fatty acids of the ω -3 family, and the high content of tocopherols, phospholipids, and carotenoids, liquid vegetable oils have a high nutritional value, are characterized by a long shelf life and low cost, and are convenient in storage, dosing, and use [8, 12]. However, the use of liquid vegetable oils for the production of pastries is limited because they are badly retained by products and show up during production and storage. This is why it is necessary to develop technological solutions that could stabilize the structure of dough and products by binding and retaining liquid oil.

To stabilize nutritional systems with liquid vegetable oils, the food industry widely employs stabilizing food additives based on high-molecular compounds, such as proteins and polysaccharides. At present, popular are food additives designed to ensure aggregate stability and/or to maintain a uniform consistency of two or more immiscible ingredients. They include thickeners, gelatinizing agents, bulking agents, and moisture retention agents [21].

Stabilizing food additives also affect the shelf life of foods because they bind water, which delays drying, hinders the development and reproduction of undesirable microorganisms, and slows down the oxidative spoilage of fats.

To form and stabilize the consistency, food technology often uses complex natural hydro-colloid polymer-based stabilizers with a wide range of functional--technological properties. The use of complex additives makes it possible to broaden the spectrum of their technological properties and favors the emergence of synergism. Each of the ingredients in stabilizing systems specifically affects the consistency, structure, outer appearance, taste perception, and stability of goods during production and storage.

The set of ingredients for mixtures of stabilizing additives changes depending on the composition, expected results, and cost. For example, the stabilizing function of polysaccharides is largely determined by interaction with the partner--protein. The protein--polysaccharide complex is present in many foods, and studying its properties and behavior in technological processes is one of the most important aspects of food science. Widely used for stabilizing the structure of foods are stabilizing systems based on natural high-molecular hydrocolloids, such as gums, modified starches, food fibers, and protein preparations. Natural stabilizers are also used in developing special and functional foods.

To increase the effectiveness of liquid vegetable oils and stabilizing food additives in pastry production, new technological solutions are necessary, making it possible to regulate the properties of semiprepared and prepared products for increasing stability, including the baking stage. This should be substantiated by the functional and technological properties of raw materials, by dosing, and by methods of introducing recipe components.

In developing a method of fabricating cookies, implying the replacement of solid-consistency fat by liquid vegetable oil to stabilize the structure of dough

and the quality of products, we used a complex food additive based of xanthan and guar gums, dietary fiber preparations, and a soybean protein isolate. All the components are on the list of food components and additives that have no adverse effect on human health when using them for food fabrication.

These food additives were chosen proceeding from studies on their functional-technological properties [22]. Preparations based on xanthan and guar gums have a high water-retaining ability, fat-emulsifying ability, and stability of emulsions; wheat gluten has a high water- and fat-retaining ability; and the soybean protein isolate has a good fat-emulsifying ability and a high stability of emulsions. The presence of the above properties makes it possible to suggest reaching the necessary stabilizing action in introducing these food additives to the composition of dough with liquid vegetable oil.

It was established in the course of our studies that the production of cookies with liquid vegetable oil implies not only a change in the traditional set of recipe components but also an increase in the moisture content of dough. Changing solid fat for liquid vegetable oil and introducing a stabilizing food additive make it possible to increase the dough moisture content by 1.5--2% and to decrease the share of fat in the recipe by 15--20% without changing the structural--mechanical properties of dough and the traditional consumer attributes of the cookies [23].

The studies have made it possible to propose an innovative method of preparing cookies with liquid vegetable oils and stabilizing natural high-molecular biopolymer-based food additives [24]. The main technological stages are preparing the recipe mixture by mixing all components except for flour and the fat phase (see figure), obtaining the fat phase from liquid vegetable oil and the complex of stabilizing food additives, and preparing a fat--flour mixture from flour and the fat phase. Dough is kneaded from the recipe and fat--flour mixtures, after which it is formed, baked, and cooled.

Preparing the fat phase from the mixture of liquid vegetable oil and the complex stabilizing additive creates conditions for a better distribution of the additive and a fuller interaction of its components with the oil. Mixing flour with the fat phase makes it possible

to create conditions for a better interaction of hydrophobic groups of flour high-molecular compounds with oil and the absorption of oil by the surface of solid particles to increase the stability of dough and product properties and to decrease the migration of oil from goods during production and storage.

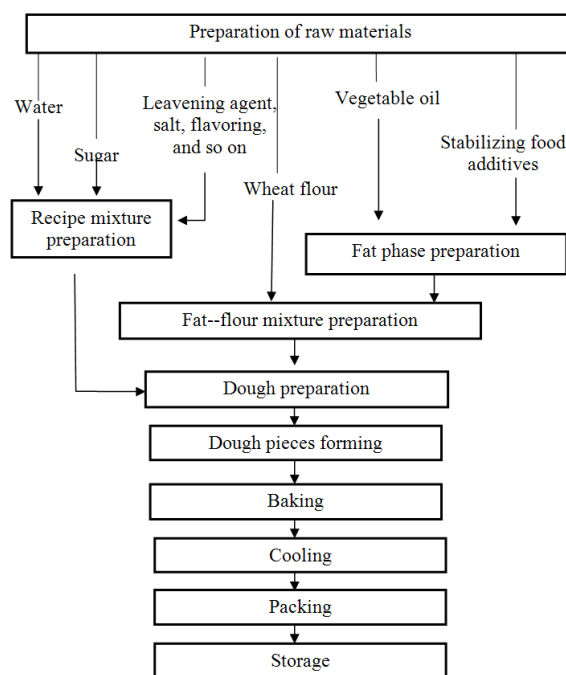


Figure Flow diagram of the production of cookies using liquid vegetable oils.

Our studies show that introducing liquid vegetable oils to pastry requires the use of stabilizing food additives and technological methods making it possible to effectively emulsify, bind, and retain liquid vegetable oil and, thus, to stabilize the structure of dough and the quality of products. The use of this technology of fabricating flour pastries with the use of raw materials containing physiologically functional ingredients makes it possible not only to obtain high-quality products but also to increase their nutritional value under the simultaneous decrease in food energy.

REFERENCES

- 1.Koz'mina, N.P., Biokhimiya khlebopecheniya (Breadmaking Biochemistry, Moscow: Pishchevaya Promyshlennost', 1971.
- 2.Puchkova, L.I., Zhiry v khlebopechenii: obzornaya informatsiya (Fats in Bread Baking: Overview), Moscow: TsNIITEN, 1976.
- 3.Zubchenko, A.V., Fiziko-khimicheskie osnovy tekhnologii konditerskikh izdelii (Physicochemical Basics of Pastry Technology), Voronezh: Voronezh. gos. tekhnol. Akad., 1997.
- 4.Matz, S.A., Matz, T.D., Cookie and Cracker Technology, 2nd ed., Westport (Conn.): AVI, 1978.
- 5.Cauvain, S. and Young, L., Baking Problems Solved, Cambridge: Woodhead, 2001; Moscow: Professiya, 2006.
- 6.Kulakova, S.N., Viktorova, E.V., and Levachev, M.M., Trans-izomery zhirnykh kislot v pishchevykh produktakh (Transisomers of fatty acids in food products), Masla i zhiry: spetsializirovannyi informatsionnyi byulleten' (Oils and fats: A specialized information bulletin), 2008, no. 3, pp. 11--14.
- 7.Sandram, K., Zameshchenie zhirnykh kislot, soderzhashchikh transizomery: ispol'zovanie pal'movogo masla kak al'ternativnogo istochnika zhirov v SShA (Replacing fatty acids containing transisomers: Using palm oil as an

- alternative source of fats in the United States), *Maslozhirovaya promyshlennost'* (Oil and fat industry), 2006, no. 1, pp. 24 – 26.
8. Jean, T, Omega-3, act II. http://baking-management.com/healthy_baking/omega3-act2-0611
9. Brooker, B.E., The role of fat in the stabilization of gas cells in bread dough, *Journal of Cereal Science*, 1996, Vol. 24. no. 3, pp. 187--198.
10. Podmore, J., Baking fats, in *The Technology of Cake Making*, Ed. by A.J. Bent, London: Blackie Academic and Professional, 1997, pp. 25--47.
11. Dremucheva, G.F., *Zhirovye produkty dlya khlebobulochnykh i muchnykh kon-diterskikh izdelii* (Fat products for baked and flour pastries), *Khleboprodukty* (Bread products), 2002, no. 8.
12. Nechaev, A.P. and Kovalenok, A.V., Optimizatsiya zhirnokislotochnogo sostava muchnykh konditerskikh izdelii (Optimizing the fatty acid composition of flour pastries), *Kon-diterskoe proizvodstvo* (Confectionary), 2006, no. 5, p.10.
13. Vas'kina, V. and Vainshenker, T., Vliyanie rastitel'nykh zhirov na kachestvo pechen'ya (The effect of vegetable fats on baking quality), *Khleboprodukty* (Bread products), 2007, no. 12, pp. 56--57; 2008, no. 1, p. 62.
14. Jill, I., How Do Different Fats Affect Baking? <http://www.madsci.org/posts/archives/1999-12/946517625.Ch.r.html>
15. Stauffer, C.E., *Fats and Oils in Bakery Product*.
shttp://uqu.edu.sa/files2/tiny_mce/plugins/filemanager/files/4281709/84607_54.pdf
16. Konova, N.I. and Renzyaeva, T.V., Vliyanie zhidkikh rastitel'nykh masel na kachestvo khleba iz pshenichnoi muki (The effect of liquid vegetable oils on the quality of wheat-flour bread), *Konditerskoe i khlebopekarnoe proizvodstvo: spetsializirovannyi buylleten'* (Confectionary and bread baking: A specialized bulletin), 2010, no. 7--8, pp. 28--30.
17. Polandova, R.D., Kozyukina, O.Yu., and Erkinbaeva, R.E., *Tekhnologii klebobu-lochnykh izdelii s udlinennymi srokami khraneniya* (Bakery technologies with extended shelf life), *Khlebopechenie Rossii* (Russia's bread baking), 2001, no. 5, pp. 16--17.
18. Manley, D., *Biscuit, Cracker and Cookie Recipes for the Food Industry*, Cam-bridge: Woodhead, 2001; St. Petersburg: Professiya, 2003.
19. Cauvain, S.P., *Breadmaking processes in Technology of Breadmaking*, Ed. by Cauvain, S.P. and Young, L.S., London: Blackie Academic and Professional, 1998, P. 18 - 44.
20. Ingredient Spotlight: How Fats are Used in Baking. <http://www.completelydelicious.com/2012/02/ingredient-spotlight-how-fats-are-used-in-baking.html>
21. Sarafanova, L.A., *Pishchevye dobavki: entsiklopediya* (Food Additives: An Encyclopedia), St. Petersburg: GIOR, 2003.
22. Renzyaeva, T.V., and Poznyakovskii, V.M., *Vzaimodeistvie sypuchego syr'ya i pishchevykh dobavok s rastitel'nykh maslom* (Interaction of free-running raw materials and food additives with vegetable oil), *Khranenie i pererabotka sel'khozcyr'ya* (Storage and processing of agricultural raw materials), 2009, no. 7, pp. 14--17.
23. Renzyaeva, T.V., Dmitrieva, E.V., and Merman, A.D., *Tekhnologiya proizvodstva pechen'ya s zhidkimi rastitel'nykh maslami* (Cookie technology using liquid vegetable oils), *Konditerskoe Proizvodstvo* (Confectionary), 2012, no. 1, pp. 16--19.
24. Renzyaeva, T.V. and Merman, A.D., RF Patent No. 2459415, *Byull. izobret.* 2012, No. 24.



UDC 637.147.2
DOI 10.12737/1514

METHOD OF OBTAINING MICROPARTICULATED CASEIN AND THE POSSIBILITY OF ITS APPLICATION IN THE PRODUCTION OF NONFAT FERMENTED MILK PRODUCTS

I.A. Smirnova, I.V. Romanovskaya, V.K. Shtrigul

Kemerovo Institute of Food Science and Technology,
bul'v. Stroitelei 47, Kemerovo, 650056 Russia
phone:/Fax: +7 (3842) 39-68-58, e-mail: milk@kemtipp.ru

(Received February 12, 2013; Accepted in revised form April 03, 2013)

Abstract: Reducing the calorie content of everyday food, including dairy beverages, is among the key recommendations of present-day dietitians. However, fat reduction worsens the organoleptically evaluated texture and flavor score of food. The organoleptic correction of nonfat products using fat simulants often needs additional financial inputs. Furthermore, fat simulants added to the product can be hazardous to human health.

Taking into consideration these facts, we have developed a casein microparticulation technology and have investigated the possibility of employing microparticulated casein in the production of nonfat fermented dairy beverages. Unlike the existing milk protein microparticulation technologies, the technology presented here uses casein in place of whey protein, which is difficult to produce and, as a consequence, expensive. A casein coagulation method has been devised, and the optimal processing parameters have been determined. A technology for producing nonfat lapper milk from skim milk has been developed. The new product has the same texture and flavor as its analogue containing 3.2 wt % fat.

Key words: microparticulation, casein, renneting, fat simulant, viscosity, active acidity, enzyme.

INTRODUCTION

The rapid progress in engineering and technology has markedly reduced the amount of manual labor in the present-day society. The decreased physical activity and sedentary lifestyle combined with traditional dietary patterns leads to overweight and obesity, which can cause so-called diseases of civilization, such as hypertension, coronary heart disease, insult, gallbladder diseases, osteoarthritis, dyspnea, rectal cancer, and diabetes [1].

The problem of instilling the culture of consumption in people and that of changing their dietary patterns should be solved at all society levels, including the government. Of great importance for solving the latter problem are public awareness of the principles of a healthy balanced diet and production of low-calorie foods.

A significant decrease in the calorie content of food can be achieved by reducing the amount of fat, the highest calorie component, whose energy value is more than two times higher than that of proteins and carbohydrates, the more so because milk fat is not an indispensable component of food from the standpoint of nutritional value.

However, low-fat dairy products may have some defects, for example, flat taste, too thin texture, and too coarse texture with signs of mealiness and curd grains (for protein foods) [2]. The nutritional value of food is of obvious significance, but the consumer's choice is actually governed by the organoleptic properties of food.

In practice, the organoleptic properties of nonfat foods is increasingly being corrected using fat simulants, which are low-calorie substances creating the illusion of the presence of fat. This property of fat substitutes is due to their particles falling in the size range from 0.5 to 2.0 μm and having a spherical or near-spherical shape. This is the reason why foods containing fat substitutes provide a creamy mouthfeel when they are masticated. Particles larger than 3 μm in aqueous dispersion are perceived as powdery, chalky, and sandy (as their size increases), and dispersed particles smaller than 0.1 μm are perceived as a true solute [3].

Fat simulants differ in their nature and may be based on a carbohydrate, protein, or fat or on their combination.

Carbohydrate-based fat substitutes are produced from natural gums, agar, modified starch, or corn fiber. They absorb water, thus imitating the fat volume and structure, and are used in the production of pastry, convenience meat products, spreads, soups, salad seasonings, glaze, and frozen desserts [4].

Protein-based fat substitutes are produced by heating and grinding (microgranulation) of milk and egg proteins or a mixture of egg and whey proteins and xanthan gum. They are unsuitable for foods whose preparation involves high-temperature treatment, because the proteins undergo denaturation at elevated temperatures, their structure breaks down, and they lose their ability to simulate fat [5].

The method of producing microgranulated whey protein (MWP) was developed in 1984 by the Canadian inventors Norman S. Singer, Shoji Yamamoto, and Joseph Latella [6]. The microgranulated protein Simplese®-100 is readily dispersible and dissolves rapidly without use of specialized equipment or technology; it acts as an ersatz dispersed phase in place of the fat droplets that traditionally function as the dispersed phase and simulates the creamy texture of the product [7, 8].

The particles of denaturated whey protein in milk-protein products and fermented dairy beverages participate in the formation of a casein clot: they incorporate in the protein matrix to function as the fat globules that they have replaced [9, 10].

However, the price of these additives is 670–730 RUB/kg, which is unacceptable for Russian manufacturers. In addition, MWP is not manufactured in Russia on the industrial scale, and this can make the production of MWP-based low-calorie foods import-dependent.

Our analysis of the literature concerning this problem suggests that Russia strongly needs domestic technologies for production of reduced-fat foods with good organoleptic properties using raw materials and equipment available for the existing enterprises.

The purpose of this study was to develop a protein-based low-calorie fat simulant and to see whether this simulant is usable in the production of nonfat lapper milk.

EXPERIMENTAL

The technical problem addressed here is to obtain ~1 µm spherical protein particles that are uniformly distributable in the raw material-product colloidal system without changes occurring in their dispersion, shape, and size in all technology steps.

The objects of this study were nonfat cow's milk (Magnitogorsk Dairy Plant) and a nonfat fermented dairy beverage produced by the thermostat method involving a casein microparticulation stage.

The following reagents were used in milk coagulation:

- heat-acid coagulation: 10% acetic acid solution (VitaKhim Perm' Co., Perm, Russia);
- acid coagulation: dry starter cultures *L. lactis*, *Str. thermophilus*, and *L. acidophilus* (Barnaul'skaya Biofabrika Co., Barnaul, Russia);
- heat-calcium coagulation: 40% calcium chloride solution (Univerkhim Co., Chelyabinsk, Russia);
- renneting: microbial chymosin Maxiren® (DSM, Netherlands).

The medium was neutralized to pH 7.00 with 10% sodium hydroxide E524 (Kaustik Co., Volgograd, Russia).

The organoleptic, physicochemical, and rheological properties of the raw materials and products were investigated by standard methods.

The raw materials and products were sampled and prepared for physicochemical characterization in conformity with ISO 707:2008 (IDF 50: 2008) "Milk and milk products – Guidance on sampling".

Organoleptic analyses were performed in conformity

with ISO 22935-2:2009 "Milk and milk products. Sensory analysis. Part 2. Recommended methods for sensory evaluation (IDT)."

Active acidity was determined potentiometrically as prescribed by the RF standard GOST R 53359-2009 (Milk and products of milk processing. Method for determination of pH). Active acidity (pH) can be measured with any potentiometer whose measurement range is pH 0–12 (14) by following the instructions for the instrument.

The viscosity of dairy raw materials and products was determined on a VPZh-4 capillary viscometer via a procedure prescribed by the RF standard GOST 33-2000. In this method, a certain volume of the liquid examined flows by gravity out of a graduated glass capillary at a constant temperature and its outflow time is measured in seconds. Kinematic viscosity is the product of the outflow time and the viscometer constant [11].

The shape of casein micelles was determined by microscopic examinations.

The size of casein micelles was determined by a turbidimetric method based on measuring the intensity of light passing through the dispersion [12]. These turbidity measurements can be carried out with a KFK-2 photoelectric colorimeter, which is intended for measuring the absorbance of colored molecular solutions. Its operation is based on the equalization, with an adjustable slit diaphragm, of two light fluxes, one passing through a cuvette with the sol analyzed and the other through a cuvette with a standard sol. A calibration plot is constructed beforehand using, e.g., an electron microscope. The particle size is derived from colorimetric data using this plot and Geller's formulas.

RESULTS AND DISCUSSION

The scientific novelty of the technology suggested here is that particles of desired size and shape are obtained by controlled coagulation of native proteins of milk, with the process terminated once the particles have reached a size of ~1 µm. This technology is unique and is not used by any manufacturer in the world. It differs from the existing technologies in that the main component of the fat simulant is casein, a readily available substance, rather than an expensive whey concentrate (Table 1).

Table 1. Some characteristics of the product obtained in this study and analogous fat substitutes

Evaluation parameter	Our product	Simplese	Olestra
Base	Casein (main milk protein)	Whey proteins	Sucrose polyester
Assimilability in organism	Completely assimilable	Completely assimilable, recognized as safe	Nonassimilable; no final data on safety
Thermal processibility	Intolerant to heat	Intolerant to heat	Heat-treatable
Calorie content, kcal/g	1–4	1–4	5
Price, RUB/t	60 000–80 000	690 000	450 000

Initially, we studied the main milk coagulation mechanisms in order to find the most appropriate method of obtaining particles of desired size and shape.

In the investigation of heat–acid coagulation, the coagulant was a 10% solution of acetic acid (VitaKhim Perm', Perm, Russia), with its dose varied between 0.2 and 1.0%. The acid type, concentration, and dosage were chosen on the basis of earlier data on the heat–acid coagulation of milk proteins [13]. Coagulation was performed between 25 and 85°C, with the temperature changed in 20°C steps. The coagulation process was terminated by rapidly cooling the system to 20°C.

The appropriateness of the size of the resulting casein particles was indirectly assessed by viscosity measurements after cooling (Table 2).

Table 2. Variation of the viscosity of the product with coagulation temperature at different doses of acetic acid

Dose of acetic acid solution, %	Viscosity of the mixture, mm ² /s, at the following temperatures			
	25±2°C	45±2°C	65±2°C	85±2°C
0.2	3.31	3.61	4.40	Pronounced coagulation
0.4	3.56	3.86	4.42	Pronounced coagulation
0.6	3.59	3.93	4.69	Pronounced coagulation
0.8	3.84	4.10	4.69	Pronounced coagulation
1.0	3.86	4.14	4.97	Pronounced coagulation

The results of this experiment indicate that increasing the dose of 10% acetic acid at a constant experimental temperature exerts an insignificant effect on milk coagulation, increasing the viscosity by only 6–8%. Raising the coagulation temperature turned out to be a more effective means to increase the kinematic viscosity by approximately 14–16%. This is due to the fact that the action of heat on protein molecules is the main dehydrating factor, which simultaneously causes the breaking of intramolecular bonds and protein denaturation.

Coagulation can theoretically be hampered by abruptly dropping the temperature. However, experience has demonstrated that milk, like any other colloidal system, is inertial and it takes a relatively long time to change its temperature. Because the state of the milk proteins changes very rapidly under the action of the acid and heat, it seems impossible to control the heat–acid coagulation process, particularly under industrial conditions.

Acid coagulation was examined as another possible way of obtaining casein-based fat simulants. Experiments were performed with lactic acid bacteria differing in their heat tolerance and acid production activity: *L. lactis*, *Str. thermophilus*, and *L. acidophilus*.

Milk coagulation was terminated by rapidly cooling the mixture to 10°C—the simplest possible method. This was done 1 h before a significant increase in viscosity took place, specifically 6, 3, and 4 h after the beginning of fermentation for *L. lactis*, *Str. thermophilus*, and *L. acidophilus*, respectively.

Pasteurized and cooled milk was fermented with pure cultures of lactic acid bacteria, which were introduced as a bulk starter (1% of the milk weight). Thereafter, milk samples were thermostated for a certain time at the optimum temperature for the development of the microorganisms. Next, the samples were cooled and their viscosity was measured.

As a result of this processing, the viscosity of the mixture increased to $(6.3–7.15) \cdot 10^6$ m²/s. This was due to the aggregation of protein molecules as a result of acid coagulation occurring via the following mechanism: lactic acid accumulating in the milk owing to lactose fermentation by the lactic acid bacteria reduces the negative charge of casein micelles and brings casein into the isoelectric state (pH 4.6–4.7). At this point in time, the interparticle repulsion potential decreases and the protein macromolecules lose their solubility and stability.

But acid coagulation is a difficult-to-control process depending on many factors that are uncorrelatable under industrial conditions, including milk composition variation with the cow's breed, individual features, state of health, and lactation period, with the way of caring for the cow, with the type of feed, and with the sanitary conditions under which the milk was produced. Note that dairy plants most often receive bulk milk, and it is difficult to control its quality and to take into account all significant factors.

In addition, as the starter cultures employed in the dairy industry are transported and stored, they may undergo progressive deactivation. Different starter batches may contain bacterial strains differing in their acid formation capacity. However, the most frequent cause of the deactivation of starter microflora is the action of bacteriophages [14].

Thus, the production of protein-based fat simulants by the acid coagulation of milk is difficult to organize and control on the industrial scale.

We also investigated the applicability of the calcium chloride coagulation of milk proteins to the production of casein-based fat simulants. Calcium chloride was introduced as its 40% solution, with the solution dose varied between 0.5 and 1.25% in 0.25% steps. As in the case of heat–acid coagulation, the milk coagulation temperature was varied between 25 and 85°C in 20°C steps. The coagulation process was terminated by rapid cooling. The viscosity of the medium was chosen to be the response parameter (Table 3).

An analysis of these experimental data demonstrated that an increase in the dose of 40% calcium chloride at a fixed temperature exerts only a slight effect on milk coagulation, increasing the viscosity of the medium by only 1–3% on the average. A more significant factor here is coagulation temperature: as the temperature is elevated from 25 to 65°C, the viscosity increases by 16–79%, depending on the calcium chloride dose.

The increase in milk viscosity is explained by the growth of protein particles. The introduction of calcium chloride into fresh milk reduces the stability of the colloidal dispersion of the calcium caseinate–calcium phosphate complex. This is accompanied by the exchange of H ions of the casein complex for Ca ions from the calcium chloride solution. As a result of this

cation exchange, the calcium caseinate–calcium phosphate complex is further enriched with calcium owing to the liberation of H ions. This acidifies the milk, bringing it from pH 6.5 to pH 5.0, and causes the aggregation of particles of the complex. Because of the specific physicochemical properties of milk, it is impossible to quickly terminate its coagulation by lowering its temperature.

Table 3. Calcium chloride dose and temperature effects on the viscosity of the milk mixture in calcium chloride coagulation

Dose of 40% CaCl ₂ , %	Viscosity of the mixture, mm ² /s, at the following temperatures			
	25±2°C	45±2°C	65±2°C	85±2°C
0.25	3.05	3.35	4.21	Pronounced coagulation
0.50	3.11	3.42	4.71	Pronounced coagulation
0.75	3.15	3.50	4.98	Pronounced coagulation
1.00	3.26	3.55	5.50	Pronounced coagulation
1.25	3.32	3.61	6.82	Pronounced coagulation

Thus, the calcium chloride coagulation of milk is difficult to monitor and control. Cooling only slows down the process slightly but does not terminate it. A significant drawback of the process is the unpleasant taste of its product that appears even in the presence of a small amount of calcium chloride.

In order to form protein particles of desired size and shape, we investigated milk renneting, in which the main coagulant is a milk-clotting enzyme. The action of milk-clotting enzymes can be corrected by varying the processing temperature, the ionic strength of the medium, the CaCl₂ concentration, and the processing time.

Investigation of the milk-clotting activity (capacity for rapidly hydrolyzing χ -casein) and total proteolytic activity (capacity for cleaving other bonds in proteins) demonstrated an obvious advantage of chymosin over the other enzymes: chymosin shows the lowest proteolytic activity relative to milk-clotting activity.

All of the milk-clotting enzymes commonly used in the dairy industry are acid proteases, which exhibit their maximum activity in acid media. The optimum active acidity for χ -casein hydrolysis with chymosin is pH 6.0, and the reaction rate varies only slightly in the pH 5.6–6.4 range. A common property of the milk-clotting enzymes is that their total proteolytic activity declines when pH is above its optimum level. We suggest that this property be used to terminate the coagulation process.

Milk-clotting enzymes vary in terms of the temperature dependence of their activity; for chymosin, the optimum temperature is 45°C.

The necessary amount of enzyme depends considerably on the physicochemical properties of the milk to be processed, but usually 2.5 g of an enzyme preparation with an activity of 100 000 U is added to 100 kg of milk. In order to check the effect of a dose of

rennet enzyme and the duration of its coagulating action on milk, we carried experiments in which the rennet enzyme dose was reduced so as to prevent pronounced coagulation of milk proteins.

An enzyme solution (0.02–0.1% of the mixture volume, 0.04% increments) was introduced into milk at 40–42°C for a higher effectiveness of the enzyme. The increasing size of casein globules was estimated as the viscosity of the medium 10, 20, and 30 min after the introduction of all reagents (Table 4).

Table 4. Variation of viscosity with the rennet enzyme dose and fermentation time

Holding time, min	Dose of rennet enzyme (as a solution with an activity of 100–150 U), %		
	0.02	0.06	0.1
	Viscosity, mm ² /s		
10	3.07	3.47	4.07
20	3.29	4.46	8.87
30	3.53	5.67	Pronounced coagulation
Total clotting time, min	70	60	30

Note that the smaller the rennet enzyme dose the longer the clotting time. Based on experimental data, we set the enzyme dose to be 0.1%, since only with this dose did we obtain the desired casein particle sizes in a short time.

To study the active acidity effect on casein coagulation with chymosin, we carried out a series of experiments in which active acidity was varied between pH 5.80 and pH 7.00 in 0.40 steps by adding a 10% acetic acid solution. The enzyme dose was fixed. The response signal was the kinematic viscosity of the medium measured after fermentation (Table 5).

Table 5. Dependence of the viscosity of the fermentation mixture on the dose of rennet enzyme (as a solution with an activity of 100–150 U) and on the active acidity of the medium

Dose of rennet enzyme (as a solution with an activity of 100–150 U), %	Viscosity, mm ² /s			
	pH 5.80	pH 6.20	pH 6.60	pH 7.00
0.02	7.03	6.95	6.72	6.24
0.06	8.15	7.52	7.25	6.65
0.1	9.05	8.92	8.72	7.85

These experiments demonstrated that, as the active acidity decreases, the viscosity of the mixture increases. This is quite natural: at pH 5.80, the system approaches the isoelectric point, at which acid coagulation dominates. Serious drawbacks of this coagulation process were revealed. This pH range is rather risky for the technology suggested. For this reason, pH 6.20 was taken to be the optimum acidity for the formation of particles of desired sizes and shapes.

We studied the effect of calcium chloride (CaCl₂) on the rennet coagulability of milk with the aim of gaining control over the growth rate of casein particles. Calcium is uninvolved in the enzymatic stage of renneting;

however, variation of its concentration in the medium can change the physicochemical conditions.

A calcium chloride dose recommended for the dairy industry (40 g of anhydrous salt as a 40% solution per 100 kg of milk) was introduced into the sample to be examined. Next, different amounts of the chymosin solution were added at pH 6.20. The same amount of enzyme was added to the reference sample at the same active acidity of the medium, but CaCl_2 was not. The viscosity data obtained in this experiment are presented in Table 6.

Table 6. Effect of calcium chloride on the viscosity of the mixture in milk renneting

Dose of rennet enzyme (as a solution with an activity of 100–150 U), %	Viscosity, mm^2/s	
	pH 6.20	
	CaCl_2	reference sample
0.02	6.95	6.97
0.06	7.52	7.48
0.1	8.92	8.87

Clearly, the viscosity of the milk samples into which CaCl_2 was introduced differs little (within the experimental error) from the viscosity of the samples obtained without adding calcium chloride. This finding confirms the data earlier published on the effect of calcium chloride on milk renneting: CaCl_2 exerts an effect on the first stage of coagulation only by changing the pH of the medium. Because the pH value in our experiment was maintained constant, optimal for the functioning of the rennet enzyme, CaCl_2 had no significant effect on the viscosity of the milk mixture.

No preliminary pasteurization was performed in this experiment. Because of this, the entire calcium remained in solution, and its amount was sufficient for milk renneting. However, dairy plants receive bulk milk (including slow-renneting milk) and it is difficult to check its renneting capacity. For this reason, it is suggested that the minimum recommended dose of calcium chloride be added into milk at the casein microparticulation stage in order to avoid spoilage losses.

By analyzing the results and parameters of this study, we established that the most rational coagulation method for obtaining the desired particle sizes and shapes is renneting. The following requirements were taken into consideration in the selection of a coagulation method for this purpose:

- acceptable organoleptic properties of the resulting mixture;
- low cost of the coagulant;
- use of standard equipment;
- controllability of the coagulation process;
- safety of the coagulant.

The renneting process is easy to control and needs no specialized equipment. A stable system can be obtained by renneting using technological manipulations. The reagents used in milk renneting do not impart a foreign smell or taste to the product. All milk-clotting enzymes are absolutely nonhazardous to human health.

Based on our studies, we have developed a technology for producing microparticulated proteins that can be used as fat simulants in dairy products.

Figure 1 schematizes the renneting process and the way in which it is terminated.

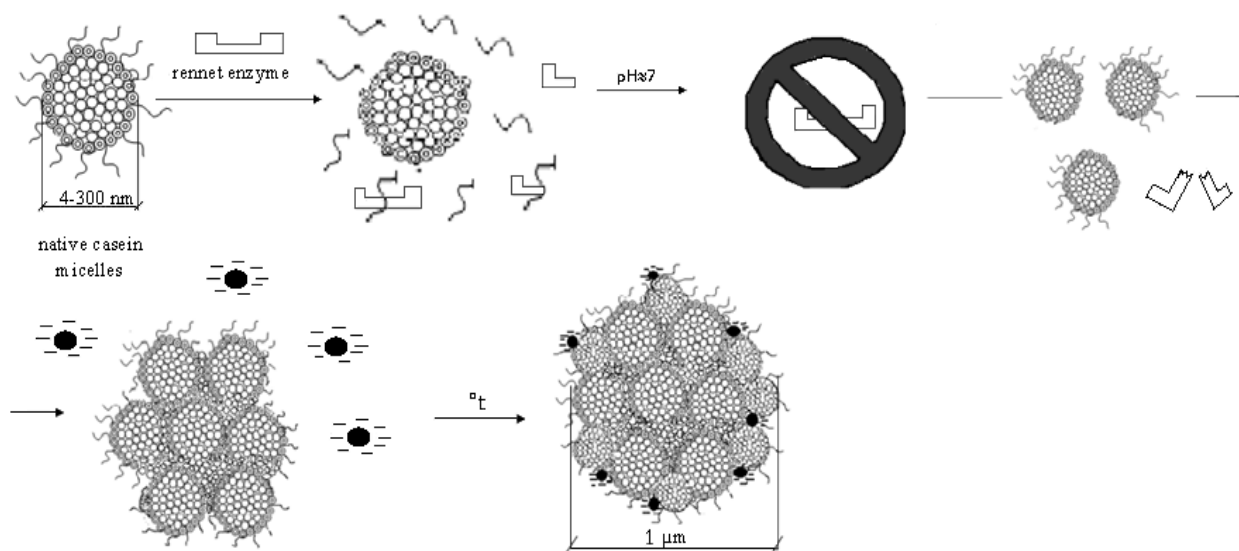


Fig. 1. Casein renneting and its termination.

For obtaining the desired particle size and shape, the renneting process should be started and terminated at a point in time such that the size of the protein particles have already increased, but no clot has formed. It is necessary here that a stable system be formed.

The average size of native casein micelles is about 40–300 nm. Provided that the optimum conditions are established, glycomacropeptide is eliminated from the surface of the micelles and hydrophobic areas appear under the action of the rennet enzyme (temperature,

calcium salts, active acidity), causing the micelles to stick together.

The process was terminated by neutralizing the medium to pH 7.00 by adding alkali solutions permitted in the food industry. This slowed down the action of the film-clotting enzyme. After heat treatment at $96 \pm 2^\circ\text{C}$, the enzyme was completely inactivated and denatured whey proteins deposited on the casein globules obtained. These proteins made the microparticles

resistant to sedimentation and sticking by increasing the negative charge on their surface. This is how the desired particle size ($\sim 1 \mu\text{m}$) was obtained.

Using the above casein microparticulation technology, we produced experimental batches of fermented milk products, including lapper milk. The production of nonfat lapper milk containing microparticulated casein is illustrated by Fig. 2.

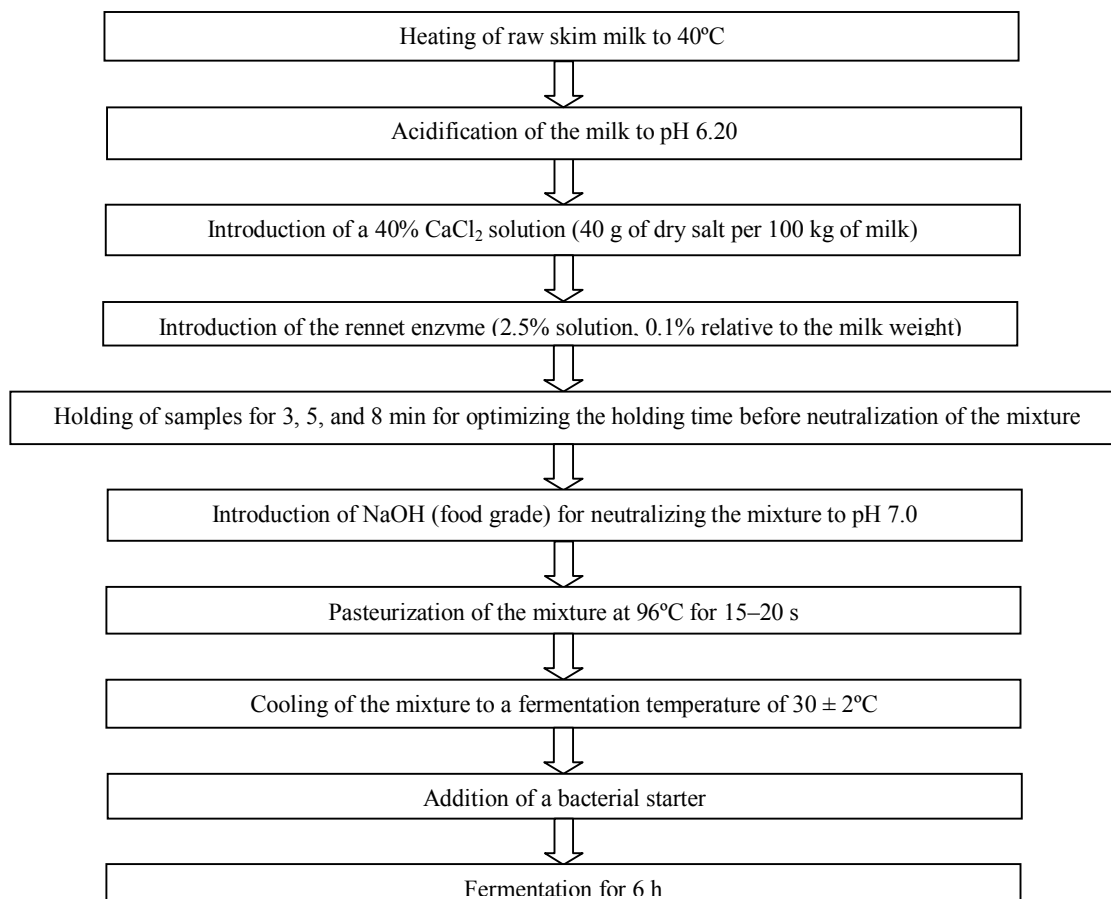


Fig. 2. Production of nonfat lapper milk containing microparticulated casein (MPC).

The reference samples were lapper milk produced using a conventional technology from nonfat milk and lapper milk with a fat content of 3.2 wt %. The quality criteria for the fermented dairy beverages were rheological properties (viscosity) and organoleptic characteristics (taste, texture). The viscosity data are listed in Table 7.

These experiments demonstrated that the viscosity of the finished product depends on the fermentation time at the microparticulation stage: as the holding time is lengthened, the viscosity of the fermented milk drink increases.

In terms of viscosity, the sample fermented for 5 min is most similar to the sample containing 3.2 wt % fat. The taste and texture of the products were evaluated in terms of the creamy mouthfeel criterion (creamy taste

and thickness), which was measured on a five-point scale. The creamy mouthfeel evaluation data for the lapper milk samples are presented as a histogram in Fig. 3.

Table 7. Viscosity of the fermented milk products obtained using the casein microparticulation stage and without microparticulation

Lapper milk viscosity, mm^2/s				
nonfat	fat content of 3.2 wt %	with microparticulated casein; fermentation for the following lengths of time, min		
		3	5	8
8.45	11.3	10.5	28.7	32.2

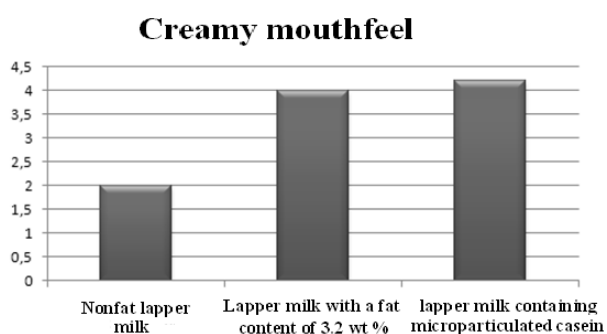


Fig. 3. Creamy mouthfeel data for lapper milk: nonfat sample and samples containing 3.2 wt % fat and microparticulated casein.

The properties of the fermented dairy beverages containing microparticulated casein demonstrated that casein microparticulation stage can be used to improve the organoleptic characteristics of nonfat fermented

milk products. Microparticulated casein makes the texture and taste of the products more pleasant for the consumer. It provides means to significantly decrease the calorie content of the products via fat reduction, without affecting the amounts of other components (proteins, vitamins, microelements). The milk products thus retain their nutritional value and wholesomeness.

The low-calorie fermented milk beverage production technology involving a casein microparticulation stage offers the following advantages:

(1) It does not need involvement of any additional raw materials in the dairy industry.

(2) It widens the range of low-calorie dairy beverages, imparts a rich taste and smooth and creamy texture to them, and thus increases the consumer demand for these foods.

(3) The new products have a high nutritional and biological value combined with their calorie content reduced by a factor larger than 2 and are thus functionally specialized.

REFERENCES

1. Vasilevskaya, L.S. and Okhnyanskaya, L.G., Fiziologicheskie osnovy problemy pitaniya (Physiological foundations of the nutrition problem), *Voprosy pitaniya* (Topics in nutrition), 2002, no. 2, pp. 19–20.
2. Shidlovskaya, V.P., *Organolepticheskie svoystva moloka i molochnykh produktov: Spravochnik* (Organoleptic Properties of Milk and Dairy Products: A Handbook), Moscow: Kolos, 2000.
3. Singer, N. S. and Moser, R.H., Microparticulated proteins as fat substitutes, in *Low Calorie Foods Handbook*, Altschul, A.M., Ed., New York: Marcel Dekker, 1993, ch. 9.
4. Akoh, C.C., Fat replacers, *Food Technology*, 1998, vol. 52, no. 3, pp. 47–53.
5. Gershoff, S. N., Nutrition evaluation of dietary fat substitutes, *Nutrition Reviews*, 1995, no. 11. http://www.findarticles.com/p/articles/mi_qa3624/is_199511.html
6. US Patent 4734287, 1988.
7. Queguiner, C., et al., Microcoagulation of a whey protein isolate by extrusion cooking at acid pH, *Journal of Food Science*, 1992, vol. 57, no. 3, pp. 610–616.
8. Schirle-Keller, J.-P., Chang, H.H., and Reineccius, G.A., Interaction of flavor compounds with microparticulated proteins, *Journal of Food Science*, 1992, vol. 57, no. 6, pp. 1448–1451.
9. Tamime, A.Y., et al., The microstructure of set-style, natural yogurt made by substituting microparticulate whey protein for milk fat, *International Journal of Dairy Technology*, 1995, vol. 48, no. 4, pp. 107–111.
10. Manylov, S.V., Issledovanie vliyaniya denaturirovannykh syvorotochnykh belkov na svoystva nizkokaloriinykh molochno-belkovykh produktov (Effect of denaturated whey proteins on the properties of low-calorie dairy protein products), *Cand. Sci. (Eng.) Dissertation*, Moscow, 2009.
11. Krus', G.N., Shalygina, A.M., and Volokitina, Z.V., *Metody issledovaniya moloka i molochnykh produktov* (Methods of Examination of Milk and Dairy Products), Moscow: Kolos, 2004.
12. Frolov, Yu.G., *Kurs kolloidnoi khimii: Poverkhnostnye yavleniya i dispersnye sistemy* (Colloid Chemistry: Surface Phenomena and Dispersions), Moscow: Khimiya, 1982.
13. Smirnova, I.A., *Biotekhnologicheskie aspekty proizvodstva termo-kislotnykh syrov* (Biotechnological Aspects of the Production of Heat–Acid Precipitated Cheese), Kemerovo: KTIPP, 2002.
14. Gudkov, A.V., *Syrodellie: Tekhnologicheskie, biologicheskie i fiziko-khimicheskie aspekty* (Cheese making: Technological, Biological, and Physicochemical Aspects), Moscow: DeLi Print, 2004.

UDC 637.131.8:579.872
DOI 10.12737/1515

EFFECT OF IRON SULFATE ON BIOSYNTHESIS OF EXTRACELLULAR METABOLITES OF PROPIONIC ACID BACTERIA

I. S. Khamagaeva

East Siberia State University of Technology and Management,
ul. Klyuchevskaya 40v, Ulan-Ude, 670013 Russia
phone:/Fax: +7 (3012) 41-72-06, e-mail: ttmp@esstu.ru

(Received May 08, 2013; Accepted in revised form May 28, 2013)

Abstract: In the work, activated cultures of propionic acid bacteria were found to exhibit high antimutagenic activity and adhesion properties, synthesize considerable amount of corrinoids and heme-containing enzymes. Increase of iron concentration in the medium was shown to intensify synthesis of extracellular metabolites promoting adaptation of the culture to the metal. Optimal technological parameters for isolation of casein phosphopeptides were determined. Ability of phosphopeptides to efficiently solubilize divalent iron was confirmed. Relationship between iron concentration and extent of solubilization was established. Iron chelated with casein phosphopeptides was noted to stay in divalent form for prolonged period.

Keywords: propionic acid bacteria, catalase, peroxidase, superoxide dismutase, casein phosphopeptides, iron solubilization

INTRODUCTION

The concept of optimal nutrition implies adequate organism supply with both macro- and micronutrients, including the essential microelements, particularly iron, as a key prerequisite for preservation of human health. Iron-deficient conditions remain a topical and untreated issue of modern medicine. Lack of iron in the organism leads to many negative consequences. One of them is the development of iron deficiency anemia [1].

Taking into account that man consumes iron in vegetable and animal products in everyday life and the presence of amino acids and peptides, as well as proteins of animal origin, promotes intake of the microelement, enrichment of diets with organic forms of iron seems reasonable. In our opinion, propionic acid bacteria, which possess the ability to synthesize considerable amounts of heme-containing enzymes and corrinoids thus increasing iron uptake, are the most convenient object for development of biotechnological production of iron in organic form [2].

Iron is known to be consumed only in the form of Fe^{2+} . However, divalent iron undergoes chemical oxidation to an insoluble, nonassimilable trivalent form. To preserve bioavailability of iron, role of chelating agents, which promote solubilization of minerals preserving their soluble state, is of interest. Casein phosphopeptides (CPPs) are among the representatives of the chelators. CPPs are phosphorylated peptides formed from caseins of cow milk upon digestion by proteases [3–5]. Casein phosphopeptides are still poorly studied as both chelating agents and potential nutraceuticals for human nutrition. Besides, there are no data in literature on the effect of CPPs on iron solubilization. Therefore, studies on iron-binding

capacity of CPPs are of interest.

The aim of the work was to study the effect of various concentrations of iron sulfate on growth and biosynthesis of extracellular metabolites by propionic acid bacteria, as well as the study on chelating properties of casein phosphopeptides.

MATERIALS AND METHODS

Bacteria and culturing conditions. Cultures of the following propionic acid bacteria (PABs) strains were subject of the study: *Propionibacterium freudenrichii* subsp. *shermanii* AC-2503, *Propionibacterium freudenrichii* subsp. *freudenrichii* AC-2500, *Propionibacterium cyclohexanicum* Kusano AC-2260, and *Propionibacterium cyclohexanicum* Kusano AC-2259, all obtained from the All-Russian Collection of Microorganisms of the Institute of Biochemistry and Physiology of Microorganisms (Moscow) and activated by a unique biotechnology method developed in the East Siberian State University of Technology and Management. Divalent salt (FeSO_4) was used as iron source. Propionic acid bacteria were cultured in serum medium supplemented with growth factors [6]. One-day culture grown on low-fat milk was used as an inoculate. Iron sulfate was added to the growth medium at concentration of 0.25–0.55 mg/mL. Propionic acid bacteria were cultured in the presence of iron sulfate for 24 h at 30°C. Culture growth kinetics was calculated according to a custom method.

Analytical procedures. The process of iron binding was followed by the amount of chelated Fe^{2+} (% iron remaining in divalent form to the total initial dose). Content of Fe^{2+} was determined using a reference method [7]. Content of Fe^{3+} was determined by

spectrophotometry. The technique was developed according to the Industry-Specific Standard 34-70-953.4-88. The method is based on the interaction of dissolved iron with sulfosalicylic acid and measurement of optical density of the colored solutions thus formed.

Determination of extracellular metabolites was performed in the end of the exponential growth phase. Catalase activity was determined using a colorimetric technique [8], peroxidase activity, by spectrophotometry using the *o*-dianisidine reagent [9], and that of superoxide dismutase, by autooxidation of adrenalin [10].

Antimutagenic activity was determined by the Ames test [2]; adhesion properties were studied on formalinized erythrocytes according to the in-depth Brilis technique; strain adhesiveness was estimated according to the index of microorganism adhesiveness (IMA) [11]; concentration of exopolysaccharides was estimated with anthrone reagent [12]; and vitamin B₁₂ content was determined by spectrophotometry [13].

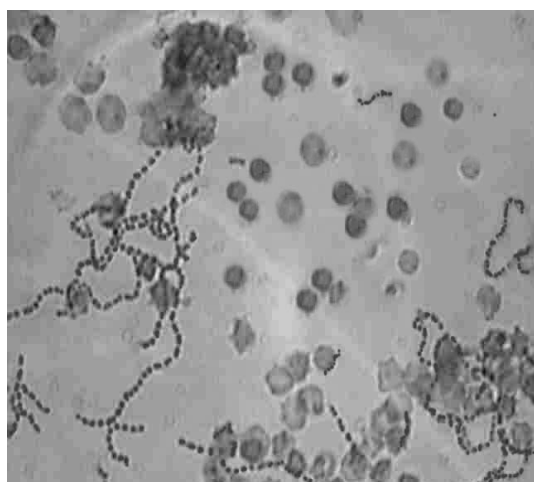
Solution of casein phosphopeptides was obtained by enzymatic hydrolysis of sodium caseinate. Metal-binding ability of CPPs depends on the extent of phosphorylation. To obtain hydrolysate with the

maximal content of low-molecular weight phosphorylated peptides and free amino acids capable of formation of soluble complexes with iron, we redefined process parameters of CPP isolation. One-stage hydrolysis of Na caseinate with pepsin and trypsin with varying hydrolysis time was used. Molecular weight distribution of peptides in the aqueous solution of casein phosphopeptides was evaluated by moderate pressure size exclusion chromatography on a TSK GEL (0.8/30 cm) column. Chelated iron content was determined by mass spectrometry. Tables discuss statistically significant differences at $p < 0.05$.

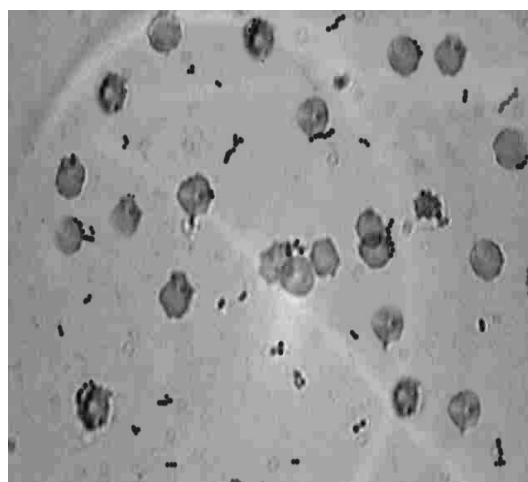
RESULTS AND DISCUSSION

Adhesion properties of propionic acid bacteria

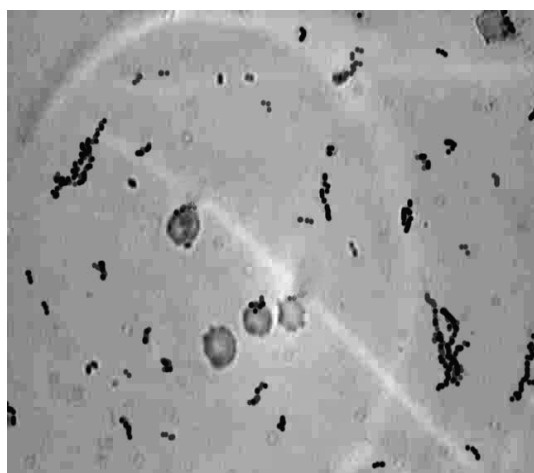
One of the current areas of modern microbiology studies adhesion process in various microorganisms. Adhesion is a intercellular interaction manifested through tight attachment of cells to a substrate. Concerning the propionic acid bacteria (PABs), we did not find any information on their adhesion properties in the literature.



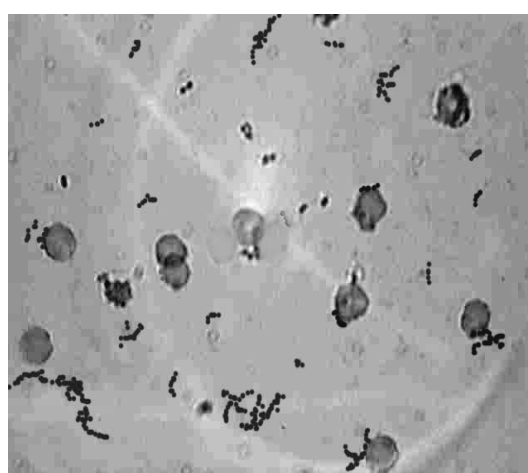
(a) *P. fredenreichii* subsp. *shermanii* AC-2503



(c) *P. freudemrichii* subsp. *fredenreichii* AC-2500



(b) *P. cyclohexanicum* Kusano AC-2259



(d) *P. cyclohexanicum* Kusano AC-2260

Fig. 1. Interaction of propionic acid bacteria with erythrocytes.

It should be noted that composition, stability, and protective properties of the macroorganism microflora largely depend on its adhesion properties. In this connection, we studied adhesion properties of various strains of propionic acid bacteria. Formalinized erythrocytes were chosen as model macroorganism cells. Process of propionic acid bacteria adhesion on erythrocytes is presented in Fig. 1.

Analysis of the data presented in Fig. 1 shows that propionic acid bacteria possess varying capability for adhesion on erythrocytes. Some strains were found to adhere in the form of individual bacterial cells (Figs. 1 b–d) or aggregates that cover erythrocyte surface almost completely (Fig. 1a).

Adhesive properties of cultures were evaluated by the average adhesion index (AAI), erythrocyte participation factor (EPF); adhesiveness was judged by the index of adhesiveness of microorganisms (IAM). According to the technique, microorganisms were considered non-adhesive at IAM values below 1.75, low adhesive, from 1.76 to 2.5; moderately adhesive, from 2.51 to 4.0, and highly adhesive, at IAM above 4.0. The results are presented in Table 1.

Table 1. Adhesiveness of propionic bacteria

Strain	AAI	EPF, %	IAM (M ± m)	Adhesiveness
<i>P. freudenreichii</i> subsp. <i>freudereichii</i> AC-2500	3.2	79	4 ± 1.5	moderately adhesive
<i>P. cyclohexanicum</i> Kusano AC-2260	3.9	82	3.7 ± 1.2	moderately adhesive
<i>P. freudereichii</i> subsp. <i>shermanii</i> AC-2503	4.6	85	5.4 ± 1.1	highly adhesive
<i>P. cyclohexanicum</i> Kusano AC-2259	3.3	80	3.1 ± 1.8	moderately adhesive

As follows from Table 1, propionic bacteria possess relatively pronounced adhesion properties. Of all studied cultures, *Propionibacterium freudenreichii* subsp. *shermanii* AC-2503 is highly adhesive, which is evidenced by adhesiveness index value (IAM = 5.4), as well as AAI (4.6) and EPF (85%) values. Consequently, the strain will attach to bowel cells better than others, creating a protective barrier. Other strains exhibited moderate adhesiveness according to all tested parameters.

Effect of iron sulfate on growth and biosynthesis of extracellular adaptation factors in propionic acid bacteria

Extracellular metabolites synthesized by microorganisms and regulating their activity are called autoregulators. It is important to stress that among the multiple functions of autoregulators factors ensuring adaptation of microorganisms to unfavorable physicochemical environmental conditions are poorly studied.

In this connection, in further studies the effect of iron sulfate on synthesis of exometabolites by propionic acid bacteria was studied. Biological effect of microorganism interaction with metals is known to be determined by concentration of the metal, its toxicity,

and metabolic potential of the microorganism [14].

Our data (Fig. 2) show that below certain concentration (0.25 mg/mL for *P. freudenreichii* subsp. *freudenreichii* AC-2500 and 0.35 mg/mL, for the rest of the strains) iron sulfate increases specific rate of propionic acid bacteria growth, which evidences iron importance for normal cell metabolism. Further increase in FeSO₄ concentration in the medium leads to growth slowdown. The number of viable cells remains high (10¹¹ CFU/cm³). It should be noted that excess metal content inhibits metabolism, turning on protective mechanisms compensating for the negative effects of the metal.

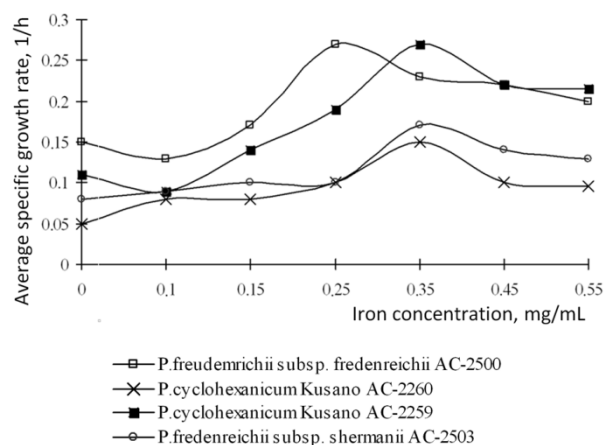


Fig. 2. Effect of iron sulfate on the growth rate of propionic acid bacteria.

Table 2. Effect of iron sulfate on the activity of antioxidant enzymes synthesized by propionic acid bacteria

Strain	Iron content, mg/mL	Enzyme activity		
		catalase, mcat/mL	peroxidase, nmol/(min mg protein)	SOD, units/mg protein
<i>P. freudenreichii</i> subsp. <i>freudenreichii</i> AC-2500	0	1280.0	1.573	1.02
	0.25	1290.5	1.572	1.77
	0.35	1300.9	1.572	1.77
	0.45	1492.5	1.570	1.78
	0.55	1490.6	1.571	1.78
<i>P. cyclohexanicum</i> Kusano AC-2260	0	1712.2	0.905	1.03
	0.25	1802.5	0.890	1.85
	0.35	1895.3	0.853	1.86
	0.45	1907.4	0.850	1.86
	0.55	1912.3	0.853	1.86
<i>P. cyclohexanicum</i> Kusano AC-2259	0	1561.9	1.118	1.01
	0.25	1807.0	1.125	1.83
	0.35	1991.1	1.122	1.83
	0.45	2007.0	1.119	1.83
	0.55	2091.3	1.119	1.84
<i>P. freudenreichii</i> subsp. <i>shermanii</i> AC-2503	0	2318.6	1.113	1.17
	0.25	2554.6	1.112	1.98
	0.35	2789.3	1.113	1.99
	0.45	2954.3	1.112	2.01
	0.55	2952.3	1.113	2.01

Studying biotechnology potential, we found that propionic acid bacteria synthesize considerable amount of heme-containing enzymes [15]. Since heme-

containing enzyme synthesis and activity depend on the content of iron ion, we studied the effect of FeSO_4 on biosynthesis of catalase, peroxidase, and superoxide dismutase. The results are presented in Table 2.

Analysis of the data presented in Table 2 shows that increase in iron concentration led to increase in the activities of catalase and SOD in all studied strains. Increase in iron sulfate concentration in the medium up to 0.45–0.55 mg/mL led to 1.5-fold increase in catalase activity and 1.7–1.85-fold increase in SOD activity (on average). As for peroxidase, its activity in all experimental samples practically did not change. Probably, this may be explained by accumulation of the endoenzyme solely. Correlation between the enzymes' activity (Y) and iron sulfate concentration was established:

$$Y_1 = -39.90x^2 + 40.61x + 19.40 \text{ for SOD and}$$

$$Y_2 = -0.115x^2 + 0.861x + 0.514 \text{ for catalase.}$$

Correlation coefficient values $R_{1,2}$ are 0.990 and 0.898, respectively.

It should be noted that increase in catalase and SOD activities considerably exceeded the capacity of propionic acid bacteria to protect themselves from oxidative stress since these very enzymes are responsible for superoxide radicals removal from cells.

As follows from the literature data, protection from toxic metal concentration in microorganisms is manifested through formation of substances capable of metal binding in the form of low-toxicity compounds. Therefore, we studied the effect of iron sulfate on synthesis of bacteria extracellular adaptation factors. The results are presented in Table 3.

Table 3. Effect of iron sulfate on synthesis of extracellular metabolites

Strain	Iron content, mg/mL	Parameters			
		Adhesion activity (IAM)	EPS, $\mu\text{g}/\text{mL}$	Inhibition (antimutagenic activity), %	Vitamin B ₁₂ concentration, $\mu\text{g}/\text{mL}$
<i>P. freudenreichii</i> subsp. <i>freudenreichii</i> AC-2500	0	4.0	29.81	43.6	13.0
	0.25	4.0	29.96	44.2	32.0
	0.35	4.2	30.05	44.8	32.5
	0.45	4.6	35.50	48.9	34.0
	0.55	5.1	36.80	48.6	34.5
<i>P. cyclohexancum</i> Kusano AC-2260	0	3.7	31.85	46.2	22.0
	0.25	3.8	32.56	48.9	26.0
	0.35	3.9	36.98	48.7	27.0
	0.45	4.4	37.20	48.6	29.0
	0.55	4.7	48.30	57.9	28.0
<i>P. cyclohexancum</i> Kusano AC-2259	0	2.8	36.65	44.8	18.0
	0.25	3.1	36.90	46.2	18.0
	0.35	3.6	36.99	47.5	18.0
	0.45	4.2	38.70	52.8	19.0
	0.55	4.6	44.78	54.2	19.5
<i>P. freudenreichii</i> subsp. <i>shermanii</i> AC-2503	0	5.4	41.30	47.7	33.0
	0.25	5.4	44.52	49.6	35.0
	0.35	5.8	49.56	50.1	35.5
	0.45	6.1	50.20	51.2	36.0
	0.55	6.3	56.58	57.3	36.0

Data presented in Table 3 evidence that the addition of iron ions to nutrient medium for PAB cultivation stimulated synthesis of extracellular metabolites. For example, higher antimutagenic activity of PABs was noted with the increase in FeSO_4 concentration, which indicates antimutagenesis induction. Increased biosynthesis of exopolysaccharides (EPS) upon the addition of iron is a manifestation of bacterial non-enzymatic protective mechanisms, when EPS prevent excess iron penetration in cells through coating of the bacterium surface. Increased adhesion is explained by not only protective response of cultures to the metal, but also the fact that, according to the literature data, the presence of di- and trivalent cations leads to shrinking of charged double layers on surfaces in aqueous media, which promotes adhesion through decrease in electrostatic repulsion.

When studying morphology of propionic acid bacteria cultured at various iron concentrations, cell aggregates (cohesion) were noted upon increase of FeSO_4 dose to 0.55 mg/mL. Probably, cells managed to maintain viability under conditions of intercellular contacts in aggregates.

The results evidence that synthesis of exometabolites promotes adaptation of propionic acid bacteria to iron ions. The tendencies revealed allow understanding of the principle of metabolic organization in propionic acid bacteria and form scientific basis for development of biologically active supplements containing iron in organic bioavailable form.

The effect of casein phosphopeptides on iron solubilization in the nutrient medium

When conducting experimental studies, we noted that at iron concentration of 0.45 mg/mL and above

color of the concentrate changes and precipitate is formed, which evidences formation of insoluble Fe^{3+} ions. In this connection, we studied the effect of casein phosphopeptides (CPPs) on solubilization (chelating) of iron in the nutrient medium. CPPs are phosphorylated peptides formed from cow milk upon their digestion by proteases.

Table 4. Molecular-weight distribution of fermentolysis fractions

Molecular weight limits, kDa	Size of peptide fractions in hydrolysates, nm	Enzymes		
		pepsin	trypsin	chymosin
>20	>10	10.5	—	20.5
20.1–18.7	7–10	9.2	—	22.6
18.7–12.5	5–7	7.6	5.7	18.4
12.5–11.0	4–5	15.7	15.4	16.7
11.0–5.1	3–4	19.5	13.2	11.8
5.1–2.8	~3	14.4	17.0	9.4
2.8–1.0	1–2	11.7	26.6	—
<1	<1	10.1	22.1	—

Table 5. Effect of iron sulfate concentration and proteolytic enzymes on chelated iron content

Iron sulfate introduced, mg/mL	Chelated iron content in aqueous solutions of casein phosphopeptides, mg			
	pepsin hydrolysis	trypsin hydrolysis	chymosin hydrolysis	chymotrypsin hydrolysis
1	0.51	0.87	0.48	0.71
2	0.88	1.99	0.98	1.12
3	1.47	2.67	1.25	2.52
4	1.99	3.13	1.87	3.25
5	2.10	4.98	2.12	4.18
6	2.89	5.25	2.58	5.16
7	2.99	6.96	2.98	6.45
8	3.58	7.27	3.15	7.15
9	4.12	8.12	4.12	8.45
10	4.69	7.72	5.12	6.89

Metal-binding capacity of CPPs is known to depend on the extent of phosphorylation. To obtain hydrolysate with the maximum content of low-molecular weight phosphorylated peptides and free amino acids that are able to form soluble complexes with iron we redefined the technological parameters of CPP isolation. A one-stage sodium caseinate hydrolysis with proteolytic enzymes was used to prepare CPPs. The results are presented in Fig. 4.

Data presented in Tables 4 and 5 and Figs. 3–7 evidence that casein phosphopeptides form nano-size chelate complexes with iron ions. These particles should easily bind cell surface, efficiently carry iron ions across the intestine wall, and protect the mineral from interactions with other components of the stomach.

As a result of the studies reported herein, technological scheme of casein phosphopeptide isolation was modified (see Fig. 8).

There is an opinion that artificial chelated forms of minerals are destroyed upon storage and lose their efficiency, therefore they are inferior to natural organic

salts of the elements. For this reason, we studied preservation of iron chelated with casein phosphopeptides in divalent form upon prolonged storage. The results are presented in Table 6.

Mass spectra of hydrolysates before and after introduction of iron

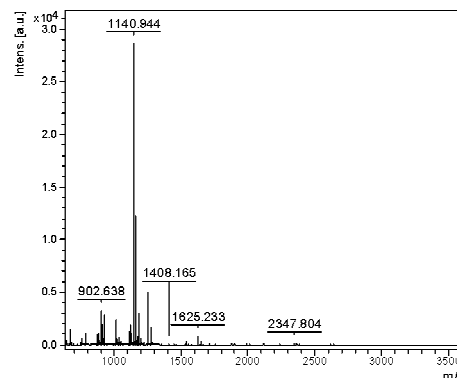


Fig. 3. Hydrolysate before the addition of iron.

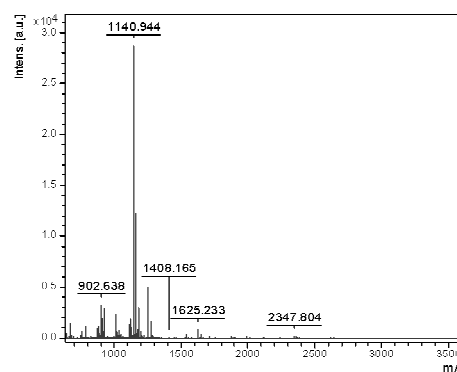
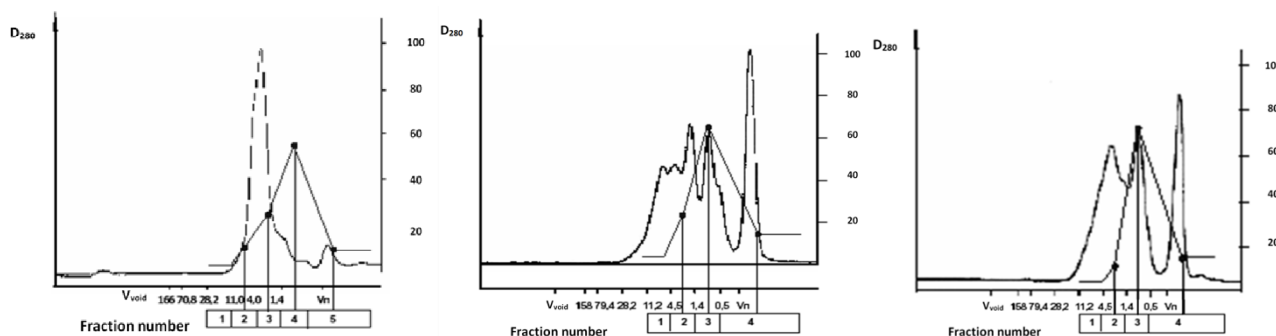


Fig. 4. Hydrolysate after the addition of iron.

Table 6. Effect of CPPs on the process of iron solubilization upon storage

Strain	CPPs content, %	Content of Fe^{2+} in storage medium (% to initially introduced dose), days			
		30	60	90	120
<i>P. freudenreichii</i> subsp. <i>freudenreichii</i> AC-2500	control	19.0	19.0	19.5	18.5
	10	58.0	62.0	62.5	60.0
	20	88.0	88.0	88.5	88.0
<i>P. cyclohexanicum</i> Kusano AC-2260	control	30.0	29.5	30.0	28.5
	10	69.0	70.5	70.0	69.0
	20	94.5	95.0	95.0	94.5
<i>P. cyclohexanicum</i> Kusano AC-2259	control	32.0	32.0	30.5	29.0
	10	60.0	60.5	60.0	59.5
	20	75.0	75.0	75.5	75.0
<i>P. freudenreichii</i> subsp. <i>shermanii</i> AC-2503	control	22.0	25.0	25.5	19.0
	10	66.0	67.0	66.0	63.5
	20	95.0	96.0	96.0	95.0



Figs. 5–7. Content of iron in chromatography fractions of iron complexes with trypsin, pepsin, and chymotrypsin hydrolysates of sodium caseinate, respectively (left to right).

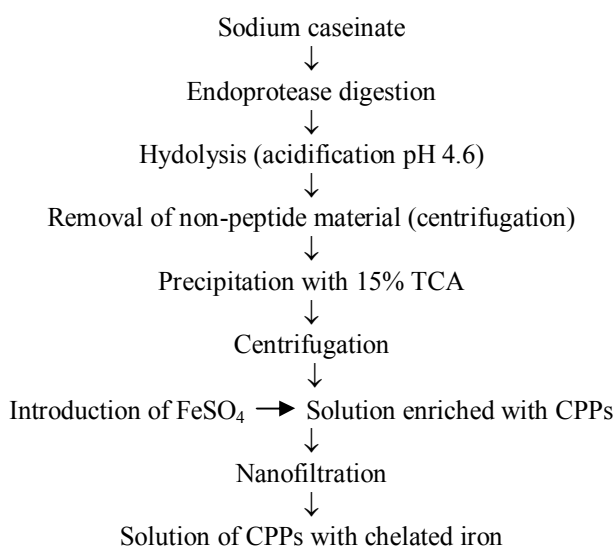


Fig. 8. Modified technological scheme of casein phosphopeptide preparation.

Data presented in Table 6 indicate that in the process of storage, chelated iron content in concentrated CPP-containing solutions practically did not change, while considerable decrease in soluble Fe^{2+} ion content was observed in control.

Altogether, the data indicate that casein phosphopeptides are promising chelating agents to obtain new bioavailable iron forms. Optimal doses of

FeSO_4 and aqueous solution of CPPs providing for the maximum amount of solubilized iron were determined.

CONCLUSIONS

1. Activated cultures of propionic acid bacteria were found to synthesize heme-containing enzymes (catalase, SOD, and peroxidase), which opens new perspectives for their practical application.

2. Optimal doses of iron sulfate providing for the active bacteria growth and high number of viable cells of propionic acid bacteria were determined.

3. Addition of iron ions to the nutrient medium was found to stimulate synthesis of extracellular metabolites that promote adaptation of propionic acid bacteria to the metal.

4. Molecular-weight distribution and order of peptide fractions in casein phosphopeptides were studied at nanolevels.

5. The method of isolation of casein phosphopeptides was optimized to provide for the maximum yield of low-molecular weight peptide nanostructures with characteristic size of 1–10 nm capable of chelating maximum amount of iron (up to 7 mg/mL).

6. Complexes of casein phosphopeptide with microelements were studied, mechanism of the mineral ion binding with peptide fractions in the complexes was characterized, and the specific content of chelated mineral in the complexes was determined.

REFERENCES

1. Avtsyn, A., Zhavoronkov, A., Rosh, M., and Strochkova, L., *Mikroelementozy cheloveka* (Human Microelementoses), Moscow, 2005.
2. Vorob'eva, L., *Propionovokisllye bakterii* (Propionic Acid Bacteria), Moscow, 1999.
3. Gapparov, M., and Stan, E., Vliyanie caseinovykh fosfopeptidov na biodostupnost' mineralov (Effect of casein phosphopeptides on bioavailability of minerals), *Voprosy pitaniya (Nutrition Aspects)*, 2003, vol. 6, pp. 40–44.
4. Savijoki, K., and Palva, A., Purification and molecular characterization of tripeptides from *Lactobacillus helveticus*, *Appl. Environ. Microbiol.*, 2000, vol. 66, pp. 794–800.
5. Furlund, C.B., Ulleberg, E.K., Devold, T.G., Flengsrud, R., and Jacobsen, M., Identification of lactoferrin peptides generated by digestion with human gastrointestinal enzymes, *J. Dairy Science*, 2013, vol. 96, pp. 75–88.
6. Khamagaeva, I., Kachanina, L., and Tumurova, S., *Biotehnologiya zakvasok propionovokisllykh bakterii* (Biotechnology of Propionic Acid Bacteria Starters), Ulan-Ude, 2006.
7. Smirnov, I., Kol'tsov, G., Gladun, V., and Levina, A., Referentnyi metod opredeleniya zheleza (Reference

method for iron determination), *Problemy gematologii i perelivaniya krovi (Hematology and Blood Transfusion Problems)*, 1999, vol. 1, pp. 50–53.

8. Korolyuk, M.A., Ivanova, L.I., Maiorova, N.O., and Tokarev, V.E., Metod opredeleniya aktivnosti katalazt (Method for determination of catalase activity), *Laboratornoe delo (Laboratory Science)*, 1988, vol. 1, p. 16.

9. Lebedeva, O.V., Ugarova, N.N., and Berezin, I.V., Kineticheskoe izuchenie reaktsii okisleniya o-dianizidina perekis'yu vodoroda v prisutstvii peroksidazy khrena (Kinetic Study of o-dianizidin oxidation with hydrogen peroxide in the Presence of Horseradish Peroxidase), *Biokhimiya (Biochemistry)*, 1977, vol. 42, no. 8, pp. 1372–1379.

10. Sirota, T.V., Novyi podkhod v issledovanii protsessa autookisleniya adrenalina i ispol'zovanie ego dlya izmereniya aktivnosti superoksidmutazy (New approach to investigation of adrenalin autooxidation and its application to measurement of superoxide dismutase activity), *Voprosy meditsynskoi khimii (Medicinal Chemistry Issues)*, 1999, vol. 3, pp. 22–33.

11. Brilis, V.I., Brilene, T.A., Lentsner, Kh.P., and Lentsner, A.A., Mikrobiologiya (Microbiology), 1982, vol. 9, pp. 75–78.

12. Nevo, A.S., Pshenichnikova, A.B., Skladnev, D.A., and Shvets, V.I., Vliyanie deiterometanola i oksida deiteriya na rostovye kharakteristiki i biosintez ekzopolisakharida obligatnymi metilotrofnymi bakteriyami (Effect of deuteromethanol and deuterium oxide on growth characteristics and biosynthesis of exopolysaccharide by obligate methylotrophic bacteria), *Biotekhnologiya (Biotechnology)*, 2003, vol. 6, pp. 38–46.

13. Kanopkaite, S., *Kobalaminy (Cobalamines)*, Vilnius: Mokslas, 1978.

14. Tutel'yan, V.A., Spirichev, V.B., Shatnyuk, and L.N., Korrektsiya mikronutrientnogo defitsyta — vazhneishii aspekt kontseptsii zdorovogo pitaniya naseleniya Rossii (Correction of micronutrient deficiency as a key aspect of the concept of healthy nutrition in Russia), *Voprosy pitaniya (Nutrition Issues)*, 1999, vol. 1, pp. 3–11.

15. Khamagaeva, I.S., Krivonosova, A.V., and Radnaeva, R.B., Biotekhnologicheskii potentsyal propionovokislykh bakterii (Propionic acid bacteria potential for biotechnology), *Molochnaya promyshlennost' (Dairy Industry)*, 2007, vol. 11, pp. 30–31.



UDC 664.014/019
DOI 10.12737/1516

NEW TECHNOLOGICAL APPROACHES TO CANNING CEPHALOPOD MOLLUSKS

L. V. Shul'gina¹, N. V. Dolbnina¹, L. Yu. Lazhentseva², and Yu. P. Shul'gin³

¹ Pacific Research Fisheries Center,
Shevchenko alley 4, Vladivostok, 690091 Russia
phone: +7 (4232) 400-921, e-mail: shulgina@mail.ru;

² Far Eastern Technical Fisheries University,
str. Lugovaya 56b, Vladivostok, 690950 Russia
phone:/Fax: +7 (4232) 44-03-06, e-mail: lazhencheva.lyubov@mail.ru

³ Far Eastern Federal University (FEFU),
str. Sukhanov 8, Vladivostok, 690091 Russia
phone:/Fax: +7 (423) 243-23-15, e-mail: yuriyshulgin@mail.ru

(Received March 11, 13; Accepted in revised form May 28, 2013)

Abstract: With significant stocks and catches of cephalopod mollusks in the Far Eastern seas, their small output as canned goods is due to a low yield of the finished product. Research was conducted on the rational use of frozen raw cephalopod mollusks in the production of sterilized canned goods. New technological approaches to canning cephalopod mollusks that ensure canning profitability and replenish the consumer market of functional seafood are justified. It was established that the exclusion of the skinning of cephalopod mollusks from the canning technology could significantly increase the output and reduce the cost of the finished product. Oil extracts of spices used in the canning of cephalopod mollusks improve their quality by reducing the thermal effects on food during sterilization and the degree of thermal damage to nutrients.

Keywords: cephalopods, canned food, technology, quality

INTRODUCTION

Cephalopod mollusks make up a massive group of sea bioresources broadly spread in the world ocean [1]. A short life cycle and quick growth of cephalopod mollusks, as well as their ability to form compact clusters determine a high level of their commercial harvesting [2, 3].

Cephalopod mollusks are easily processable, allowing for the use of various processing methods and a wide range of products, including fermented ones [4–11].

The main commercial species of cephalopod mollusks in the Far Eastern seas are octopuses (*Octopus dofleini*) and the Commander (*Berryteuthis magister*) and Pacific (*Todarodes pacificus*) squids [12]. Annual squid catches are at least 240 000 t, and those of octopuses, 800 000–900 000 t. Despite these solid catches, the current highly processed goods of cephalopod mollusks are produced in amounts insufficient for the country's population. In the consumer market, they are represented mainly by fresh frozen products. In small amounts, cephalopod mollusks are processed into dried, seasoned, and culinary products and preserves, filled with various sauces, but these products have limited storage life and conditions, causing difficulties in their transportation and marketing. The annual output of canned squids is no more than 1.6 million standard cans, and canned

octopuses are not produced domestically.

At the same time, the nutritive tissues of cephalopod mollusks are characterized by high organoleptic properties, the presence of complete proteins, and insignificant amount of lipids, as well as a complex of mineral substances [13–20].

Various biologically active substances, including those that are rarely found in terrestrial animals and plants [21–27], have been found in the tissues of cephalopod mollusks; therefore, cephalopod-based products are very useful for various groups of the population and are recommended by nutritionists as ingredients of many diets. In recent decades, biologically active food additives and enzymatic preparations have been developed on the basis of cephalopod mollusks [28–31].

One of the reasons for the low use of raw materials from cephalopod mollusks in canning is the low yield of end products due to high losses of their nutritive part during processing, which makes them unprofitable as canned food under current conditions. The loss of raw materials during canning is explained by the fact that the traditional cephalopod canning technologies require thermal, enzymatic, or mechanical removal of skin integuments from the heads, pallia, and tentacles of cephalopods. At the same time, the skin of cephalopod mollusks belongs to nutritive tissues, containing amino acids, such as proline and oxyproline,

which are collagen components [14, 32]. China has developed a technology of producing collagen from the cephalopod skin left after the core production [33]. The preservation of cephalopod skin integuments during canning would increase the utilization factor of this valuable raw material and its end-product yield.

Another important factor of the low motivation of producers in cephalopod canning is the worsening of organoleptic characteristics of the product after sterilization due to the interaction of reducing sugars with amino acids during thermal conditioning (the Maillard reaction) and the formation of melanoidins. As is known, melanoidin formation leads to the browning of sterilized mollusk meat, the appearance of a caramelization smell, and the loss of its inherent flavor characteristics [34, 35]. A decreased thermal effect on the product during sterilization makes it possible to reduce the activity of the Maillard reaction and improve the quality of canned goods.

The goal of this study was to justify and develop new technological approaches to cephalopod canning that reduce raw-material losses and ensure the high quality of end products.

OBJECTS AND METHODS OF RESEARCH

The object of research was frozen raw materials of squids and octopuses. Additional materials used were edible salt, vegetables, legumes, vegetable oil, olives, and spices. Glass jars III-5-58-120-00 with a capacity of 120 cm³ (Germany) with twist-off tin lids were used for canning. When developing sterilization regimes for canning cephalopods, we used the spores of the *Cl. sporogenes-25* test strain, obtained at the laboratory of microbiology of OAO Giprorybflot (St. Petersburg).

Samples for analysis, the general chemical composition, and the safety indicators of raw materials and end products were obtained by standard methods. An atomic adsorption photometer, Nippon Jarall Asl, model AA-855 (Japan), was used to detect mineral substances. The amino-acid composition of proteins was identified with an ammo-acid analyzer, Hitachi L-8800 (Japan). The biological value of proteins was evaluated by the amino-acid score in line with the recommended composition of the "ideal" protein according to the FAO/WHO scale. The taurine amino acid was detected by the spectrophotometric method [36]. The biological value of raw materials and products was determined by the relative biological value (RBV) indicator using ciliated infusorian *Tetrahymena pyriformis* in line with the recommendations of Yu.P. Shul'gin et al. [37]. The output of intermediate products and canned goods was determined by the results of control tests.

RESULTS AND DISCUSSION

Studies on frozen raw materials from commercial catches in recent years show that the average mass of a squid specimen is no more than 0.3 kg, and that of an octopus, no more than 3.2 kg. The general chemical composition of the nutritive part of cephalopod mollusks is given in Table 1. The mollusks somewhat differed in protein and moisture contents: the Commander squid (a deepwater species) has tissues

more watery than those of the Pacific squid and octopuses and contains fewer proteins.

Table 1. Chemical composition of the nutritive part of cephalopods

Substances	Quantity, % of the total body mass		
	<i>Todarodes pacificus</i>	<i>Berryteuthis magister</i>	<i>Octopus dofleeni</i>
Moisture	75.3±4.1	82.1±4.8	78.7±4.3
Protein	19.5±1.8	12.5±1.5	16.1±1.4
Carbohydrates	2.1±0.3	2.3±0.3	2.5±0.5
Fat	1.4±0.2	1.3±0.5	0.5±0.2
Minerals	1.7±0.2	1.8±0.2	2.2±0.3

The traditional preparation of semiproducts for canning included the cutting of cephalopod mollusks, during which the insides and skin were removed. It was established that the nutritive part of mollusks before skin removal was about two-thirds of their total body mass. After skinning, it was observed that nutritive mass losses during cephalopod skinning were from 18.8 ± 1.3 to 33.6 ± 2.0%. The highest processing losses were characteristic of octopuses, whose skin with suckers on their arms comprises a substantial share in the total mass of their nutritive part.

The investigation of the general chemical composition of skinned and unskinned cephalopod semiproducts did not reveal any actual differences in the content of individual nutrients.

Comparative analysis of the amino-acid composition of skinned and unskinned cephalopod semiproducts also showed their similarity. The sum of essential amino acids (EAAs) in the squid tissues was practically the same and exceeded slightly the sum of essential amino acids of the reference protein (Table 2). Threonine was a deficient essential amino acid in the squid proteins, and valine, in the octopus proteins.

Table 2. Essential amino acids in the nutritive tissues of cephalopods

Amino acid	FAO/WHO reference	Content in semiproducts (g/100 g of protein) from		
		<i>Berryteuthis magister</i>	<i>Todarodes pacificus</i>	<i>Octopus dofleeni</i>
Valine	5.0	5.0	6.3	2.9
Isoleucine	4.0	5.1	5.9	4.0
Leucine	7.0	10.2	9.4	6.9
Lysine	5.5	7.3	8.2	5.7
Methionine + cystine	3.5	3.4	4.5	5.0
Threonine	4.0	3.1	1.7	5.8
Phenylalanine + tyrosine	6.0	8.4	6.9	6.7
Tryptophane	1.0	1.0	1.0	1.1
Sum of EAAs	36.0	39.9	39.9	38.1

The characteristic feature of the squid and octopus proteins' composition was high contents of proline, taurine, and other nitrogenous matters, which take part in the osmoregulation of mollusks [38].

Proline is a major amino acid that ensures the synthesis of collagen in the human organism, which, in

turn, is the main building material for bones, tendons, ligaments, and the skin, ensuring the formation of strong and elastic tissues on the surface of mechanical damages of various organs [39].

Taurine is a sulfur-containing amino acid, which is contained formlessly in the cardiac-muscle cells, skeletal muscles, central nervous system, retina, and other tissues [40, 41]. In the human organism, it suppresses the increase in the level of cholesterol in the blood, normalizes the functions of the visual organs, prevents a high aggregation of thrombocytes and the convulsive activity of the brain, and displays antitoxic and antioxidant properties, having powerful adaptogenic and health-improving effects.

As is known, taurine is present in the cephalopod tissues in amounts exceeding 100 times and more its content in plants and other animals [21, 42].

The skinned meat and skin integuments of cephalopod mollusks did not differ much in proline and taurine contents (Table 3). The muscle tissue of squids contained more of them than their skin. In octopuses, high amounts of taurine were detected both in the muscle tissue and in the skin. The proline content in the octopus tissues was smaller than in squids, but its amount in different parts of octopuses was equal.

Table 3. Proline and taurine contents in cephalopod tissues

Cephalopods	Quantity, g per 100 g of proteins			
	proline		taurine	
	skinless meat	skin	skinless meat	skin
<i>Todarodes pacificus</i>	3.9–7.3	2.8–4.9	0.5–1.3	0.4–1.1
<i>Beryteuthis magister</i>	2.4–5.6	1.2–4.8	0.5–1.1	0.3–1.0
<i>Octopus dofleini</i>	1.8–3.8	1.4–3.9	1.2–2.6	1.0–2.5

It follows from the above data that, if the cephalopod skin is preserved during the preparation of semiproducts for canning, the factor of raw material use will increase, as well as the output of mass consumer and directed-action products with high contents of rare nutrients, valuable for humans.

To assess the possibility of producing more high-quality preserves from a unit of raw materials on the basis of unskinned semiproducts, "natural," "blanched in oil," and "blanched and smoked in oil" samples of canned goods were manufactured.

Taking into account the proposed assortment, after the cutting of mollusks and the careful washing and removal of excess moisture, the semiproducts underwent additional preprocessing. In order to obtain a natural sample, a raw cephalopod semiproduct was sliced: the pallium, into slices of no more than 7–8 mm wide; the octopus arms, into rings; and the squid tentacles were left intact for prepacking. For the samples blanched in oil, a dressed semiproduct was blanched; squid semiproducts were blanched in boiling water for three minutes; the octopus samples were blanched for 40 min. After blanching and additional dewatering, a semiproduct was cut into pieces of no more than 10×40 mm. The samples smoked in oil were

obtained from blanched semiproducts that were grilled until the meat had a slight smoking flavor. The soft-smoked cephalopod meat was cooled on grills to 30–35°C and then cut into pieces of no more than 10×40 mm.

To compare the yield and quality indicators of the end products, reference samples of canned products were made from skinned semiproducts obtained according to the traditional technology.

The appearance of a sliced semiproduct from unskinned squids differed slightly from samples of skinned mollusks. A semiproduct from an unskinned octopus differed from a skinned sample in its characteristic purple tincture.

The quantity of semiproducts obtained for canning reference (skinned) and test (unskinned) cephalopod samples depending on the canning method is given in Fig. 1.

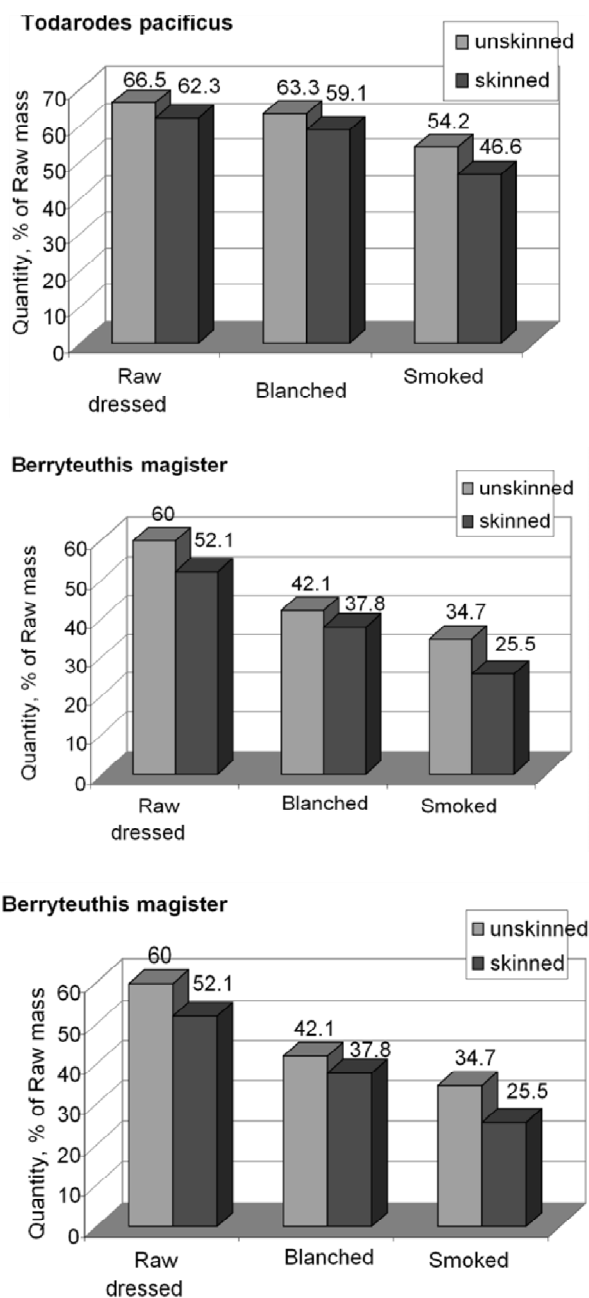


Fig. 1. Quantity of cephalopod semiproducts unskinned and skinned for various canning assortments.

As we see, if skinning is excluded from the

technology of cephalopod canning, the semiproduct yield for various assortments will be much greater than after skinning, improving economic performance.

A prepared sliced cephalopod semiproduct was packed in glass jars. The packing rates for components for the proposed canning assortments are given in Table 4.

Table 4. Packing rates for glass-jar components for various cephalopod canning assortments

Canned goods	Component mass, g					
	Cephalopods	saline solution	oil	salt	olives	paprika
Natural unskinned squid	90	20	-	-	-	-
Natural unskinned octopus	90	20	-	-	-	-
Natural mixed octopus and surf clam	90	20	-	-	-	-
Octopus in oil	89	-	20	1	-	-
Octopus with paprika in oil	88.3	-	20	1	-	0.7
Octopus with olives in oil	70	-	20	1	19	-
Squid in oil	70	-	20	1	19	-
Soft-smoked octopus in flavored oil	89	-	20	1	-	-
Soft-smoked squid in flavored oil	89	-	20	1	-	-

To obtain natural preserves, jars with a sliced blanched semiproduct (the pallium, squid tentacles, and octopus arms) were filled with 20 cm³ of filtered 2 % salt brine.

For mixed natural octopus and surf clam preserves, we used a bivalve mollusk, the Sakhalin surf clam, prepared in the following way: after unfreezing, cleaning, and washing, the surf clam muscle together with the pallium was loaded into a boiling 2% salt brine at a ratio of 1 : 3, four minutes after the simmer, the surf clam muscle was taken out of the salt brine, cooled, and cut into two-to-three parts. Fifty grams of octopus cut into pieces and 40 g of surf clam were packed into a jar, and the jar was filled with salt brine.

The preserves were sterilized at no more than 115°C, since a higher temperature has a negative effect on the protein and carbohydrate components of seafood [43]. The preserves were sterilized and cooled in water with back pressure (0.18 MPa) in an AB-2 autoclave; all preserves were cooled in water with back pressure.

Rational formulas of sterilization regimes were developed to ensure the commercial sterility of preserves. The values of the normative sterilizing effect (F_n) for the test and reference canned samples were estimated after determining the heat resistance of the spores (constants $D_{121.1}^{\circ\text{C}}$ and $Z^{\circ\text{C}}$) of the test strain, *C. sporogenes-25*, in an extract from unsterilized jars with products for each assortment separately. It was established that the time of sterilization proper to obtain

commercially sterile natural preserves was at least 45 min. and at least 50 min. for other types.

The amount of preserves made from unskinned cephalopods was much larger than that made from skinned semiproducts. Table 5 shows that the exclusion of the skinning operation from the cephalopod canning technology increased the yield of the end product, depending on the product assortment and type, by 12.9–52.8%.

Table 5. Increased output of preserves made from cephalopod unskinned semiproducts

Canned cephalopods	Increased output (%) of preserves from		
	squid		octopus
	Commander	Pacific	
Natural	12.9	19.1	42.1
Blanched in oil	14.8	27.1	52.8
Soft-smoked in oil	31.1	37.2	50.2

The raw material saving per unit of end product helped improve cephalopod canning profitability. Thus, the economy of raw materials to produce 1000 standard cans of natural preserves from Pacific squid amounted to 2523.48 rubles; from Commander squid, 15 146.3 rubles; and from octopus, 9292.0 rubles.

The like finished preserves from unskinned and skinned cephalopods had no significant differences in their nutritive and energy values.

When evaluating the amino-acid composition of preserves from unskinned semiproducts, high contents of proline and taurine were established. Table 6 shows that 100 g of unskinned cephalopod preserves meet the daily requirement for these substances of 10% and higher. The high contents of proline and taurine in the new cephalopod preserves make them functional products.

Table 6. Proline and taurine contents in unskinned cephalopod preserves

Variants of preserves	Recommended daily consumption for humans	Content in preserves, g per 100 g of product	Share of recommended daily consumption, %
proline			
Natural unskinned (Commander) squid	4.5 g	0.64±0.5	14.2
Natural unskinned octopus		0.48±0.04	10.7
(Pacific) squid in oil		1.2±0.3	26.6
taurine			
Soft-smoked squid in oil	400.0 mg	234.0±0.51 mg	58.5
Natural unskinned octopus		321.0±0.22 mg	80.25

In preserves from skinned semiproducts, the cephalopod meat was more compact and less juicy compared to the test samples, which was due to the loss of tissue juice during preprocessing. In the samples of preserves in oil, whose sterilization time was 5 min.

longer than that of natural preserves, a slight caramelization flavor was present due to thermal damage of sterilized objects and to the formation of Maillard reaction products.

A known method of reducing the heat resistance of the spores of microorganisms and, consequently, of reducing the severity of preserve sterilization regimes is to create an acidic medium of canned products, which is of little use for the assortment of preserves in oil. Therefore, we should seek techniques to reduce the excessive thermal load on products during sterilization, to diminish the thermal resistance of microorganisms, but at the same time to guarantee their commercial sterility.

It has been established previously that the oily extracts of spices used in the fish canning technology have a marked antimicrobial activity and can inhibit the development of the vegetative cells of microorganisms and reduce the thermal resistance of spore microorganisms in canned goods [44, 45]. Therefore, to ensure the full reduction of the values of the normative sterilizing effect (F_n) and, consequently, of the thermal load (heat damage) on the product, oil was replaced with a spicy--oily extract, the so-called flavored oil, during canning.

Flavored vegetable oil, prescribed for canning recipes, was prepared as follows: ground spices were mixed with oil, heated to 100°C, at a ratio of 5 : 100 and seasoned for 24 h, after which the liquid part was separated from the lees [44]. The flavored oil acquired a tincture characteristic of the spice used (cadmium orange, orange, or other).

The reference samples of preserves were filled with the vegetable oil used to produce spice--oily extracts.

The lethal time (constant $D_{121.1}^{\circ C}$) for the spores of the test strain, *C. sporogenes-25*, in the extractions of all preserves in spicy--oily extract was lower than for the

like preserves in vegetable oil. Figure 2 shows that the test samples of "Octopus in oil" had a value of constant $D_{121.1}^{\circ C}$ lower by 0.11 conventional minute than in the like reference samples. Taking into account the obtained values of constant $D_{121.1}^{\circ C}$, we calculated indicators F_n for the test samples of preserves that were lower compared to the reference samples.

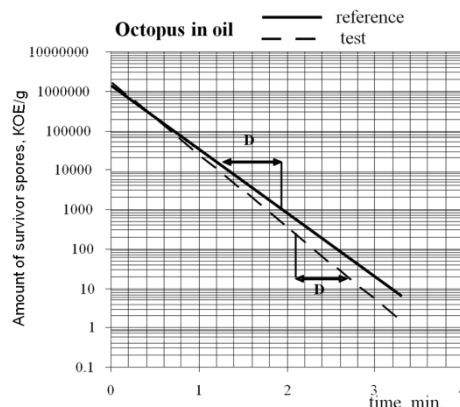


Fig. 2. Survivability and lethal-time curves ($D_{121.1}^{\circ C}$) of the *C. sporogenes-25* spores in the reference and test samples of "Octopus in oil."

The obtained data were used to determine the duration of the sterilization proper of preserves, which ensured the necessary values of the actual sterilizing effect (F_a) during the sterilization of preserves.

It was established that, to reach the necessary sterilizing effect, the duration of the sterilization proper of the test samples of preserves was 5 min. shorter compared to the reference samples (Table 7).

Table 7. Duration of sterilization and the actual sterilizing effect (F_f) for the test and reference samples of preserves

Preserves	Preserves in					
	vegetable oil			spicy--oily extract		
	F_n , conv. min.	Sterilization time, min.	F_f , conv. min.	F_n , conv. min.	Sterilization time, min.	F_f , conv. min.
Blanched in oil	5.28	20–50–20	6.9	4.50	20–45–20	5.68
Soft smoked in oil	5.28	20–50–20	6.9	4.64	20–45–20	5.8

The reliability of the preliminary developed sterilization regimes was confirmed by the results of laboratory testing by the method of artificial inoculation of preserves in which vegetable oil was fully replaced with the spicy-oily extract. To this end, 30 jars were taken and spores of *C. sporogenes-25* were introduced into the center of each jar, after which the jars were sterilized, and their commercial sterility was analyzed. To compare the quality of preserves, five jars of each assortment, not inoculated with bacterial spores, were sterilized, as well as preserves in vegetable oil. After sterilization, all the preserves were commercially sterile, which indicated the reliability of regimes with shortened sterilization times.

Sterilized preserves in spicy--oily extracts did not differ from samples in vegetable oil and were characterized by attractive appearance and low spicy flavor. All the test samples of preserves were free from the caramelization flavor.

Thus, the use of spicy--oily extracts in the production of preserves "in oil" made it possible to reduce the duration of the sterilization proper of preserves, which led to a reduced thermal load on the product and, consequently, a reduced intensity of the Maillard reaction.

The efficiency of the positive effect of replacing vegetable oils in the composition of cephalopod preserves "in oil," caused by the reduced duration of their sterilization by 5 min., was evaluated by the effect

of heat damage on microbial and raw-material cells, including the survivability of protein and biologically valuable nutrients.

During the sterilization of preserves, part of spore-forming cells of *Bacillus subtilis* (*B. subtilis*) is able to survive and remain viable for the whole storage period [45]. However, the presence of bacilli, even in a dormant state, affects the quality of preserves and leads to the "aging" of protein structures. The sanitary standards permit the presence of *B. subtilis* within the "residual" microflora in sterilized preserves, but their number in sterilized preserves of group A should not exceed 11 cells per 1 g of the product.

Therefore, the number of *B. subtilis* cells was determined before and after the sterilization of the newly developed preserves in which spicy--oily extracts were used. Preserves with the vegetable oil used to obtain the spicy--oily extracts were used as reference products. It was established that before sterilization the average number of bacilli in 1 g of preserves was 320 ± 64 cells. After sterilization, 1 g of commercially sterile cephalopod preserves in vegetable oil revealed from 3 to 13 viable *B. subtilis* cells. Bacilli were not found in preserves with spicy--oily extracts, which indicated the expressed sporicidal effect of the oil filling.

An indicator of the degree of survival of the nutritive value of a product during sterilization is heat damage to proteins, which affects their digestibility. To evaluate the effect of spicy--oily extracts and sterilization regimes on the digestibility of the protein component of preserves developed for assortments on various oil bases, special research was conducted by biotesting. Figure 3 shows the results of digesting protein products before and after sterilization in the test and reference samples of preserves.

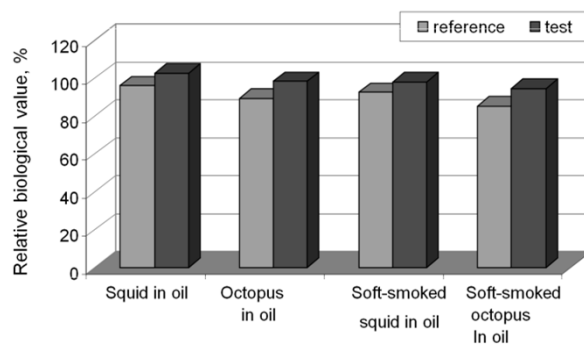


Fig. 3. Digestibility of canned cephalopod products in oil (reference) and in spicy--oily extracts (test).

As is seen from the figure, the replacement of vegetable oil with spicy--oily extracts was accompanied by increased bioavailability of the protein component of preserves. It is possible that minor liposoluble components of spices affected positively the digestion of proteins in products filled with spicy--oily extracts.

As is known, high-temperature processing destroys fatty acids [46]. The effect of spicy--oily extracts on the stability of the lipid component in cephalopod preserves filled with oil was assessed by comparing the fatty--acid composition of the reference and test samples of sterilized products. Table 8 shows the results of the study of the fatty--acid composition of the oil component in the reference (with vegetable oils or their blends) and test (filled with spicy--oily extracts prepared on the same oils or their blends) samples of cephalopod preserves.

Table 8. Comparative characteristics of the fatty--acid composition of the oil base of the reference and test samples of seafood preserves

Fat phase of preserves	Sum of fatty acids in preserves (% of the total amount of fatty acids)					
	in vegetable oil			in spicy--oily extract		
	saturated	monounsaturated	polyunsaturated	saturated	monounsaturated	polyunsaturated
Squid in oil						
Corn oil	17.2	27.6	55.2	14.9	26.7	58.4
Sunflower oil	17.5	26.4	56.1	14.0	25.6	61.1
Octopus in oil						
Sunflower oil	21.7	26.1	52.2	17.3	25.4	57.3
Soft-smoked squid in flavored oil						
Soybean oil	20.8	25.5	55.7	16.6	22.1	61.3
Soybean and corn oil blend (55:45)	16.5	25.7	57.8	15.9	24.6	59.5
Soybean and sunflower oil blend (60:40)	17.6	24.1	8.3	16.2	23.7	60.1
Soft-smoked octopus in flavored oil						
Olive oil	21.0	16.3	62.7	17.2	12.5	70.3
Soybean and sunflower oil blend (60:40)	21.2	24.5	54.3	17.6	23.4	59.0

The quoted results show that the oil component in the reference and test samples of preserves differed in fatty acid contents. In all the assortments of preserves in

vegetable oils, the sum of polyunsaturated fatty acids was much lower than their amount in preserves filled with spicy--oily extracts. This indicates that a longer

duration of the sterilization proper of preserves (the reference preserves by 5 min.) leads to the largest heat damage to the carbon chains of high-molecular unsaturated fatty acids. During their destruction, fatty acids with smaller carbon chains are formed and accumulated. Oil blending improves the resistance of the oil component in the composition of preserves to the sterilization temperature, especially when they are used in spicy--oily extracts. Consequently, the full replacement of vegetable oils with spicy--oily extracts makes it possible to reduce the degree of heat damage to the nutrient material of products when cephalopod preserves are sterilized.

The research results were implemented during the development of technological instructions and technical specifications for the production of new preserves. Regional and industry degustations pointed to their high consumer attributes. The fish-canning enterprise ZAO

APK Slavyanskii-2000, Primorski krai) manufactured batches of new cephalopod preserves that were in demand among buyers.

CONCLUSIONS

New technological approaches have been developed to the canning of cephalopod mollusks that ensure canning profitability and replenish the consumer market with functional seafood.

The exclusion of the skinning process from the cephalopod canning technology helps increase considerably the yield of high-quality products, reducing their cost, and broaden the range of products.

The use of spicy--oily extracts as an oil filling in the cephalopod canning technology improves product quality by reducing the necessary level of thermal effect on products during sterilization and the degree of heat damage to their nutrients.

REFERENCES

- Jereb, P., and Roper, C.F.E., *Cephalopods of the World. An Annotated and Illustrated Catalogue of Cephalopod Species Known to Date*, Vol. 1: *FAO Species Catalogue for Fishery Purposes*, 2005, Rome: FAO.
- Boyle, P., *Bulletin of Marine Science*, 2002, vol. 71, no. 1, pp. 13–16.
- Rocha F., Guerra A. and Gonzales A.F., *Biological Reviews of the Cambridge Philosophical Society*, 2001, vol. 76, pp. 291–304.
- Duvalina, I.A. and Efremov, O.V., *Rybprom (Fish industry)*, 2009, no. 2, pp. 33–35.
- Podkorytova, A.V. and Slapoguzova, Z.V., *Rybnoe khozyaistvo (Fishery)*, 2007, no. 3, pp. 99–102.
- RF Patent No. 1837802, 1993.
- RF Patent No. 2115345, 1998.
- Jpn. Patent No. 25866-65, 1965.
- Fr. Patent No. 86101825.7, 1986.
- Jpn. Patent No. 850517, 1993.
- Gr. Patent No. 160397, 2012.
- Report on the Main Fishery Research Results in 2010*, 2011, Moscow: VNIRO.
- Zyuz'gina, A.A. and Kupina, N.M., *Khanenie i pererabotka sel'khozsyrya (Storage and processing of agricultural raw materials)*, 2000, no. 10, pp. 40–42.
- Kupina, N.M. and Zyuz'gina, A.A., *Khanenie i pererabotka sel'khozsyrya (Storage and processing of agricultural raw materials)*, 2002, no. 7, pp. 27–29.
- Papan, F., Jazayeri, A., Motamedi, H., and Mahmoudi, S., *Journal of American Science*, 2011, vol. 7, no. 1, pp. 154–157.
- Nurjanah, Jacob, A.M., Nugraha, R., Sulastri, S., Nurzakiah, and Karmila, S., *Advance Journal of Food Science and Technology*, 2012, vol. 4, no. 4, pp. 220–224.
- Nutritional and Functional Properties of Squid and Cuttlefish*, Ed. by Masayo, O., Fujii, and Tateo, 2000, Tokyo: National Cooperative Association of Squid Processors.
- Ramasamy, P., Subhadrappa, N., Sudharsan, S., Seedeivi, P., Shanmugam, V., and Shanmugam, A., *African Journal of Food Science*, 2012, vol. 6, no. 22, pp. 535–538.
- Rosa, R., Nunes, M.L., Sousa, R. C., *Bulletin of Marine Science*, 2002, vol. 71, pp. 739–751.
- Rosa, R., Pereira, J., Nunes, M.L., *Marine Biology Research*, 2005, vol. 146, no. 4, pp. 739–751.
- Ayushin, N.B., Petrova, I.P., and Epshtein, L.M., *Izvestiya Tikhookeanskogo nauchno-issledovatel'skogo rybokhozyaistvennogo tsentra (Bulletin of the Pacific research fishery center)*, 1999, vol. 125, pp. 52–55.
- Bernay, B., Baudy-Floch, M., Gagnon, J., and Henry, J., *Peptides*, 2006, vol. 27, no. 6, pp. 1259–1268.
- De Koning, A.J., *Journal of the Science of Food and Agriculture*, 2006, vol., 61, no. 1, pp. 129–132.
- Chacko, D. and Patterson, J., *Indian Journal of Microbiology*, 2005, vol. 45, no. 3, pp. 223–226.
- Gomarhi, P., Nair, J.R., and Sherief, P.M., *Indian Journal of Marine Sciences*, 2010, vol. 39, pp. 100–104.
- Nair, J.R., Pillai, D., Joseph, S.M., Gomathi, P., Senan, P.V., and Sherief, P.M., *Indian Journal of Geo-Marine Sciences*, 2011, vol. 40, no. 1, pp. 13–27.
- Nirmale, V., Nayak, B.B., Kannappan, S., and Basu, S., *Journal of the Indian Fisheries Association*, 2002, vol. 29, pp. 65–69.
- Borovskaya, G.A., Mikheev, E.V., Epshtein, L.M., et al., *Izvestiya TINRO (TINRO bulletin)*, 2006, vol. 146, pp. 294–299.
- RF Patent No. 2171066, 2000.
- RF Patent No. 22550047, 2005.

31. Mikheev, E.V. and Kovalev, N.N., *Izvestiya TINRO (TINRO bulletin)*, 2009, vol. 159, pp. 326–338.
32. Kozyreva, O.B., *Izvestiya TINRO (TINRO bulletin)*, 1999, vol. 125, pp. 8–84.
33. China Patent No. 101245104, 2012.
34. Safronova, T.M., *Aminosakhara promyslovykh ryb i bespozvonokhnukh i ikh rol' v formirovani kachestva produktov (Amino Sugars of Commercial Fishes and Invertebrates and Their Role in the Formation of Food Quality)*, Moscow: Pishchevaya promyshlennost', 1980.
35. Michiro, S. and Hirobumi, K., *Bulletin of the Japanese Society of Scientific Fisheries*, 1980, vol. 46, no. 10, pp. 1261–1264.
36. Charles, J. and Parker, J.R., *Journal of Analytical Biochemistry*, 1980, vol. 108, pp. 303–305.
37. Shul'gin, Yu.P., Shul'gina, L.V., and Petrov, V.A., *Uskorennaya biotis otsenka kachestva i bezopasnosti syr'ya i produktov iz vodnykh bioresursov (Accelerated Biotic Assessment of the Quality and Safety of Raw Materials and Products from Aquatic Bioresources)*, Vladivostok: TEA, 2006.
38. Ivanovo, A.M., Rainer, S.F., and Wadley, V.A., *Comp. Bioche. Physiol.*, 1981, vol. 70, no. 1. pp. 17–22.
39. Williamson, MR., *Bioche. J.*, 1994, vol. 297, pp. 249–260.
40. Hittable, R.J., *Taurine Nutr. and Neurol. Proc. Simp. Taurine: Quest. and Answers*, 1982, New York, pp. 97–98.
41. Ayushin, N.B., *Izvestiya Tikhookeanskogo nauchno-issledovatel'skogo rybokhozyaistvennogo tsentra (Bulletin of the Pacific research fishery center)*, 2001, vol. 129, pp. 129–145.
42. Sajama, M. and Kobayashi, H., *Bulletin of the Japanese Society of Scientific Fisheries*, 1980, vol. 46, no. 10, pp. 1261–1264.
43. Shvidkaya, Z.P. and Blinov, Yu.G., *Khimicheskie i biotekhnologicheskie aspekty teplovogo konservirovaniya gidrobiontov dal'nevostochnykh morei (Chemical and Biotechnological Aspects of Thermal Canning of Hydrobionts of Far Eastern Seas)*, Vladivostok: Dal'nauka, 2008.
44. RF Patent No. 2427277, 2011.
45. Lazhentseva, L.Yu. and Kim, E.N., *Pishchevaya promyshlennost' (Food industry)*, 2012, no. 6. pp. 38–40.
46. Brazhnikov, A.M., *Teoriya termicheskoi obrabotki myasoproduktov (The Theory of Thermal Processing of Meat Products)*, Moscow: Agropromizdat, 1987.



UDC 577.112.387.2

DOI 10.12737/1542

EXPRESSION OF RECOMBINANT L-PHENYLALANINE AMMONIA-LYASE IN ESCHERICHIA COLI

O. O. Babich, L.S. Dyshlyuk, and I. S. Milent'eva

Kemerovo Institute of Food Science and Technology,
bul'v. Stroitelei 47, Kemerovo, 650056 Russia
phone:/Fax: +7 (3842) 39-68-73, e-mail: olich.43@mail.ru

(Received May 22, 2013; Accepted in revised form June 24, 2013)

Abstract: The *pal* gene coding for L-phenylalanine ammonia-lyase of *Rhodospodium toruloides* (GenBank entry no. X12702.1) with optimized sequence was cloned into an expressing vector pET28a. Three parameters of expression (inductor type, duration, and temperature of induction) were optimized, which resulted in a strain producing recombinant L-phenylalanine ammonia-lyase with the maximal productivity, that is, $35 \pm 1\%$ to total cell protein, upon utilization of 0.2% lactose (according to Studier) induction during 18 h at 37°C. The recombinant L-phenylalanine ammonia-lyase was found to be insoluble by 99%. Solubility of the protein did not improve upon utilization of 1 mM IPTG as an inductor instead of 0.2% lactose, or upon bacterium cultivation at various temperatures, that is 25°C and 37°C.

Keywords: L-phenylalanine ammonia-lyase, cloning, expression, recombinant protein, induction, L-phenylalanine, phenylketonuria

INTRODUCTION

L-Phenylalanine ammonia-lyase (PAL, EC 4.3.1.5) catalyzes the reaction of reversible deamination of L-phenylalanine to *trans*-cinnamic acid and ammonia [1]. PAL is the key enzyme of phenylpropanoids metabolism in plants and fungi, where it is involved in biosynthesis of secondary metabolites (flavonoids, furanocoumarins, and components of cell wall) and exists in multiple isoforms [2]. First three-dimensional structure of PAL from the yeast species *Rhodospodium toruloides* has been determined at 2.1 Å resolution. Molecular weight of PAL is 76880 Da. Molecule of the enzyme contains 716 amino acid residues. Typically, optimal pH values for PAL are in the range of 8.2 to 9.0. Optimal temperature lies within the range of 35 to 55°C in function of the enzyme source [3].

Enzyme isolation is of interest for application as a therapeutic agent in treatment of phenylketonuria; it may be used directly as a drug in phenylketonuria therapy or in production of phenylalanine-free food [1, 2]. In addition to medicinal applications, PAL may be used in biotechnology to produce L-phenylalanine from *trans*-cinnamic acid [3].

Application of *Escherichia coli* strain producing recombinant L-phenylalanine ammonia-lyase as a source of the enzyme in industry seems promising [4, 5].

Escherichia coli is one of the most efficient and simple ways of large-scale production of recombinant proteins in view of the well-studied genetics of the microorganism, availability of convenient expression vector systems and host strains, simple use, low price,

and high levels of target gene expression reaching 40–45% to the total cell protein [5, 6].

The aims of the present work were cloning of L-phenylalanine ammonia-lyase gene and its expression in *E. coli* cells, as well as characterization of the expression product.

MATERIALS AND METHODS

Reagents. Acrylamide, *N,N'*-methylene-bisacrylamide, sodium dodecylsulfate (SDS), bromophenol blue, glycogen, glycerol, 2-mercaptoethanol, ammonium persulfate, Tween 20, Triton X-100, Tris(hydroxymethyl)aminomethane (Tris), *N,N,N',N'*-tetramethylethylenediamine (TEMED), ethylenediaminetetraacetic acid (EDTA), and glucose from Serva (Germany); agarose, ethidium bromide, bovine serum albumin (BSA), deoxyribonucleoside 5'-triphosphates, mineral oil, protease K, isopropyl β-D-1-thiogalactopyranoside (IPTG), and lysozyme from Sigma (United States); yeast extract, bacto-tryptone, and agar from Dafco (United Kingdom). Phenol, lysozyme, chloroform, ethanol, acids, alkalis, and salts (analytically and chemically pure grades) from Reakhim (Russia); LB medium from Gibco BRL (United States); kanamycin sulfate from Sintez (Kurgan, Russia); restriction endonucleases NcoI and HindIII, T3 DNA ligase, Pfu-pol, and Taq-pol from Sibenzim (Russia).

Bacterial strains. Cells of *E. coli* strain BL21[DE3]Star (Invitrogen, United States) of F- ompT hsdSB (rB-mB-) gal dcm rne131 (DE3) phenotype

containing λ De3 lyzogene and rne131 mutation in the genome were used for the target protein expression. Mutant gene rne (rne131) codes for a shortened RNAase E form, which decreases intracellular degradation of mRNA leading to increase in its enzymatic stability.

Plasmid DNA. Vector pET28a, containing promoter for T7 phage polymerase, lac-operon, ribosomal complex binding site (RBS), starting codon for translation of the cloned fragments, and a polyhistidine-tag fragment within the reading frame, was used for expression in *E. coli* cells. Any nucleotide sequence cloned in the vector is expressed as a protein fused with polyhistidine for convenience of further purification by immobilized metal affinity chromatography.

Gene synthesis was performed in such a way that it would contain restriction sites NcoI and HindIII for amplification and further insertion into the gene fragment of polylinker pET28a.

Amplification of the *pal* gene was performed by the method of polymerase chain reaction (PCR). Oligonucleotide primers were designed using the OLIGO (version 3.3) software taking into account the data on primary structure of the *pal* gene. To amplify the coding region of the *pal* gene from *R. toruloides*, sequence from GenBank database (X12702.1) was used as a template. At their 5'-ends, primers contained additional sequences incorporating restriction sites NcoI in case of the forward primer and HindIII, in case of the reverse one, in order to amplify the gene structural region and insert it into a polylinker of the pET28a expressing vector at relevant sites. Reverse primer was constructed so that the amplicon would not contain a stop codon and joining of the reading frames of the gene and *His₆* sequences would be ensured.

Polymerase chain reaction was performed in 20–50 μ L solution prepared on the basis of ten-fold buffer for Taq polymerase containing deoxynucleoside triphosphate, 200 μ M each, 0.5 μ M of each primer, 2 mM MgSO₄, 10 ng template, 2 units Taq DNA polymerase, and 0.1 units Pfu DNA polymerase. Temperature of annealing of oligonucleotides was calculated according to an empiric formula $T_m = 67.5 + 34[\% \text{GC}] - 395/n$, where $\%GC = (G + C)/n$, n is the number of nucleotides. Analysis of PCR products was performed by electrophoresis in 1% agarose gel.

Sanger sequencing was performed on an ABI3730xl (Applied Biosystems, United States) equipment using BigDye[®] Terminator v3.1 Cycle Sequencing Kit according to the manufacturers' protocols.

DNA hydrolysis by restriction endonucleases NcoI and HindIII was performed in buffer solutions under optimal conditions of incubation medium recommended for each of the enzymes by the manufacturers. Completion of hydrolysis was controlled by electrophoresis in agarose gel. Reaction mixture was purified from the reaction products using the QuickClean kit.

Isolation of DNA fragments from agarose gel. Samples of DNA were separated by electrophoresis in Tris–acetate buffer in a 0.7–0.8% agarose gel (Bio-Rad, United States) containing 0.3 μ g/mL ethidium bromide and analyzed by fluorescence under ultraviolet light at 254 nm. Gel pieces containing fragments of interest

were cut out and transferred into microcentrifuge tubes, then DNA fragments were eluted from the gel using the “Isolation of DNA from agarose gels” kit (Boeringer Mannheim, Germany). Sodium perchlorate was added to the tubes in the amount of 400 μ L per 100 mg weight of the cut out gel. The mixture was heated to 65°C, then agarose was dissolved in salt buffer. Glass milk microbeads were introduced into the suspension at the amount of 20 μ L per 100 mg of gel weight. In the salt solution, DNA contained in the gel adsorbed on the surface of the microbeads. They were washed (consecutive precipitation–resuspension) with the same salt solution once and with 70% ethanol, two times. DNA was desorbed from the beads by resuspension in TE buffer (10 mM Tris-HCl buffer, pH 7.4, 1 mM EDTA) in the amount of 50 μ L per 100 mg gel weight.

Ligation. Products of hydrolysis of the vector DNA obtained as described above and the *pal* gene amplicon were ligated by phage T4 DNA ligase. Concentrations of the vector and gene in the reaction mixture were 5 ng/mL each. Concentration of phage T4 DNA ligase was 5 units/ μ L. Reaction was performed at 15°C during 24 h.

Preparation of competent *E. coli* cells for transformation. To prepare competent cells for the following transformation by electroporation, individual colony was grown on LB agar and placed into 5 mL LB medium. Cells were grown during night at 37°C and constant stirring (250 rpm). Two milliliter of the night culture were placed into 200 mL LB medium. Cells were grown at 37°C at constant stirring (250 rpm) till the optical density at 600 nm reached 0.6, then they were sedimented by centrifugation during 10 min at 4000 g at 4°C. Cells were washed in deionized water in the initial volume followed by centrifugation. The procedure of washing was performed three times. After washing, cell sediment was resuspended in small volume of deionized water and centrifuged during 30 s at 5000 rpm in a microcentrifuge. Three volumes (of the cell sediment volume) of 15% glycerol solution were added to the sediment, it was resuspended and quickly frozen in liquid nitrogen. Cells ready for transformation were stored at –70°C.

Transformation of *E. coli* cells. Transformation of competent cells was performed by electroporation. Plasmid DNA (2 μ L) at concentration of 0.3–1.0 ng/ μ L was added to 12 μ L of competent cells and mixed; electroporation was performed in a GVI-1 generator of high-voltage impulses in sterile cells under electrical impulse strength of 10 kV/cm and duration of 4 ms. After transformation, cells were put in 1 mL SOC medium (2% bacto-tryptone, 0.5% yeast extract, 10 mM NaCl, 2.5 mM KCl, 10 mM MgCl₂, 10 mM MgSO₄, and 20 mM glucose) and incubated for 40 min at 37°C. After incubation 10–250 μ L cell suspension were inoculated into a selective LB medium containing kanamycin (25 μ g/mL) to select the recombinant clones.

Induction of gene expression with IPTG. Induction of expression of genes coding for the recombinant enzyme in producer strain was performed using IPTG at final concentration of 1 mM. For this purpose, a single producer strain colony was inoculated onto standard liquid medium LB containing kanamycin at concentration of 25 μ g/mL and 1% glucose and

fermented at 37°C in a rotor-type temperature-controlled shaker overnight at 250 rpm. Then, after optical density at 600 nm was measured, the culture was diluted with the LB liquid medium containing kanamycin at concentration of 25 µg/mL to the optical density of 0.1 OU and fermented during 2–3 h at 37°C to the optical density of 0.6–0.8 OU. Then, the culture was divided into two equal parts: IPTG was added to one of the parts to the final concentration of 1 mM and it was fermented during 5 h at temperature of 25°C or 37°C, cell aliquots collected for analysis at certain time intervals. The aliquots were stored at –20°C.

Autoinduction of expression with 0.2% lactose. To induce autoinduction of expression according to Studier [7], modified PYP-5052 medium, containing 1% peptone, 0.5% yeast extract, 50 mM Na₂HPO₄, 50 mM K₂HPO₄, 25 mM (NH₄)₂SO₄, 2mM MgSO₄, 0.5% glycerol, 0.05% glucose, and 0.2% lactose, was used.

A single colony of producer strain was inoculated into PYP-5052 medium containing 25 µg/mL kanamycin. After that, the colony was fermented at 25°C or 37°C in a temperature-controlled rotor-type shaker at 250 rpm during 32, or 18 h, or till no significant change in optical density at 600 nm occurred per 1 h. Then, an aliquot of cells was collected for analysis. Aliquots were stored at –20°C.

Polyacrylamide gel electrophoresis (PAGE). Electrophoresis of cell lysates and proteins was performed according to disk-electrophoresis procedure in 10% PAGE under denaturing conditions according to Laemmli.

Destruction of bacterial cells under native conditions. Bacterial cells were destroyed under native conditions using ultrasonic treatment. Wet cell sediment obtained from 300 µL culture medium were resuspended in 30 mL buffer (50 mM Tris-HCl, pH 8.0, 20 mM EDTA, pH 8.0) and sonicated for 10 min at the amplitude of 60%, sonication duration 30 s, pause of 30 s, and a working temperature of 4°C. Destruction was controlled by inoculation of cells after sonication on a standard agarized LB medium containing kanamycin at concentration of 25 µg/mL. After sonication, cell lysate was centrifuged during 20 min at 15000 g, and the precipitate and sediment were used for analysis of p17 protein localization.

Computer methods of data analysis. Analyses of nucleotide and amino acid sequences were performed using a Lasergene v.7.1.0 (DNASTar, United States) and BioEdit v.5.0.9 software packages.

Search for homologous sequences was performed using the BLAST2 (<http://www.wbi.ac.uk/blastall/>) software. Comparison of amino acid sequences was performed using a ClustalW1.8 (<http://www.ebi.ac.uk/clustalw/index.html>) software.

RESULTS AND DISCUSSION

Cloning of the pal gene in E. coli cells. Due to the difficulties in genome organization of the *pal* gene (6 introns), it was synthesized using the sequence of the *pal* gene isolated from *R. toruloides* (GenBank: X12702.1). The gene was treated by restriction endonucleases NcoI and HindIII to obtain sticky ends.

Expression vector pET28a designed for expression

of recombinant proteins in *E. coli* and containing kanamycin resistance gene was chosen for cloning. In addition to that, the vector contains sequence coding for His-Tag end near the polylinker, which considerably simplifies chromatography on a Ni-containing carrier. To prepare for cloning, the vector was treated with restriction endonucleases NcoI and HindIII and purified from the reaction products with the QuickClean kit. After hydrolysis with restriction endonucleases, the vector gained sticky ends complementary to the *pal* gene.

Preparation of the PAL protein producer strain. Cells of *E. coli* strain BL21[DE3]Star containing the gene coding for T7 phage polymerase under the control of an inducible bacterial promoter in their genome were transformed with pET28a DNA containing the *pal* gene coding for L-phenylalanine ammonia-lyase from *Rhodospiridium toruloides* (GenBank: X12702.1) by electroporation. The strain was chosen because it contains the DE3 lysogen carrying a gene coding for phage T7 polymerase under the control of the lacUV5 inducible promoter necessary for the expression of the gene cloned in the pET28a plasmid. Besides, these cells do not contain protease lon and carry a mutation in the gene coding for the outer membrane protease OmpT.

The absence of these two proteases decreases degradation of heterologous proteins. Also, the strain carries a mutant *rne* gene coding for a truncated RNAase, which should lead to increase in the stability of mRNA in cell due to decrease in its enzymatic degradation [8, 9].

These manipulations resulted in the *E. coli* strain BL21[DE3]Star pET28aPAL producing the L-phenylalanine ammonia-lyase of *Rhodospiridium toruloides*, which we will call BL21PAL further on.

Biosynthesis of the PAL recombinant protein by E. coli strain BL21PAL after induction of expression with 1 mM IPTG. To culture the obtained PAL protein producer strain, standard agarized LB medium containing kanamycin at concentration of 25 µg/mL and 1% glucose was used. The level of the enzyme expression was optimized in function of time and temperature of induction. Fermentation was performed in 2-L flasks in 250 mL medium containing kanamycin at concentration of 25 µg/mL in a temperature-controlled rotor-type shaker at 37°C and 250 rpm. IPTG at concentration of 1 mM was used as an inductor. Expression induction was performed when optical density of cell culture at 600 nm reached 0.6–0.8 OU. Then, after a certain period of time (from 15 min to 1 h) aliquots of the cell culture were collected. Cell culture without induction was used as control. Without the induction, cells grow according to a logarithmic law: linear growth is observed till the optical density of 0.6–0.8 OU, then exponential growth occurs to 3.8–4.2 OU; after that the growth curve reaches a plateau of the stationary growth phase. After the addition of the inductor (1 mM IPTG) to cell culture cells grow more slowly, optical density of the culture grows from 0.6 to 1.5 OU within 4 h, however, later on exponential growth phase with late transfer to a stationary growth phase occurs. When studying the dynamics of biosynthesis of the PAL recombinant protein by *E. coli*

cells after expression induction with 1 mM IPTG, maximal expression of the *pal* gene in *E. coli* strain BL21PAL was noted after 3 h of fermentation. According to densitometry analysis, protein yield was 32% to the total protein (Fig. 1). When expression was induced at 25°C, longer (9 h) transfer of culture cells to exponential growth phase occurred.

Maximal level of expression (32%) at all temperatures was the same. Without the induction of expression, undeliberate synthesis of recombinant protein, or “T7 promoter leakage”, often observed in this expression system [10], occurred.

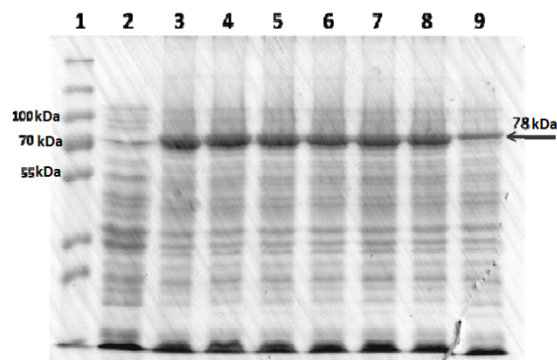


Fig. 1. Analysis of *E. coli* strain BL21PAL cell lysates after induction of expression under various condition:

1, molecular weight marker “PageRuler™ Prestained Protein Ladder”, Fermentas; 2, negative control (lysate of producer strain cells without the addition of an inductor); 3, *E. coli* strain BL21PAL cell lysate after induction of expression with 0.2% lactose according to Studier at 25°C during 32 h; 4, *E. coli* strain BL21PAL cell lysate after induction of expression with 0.2% lactose according to Studier at 37°C during 18 h; 5, *E. coli* strain BL21PAL cell lysate after induction of expression with 1 mM IPTG at 37°C during 3 h; 6, *E. coli* strain BL21PAL cell lysate after induction of expression with 1 mM IPTG at 37°C during 5 h; 7, *E. coli* strain BL21PAL cell lysate after induction of expression with 1 mM IPTG at 25°C during 5 h; and 8, *E. coli* strain BL21PAL cell lysate after induction of expression with 1 mM IPTG at 25°C during 8 h.

Biosynthesis of the PAL recombinant protein by *E. coli* strain BL21PAL after autoinduction of expression with 0.2% lactose according to Studier. Fermentation was performed in 2-L flasks in 250 mL PYP-5025 medium for autoinduction containing kanamycin at concentration of 100 µg/mL in a temperature-controlled rotor-type shaker at 250 rpm during 19 h at temperature of 37°C and during 32 h at temperature of 25°C.

Average optical density (OD600) of the *E. coli* strain BL21PAL cell culture was the same at different temperatures of cultivation and was 7 OU. After PAGE of *E. coli* BL21PAL cell lysates with autoinduction of expression with 0.2% lactose, PAL protein content in *E. coli* cells was determined by densitometry of the obtained electrophoregrams using the TotalLab software. The results of the densitometry analysis showed that, in *E. coli* cells of BL21PAL, PAL protein accumulated in the amount of 35% to the total cell protein at fermentation temperature of 37°C and 33%, at temperature of 25°C (Figs. 2 and 3).

The method of expression induction was chosen as the simplest efficient and cheap alternative to classic induction using IPTG in expression systems based on lactose operon. When autoinduction is used, there is no need in the following cell culture optical density monitoring or addition of an inductor.

From the moment of the colony inoculation into an autoinduction medium to the collection of bacteria biomass with OD600 = 7–15 with synthesized target proteins, 15–20 h pass.

The phenomenon of expression autoinduction is based on the mechanisms that bacteria utilize to regulate consumption of carbon and energy source from the nutrient medium. If there is glucose in the medium, catabolic repression and exclusion of the inductor prevent lactose consumption by lac-permease, product of the lacY gene [11, 12].

When glucose resources are exhausted, lac-permease starts to consume lactose, and β-galactosidase inside bacterial cells turns lactose into a natural inductor, allolactose [6].

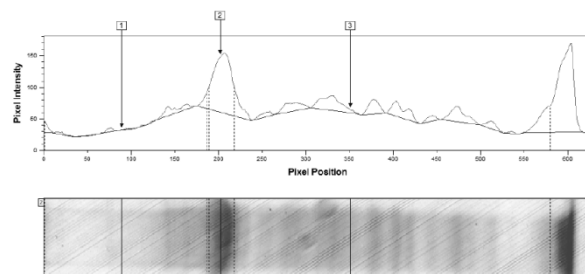


Fig. 2. Densitogram of *E. coli* strain BL21PAL cell lysate after expression induction with 0.2% lactose according to Studier at 25°C during 32 h.

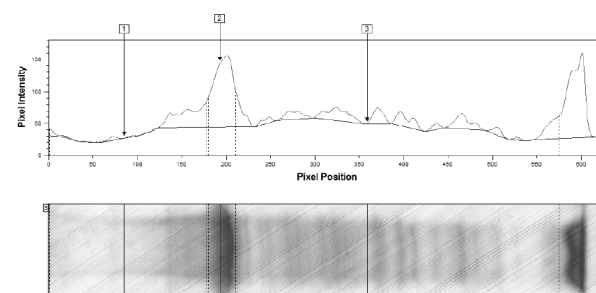


Fig. 3. Densitogram of *E. coli* strain BL21PAL cell lysate after expression induction with 0.2% lactose according to Studier at 37°C during 18 h.

Utilization of a substance not associated with induction and lactose operon (for example, glycerol) as a source of carbon and energy allows to almost double the yield of the target protein by comparison with the equivalent amounts of lactose as a primary energy source. This is because T7 RNA polymerase is so much active that induction may direct most of cellular transcription and translation toward production of target protein [13], which may overlap with the ability to metabolize lactose for energy needs. Glycerol does not overlap with the induction of the target protein and

serves as an efficient source of carbon and energy. The presence of 0.05% glucose in the autoinduction medium accelerates the process of bacterial cell growth at initial stages and simultaneously blocks induction with 0.2% lactose present in the medium, while 0.5% glycerol, also present in the medium, is an efficient source of carbon and energy.

The maximal level of expression of the PAL recombinant protein in *E. coli* strain BL21PAL cells was 35% upon utilization of autoinduction medium in contrast to the maximal level of 32% upon induction with IPTG. Increase in the maximal level of expression upon autoinduction with 0.2% lactose was 7–8%, if compared to induction with IPTG. The data evidence that utilization of a simpler and cheaper autoinduction for synthesis of recombinant protein p17 leads to similar results obtained upon utilization of 1 mM IPTG as inductor, while bacterial biomass and, thus, protein yield, increased 6–7 times.

Solubility of the PAL recombinant protein upon its synthesis in E. coli strain BL21PAL was determined by disc-electrophoresis of *E. coli* cells destroyed upon induction of expression with 0.2% lactose during 18 h at 37°C according to Studier in PAGE. Both sediment and supernatant formed upon sedimentation of cell debris were analyzed.

It was demonstrated that 99% of PAL recombinant protein synthesized in *E. coli* strain BL21PAL cells upon expression induction under optimal conditions is in the sediment formed upon sedimentation of cell debris and probably only the insignificant amount (1%) is in the supernatant (Fig. 4).

Utilization of 1 mM IPTG instead of 0.2% lactose as an inductor did not change protein solubility, neither did bacteria cultivation at different temperatures, 25°C or 37°C.

Accumulation of PAL protein in cells of producer strain in insoluble form indirectly evidences its non-native conformation (tertiary structure).

The data on solubility do not agree with the literature data, which demonstrate that utilization of different techniques to express the *pal* gene coding for L-phenylalanine ammonia-lyase of *Rhodospiridium toruloides* (GenBank: X12702.1) in *E. coli* cells results in a soluble target protein. The probable reason for accumulation of PAL in cells of the producer strain in insoluble form is utilization of the gene with modified

codon sequence for expression. As a result of codon composition optimization, regions necessary for ribosome slow-down at the borders of domain folding could be impaired, which could have led to start of new domain translation when folding of the previous one was not complete, which, in turn, could lead to formation of insoluble protein aggregates.

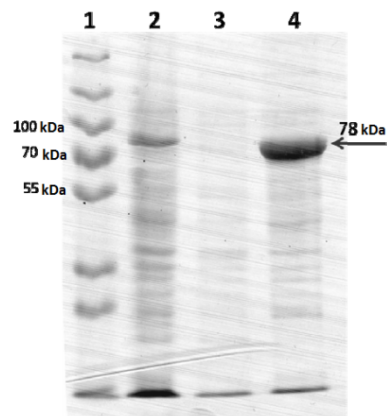


Fig. 4. Determination of PAL recombinant protein solubility upon its synthesis in *E. coli* strain BL21PAL cells: 1, molecular weight marker “PageRuler™ Prestained Protein Ladder” (Fermentas); 2, lysate of *E. coli* strain BL21PAL cells destroyed by sonication; 3, supernatant formed upon centrifugation of the lysate of *E. coli* strain BL21PAL cells destroyed by sonication; and 4, sediment formed upon centrifugation of the lysate of *E. coli* strain BL21PAL cells destroyed by sonication.

Therefore, *E. coli* strain producing L-phenylalanine ammonia-lyase of *Rhodospiridium toruloides* was obtained. Optimization of expression resulted in the maximum level of expression of 35% upon induction with 0.2% lactose according to Studier during 18 h at 37°C. When expressed in *E. coli* cells, the recombinant L-phenylalanine ammonia-lyase was insoluble (formed inclusion bodies) under all conditions studied.

ACKNOWLEDGMENTS

The work was performed in frames of the Federal Target Program “Research and Academic Staff of Innovative Russia” in the years 2009–2013, state contract no. 16.740.11.0239.

REFERENCES

1. Sarkissian, C.N., and Gamez, A., Phenylalanine ammonia lyase, enzyme substitution therapy for phenylketonuria, where are we now? *Mol. Genet. Metab.*, 2005, vol. 86, pp. S22–26.
2. Sarkissian, C.N., Shao, Z., Blain, F., Peevers, R., Su, H., Heft, R., Chang, T.M.S., and Scriver, C.R., A different approach to treatment of phenylketonuria: Phenylalanine degradation with recombinant phenylalanine ammonia lyase, *Proc. Natl. Acad. Sci. U.S.A.*, 1999, vol. 96, no. 5, pp. 2339–2344.
3. Evans, C.T., Hanna, K., Payne, C., Conrad, D., and Misawa, M., Biotransformation of trans-cinnamic acid to L-phenylalanine: Optimization of reaction conditions using whole yeast cells, *Enzyme Microb. Technol.*, 1987, vol. 9, pp. 417–421.
4. Baneyx, F., Recombinant protein expression in *Escherichia coli*, *Curr. Opin. Biotechnol.*, 1999, vol., 10, pp. 411–421.
5. Hannig, G., and Makrides, S.C., Strategies for optimizing heterologous protein expression in *Escherichia coli*, *Trends in Biotechnology*, 1998, vol. 16, pp. 54–60.
6. Beckwith, J., The operon: An historical account in *Escherichia Coli and Salmonella Typhimurium: Cellular*

and *Molecular Biology*, Neidhardt, F.C., Ed., Washington, D.C.: American Society for Microbiology, 1987, pp. 1439–1452.

7. Studier, F.W., Protein production by auto-induction in high density shaking cultures, *Protein Expr. Purif.*, 2005, vol. 41, pp. 207–234.

8. Kido, M., Yamanaka, K., Mitani, T., Niki, H., Ogura, T., and Hiraga, S., RNase E polypeptides lacking a carboxyl-terminal half suppress a mukB mutation in *Escherichia coli*, *J. Bacteriol.*, 1996, vol. 178, pp. 3917–3925.

9. Lopez, P.J., Marchand, I., Joyce, S.A., and Dreyfus, M., The C-terminal half of RNase E, which organizes the *Escherichia coli* degradosome, participates in mRNA degradation but not rRNA processing in vivo, *Mol. Microbiol.*, 1999, vol. 33, pp. 188–199.

10. Grossman, T.H., Kawasaki, E.S., Punreddy, S.R., and Osburne, M.S., Spontaneous cAMP-dependent derepression of gene expression in stationary phase plays a role in recombinant expression instability, *Gene*, 1998, vol. 209, pp. 95–103.

11. Inada, T., Kimata, K., and Aiba, H., Mechanism responsible for glucose-lactose diauxie in *Escherichia coli*: challenge to the cAMP model, *Genes Cells*, 1996, vol. 1, pp. 293–301.

12. Kimata, K., Takahashi, H., Inada, T., Postma, P., and Aiba, H., cAMP receptor protein-cAMP plays a crucial role in glucose-lactose diauxie by activating the major glucose transporter gene in *Escherichia coli*, *Proc. Natl. Acad. Sci. U.S.A.*, 1997, vol. 94, pp. 12914–12919.

13. Studier, F.W., and Moffatt, B.A., Use of bacteriophage T7 RNA-polymerase to direct selective high-level expression of cloned genes, *J. Mol. Biol.*, 1986, vol. 189, pp. 113–130.



UDC 621.929.2/.9
DOI 10.12737/1558

DEVELOPMENT OF MATHEMATICAL MODELS OF CENTRIFUGAL MIXING UNITS OF NEW DESIGN FOR THE PRODUCTION OF DRY COMBINED FOOD PRODUCTS

V. N. Ivanets and D. M. Borodulin

Kemerovo Institute of Food Science and Technology,
bul'v. Stroitelei 47, Kemerovo, 650056 Russia
phone: +7(3842) 39-68-42, e-mail: Borodulin_dmitri@list.ru

(Received January 17, 2013; Accepted in revised form February 25, 2013)

Abstract: A method of modeling the continuous process of the mixing of bulk materials on the basis of cybernetic analysis with some elements of automatic control theory (ACT) [6, 9] has been considered. In this case, a mixing unit (MU) is represented in the form of a dynamic system, which is characterized by the known topology of the motion of material flows and subjected to various external disturbances.

The two developed mathematical models allow us to determine the degree of the smoothening of input material flow fluctuations from volumetric dosers by the mixers incorporated into a MU. The obtained numerical values of smoothability indicate that it is reasonable to equip the studied mixers of new design with volumetric dosers. This allows us to meet the requirements to MUs from both the engineering and economical viewpoints.

Key words: centrifugal mixer, time-and-frequency analysis, bulk materials, combined food products, modeling, cybernetic analysis

INTRODUCTION

The contemporary state of the market of food industry equipment is characterized by a considerable increase in the demand for machines and apparatuses that allow the production of high-quality food products of increased nutritional value (enriched with vitamins and biologically essential components) at low expenditures. In particular, the population should have new combined food products that compensate the deficiency of different food components and micronutrients in its ration due to considerable ecological disturbances in different regions of Russia and other countries.

Since the content of many food additives in the major product is small (1% and lower), the key problem consists in their uniform distribution over the entire volume. Using the results of studies, it has been revealed that continuous centrifugal mixers (CCMs) [2, 5] characterized by a high intensity of mixing due to the targeted organization of the motion of thin disperse layers are most promising for the solution of this problem. Centrifugal mixers enable the production of good-quality mixtures at a component ratio of 1:100 [2]. However, a single CCM is usually insufficient at higher ratios. In this connection, we propose to incorporate two serially arranged centrifugal mixers with a good smoothability into a single MU. In this case, it is possible to use volumetric dosers with certain advantages (high material feed rate, small dimensions,

low cost and maintenance expenditures) for the preparation of mixtures with high ratios of mixed components. For this reason, the objective of our work is to compare the operational efficiencies of two centrifugal MU of new design (differ from each other by the set of equipment incorporated in them), in which it is possible to obtain dry combined food products with a high ratio of mixed components, using cybernetic analysis and some ACT elements [6, 7, 9].

When studying the operation of certain mixing equipment, we artificially imposed a disturbance of one or another kind onto the input feed flow and then analyzed its consequences at the output of an apparatus (plotted a response curve) [10]. The function determined from the given curve for the residence time distribution of particles in centrifugal mixers was used in combination with the accepted flow pattern of mixed materials in an apparatus to predict the process of mixing in it [1, 8].

A number of scientific works [1, 6, 8, 13, 15] are devoted to the problems of the modeling of mixing processes. In our work, we have detailed the questions of the creation of a MU mathematical model, which would allow us to match the time-and-frequency characteristics of CCMs and dosers incorporated into a MU in the interactive operational mode of a computer. As a result, this provides the possibility of decreasing the amplitude of fluctuations in the output material flow of a mixer and improving the quality of a ready mixture.

OBJECTS AND METHODS OF STUDY

In the first case, the object of the study aimed at implementing the method of the sequential dilution of a mixture is a mixing unit that incorporates a block of two spiral and one batch dosers (D, $i=1, N$) and two serially arranged CCMs. Spiral doser D₁ and batch doser D₂ deliver initial mixture components through summing element SE₁ into CCM₁. This results in the mixing of components at a ratio of 1 : 500. The obtained mixture enters SE₂, into which the major component (incorporated into the mixture in a great amount) is simultaneously fed with spiral doser D₃, and then into CCM₂, where the components are finally mixed at a ratio of 1 : 20. As a result, the mixture with a ratio of mixed components of 1 : 1000 is obtained at the output of CCM₂.

The general structural functional scheme of the studied mixing unit operating by the method of the sequential dilution of a mixture is shown in Fig. 1. The dosers form the signals of the mass flow rates of materials that have masses $Q_{d1}(t)$ and $Q_{d2}(t)$ and concentrations $X_{d1}(t)$ and $X_{d2}(t)$ and are fed into SE₁, thereupon the summary flow with parameters $X_{dc1}(t)$ and $Q_{dc1}(t)$ enters CCM₁. The mixture that leaves the first mixer and has a weight $Q_{M1}(t)$ and a concentration $X_{M1}(t)$ and the material flow with parameters $X_{d3}(t)$ and $Q_{d3}(t)$ from spiral doser D₃ are fed into SE₂. As a result, the material mass $Q_{M1}(t)+Q_{d3}(t)$ with a concentration $X_{M1}(t)+X_{d3}(t)$ enters CCM₂, and a mixture with parameters $Q_{M2}(t)$ and $X_{M2}(t)$ leaves it.

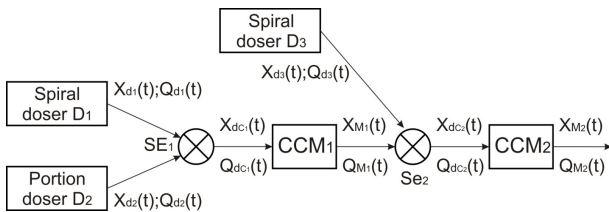


Fig. 1. Structural functional scheme of the studied mixing unit.

To perform the monitoring and control of the principal parameters of the continuous process of mixing, let us use the structural functional scheme implying the estimation of the impulse responses of dosers and the transfer functions of mixers that are incorporated into the MU [6, 9, 10]. The transfer function of a mixer is the ratio of the output signal $y(S)$ to the input signal $x(S)$, both are Laplace transformed, at zero initial conditions. The transfer function is governed only by CCM internal properties, represents a dimensionless function of complex variables, and is denoted as $W(S)=y(S)/x(S)$.

From Fig. 1 it can be seen that the two-stage MU consists of the two blocks of dosers $W_{DB1}(S)$ and $W_{DB2}(S)$ that have certain impulse responses, form signals of different kinds, and operate in parallel for SE₁ and SE₂. The principal elements of the scheme are the CCMs of new design developed by us with a horizontal rotor in the form of three and one hollow truncated cones ($W_{CM1}(S)$ and $W_{CM2}(S)$) [11, 12].

The MU output signal for the given scheme in the operator form ($W_{MU}(S)$) is determined by the formula

$$W_{MU}(S) = [W_{DB1}(S) \times W_{CM1}(S) + W_{DB2}(S)] \times W_{CM2}(S), \quad (1)$$

where $W_{DB1,2}(S)$ are the impulse responses of the block of dosers, $W_{CM1,2}(S)$ is the CCM transfer function, and S is an independent complex variable that stands for differentiation with respect to time.

Here, the first block of dosers consists of a spiral doser and a batch doser. When the spiral doser forms a signal, the feed of a component $X_{d1}(t)$ fluctuates by a time-dependent sinusoidal law with an average value X_{d01} and an amplitude X_{dm1} :

$$X_{d1}(t) = X_{d01} + X_{dm1} \times \sin(\omega_{d1}t), \quad (2)$$

Performing the Laplace transform of the given signal from the time-dependent form to the operator form, we obtain the following expression:

$$W_1(S) = \frac{X_{d01}}{S} + \frac{X_{dm1} \times \omega_{d1}}{S^2 + \omega_{d1}^2}, \quad (3)$$

where X_{d01} is the constant flow rate of a component dosed with a spiral doser and X_{dm1} and ω_{d1} is the amplitude and frequency of fluctuations.

For the formation of a square-wave signal from the batch doser $X_{d2}(t)$, let us use the Fourier tenth-order expansion [6], which is represented by the following function in the temporal region:

$$X_{d2}(t) = \frac{A_{02}}{2} + \sum_{k=1}^{10} \left(A_{k2} \cdot \cos \frac{2k\pi}{T_{d2}} t + B_{k2} \cdot \sin \frac{2k\pi}{T_{d2}} t \right), \quad (4)$$

The Laplace transform of this signal gives the following expression:

$$W_2(S) = \frac{A_{02}}{2S} + \sum_{k=1}^{10} \left(\frac{A_{k2} \times S}{S^2 + \omega_{d2}^2} + \frac{B_{k2} \times \omega_{d2}}{S^2 + \omega_{d2}^2} \right), \quad (5)$$

where $\omega_{k2}=2\pi k/T_{d2}$ is the angular fluctuation frequency corresponding to the k^{th} harmonic of the Fourier expansion of a square-wave signal from the batch doser, T_{d2} is the period of its fluctuations, and A_{02} , A_{k2} , and B_{k2} are coefficients in the Fourier expansion of the signal.

$$\begin{cases} A_{02} = \frac{2}{T_{d2}} \int_0^{T_{d2}} X(t) dt \\ A_{k2} = \frac{2}{T_{d2}} \int_0^{T_{d2}} X(t) \times \cos\left(\frac{2k\pi}{T_{d2}} t\right) dt, \\ B_{k2} = \frac{2}{T_{d2}} \int_0^{T_{d2}} X(t) \times \sin\left(\frac{2k\pi}{T_{d2}} t\right) dt \end{cases} \quad (6)$$

Then, taking into account Eqs. (3) and (5), the summary signal $W_{DB1}(S)$ in the operator form will be

$$W_{DB1}(S) = \frac{X_{d01}}{S} + \frac{X_{dm1} \times \omega_{d1}}{S^2 + \omega_{d1}^2} + \frac{A_{02}}{2S} + \sum_{k=1}^{10} \left(\frac{A_{k2} \times S}{S^2 + \omega_{d2}^2} + \frac{B_{k2} \times \omega_{d2}}{S^2 + \omega_{d2}^2} \right), \quad (7)$$

The second block incorporates a spiral doser. Its signal in the time-dependent and operator forms is

$$X_{d3}(t) = X_{d03} + X_{dm3} \times \sin(\omega_{d3}t), \quad (8)$$

$$W_3(S) = \frac{X_{d03}}{S} + \frac{X_{dm3} \times \omega_{d3}}{S^2 + \omega_{d3}^2}, \quad (9)$$

When forming a CCM mathematical model, it is necessary to characterize the dynamics of the displacement of a material inside it. Professor Yu. I. Makarov in his work [10] considered a CCM as a control element with pronounced low-frequency filter properties. He has proved that the continuous process of mixture preparation can be described by the models that incorporate the corresponding combinations of serial and parallel plug-flow and stirred-tank zones. For the quantitative analysis of the operation of a CCM, its dynamic characteristics are usually approximated by first- or second-order aperiodic elements [6, 9].

The first-order element has the following form:

$$W_{CM}(S) = \frac{K \times e^{-\tau S}}{T_1' \times S + 1}, \quad (10)$$

The second-order element is

$$W_{CM}(S) = \frac{K \times e^{-\tau S}}{T_2^2 \times S^2 + T_1 \times S + 1}, \quad (11)$$

where K is the transfer coefficient ($K = 1$), T_1' and T_1 are time constants (for the first and second CCMs) that characterize the time interval, within which the concentration decreases from a maximum value to a nearly zero level, T_2 is the time constant that characterizes the period of attaining the maximum change rate of the output concentration of a mixture from a mixer in the transition regime with an impulse dosing disturbance, and τ is the delay period.

Substituting the impulse responses of all the blocks and the transfer functions of MU mixers (Eqs. (7), (9), (10), and (11)) into Eq. (1), we obtain

$$W_{MU}(S) = \left[\left(\frac{X_{d01}}{S} + \frac{X_{dm1} \times \omega_{d1}}{S^2 + \omega_{d1}^2} + \frac{A_{02}}{2S} + \sum_{k=1}^{10} \left(\frac{A_{k2} \times S}{S^2 + \omega_{d2}^2} + \frac{B_{k2} \times \omega_{d2}}{S^2 + \omega_{d2}^2} \right) \right) \times \frac{K \times e^{-\tau S}}{T_2^2 \times S^2 + T_1 \times S + 1} + \frac{X_{d03}}{S} + \frac{X_{dm3} \times \omega_{d3}}{S^2 + \omega_{d3}^2} \right] \times \frac{K \times e^{-\tau S}}{T_1' \times S + 1}, \quad (12)$$

The obtained model describes the process of the mixing of bulk components in the case of the sequential dilution of a mixture.

Let us further consider a procedure in the space of MU model states. To accomplish this, let us convert the

general structural functional scheme of the studied MU (Fig. 1) into the block structural scheme, whose elements are specified in the form of transfer functions (Fig. 2). The block structural scheme differs from the previous scheme by that the output signals of the block of the first- and second-stage dosers are substituted by parallel virtual elements linked to the output of corresponding mixers.

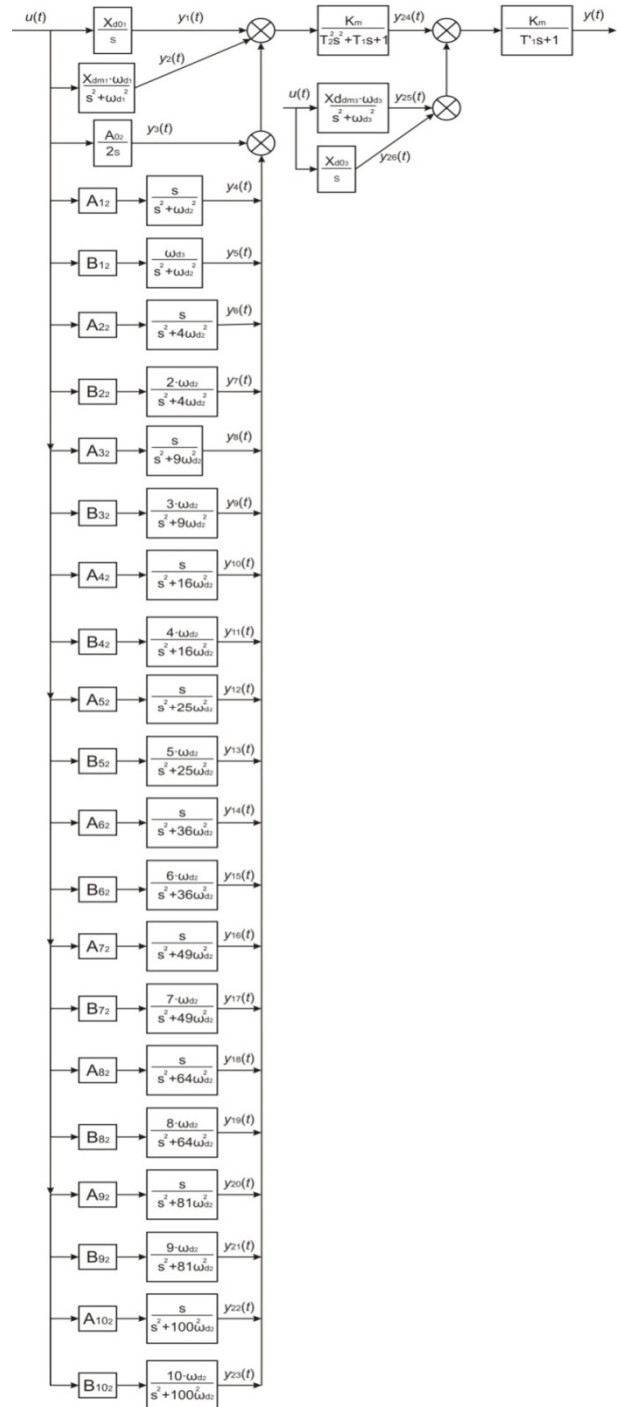


Fig. 2. Block structural scheme of the mixing unit.

The transfer functions describing the virtual elements are such that the signal that appears at the output of the mixers upon the synchronous fictitious control action $u(t)$ onto their outputs in the form of a unit impulse function is equal to the summary action of

real dosing impulses. From the block structural scheme it can be seen that it has two inputs and one output.

Let us transform the obtained transfer functions (Eqs. (7), (9), and (12)) into the corresponding differential equations. By way of example, let us consider the first summand of Eq. (7) $\frac{X_{d01}}{S}u(t)$, which is the image of the function $y_1(t)$, i.e., $\frac{X_{d01}}{S}u(t) = Y_1 \rightarrow y_1$. Multiplying both sides of the equation by S with consideration for $S \times Y_1 \rightarrow \dot{y}_1$, we obtain the differential equation $\dot{y}_1 = X_{d01} \times u(t)$. Transforming the other elements (summands) in a similar way, we obtain the following system of differential equations:

$$\left\{ \begin{aligned} \frac{dy_1(t)}{dt} &= X_{d01} \times u(t) \\ \frac{d^2y_2(t)}{dt^2} + \omega_{d1}^2 \times y_2(t) &= X_{dm1} \times \omega_{d1} \times u(t) \\ \frac{dy_3(t)}{dt} &= \frac{A_0}{2} \times u(t) \\ \frac{d^2y_4(t)}{dt^2} + \omega_{d2}^2 \times y_4(t) &= A_1 \times u(t) \\ \frac{d^2y_5(t)}{dt^2} + \omega_{d2}^2 \times y_5(t) &= B_1 \times \omega_{d2} \times u(t) \\ \frac{d^2y_6(t)}{dt^2} + 4\omega_{d2}^2 \times y_6(t) &= A_2 \times u(t) \\ \frac{d^2y_7(t)}{dt^2} + 4\omega_{d2}^2 \times y_7(t) &= 2B_2 \times \omega_{d2} \times u(t) \\ \frac{d^2y_8(t)}{dt^2} + 9\omega_{d2}^2 \times y_8(t) &= A_3 \times u(t) \\ \frac{d^2y_9(t)}{dt^2} + 9\omega_{d2}^2 \times y_9(t) &= 3B_3 \times \omega_{d2} \times u(t) \\ \dots\dots\dots \\ \frac{d^2y_{22}(t)}{dt^2} + 100\omega_{d2}^2 \times y_{22}(t) &= A_{10} \times u(t) \\ \frac{d^2y_{23}(t)}{dt^2} + 100\omega_{d2}^2 \times y_{23}(t) &= 10B_{10} \times \omega_{d2} \times u(t) \\ T_2^2 \frac{d^2y_{24}(t)}{dt^2} + T_1 \frac{dy_{24}(t)}{dt} + y_{24}(t) &= Km \sum_{i=1}^{23} y_i \\ \frac{d^2y_{25}(t)}{dt^2} + \omega_{d3}^2 \times y_{25}(t) &= X_{dm3} \times \omega_{d3} \times u(t) \\ \frac{dy_{26}(t)}{dt} &= X_{d03} \times u(t) \\ T_1' \frac{dy(t)}{dt} + y(t) &= Km(y_{24}(t) + y_{25}(t) + y_{26}(t)) \end{aligned} \right. , \quad (13)$$

where $y_1(t), y_2(t), y_3(t), y_4(t) \dots y_{25}(t)$ are the internal signals that characterize the operation of corresponding transfer functions in the elements of the block structural scheme. The sum of $y_1(t)$ and $y_2(t)$ is the signal formed by the spiral doser, and the sum of $y_3(t), y_4(t) \dots y_{23}(t)$ is the signal formed by the batch dosers in the first block. The signals $y_{25}(t)$ and $y_{26}(t)$ are formed by the spiral

doser of the second block, $y_{24}(t)$ corresponds to the output signal of the first-stage CCM, and $y(t)$ corresponds to the output signal of the second-stage CCM or the MU as a whole.

To solve system (14), let us reduce the order of the differential equations via the substitution of variables.

$$\begin{pmatrix} y_1(t) \\ y_2(t) \\ \dot{y}_2(t) \\ y_3(t) \\ \dots\dots\dots \\ y_k(t) \\ \dot{y}_k(t) \\ \dots\dots\dots \\ y_{26}(t) \\ y(t) \end{pmatrix} = \begin{pmatrix} x_1(t) \\ x_2(t) \\ x_3(t) \\ x_4(t) \\ \dots\dots\dots \\ x_{2k-3}(t) \\ x_{2k-2}(t) \\ \dots\dots\dots \\ x_{49}(t) \\ x_{50}(t) \end{pmatrix}, \quad (k = \overline{4,25}), \quad (14)$$

Such a transformation allows us to write the system of the differential equations describing the behavior of the MU with a batch doser signal that has n Fourier expansion harmonics in the Cauchy normal form.

$$\left\{ \begin{aligned} \dot{x}_1(t) &= X_{d01} \times u(t) \\ \dot{x}_2(t) &= x_3(t) \\ \dot{x}_3(t) &= -\omega_{d1}^2 \times x_2(t) + X_{dm1} \times \omega_{d1} \times u(t) \\ \dot{x}_4(t) &= \frac{A_0}{2} \times u(t) \\ \dot{x}_{4k+1}(t) &= x_{4k+2}(t) \quad (k = \overline{1,n}) \\ \dot{x}_{4k+2}(t) &= -k^2 \times \omega_{d2}^2 \times x_{4k+1}(t) + A_k \times u(t) \\ \dot{x}_{4k+3}(t) &= x_{4k+4}(t) \\ \dot{x}_{4k+4}(t) &= -k^2 \times \omega_{d2}^2 \times x_{4k+3}(t) + kB_k \times \omega_{d2} \times u(t) \\ \dot{x}_{4n+5}(t) &= x_{4n+6}(t) \\ \dot{x}_{4n+6}(t) &= \frac{Km}{T_2^2} (x_1(t) + x_2(t) + x_4(t) + \sum_{k=1}^{2n} x_{2k+3}(t)) - \\ &\quad - \frac{1}{T_2^2} \times x_{4n+5}(t) - \frac{T_1}{T_2^2} \times x_{4n+6}(t) \\ \dot{x}_{4n+7}(t) &= x_{4n+8}(t) \\ \dot{x}_{4n+8}(t) &= -\omega_{d3}^2 \times x_{4n+7}(t) + X_{dm3} \times \omega_{d3} \times u(t) \\ \dot{x}_{4n+9}(t) &= X_{dm3} \times u(t) \\ \dot{x}_{4n+10}(t) &= \frac{Km}{T_1'} (x_{4n+5}(t) + x_{4n+7}(t) + x_{4n+9}(t)) - \frac{1}{T_1'} \times x_{4n+10}(t) \end{aligned} \right. , \quad (15)$$

It should be noted that the output signal $y(t)$ of the second CCM is related with the state variable $x_{4n+10}(t)$ according to Eq. (15) via the relationship $y(t) = x_{4n+10}(t)$, which is the output equation for the considered MU.

Obtained model (16) that contains information on the formation of flow signals in the blocks of dosers also allows us to trace their fluctuations in parallel (during a single calculation procedure) with the output

signal that has passed the first CCM and is received at the output of the second mixer.

Let us model a two-stage MU consisting of three spiral dosers and two CCMs in a similar manner. Its structural functional scheme is shown in Fig. 3.

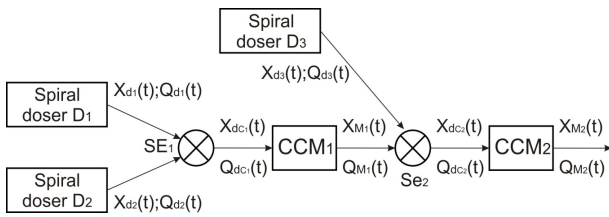


Fig. 3. Structural functional scheme of the mixing unit.

The output signal of the MU, where the first block incorporates two spiral dosers, in the operator form ($W_{MU}(S)$) is represented by Eq. (1), and its impulse response is determined as

$$W_{DB1}(S) = \frac{X_{d01}}{S} + \frac{X_{dm1} \times \omega_{d1}}{S^2 + \omega_{d1}^2} + \frac{X_{d02}}{S} + \frac{X_{dm2} + \omega_{d2}}{S^2 + \omega_{d2}^2}, \quad (16)$$

The second block incorporates a spiral doser, whose impulse response is represented by Eq. (9). The transfer functions of the mixers are expressed by Eqs. (10) and (11).

Substituting the impulse responses of all the MU blocks and apparatuses (Eqs. (16), (9), (10), and (11)) into Eq. (1), we obtain the following model for the process of the mixing of bulk materials:

$$W_{MU}(S) = \left[\left(\frac{X_{d01}}{S} + \frac{X_{dm1} \times \omega_{d1}}{S^2 + \omega_{d1}^2} + \frac{X_{d02}}{S} + \frac{X_{dm2} + \omega_{d2}}{S^2 + \omega_{d2}^2} \right) \times \frac{K \times e^{-\tau S}}{T_2^2 \times S^2 + T_1 \times S + 1} + \frac{X_{d03}}{S} + \frac{X_{dm3} \times \omega_{dm3}}{S^2 + \omega_{d3}^2} \right] \times \frac{K \times e^{-\tau S}}{T_1' \times S + 1}, \quad (17)$$

Let us consider a procedure in the space of MU model states and, to accomplish this, transform the general structural functional scheme of the studied MU (Fig. 3) into the scalarized block structural scheme (Fig. 4).

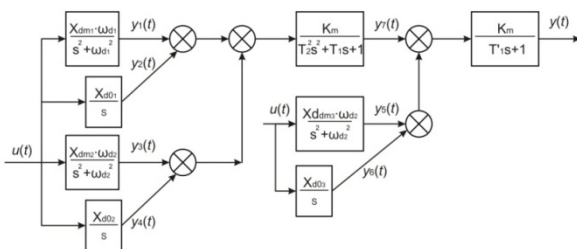


Fig. 4. Block structural scheme of the mixing unit.

Applying the above considered expressions, we write the following system of differential equations:

$$\begin{cases} \frac{d^2 y_1(t)}{dt^2} + \omega_{d1}^2 \times y_1(t) = X_{dm1} \times \omega_{d1} \times u(t) \\ \frac{dy_2(t)}{dt} = X_{d01} \times u(t) \\ \frac{d^2 y_3(t)}{dt^2} + \omega_{d2}^2 \times y_3(t) = X_{dm2} \times \omega_{d2} \times u(t) \\ \frac{dy_4(t)}{dt} = X_{d02} \times u(t) \\ \frac{d^2 y_5(t)}{dt^2} + \omega_{d3}^2 \times y_5(t) = X_{dm3} \times \omega_{d3} \times u(t) \\ \frac{dy_6(t)}{dt} = X_{d03} \times u(t) \\ T_2^2 \frac{d^2 y_7(t)}{dt^2} + T_1 \frac{dy_7(t)}{dt} + y_7(t) = K_m (y_1(t) + y_2(t) + y_3(t) + y_4(t)) \\ T_1' \frac{dy_8(t)}{dt} + y_8(t) = K_m (y_5(t) + y_6(t) + y_7(t)) \end{cases}, \quad (18)$$

To solve it, let us reduce the order of the differential equations.

$$\begin{pmatrix} y_1(t) \\ \dot{y}_1(t) \\ y_2(t) \\ y_3(t) \\ \dot{y}_3(t) \\ y_4(t) \\ y_5(t) \\ \dot{y}_5(t) \\ y_6(t) \\ y_7(t) \\ \dot{y}_7(t) \\ y_8(t) \end{pmatrix} = \begin{pmatrix} x_1(t) \\ x_2(t) \\ x_3(t) \\ x_4(t) \\ x_5(t) \\ x_6(t) \\ x_7(t) \\ x_8(t) \\ x_9(t) \\ x_{10}(t) \\ x_{11}(t) \\ x_{12}(t) \end{pmatrix}, \quad (19)$$

Using Eqs. (19) and (20) as a basis, we obtain the resulting equation system (in the Cauchy normal form) describing the behavior of the mixing unit:

$$\begin{cases}
 \dot{x}_1(t) = x_2(t) \\
 \dot{x}_2(t) = -\omega_{d2}^2 \times x_1(t) + X_{dm1} \times \omega_{d1} \times u(t) \\
 \dot{x}_3(t) = X_{d01} \times u(t) \\
 \dot{x}_4(t) = x_5(t) \\
 \dot{x}_5(t) = -\omega_{d2}^2 \times x_4(t) + X_{dm2} \times \omega_{d2} \times u(t) \\
 \dot{x}_6(t) = X_{d02} \times u(t) \\
 \dot{x}_7(t) = x_8(t) \\
 \dot{x}_8(t) = -\omega_{d3}^2 \times x_7(t) + X_{dm3} \times \omega_{d3} \times u(t) \\
 \dot{x}_9(t) = X_{d03} \times u(t) \\
 \dot{x}_{10}(t) = x_{11}(t) \\
 \dot{x}_{11}(t) = \frac{K_m}{T_2} (x_1(t) + x_3(t) + x_4(t) + x_6(t)) - \\
 \quad - \frac{1}{T_2} \times x_{10}(t) - \frac{T_1}{T_2} \times x_{11}(t) \\
 \dot{x}_{12}(t) = \frac{K_m}{T_1} (x_7(t) + x_9(t) + x_{10}(t)) - \frac{1}{T_1} \times x_{12}(t)
 \end{cases} \quad (20)$$

According to Eq. (20), the output equation for the considered MUs is

$$y(t) = x_{12}(t), \quad (21)$$

The obtained models can be implemented via different mathematical software that provides the possibility of calculating the MU time-and-frequency characteristics using the known values of doser impulse responses and mixer transfer functions.

RESULTS AND DISCUSSION

The frequency method of determining the smoothening degree requires the knowledge of the frequency transfer function of a mixer that operates in a certain regime (rotor speed, internal and external recycle ratios, taper angle, etc.). The given studies were performed on the white flour-potassium iodide mixture.

To determine the smoothability of the two centrifugal MUs (the first of them is schematized in Fig. 1, and the scheme of the second MU is shown in Fig. 2), the transfer functions of the mixers incorporated in them were represented as $W(j\omega) = j \times Im(\omega) + Re(\omega)$. After $Re(\omega)$ and $Im(\omega)$ were determined, we plotted the amplitude frequency characteristic $A(\omega) = \sqrt{Im^2(\omega) + Re^2(\omega)}$.

The studied MUs contain two CCMs each and identical spiral dosers, whose frequencies will be used to estimate the smoothability. For this reason, the obtained amplitude frequency characteristics will be identical for both mixing units.

Hence, the amplitude frequency characteristics of the first-stage CCMs of the studied MUs are plotted in Fig. 5.

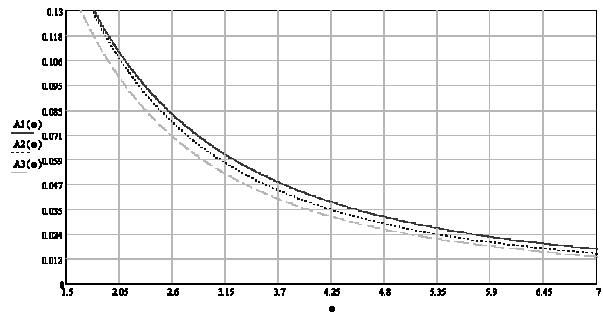


Fig. 5. Amplitude frequency characteristics A1, A2, and A3 of CCM rotor speeds for the three operational regimes [12] at 10, 12.5, and 15 s⁻¹, respectively.

From Fig. 5 it can be seen that the MU operating in the third regime has the best smoothing characteristics. The CCM smoothability was estimated from the plots for the third operational regime at a specified operational frequency of dosers. For example, if a dosing signal with a frequency $\omega = 4.02 \text{ s}^{-1}$ is sent to the input of a mixer (first doser signal), the length of the transfer function vector is $R(\omega) = A(\omega) = 0.032$. The smoothability of the first-stage centrifugal mixer was then determined as

$$S(4.02) = \frac{1}{R(4.02)} = \frac{1}{0.032} = 31.25, \quad (22)$$

Hence, the centrifugal mixer smoothenes feed flow fluctuations at the given frequency of input signals by 31.25 times.

Let us further consider the amplitude frequency characteristic for the second-stage CCM [11] of the studied MUs (Fig. 6).

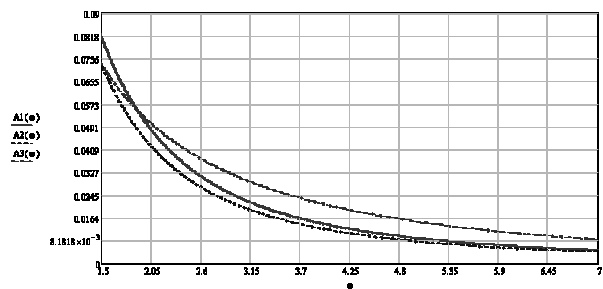


Fig. 6. Amplitude frequency characteristics A1, A2, and A3 of CCM rotor speeds for the three operational regimes at 10, 12.5, and 15 s⁻¹, respectively.

If a dosing signal with a frequency $\omega = 4.02 \text{ s}^{-1}$ (third doser signal) is sent to the input of the mixer (at $n = 15 \text{ s}^{-1}$), the length of the frequency transfer function vector is $R(\omega) = A(\omega) = 0.0123$. The smoothability of the first-stage centrifugal mixer is further determined as

$$S(4.02) = \frac{1}{R(4.02)} = \frac{1}{0.0123} = 81.3, \quad (23)$$

Hence, the centrifugal mixer smoothenes feed flow

fluctuations at the given frequency of input signals by 81.3 times.

The data for all the MU operational regimes are given in Table 1.

Table 1. Smoothability of the mixing units

	CCM operational regimes (rotor speed, s ⁻¹)	Input signal frequency, s ⁻¹	
		2.093	4.02
White flour potassium iodide mixture			
First-stage CCM [1]	10	9.17	24.39
	12.5	9.43	28.57
	15	10.00	31.25
Second-stage CCM [4]	10	20.36	45.87
	12.5	24.44	91.46
	15	19.23	81.3
MU	10	29.53	70.26
	12.5	33.87	120.03
	15	39.53	112.55

Hence, it follows from the results of frequency analysis that the smoothability $S(\omega)$ grows with an increase in the operational speeds of CCM rotors and the input signals formed by the dosers. Its considerable growth occurs upon the switch from the first CCM operational regime to the second regime at both stages. The highest value of $S(\omega)$ for the studied MUs is observed at a CCM rotor speed of 12.5 s⁻¹.

To determine the degree of the smoothening of real dosing station signals, we also performed the time analysis of the MUs.

Let us first perform the analysis of the first MU (Fig. 1) at a CCM rotor speed of 10 s⁻¹. Let us determine the real signal of the MU first-stage doser block from Eq. (2) using, for example, the *MathCAD* software for the case when the major component (white flour) is dosed with a spiral doser and the key component (potassium iodide) is dosed with a batch doser. The concentration of potassium iodide in the flour was found potentiometrically on an Elis-131-1 ion selective electrode, with which the equilibrium concentration of iodine ions in a solution was determined. The measurements of pI were performed on an ANION-4100 ion conductivity meter. The iodide selective electrode was preliminary calibrated against standard potassium iodide solutions with a mass concentration of 2. 1.5, 1, 0.5, and 0.1 g/dm³ [3]. The obtained signal is shown in Fig. 7.

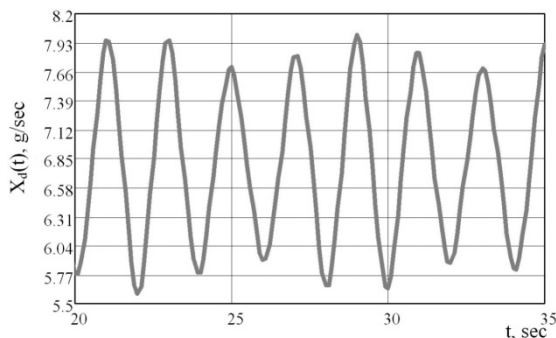


Fig. 7. Signal of the first block of dosers (spiral and batch).

The amplitude of the input signal of the first block of dosers is

$$X_{dm}^{IN} = \frac{X_{d0}^{max} - X_{d0}^{min}}{2} = \frac{8.036 - 5.564}{2} = 1.236, \text{ g/s.} \quad (24)$$

The obtained signal was further sent to the input of the MU first-stage CCM [12]. The response of the system to the input signal is shown in Fig. 8.

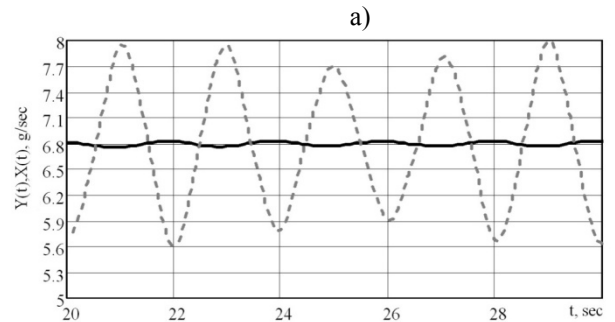
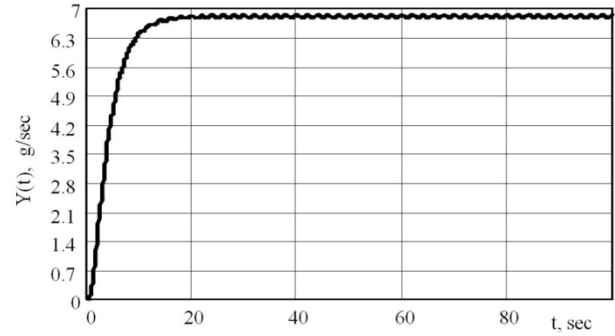


Fig. 8. Response of the system to the input signal of the first block of dosers: (a) output signal of the first-stage centrifugal mixer, (b) ratio of the amplitudes of the input (---) and (—) output signals.

The analysis of the obtained plots allows us to determine the real degree of the smoothening of feed flow fluctuations for the first block of dosers and also the numerical values of the real transfer functions of the first-stage CCMs $W_{CMI}(S)$.

By way of example, let us calculate $S(\omega)$ of a CCM. To accomplish this, let us calculate the amplitude of the mixer's output signal by the formula

$$X_{dm}^{OUT} = \frac{X_{d0}^{max} - X_{d0}^{min}}{2} = \frac{6.832 - 6.766}{2} = 0.033, \text{ g/s.} \quad (25)$$

Then we find

$$R(\omega) = \frac{X_{dm}}{X_{d0}} = \frac{0.033}{6.799} = 0.00482, \quad (26)$$

Thereupon we calculate the mixer's smoothability as

$$S(\omega) = \frac{1}{R(\omega)} = \frac{1}{0.00482} = 207.22, \quad (27)$$

The CCM transfer function can be calculated from the ratio of the amplitudes of the input and output signals, and its numerical value is then equal to

$$W_{CM1}(S) = \frac{X_{dm}^{OUT}}{X_{dm}^{IN}} = \frac{0.033}{1.236} = 0.027, \quad (28)$$

The smoothability of the mixer at rotor speeds of 12.5 and 15 s⁻¹ was determined in a similar way. The obtained results were compiled in Table 2.

Table 2. Smoothability and transfer function of the first-stage mixer

n, s^{-1}	$X_{dm}^{IN}, g/s$	$X_{dm}^{OUT}, g/s$	$S(\omega^*)$	$W_{CM1}(S^{**})$
10	1.236	0.033	207.22	0.027
12.5	1.236	0.031	222.9	0.025
15	1.236	0.025	272.9	0.02

* ω is the fluctuation frequency created by a doser, s⁻¹.

** S is an independent complex variable that stands for differentiation with respect to time.

The results of the performed analysis indicate that the CCM [12] smoothens well input material flow fluctuations produced by the first block of volumetric dosers. The best result was obtained at a rotor speed of 15 s⁻¹.

The signal from the second block of dosers was then superimposed to the output signal of the first-stage CCM, thus leading to an increase in its amplitude and the numerical value of its impulse response (signals from the first-stage CCM and the second-stage block of dosers). The graphical interpretation of the given signal is shown in Fig. 9.

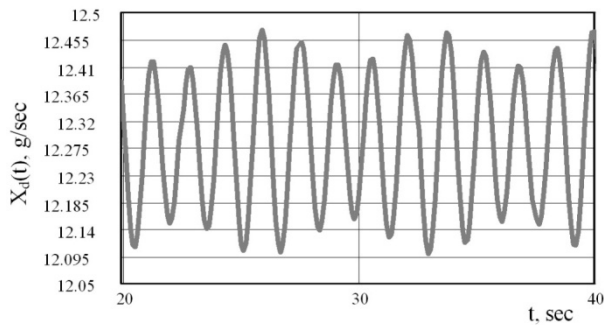


Fig. 9. Summary signal from the first CCM and the second block of dosers.

The amplitude of this signal is equal to

$$X_{dm}^{IN} = \frac{X_{d0}^{max} - X_{d0}^{min}}{2} = \frac{12.474 - 12.098}{2} = 0.188, g/s. \quad (29)$$

To determine the impulse response of the first-stage CCM and the second-stage block of dosers, the amplitude calculated by Eq. (30) should be divided by X_{dm}^{IN} obtained by Eq. (26):

$$W_{CM1+BD2}(S) = \frac{X_{dm}^{OUT}}{X_{dm}^{IN}} = \frac{0.1883}{0.033} = 5.371, \quad (30)$$

The obtained signal was further sent to the input of the MU second-stage CCM [11]. The response of the system to the input signal is shown in Fig. 10.

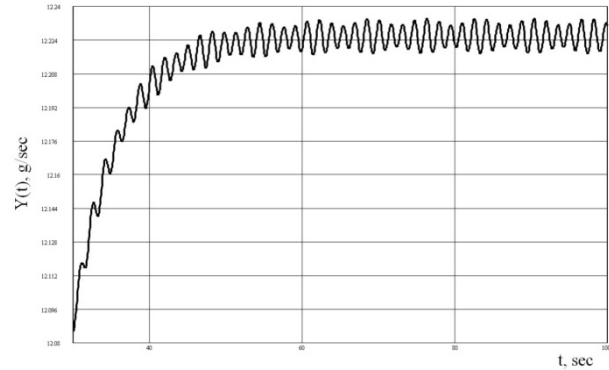


Fig. 10. Response of the system to the input signal of the second-stage block of dosers and the first CCM.

The ratios of the amplitudes of the input and output signals for the second CCM [11] are plotted in Fig. 11.

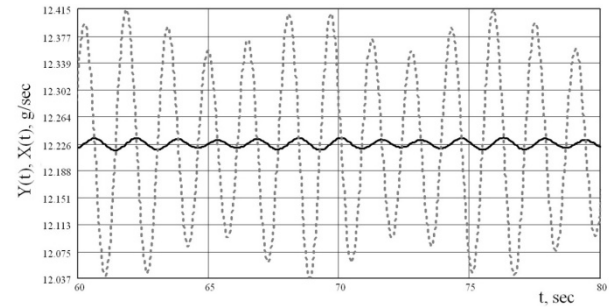


Fig. 11. Magnified system response fragment for the steady-state operational regime. Ratio of the amplitudes of the input (—) and output (---) signals.

Since the second-stage CCM is the end element in the functional structural scheme (Fig. 1), its output signal $y(t)$ may be considered as the output impulse of the entire studied MU, and the transfer function $W_{CM2}(S)$ becomes $W_{MU}(S)$.

For further analysis, let us calculate $S(\omega)$ and $W_{CM2}(S)$ of the CCM at $n = 10 s^{-1}$. To accomplish this, let us calculate the amplitude of the mixer's output signal by the formula

$$X_{dm}^{OUT} = \frac{X_{d0}^{max} - X_{d0}^{min}}{2} = \frac{12.294 - 12.144}{2} = 0.075, g/s. \quad (31)$$

Further, we find

$$R(\omega) = \frac{X_{dm}}{X_{d0}} = \frac{0.075}{12.219} = 0.00614, \quad (32)$$

Then we determine the smoothability of the mixer as

$$S(\omega) = \frac{1}{R(\omega)} = \frac{1}{0.00614} = 162.867, \quad (33)$$

The transfer function of the second-stage CCM (or the MU transfer function) will be

$$W_{CM2}(S) = \frac{X_{dm}^{OUT}}{X_{dm}^{IN}} = \frac{0.075}{0.188} = 0.399, \quad (34)$$

The smoothability of the second-stage mixer and its transfer function at rotor speeds of 12.5 and 15 s⁻¹ was determined in a similar way. The obtained results were compiled in Table 3.

The results of the performed analysis indicate that the second-stage CCM [11] slightly worse smoothens input material flow fluctuations in comparison with the first-stage CCM [12]. This is explained by that the rotor of the second mixer consists of a single cone, so mixed particles reside in the working zone of the mixer for a shorter time.

Let us further perform the analysis of the second MU, whose regime parameters are the same as for the first MU. The real signal of the first-stage block of MU spiral dosers was determined by Eq. (15) for the white flour potassium iodide feed. The obtained signal is plotted in Fig. 12.

Table 3. Smoothability and transfer function of the second-stage mixer

<i>n</i> , s ⁻¹	First mixer and second block of dosers		Second mixer or mixing unit		
	<i>X</i> _{dm} ^{IN} , g/s	<i>W</i> _{CM1+DB2} (<i>S</i>)	<i>X</i> _{dm} ^{OUT} , g/s	<i>S</i> (<i>ω</i> [*])	<i>W</i> _{CM2} (<i>S</i> ^{**}) (<i>W</i> _{MU} (<i>S</i>))
10	0.188	5.37	0.075	162.86	0.399
12.5	0.186	6.103	0.11	111.2	0.59
15	0.182	3.15	0.109	111.6	0.595

* *ω* is the fluctuation frequency created by a doser, s⁻¹.
 ** *S* is an independent complex variable that stands for differentiation with respect to time.

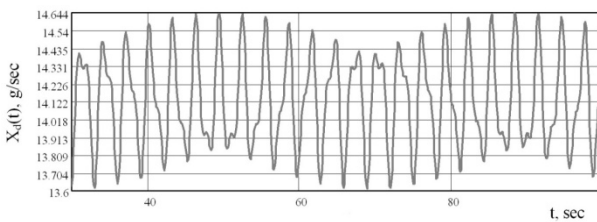


Fig. 12. Signal of the first block of dosers (both are spiral).

The amplitude of the given signal is *X*_{dm}^{IN} = 0.516 g/s.

Sending the given signal to the input of the MU first-stage CCM [12], we obtain the system's response shown in Fig. 13.

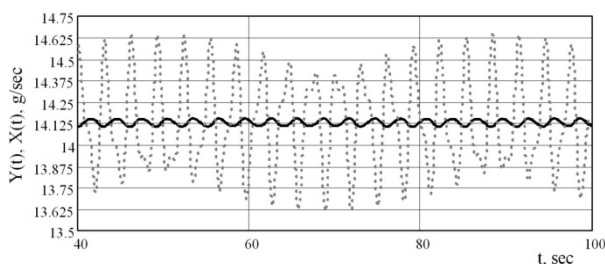


Fig. 13. Magnified system response fragment. Ratio of the amplitudes of the input (---) and output (—) signals.

The output signal amplitude is *X*_{dm}^{OUT} = 0.025 g/s.

The ratio of the amplitude to the average mass flow rate is *R*(*ω*) = 0.0018.

Then the smoothability of the first-stage CCM is

$$S(\omega) = \frac{1}{R(\omega)} = \frac{1}{0.0018} = 554.67, \quad (35)$$

and its transfer function is

$$W_{CM1}(S) = \frac{X_{dm}^{OUT}}{X_{dm}^{IN}} = \frac{0.025}{0.516} = 0.049, \quad (36)$$

The parameters of the implementation of the mathematical model of the MU first stage for the operation of the CCM at rotor speeds of 12.5 and 15 s⁻¹ are given in Table 4.

Table 4. Smoothability and transfer function of the first-stage mixer

<i>n</i> , s ⁻¹	<i>X</i> _{dm} ^{IN} , g/s	<i>X</i> _{dm} ^{OUT} , g/s	<i>S</i> (<i>ω</i> [*])	<i>W</i> _{CM1} (<i>S</i> ^{**})
10	0.516	0.025	554.67	0.049
12.5	0.516	0.025	591.13	0.046
15	0.516	0.02	716.46	0.038

* *ω* is the fluctuation frequency created by a doser, s⁻¹.
 ** *S* is an independent complex variable that stands for differentiation with respect to time.

From Table 4 it can be seen that the CCM [12] has the highest smoothability at a rotor speed of 15 s⁻¹.

Further, the output signals of the first-stage CCM and the second block of dosers superimpose over each other. The graphical interpretation of the summary signal is shown in Fig. 14.

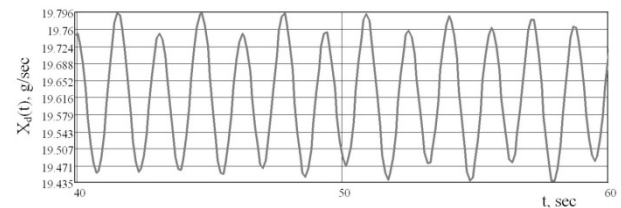


Fig. 14. Summary signal from the first CCM and the second block of dosers.

The amplitude of the given signal and the CCM transfer function are *X*_{dm}^{IN} = 0.181 g/s and *W*_{CM1+BD2}(*S*) = 7.1, respectively.

The obtained signal was sent to the input of the MU second-stage CCM [11]. The response of the system to the input signal is shown in Fig. 15.

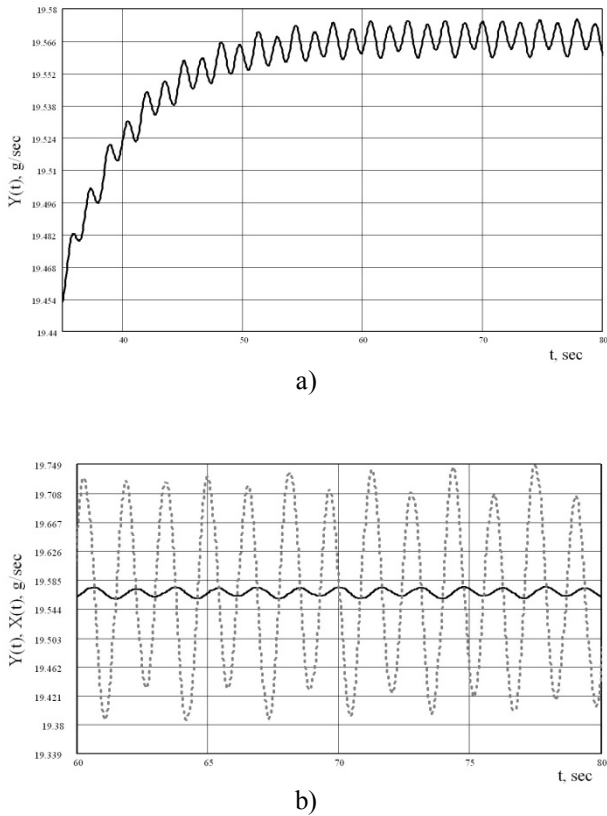


Fig. 15. Response of the system to the input signal of the first block of dosers and the continuous centrifugal mixer: (a) output signal of the second-stage CCM, (b) magnified fragment of the ratio of the amplitudes of the input (---) and output (—) signals.

The amplitude of the output signal of the second-stage mixer is

$$X_{dm}^{OUT} = \frac{X_{d0}^{max} - X_{d0}^{min}}{2} = \frac{19.624 - 19.606}{2} = 0.00889, \text{ g/s.} \quad (37)$$

$$R(\omega) = \frac{X_{dm}}{X_{d0}} = \frac{0.00889}{19.615} = 0.00045, \quad (38)$$

The smoothability of the second-stage CCM is

$$S(\omega) = \frac{1}{R(\omega)} = \frac{1}{0.00045} = 2204, \quad (39)$$

The transfer function of the second-stage CCM (or the MU) is

$$W_{CM2}(S) = \frac{X_{dm}^{OUT}}{X_{dm}^{IN}} = \frac{0.00889}{0.181} = 0.049, \quad (40)$$

The results obtained at rotor speeds of 12.5 and 15 s⁻¹ are given in Table 5.

Table 5. Smoothability and transfer function of the second-stage mixer

$n, \text{ s}^{-01}$	First mixer and second block of dosers		Second mixer or mixing unit		
	$X_{dm}^{IN}, \text{ g/s}$	$W_{CM1+DB2}(S)$	$X_{dm}^{OUT}, \text{ g/s}$	$S(\omega^*)$	$W_{CM2}(S^{**}) (W_{MU}(S))$
10	0.181	7.1	0.00889	2204	0.049
12.5	0.18	7.51	0.0088	2228	0.049
15	0.176	8.94	0.025	797.95	0.139

* ω is the fluctuation frequency created by a doser, s⁻¹.

** S is an independent complex variable that stands for differentiation with respect to time.

The results of the performed analysis indicate that the second-stage CCM [11] has the same numerical values of the transfer function as for the first-stage CCM [12]. The difference exists only between the values obtained at $n = 15 \text{ s}^{-1}$, thus confirming the fact that the mixture components reside in the working zone of a mixer for a minimum period of time. For this reason, the second-stage CCM has not enough time to smoothen input flow fluctuations to an adequate degree.

Let us further consider some parameters of the implementation of the mathematical model of the studied MUs on the sugar-millet, salt-semolina, and river sand-ferromagnetic powder mixtures from Table 6 and 7.

Hence, the operational frequency regimes of dosers and CCMs have been matched for the preparation of high-quality mixtures with a high ratio of mixed components on the basis of cybernetic approach with some ACT elements. Theoretical and experimental analyses have allowed us to determine the obtained result error, which does not exceed $\pm 10.56 \%$. Consequently, the represented models adequately describe the obtained experimental data.

The smoothabilities of mixers with respect to input material flow fluctuations have been determined using the frequency and time methods. Their numerical values lie within a range from 50 to 2230 times. The discrepancy between the results of time-and-frequency analyses in the case of obtaining the white flour-potassium iodide mixture at a CCM rotor speed of 12.5 s^{-1} is 8.1%. Hence, the use of these methods of analysis is absolutely allowable.

The implementation of the mathematical models of mixing units that operate by the principle of the sequential dilution of a mixture shows that the best smoothability is attained for the mixing of components at first- and second-stage CCM rotor speeds of 15 and 10 s^{-1} , respectively.

It has been established that it is necessary to prolong the time of the residence of mixed components in the working zone by sequentially passing them through a greater number of cones to increase the smoothability of mixers.

Table 6. Smoothability and transfer function of the first mixing unit

First CCM					First CCM and second block of dosers		Second CCM or mixing unit		
n, s^{-1}	$X_{dm}^{IN}, g/s$	$X_{dm}^{OUT}, g/s$	$S(\omega^*)$	$W_{CM1}(S^{**})$	$X_{dm}^{IN}, g/s$	$W_{CM1+DB2}(S)$	$X_{dm}^{OUT}, g/s$	$S(\omega^*)$	$W_{CM2}(S^{**})$ ($W_{MU}(S)$)
Sugar-millet mixture									
10	1.35	0.042	287.9	0.031	0.363	8.69	0.029	775.7	0.081
12.5	1.35	0.028	430	0.021	0.354	12.65	0.292	77.35	0.825
15	1.35	0.03	404.8	0.022	0.355	11.94	0.071	322	0.2
Salt-semolina mixture									
10	1.47	0.012	1478	0.0082	0.383	31.65	0.066	522.4	0.173
12.5	1.47	0.018	1012	0.012	0.386	21.83	0.037	942.7	0.095
15	1.47	0.012	1502	0.008	0.383	32.1	0.038	910.2	0.1
River sand-ferromagnetic powder mixture									
10	1.23	0.04	220.97	0.033	0.262	6.55	0.022	772.5	0.083
12.5	1.23	0.03	294.14	0.024	0.255	8.47	0.023	740.1	0.089
15	1.23	0.027	332.36	0.022	0.252	9.48	0.023	742	0.09

* ω is the fluctuation frequency created by a doser, s^{-1} .

** S is an independent complex variable that stands for differentiation with respect to time.

Table 7. Smoothability and transfer function of the second mixing unit

First CCM					First CCM and second block of dosers		Second CCM or mixing unit		
n, s^{-1}	$X_{dm}^{IN}, g/s$	$X_{dm}^{OUT}, g/s$	$S(\omega^*)$	$W_{CM1}(S^{**})$	$X_{dm}^{IN}, g/s$	$W_{CM1+DB2}(S)$	$X_{dm}^{OUT}, g/s$	$S(\omega^*)$	$W_{CM2}(S^{**})$ ($W_{MU}(S)$)
Sugar-millet mixture									
10	0.65	0.031	514.1	0.048	0.353	11.21	0.028	965.3	0.079
12.5	0.65	0.031	761.2	0.033	0.348	16.35	0.017	1593	0.049
15	0.65	0.022	726	0.034	0.348	15.61	0.02	1357	0.057
Salt-semolina mixture									
10	0.93	0.006	3451	0.0069	0.381	58.75	0.079	496.9	0.207
12.5	0.93	0.006	1868	0.013	0.385	32.15	0.042	926.2	0.11
15	0.93	0.008	2734	0.0087	0.382	46.71	0.044	892	0.115
River sand-ferromagnetic powder mixture									
10	0.63	0.037	275.4	0.058	0.259	7.087	0.022	824.4	0.084
12.5	0.63	0.037	362.8	0.044	0.253	9.113	0.023	780.3	0.091
15	0.63	0.025	409.3	0.039	0.251	10.187	0.019	924.6	0.078

* ω is the fluctuation frequency created by a doser, s^{-1} .

** S is an independent complex variable that stands for differentiation with respect to time.

The developed mathematical models have allowed us to compare the operational efficiency of two centrifugal MUs. The analysis of results shows that the

second MU that incorporates three spiral dosers has the highest smoothability.

REFERENCES

1. Akhmadiev, F.G. and Aleksandrovskii, A.A., Modelirovanie i realizatsiya sposobov prigotovleniya smesei (Modeling and implementation of mixture preparation methods), *Zhurnal Vsesoyuznogo Khimicheskogo Obshchestva imeni D.I. Mendeleeva (Journal of All-Union Mendeleev Chemical Society)*, 1988, vol. 33, no. 4, p. 448.
2. Borodulin, D.M. and Ivanets, V.N., *Razvitie smesitel'nogo oborudovaniya tsentrobezhnogo tipa dlya polycheniya sukhikh i wvlazhnennykh kombinirovannykh produktov (Development of Centrifugal Mixing Equipment for the Preparation of Dry and Wetted Combined Food Products)*, Kemerovo: KemTIPP, 2012.
3. Gel'man, M.I. and Kirsanova, N.V., *Praktikum po fizicheskoi khimii. Uchebnoe posobie (Workshop on Physical Chemistry: Tutorials)*, St. Petersburg: Lan', 2004.
4. Ivanets, V.N., Smesiteli poroshkoobraznykh materialov dlya vitaminizatsii pishchevykh i kormovykh produktov (Mixers of powder-like materials for the vitaminization of food and fodder products), *Izvestiya Vysshikh Uchebnykh Zavedenii. Pishchevaya Tekhnologiya (News of Institutes of Higher Education. Food Technology)*, 1988, no. 1, pp.89-97.
5. Ivanets, V.N. and Poznyakovskii, V.M., *Gigienicheskie aspekty, tekhnologiya, i apparaturnoe oformlenie vitaminizatsii pishchevykh produktov (Hygienic Aspects, Technology, and Equipment Implementation of Food Product*

Vitaminization), Kemerovo: KemTIPP, 1991.

6. Ivanets, V.N. and Fedosenkov, B.A., *Protsessy dozirovaniya sypuchikh materialov v smeseprigotovitel'nykh agregatakh nepreryvnogo deistviya: obobshchennaya teoriya i analiz* (Bulk Material Dosing Processes in Continuous Mixture Preparing Units: Generalized Theory and Analysis), Kemerovo: KemTIPP, 2002.

7. Ivanets, V.N., Zhukov, A.N., and Borodulin, D.M., *Analiz chastotno-vremennykh kharakteristik smesitelya nepreryvnogo deistviya tsentrobezhnogo tipa* (Analysis of the time-and-frequency characteristics of a continuous centrifugal mixer), *Khranenie i Pererabotka Sel'khozsyrya* (Storage and Processing of Farm Products), 2004, no. 2, pp. 52-54.

8. Kafarov, V.V. and Dorokhov, I.N. *Sistemnyi analiz protsessov khimicheskoi Tekhnologii* (System Analysis of Chemical Engineering Processes), Moscow: Nauka, 1976.

9. Lazareva, T.Ya. and Martem'yanov, Yu.F., *Osnovy teorii avtomaticheskogo upravleniya. Uchebnoe posobie* (Foundations of Automatic Control Theory: Textbook), Tambov: Izd. Tambov. Gos. Univ., 2004.

10. Makarov, Yu.I., *Apparaty dlya smesheniya sypuchikh materialov* (Apparatuses for the Mixing of Bulk Materials), Moscow: Mashinostroenie, 1973.

11. RF Patent 2361653, *Byull. Izobret.*, 2009, no 20.

12. RF Patent 2207186, *Byull. Izobret.*, 2003, no. 18.

13. Dehling, H.G., Hoffmann, A.C., and Stuu, H.W., Stochastic models for transport in a fluidized bed, *SIAM Journal on Applied Mathematics*, 1999, vol. 60, no. 1, p. 337-358.

14. Hoffmann, A.C. and Paarhuis, H.I., A study of the particle residence time distribution in continuous fluidized beds, *Institution of Chemical Engineers Symposium Series*, 1990, vol. 121, p. 37-49.

15. Salahudeen, S.A. and AlOthman, O., Optimization of rotor speed based on stretching, efficiency, and viscous heating in nonintermeshing internal batch mixer: simulation and experimental verification, *Journal of Applied Polymer Science*, 2013, vol. 127, no. 4, pp. 2739-2748.



UDC 637.024, 548.5, 532.5.
DOI 10.12737/1559

LACTOSE CRYSTALLIZATION: CURRENT ISSUES AND PROMISING ENGINEERING SOLUTIONS

A.E. Rjabova, V.V. Kirsanov, M.N. Strizhko, A.S. Bredikhin, V.K. Semipyatnyi,
V.V. Chervetsov, A.G. Galstyan

All-Russia Dairy Research Institute,
Lusinovskaya ul. 35, Moscow, 115093 Russia
phone::/Fax: (499)236-02-36, E-mail: conservlab@mail.ru

(Received March 05, 2013; Accepted in revised form March 12, 2013)

Abstract: Current technological aspects of lactose crystallization are considered. A promising lactose crystallization method involving simulation seed crystals is reported. Advanced engineering solutions for continuous crystallization using spraying in vacuo and scraped-surface heat exchangers are presented.

Key words: lactose, heterogeneous and homogeneous crystallization, simulation seed crystals, continuous crystallization of lactose, scraped-surface plate-type cooling crystallizer, vacuum spray crystallizer.

INTRODUCTION

Lactose crystallization is among the necessary technological operations in the production of sweetened canned condensed milk. This operation consists of creating appropriate conditions for extensive formation of crystallization centers and for subsequent controllable crystal growth at certain processing parameters and under post-production storage conditions.

The lactose crystallization kinetics can be described in terms of a $C = f(t)$ function, where C is the lactose concentration in the solution (%) and t is time (s). The corresponding crystallization curve can conventionally be divided into the following three segments: induction period, in which $C = \text{const}$; rapid increase in the concentration with time; slow variation of the concentration at the late stages of the process.

The first period is characterized by the formation of crystal nuclei; the second and third periods, by their growth. A nucleus (crystallization center) is the minimum amount of a new phase that is capable of independently existing [1, 10]. Once stable nuclei have formed in the new phase, they begin to grow. The main processes determining the crystal growth rate are the diffusion of the constituent particles to the surface of the growing crystal and their incorporation in the crystal lattice. In turn, the latter process includes the adsorption of particles by the surface, their migration on the surface, and their incorporation in the lattice as such.

The factors on which the crystal growth rate depends are the solution temperature, stirring intensity, the presence of impurities, degree of supersaturation, viscosity, etc. The effect of a given factor depends on crystallization conditions. For example, the variation of the crystal growth rate with the degree of supersaturation depends on whether the solution is stirred or not. On the whole, the value of supersaturation is so significant that its variation alters the growth

mechanism [2–4, 9–11]. A large number of crystal growth theories have been devised to account for the complicated dependence of the growth rate on various factors. However, there is still no unified theory completely describing the multiformity of the crystallization process.

Contributions to classical crystallization theory were made by J. Gibbs, M. Volmer, W. Kossel, I.N. Stranskoi, and R. Kaishev. The theory is based on the thermodynamic conception that an isolated system is absolutely stable when its entropy is invariable [5].

The present-day technologies of production of sweetened condensed dairy products necessarily include the introduction of seed crystals for preventing the consistency defects arising from uncontrolled lactose crystallization. The seeds used in these technologies are microcrystalline lactose with a crystal size of 2–3 μm , supersaturated solutions or suspensions of lactose containing crystal nuclei, and water-soluble crystalline macromolecular organic compounds mixed with lactose [6, 7].

The seed material is introduced at the enhanced crystallization temperature, which depends on the lactose concentration in the system. At this temperature, the maximum degree of lactose supersaturation is rapidly reached at a minimum increase in the viscosity of the milk. The enhanced crystallization temperature is determined from Hudson's plot shown in Fig. 1.

To determine the enhanced crystallization temperature of lactose, the weight fraction of lactose in the aqueous part of condensed milk (lactose number) is first determined. Next, the intersection point between the vertical line corresponding to this lactose weight fraction and the enhanced crystallization curve is found. This intersection point indicates the mass crystallization temperature in the ordinate axis.

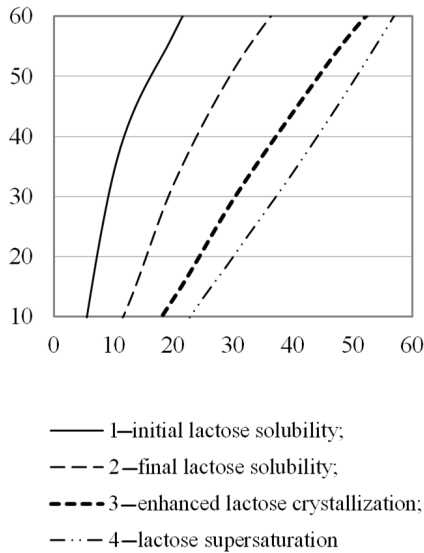


Fig. 1. Plot for determining the enhanced lactose crystallization temperature.

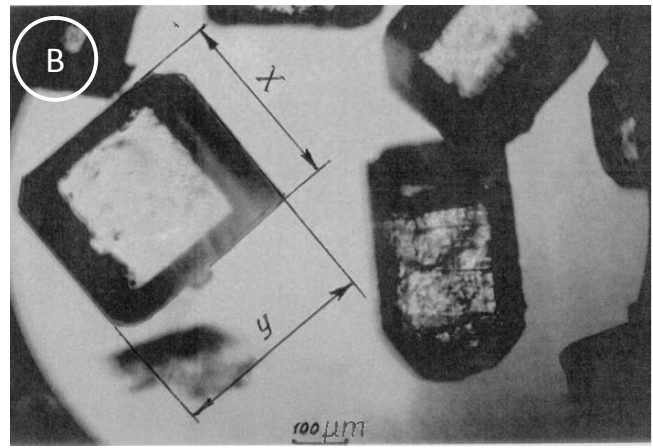
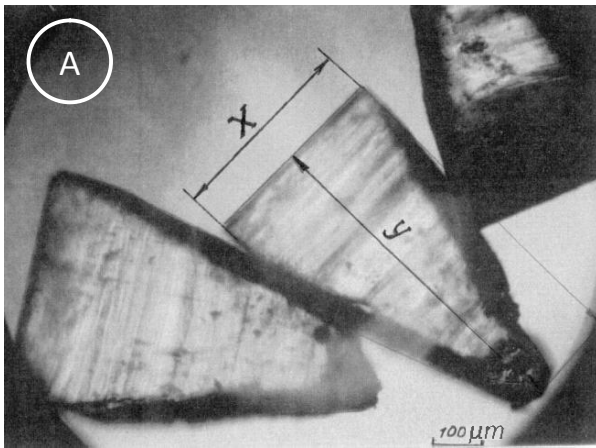


Fig. 2. Microstructure and classical shape of crystals of (A) α -lactose monohydrate and (B) sucrose.

Figure 2 shows the lactose and sucrose crystal shapes.

Tables 1 and 2 list the values of crystallization efficiency criteria and lactose crystals settling velocity data, respectively.

Table 1. Crystallization efficiency criteria

Number of crystals in 1 mL ³ of sweetened condensed milk, thousands	Average particle size, μm	Consistency of sweetened condensed milk
400–300	≤ 10	Uniform
300–100	12–15	Slight floury
100–50	16–20	Floury
50–25	21–24	Strong floury
≤ 25	≥ 25	Sandy

The mutarotation phenomenon takes place in lactose solutions. The lactose isomers are in dynamic equilibrium. α -Lactose turns into β -lactose via the tautomeric aldehyde form, which has a carbonyl group. α -Lactose crystallizes under commonly used process conditions, because it is less soluble than the β -form. β -Lactose begins to turn into α -lactose once the latter has

The lactose weight fraction in condensed milk (L_{pr} , %) is calculated via the formula

$$L = \frac{L_n \times F_{pr}}{F_n} \tag{1}$$

where L_n is the lactose weight fraction in normalized milk (%), F_{pr} is the weight fraction of fat in the product (%), and F_n is the weight fraction of fat in normalized milk (%).

The lactose weight fraction in the aqueous part of condensed milk (lactose number, L_{con} , %) is calculated via the formula

$$L_{con} = \frac{100 \times L_{pr}}{L_{pr} + W_{pr}} \tag{2}$$

where L_{pr} is the lactose weight fraction in sweetened condensed milk (%) and W_{pr} is the water weight fraction in sweetened condensed milk (%).

precipitated. This can be explained by the disturbance of the dynamic equilibrium between the isomers.

Table 2. Lactose crystals settling velocity in sweetened condensed whole milk as a function of viscosity and crystal size

Consistency	Viscosity, Pa.s	Crystal size, μm	Settling velocity, cm/day (*)
Velvety (uniform)	2.0	10	0.0470 (5.7)
	3.0	10	0.0309 (8.6)
	5.0	10	0.0188 (14.0)
	10.0	10	0.00941 (28.6)
Floury (nonuniform)	2.0	20	0.189 (1.4)
	3.0	20	0.124 (2.1)
	5.0	20	0.0754 (3.2)
	10.0	20	0.0377 (7.0)
Sandy	2.0	40	0.766 (0.33)
	3.0	40	0.497 (0.53)
	5.0	40	0.300 (0.86)
	10.0	40	0.149 (1.8)

* Sediment formation time in months

This process continues until the solution is completely exhausted. Even if seed crystals have been introduced, it is practically impossible to completely eliminate the supersaturation of the solution and to bring crystallization to completion at the product cooling stage, so lactose crystals continue growing during long-term storage at low temperatures, and this can lead to the formation of large crystals. Recrystallization processes consisting in the growth of larger crystals at the sacrifice of small crystals are also possible here. This recrystallization, which progressively spoils canned dairy products, most often occurs under uncontrolled temperature variations during storage [8, 11].

If the product is additionally heated after the introduction of seed crystals, the crystallization process will be inefficient. This technology is used in the production of boiled sweetened condensed milk.

Having analyzed the literature and internet sources dealing with crystallization, including the crystallization of salts, various alloys, and biological fluids, we considered the possibility of replacing conventional seed materials with alternative crystalline substances. It was found that continuous lactose crystallization methods are promising.

The purpose of this work is to investigate the basic principles of the heterogeneous lactose crystallization technology and to design apparatuses for continuous crystallization using spraying in vacuo and scraped-surface heat exchangers.

The introduction of this crystallization technology in the dairy industry would shorten the processing time and significantly reduce the working area requirements.

EXPERIMENTAL

The objects of this study were lactose and demineralized whey solutions and sweetened condensed milk. The simulation seed materials were calcium carbonate, titanium dioxide, and silicon dioxide powders with a crystal size of 1–4 μm . The amount of seeds added was 0.02–0.1% of the product weight. The seed material was introduced at $(33.5 \pm 1.5)^\circ\text{C}$. The linear dimensions of the lactose crystals in the samples examined were determined using L.V. Chekulaeva's procedure. The crystal size uniformity coefficient was determined via N.A. Figurovskii's formula.

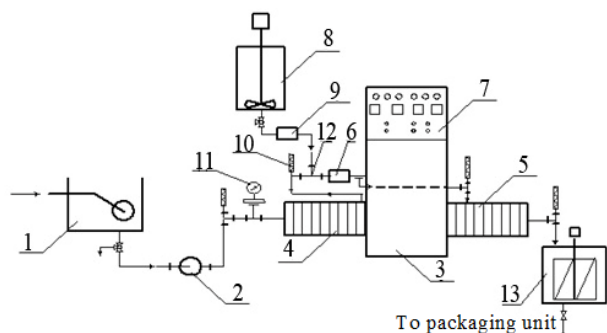


Fig. 3. Schematic of the improved unit for continuous cooling of sweetened condensed milk: (1) receiver tank, (2) product supply pump, (3) scraped-surface heat exchanger, (4) first cooling section, (5) second cooling section, (6) disc treater, (7) control board, (8) seed tank, (9) dosing pump, (10) resistance thermometer, (11) membrane manometer, (12) jet mixer, and (13) buffer tank.

The improved pilot plant based on a scraped-surface heat exchanger for continuous crystallization of lactose in canned dairy products is schematized in Fig. 3.

The plant consists of the following elements: receiver tank 1; positive displacement pump 2 for product supply, fitted with an IG5-Rus frequency changer (LG Corp.); two-section scraped-surface heat exchanger 3 with a disc treater 6 equipped with an IG5-Rus frequency changer (LG Corp.); jacketed seed tank 8 with an impeller; dosing pump 9; jet mixer 12; resistance thermometers 10; membrane manometers 11; control board 7; stirred buffer tank 13.

The unit was operated in the following way. After vacuum evaporation, the condensed lactose-containing product, whose temperature was $55\text{--}60^\circ\text{C}$, entered the receiver tank, from which it was pumped into the first section of the scraped-surface plate-type heat cooler, where it was cooled to the lactose mass crystallization temperature. Next, the product entered the disc treater that consisted of a system of rotating and fixed discs. Passing through the gaps between the discs, the product was subjected to intensive mechanical treatment. A dispersion of microcrystalline lactose from the seed preparation tank was injected with the dosing pump through the jet mixer into the product stream entering the disc treater. In the jet mixer, the injected liquid stream was preliminarily broken up by the product stream passing through the mixer. Next, the seed-containing dispersion droplets were further reduced and uniformly incorporated in the product in the disc treater. This ensured the uniform distribution of the seed crystals over the entire volume of the product. Since the actuator of the disc treater was equipped with a frequency changer, it was possible to vary the intensity of mechanical treatment to alter the crystal size.

The product that left the disc treater was directed to a holder and then to the second section of the cooler, where it was cooled to room temperature ($18\text{--}20^\circ\text{C}$). Prior to be canned, the product was stirred in the buffer tank.

The improved pilot plant based on vacuum spray crystallization is schematized in Fig. 4.

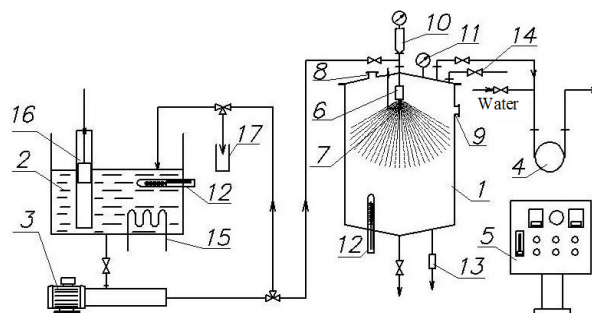


Fig. 4. Setup for investigating the continuous vacuum crystallization process: (1) vacuum chamber, (2) product tank, (3) screw pump, (4) liquid ring vacuum pump, (5) control board, (6) spray nozzle, (7) movable temperature sensor, (8) two lamps, (9) inspection window, (10) air dome with a pressure–vacuum gage, (11) standard vacuum gage, (12) resistance thermometer, (13) vacuum relief valve, (15) electric heater, (16) flowmeter, (17) measuring vessel, and (18) crate with beakers.

This setup includes a 0.075-m³ vacuum chamber 1 with a spray nozzle 6 mounted at its top. The lid of the vacuum chamber has two lamps 8, a vacuum gage 11, a well for the movable temperature sensor 7, a pipe with a vacuum relief valve 14, and an air suction pipe. In the upper part of the sidewall, there are two inspection windows for watching the spraying process and photographing. The bottom of the vacuum chamber has an emptying pipe, a temperature sensor 12, and a sampler 13. There is a crate with beakers 18 inside the vacuum chamber for determination of the irrigation density. The setup includes an OVN-4 screw pump 3 fitted with an IG5-Rus frequency changer (LG Corp.), an MEX-50 liquid ring vacuum pump 4 (Italy), a control board 5, and a 0.006-m³ product tank 2 with an electric heater 15 operable in automatic and manual modes, a resistance thermometer 12, and a float-type flowmeter 16. The capacity of the screw pump is measured using a measuring vessel 17. Temperature is measured with TSP-0879-01 resistance thermometers with a TRM-2 microprocessor-based temperature controller.

The unit was operated in the following way. The initial product from tank 2 was delivered by the screw pump 3 at a preset rate through the spray nozzle with a given geometry into the vacuum chamber pumped down to a preset depression. The sprayers were geometrically similar conical nozzles with an outlet orifice diameter of $d_c = 0.82 \times 10^{-3} - 2.15 \times 10^{-3}$ m. Experiments were carried out on distilled water, a 50% lactose solution, and condensed whey with a dry matter content of 50±1% at 60–80°C and on sweetened condensed milk with a water content of 26.5% at 50–90°C. The following parameters were monitored during the experiment: product tank temperature, vacuum chamber temperature at fixed distances from the nozzle, throughput capacity (by a volumetric method), pressure before the nozzle, and depression in the chamber.

The product samples obtained in these experiments were packed in tin cans (400 g of product in each) and were stored for 120 days at 6–10°C. The lactose crystal size was determined in the freshly prepared product, in the product that had been stored for 48 h, and then at 15-day intervals.

RESULTS AND DISCUSSION

Simulation seed materials

It was established that the minimum necessary dosage and particle size of a seed material depend crucially on what the seed material is and when it is introduced. Preliminary crystallization efficiency data (obtained after 48-h-long storage) as a function of the quantity of seeds introduced are presented in Fig. 5.

It follows from the data presented in Fig. 5 that the crystallization efficiency depends significantly on the kind and amount of simulation seed material. The highest efficiency (96%) was achieved with 0.2% SiO₂, and the lowest efficiency was observed for 0.01% TiO₂. A decrease in the dosage of a simulation seed material exerts an adverse effect irrespective of what the material is. Preliminary studies demonstrated that, when the amount of seed material is 0.05% or below, up to 38% of the samples undergo no crystallization. Note that the efficiency of the process does not depend significantly

on whether 0.1 or 0.2% seed material is added. For this reason, subsequent studies were carried out for a seed material dose of 0.1%.

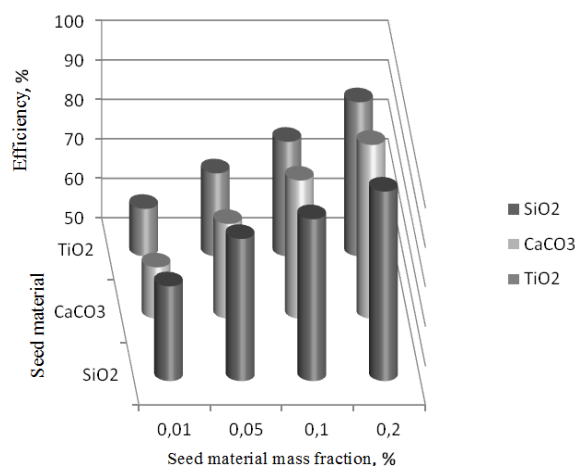


Fig. 5. Crystallization efficiency as a function of the kind and amount of seed material introduced.

The resulting samples were stored for 90 days at 6–10°C. The crystal size of lactose in the samples was determined at 15-day intervals. The results of these measurements are presented in Fig. 6.

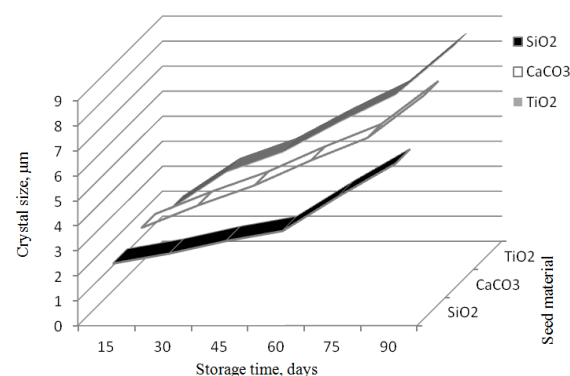


Fig. 6. Crystallization efficiency during storage as a function of the kind and amount of seed material introduced.

Silicon dioxide proved to be the most effective seed material: with a SiO₂ dose of 0.1% relative to the product weight, the average crystal size of lactose did not exceed 6.4 μm on the 90th day. A seed dose was considered to be effective when its increase did not exert any significant effect on lactose crystallization.

It was found that use of a simulation seed material does not change the classical shape of lactose crystals (Fig. 7).

On the whole, the seed efficiency decreases in the following order: SiO₂ > TiO₂ > CaCO₃.

These data suggest that use of alternative seed materials in lactose crystallization from saturated solutions needs to be further studied.

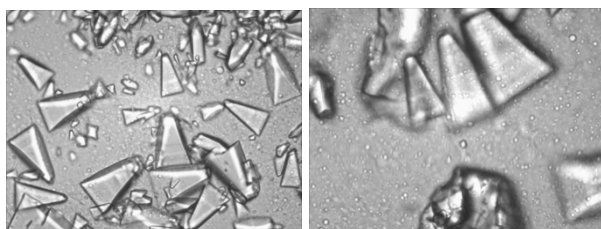


Fig. 7. Lactose crystals with simulation nuclei.

Continuous crystallization in a scraped-surface heat exchanger

The experiments carried out in this study can be divided into two groups. In the first group, the seed materials was a suspension of lactose powder in a vegetable oil (combined seed material); in the second group, the seed material was the finished product that had been subjected to crystallization.

Below, we will consider the most important results of these experiments. The first group of experiments included two variants.

First variant. The seed material as a suspension of lactose powder in a vegetable oil (0.12% of the product weight) from tank 8 was continuously introduced with the dosing pump 9 into the product stream through the special-purpose jet mixer 12 downstream of the first section of the cooling crystallizer (Fig. 3) at the lactose mass crystallization temperature. Next, the product was directed to the disc treater, where it was subjected to intensive hydrodynamic treatment ($n = 1000$ rpm). As a result, the seed material and fat were uniformly distributed throughout the product volume and the fat was finely dispersed. The product processed in this way entered the holder, which was a tube segment 50 mm in diameter connecting the disc treater with the second section. The residence time of the product in the holder was 4 s at a preset crystallizer throughput capacity of 300 kg/h.

In the second section, the product was cooled to 20°C, the temperature prescribed by the technical regulations.

The seed introduction temperature was varied between 30 and 35°C in 1°C steps. The product was sampled after the second cooling stage. The size distribution of lactose crystals in the samples was determined via a standard procedure.

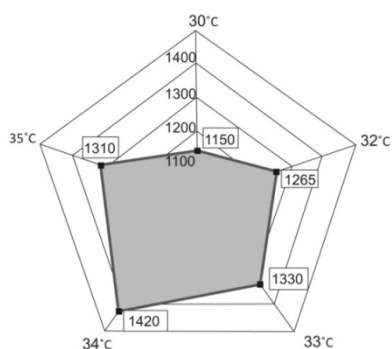


Fig. 8. Dependence of the extent of crystallization of lactose on the seed introduction temperature.

Figure 8 shows how the extent of crystallization of lactose in the product depends on the seed introduction

temperature. It is clear from the plot that the number of the resulting crystals depends on the mass crystallization temperature and reaches its maximum value of 1420 thousands per cubic millimeter (average crystal size of 4.5–5.0 μm) at 34°C.

Second variant. In order to evaluate the effect of hydrodynamic treatment intensity on the crystal size distribution of lactose, we carried out a series of experiments at different rotational speeds of the working elements of the disc treater. Sweetened condensed milk at 55°C was fed into the first section of continuous cooling crystallizer, where it cooled to 34°C. At this temperature, the combined seed material was introduced into the product. After the introduction of the seed material, the product was subjected to intensive mechanical treatment in the disc treater. The rotational speed of the working elements of the disc treater was varied from one series of experiments to another and was 200, 600, or 1000 rpm. The product leaving the disc treater was directed through the holder to the second section of the continuous cooling crystallizer, where it was cooled to 20°C.

For proving the efficiency of the method suggested here, we cooled the product in the conventional way. In this experiment, the product temperature decreased from 55 to 20°C in 40 min. The linear dimension of 100 lactose crystals was measured in the samples, and the average value was then determined (Table 3).

Table 3. Crystal size data for lactose

Parameter	Conventional crystallization	Continuous crystallization					
		after the disc treater for different rotational speeds, rpm			after the second cooling section for different rotational speeds, rpm		
		200	600	1000	200	600	1000
Average lactose crystal size, μm	6.35	7.72	6.26	5.03	5.84	4.83	4.18
Size uniformity coefficient	0.65	0.63	0.71	0.76	0.83	0.87	0.91

From the cumulative size distribution curves (Fig. 9), we derived the size uniformity coefficient.

Based on the data presented in Table 3, we plotted the dependence of the average lactose crystal diameter on the rotational speed of the working elements of the disc treater (Fig. 10). It can be seen from the plot that the average lactose crystal diameter definitely depends on the rotational speed of the working elements: as the rotational speed is increased, the lactose crystal diameter at the apparatus outlet decreases on the average by 30%. This seems to be a significant factor for enhancing the quality and storability of the finished product.

The second series of experiments was aimed at organizing a continuous process for lactose crystallization in the sweetened condensed milk without use of lactose powder. The seed material in these experiments was the finished product that had been

subjected to crystallization. This variant of the process is prescribed by the RF Regulations TPI GOST R 53436-001.

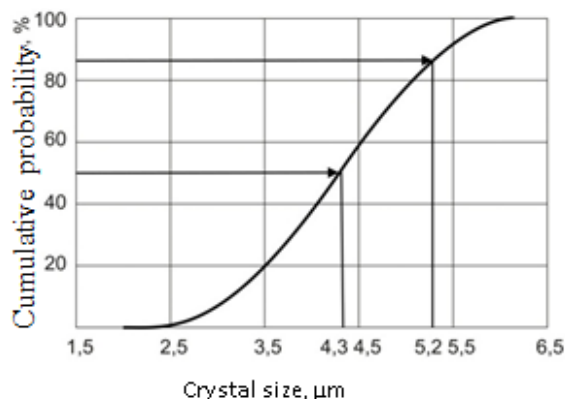


Fig. 9. Cumulative crystal size distribution function for lactose.

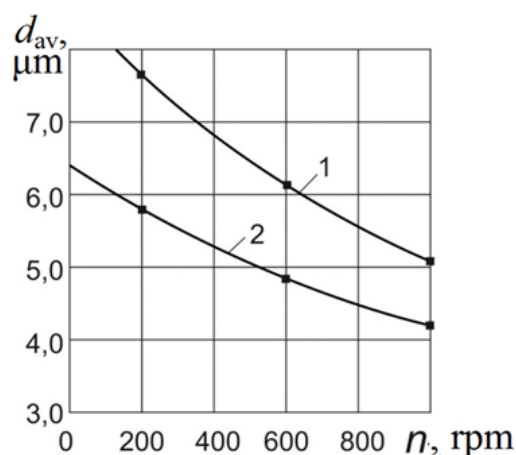


Fig. 10. Average lactose crystal diameter as a function of the rotational speed of the working elements of the disc treater: crystals (1) after the disc treater and (2) after the second section of the cooling crystallizer.

In conventional (batch) crystallization, it is allowable to replace lactose powder with an earlier obtained finished product having good organoleptic properties (1.5–2.0% of the weight of the product being processed).

The design of our pilot plant allows this replacement to be made. In this case, a small amount of combined seed material that is necessary only for starting the plant is prepared in the seed tank. After the entire seed material is consumed, part (1.5–2.0%) of the finished product is continuously supplied to the seed tank via a special-purpose pipeline. This part of the product is injected into the product stream with a dosing pump through a special-purpose mixer. Next, the product enters the disc treater, which ensures perfect mixing and exerts strong hydrodynamic action on the product, thus intensifying crystal nucleation and growth. After passing through the holder, the product cools to the final temperature prescribed by the technical regulations in the second section of the scraped-surface plate-type heat exchanger, which is employed as the lactose cooling crystallizer. Note that the seed material in the plant startup period can be the finished product with good velvety consistency from an earlier batch. This approach

excludes lactose powder from the technology, making this variant of the crystallization process very advantageous.

For experimental confirmation of the possibility of carrying out continuous lactose crystallization with part of the finished product used as the seed material and for optimizing the processing conditions, we performed the second series of experiments, in which part of the finished product as the seed material was returned via a special-purpose pipeline into the seed tank and was then injected with the dosing pump into the product stream cooled to the lactose mass crystallization temperature. The experiments in which part of the finished product was recycled in this way yielded good results: all samples examined had over 1 million lactose crystals per cubic millimeter of the finished product, and the average crystal size was 4–5 μm . This ensured the uniform velvety consistency of the product. Note the very favorable crystal size distribution: the first group of crystals (below 10 μm) included 98–99% of the total number of crystals, and the crystallization uniformity coefficient was 0.87–0.92. For the sake of comparison, we carried out experiments on the same product using the conventional (batch) method of lactose crystallization.

The continuous crystallization experiments were performed at different seed introduction temperatures (30–35°C). The product was sampled using four samplers: (I) sampler placed downstream of the jet mixer before the inlet of the disc treater, (II) sampler placed before the holder, (III) sampler placed before the second section of the crystallizer, and (IV) finished-product sampler mounted at the outlet of the apparatus.

Figure 11 illustrates the kinetics of the continuous crystallization of lactose at different seed introduction temperatures. The total residence time of the product in the apparatus was 30 s, which consisted of the following periods: 8 s, the first section of the cooling crystallizer; 2 s, disc treater; 4 s, holder; 16 s, the second section of the crystallizer.

As the seed material is injected into the product stream and as the product is subsequently processed in the disc treater (2 s), rapid nucleation of lactose crystals takes place to the extent of 0 to 600–700 thousands per cubic millimeter; after the holder, the number of crystals increases to 1000–1200 thousands per cubic millimeter; at the apparatus outlet, it is as large as 1300 thousands per cubic millimeter. The average crystal diameter increase simultaneously from 3.7 μm at the beginning of the process to 5.4 μm at the outlet of the apparatus.

Lactose crystallization in the continuous cooling crystallizer begins at point B, which corresponds to the point at which the seed material is introduced into the product stream. The segment AB of the curves indicates the induction period in lactose crystallization. In the curve segment BC, which corresponds to processing in the disc treater, intensive lactose crystallization takes place (dashed straight line slightly deviating from the vertical). The segment CD indicates the end of product processing in the disc treater and is characterized by a further rapid increase in the number of lactose crystals and by a distinct branching of the kinetic curve into the

curves corresponding to different seed introduction temperatures. The segment DE corresponds to product passage through the holder and is characterized by a further increase in the number of lactose crystals. The segment EF corresponds to the cooling of the product from the seed introduction temperature to the final temperature specified in the technical regulations in the second section of the crystallizer. In this period, the rate of increase of the number of crystals decreases and the curves tend to their maximum level. This indicates the end of crystallization at the given supersaturation.

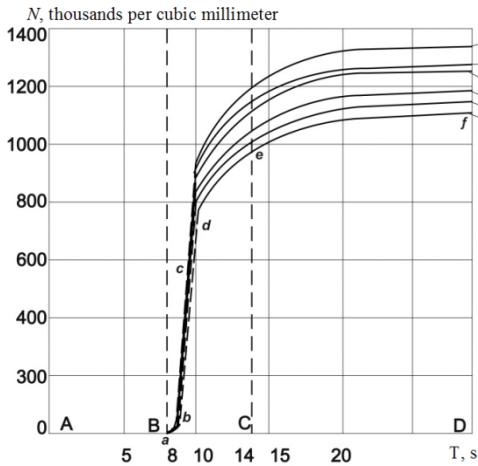


Fig. 11. Lactose crystallization kinetics at seed introduction temperatures of (1) 30, (2) 31, (3) 32, (4) 33, (5) 34, and (6) 35°C.

The data plotted in Fig. 11 also suggest that the optimal seed introduction temperature is 34°C, at which the most extensive crystallization is observed.

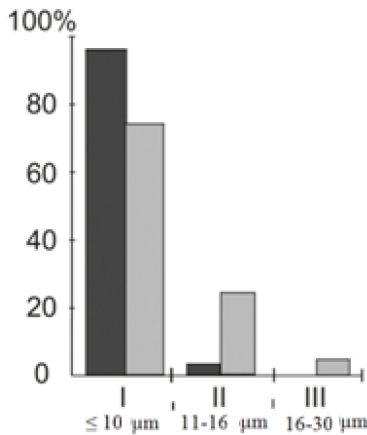


Fig. 12. Histogram of the size distribution of lactose crystals.

Figure 12 presents the histogram of the size distribution of lactose crystals. It is clear that, in continuous lactose crystallization in the sweetened condensed milk, the greater part of the crystals (98%) belongs to the first size group ($\leq 10 \mu\text{m}$) and there are no lactose crystals belonging to the third group 16 to 30 μm). The processing of a reference sample by the conventional method yielded the following crystal size

distribution: first group, 75%; second group, 22%; third group, 3%. This size distribution is obviously worse.

Continuous crystallization using product spraying in vacuo

Using a model of the product (aqueous solution of lactose with a dry matter content of 50%), we optimized the spray nozzle geometry and selected a nozzle for the vacuum crystallizer (Fig. 13).

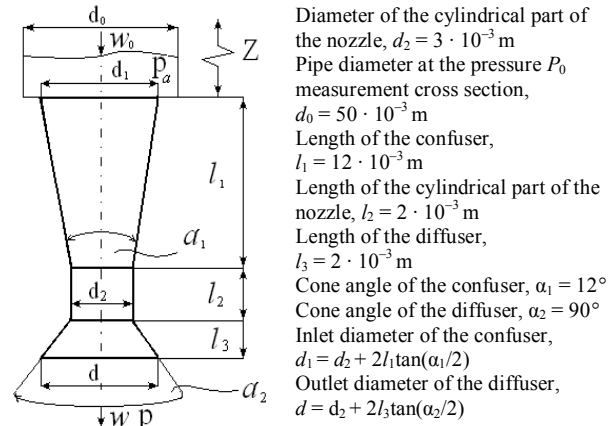


Fig. 13. Schematic of the spray nozzle of the vacuum crystallizer.

We elucidated the dependences of the spray angle on the product inlet pressure at a fixed depression in the vacuum chamber and on the product inlet temperature (Figs. 14, 15).

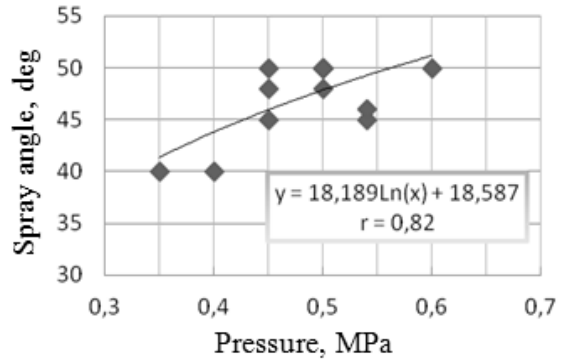


Fig. 14. Spray angle as a function of inlet pressure at 60°C.

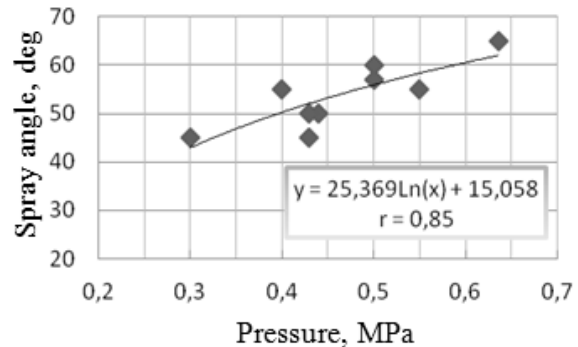


Fig. 15. Spray angle as a function of inlet pressure at 80°C.

It was experimentally confirmed that it is possible to generate a large number of lactose crystals in the lactose-containing product by spraying the latter in a chamber at a residual pressure of 550–700 Pa and a temperature of 60–90°C, which is well above the boiling point at this pressure.

It was also proved experimentally that the final product temperature depends on the initial temperature at a constant product inlet temperature and a constant depression in the vacuum chamber (Fig. 16). It was elucidated how the final product temperature depends on the injection pressure (Fig. 17).

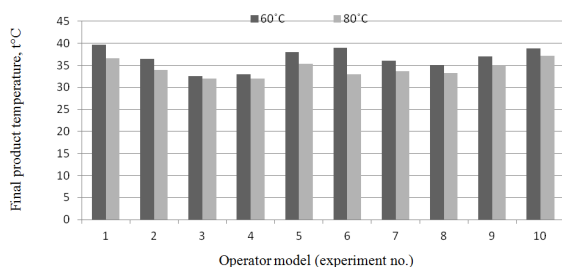


Fig.16. Final product temperature as a function of the initial product temperature.

CONCLUSIONS

This study of the continuous crystallization of lactose in sweetened condensed milk suggests the following conclusions:

(1) The heterogeneous crystallization of lactose is promising for production of sweetened condensed dairy products.

(2) Experiments proved the theoretical prediction that continuous crystallization can be carried out in an apparatus based on scraped-surface plate-type heat exchanger.

(3) Two variants of seed introduction at the optimal mass crystallization temperature of lactose were considered. Both are efficient and can be industrially used in the operation of a continuous cooling crystallizer.

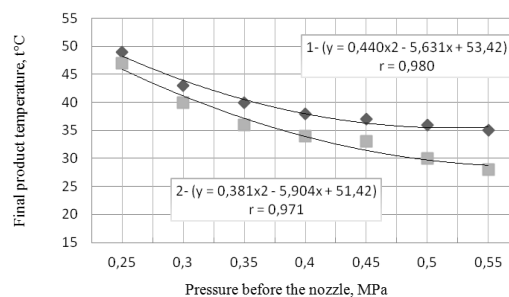


Fig. 17. Final product temperature as a function of the pressure before the nozzle.

(4) Use of the disc treater in combination with the continuous cooling crystallizer ensures uniform distribution of the seed material over the entire product volume. Moreover, the hydrodynamic action of the disc treater on the product intensifies the crystallization process and favors the formation of smaller crystals.

(5) Vacuum spray crystallization is a promising method for processing lactose-containing feedstocks.

REFERENCES

- Zel'dovich, Ya.B., K teorii obrazovaniya novoi fazy: kavitatsiya (On the theory of the formation of a new phase: cavitation), *Zhurnal eksperimental'noi i teoreticheskoi fiziki* (Journal of experimental and theoretical physics), 1942, vol. 12, nos. 11–12, pp. 525–538.
- Polyanskii, K.K. and Shestov, A.G., *Kristallizatsiya laktozy: fiziko-khimicheskie osnovy* (Lactose Crystallization: Physicochemical Foundations), Voronezh: Voronezh. Gos. Univ., 1995.
- Gnezdilova, A.I., Razvitie nauchnykh osnov kristallizatsii laktozy i sakharozy v mnogokomponentnykh vodnykh rastvorakh (Development of the scientific foundations of lactose and sucrose crystallization from multicomponent aqueous solutions), *Doctoral (Eng.) Dissertation*, Vologda, 2000.
- Polyanskii, K.K., *Kristallizatsiya laktozy v proizvodstve molochnykh produktov* (Lactose crystallization in the production of dairy products), *Doctoral (Eng.) Dissertation*, Moscow, 1981.
- Stranskii, I.N. and Kaishev, R., K teorii rosta kristallov i obrazovaniya kristallicheskih zarodyshei (On the theory of crystal growth and nucleation), *Uspekhi khimii* (Russian chemical reviews), 1939, vol. 21, no. 4, pp. 408–465.
- Khramtsov, A.G., *Molochnyi sakhar* (Lactose), Moscow: Agropromizdat, 1987.
- Chekulaeva, L.V., Polyanskii, K.K., and Golubeva, L.V., *Tekhnologiya produktov konservirovaniya moloka i molochnogo syr'ya* (Production of Canned Milk and Dairy Products), Voronezh: Voronezh. Gos. Univ., 1996.
- Golubeva, L.V., Chekulaeva, L.V., and Polyanskii, K.K., *Khranimosposobnost' molochnykh konservov* (Storability of Canned Dairy Products), Moscow: DeLi Print, 2001.
- Shabalin, V.N. and Shatokhina, S.N., *Morfologiya biologicheskikh zhidkostei cheloveka* (Morphology of Human Biological Fluids), Moscow: Khrizostom, 2001.
- Rosenberger, F., *Fundamentals of Crystal Growth*, Berlin: Springer, 1979.
- Hartel, R.W., *Crystallization in Foods*, New York: Aspen, 2001.

UDC 66.067.38
DOI 10.12737/1560

INTENSIFICATION OF ULTRAFILTRATION CONCENTRATING BY THE SEPARATION OF THE CONCENTRATION BOUNDARY LAYER

B. A. Lobasenko¹ and A. G. Semenov²

Kemerovo Institute of Food Science and Technology,
bul'v. Stroitelei 47, Kemerovo, 650056 Russia

¹phone/Fax: +7(3842) 39-68-42, e-mail: lobasenko@mail.ru

²phone/Fax: +7(3842) 68-00-49, e-mail: agsem55@yandex.ru

(Received January 10, 2013; Accepted in revised form February 11, 2013)

Abstract: The possibility of intensifying the ultrafiltration concentrating of food substance solutions by the separation of the near-membrane flow part that comprises the concentration boundary layer (or diffusion layer) enriched by a useful component has been investigated in this study. A mathematical model of the longitudinal development of polarization on a membrane with consideration of its selectivity (rejection coefficient) has been proposed. The efficiency of the separation of the near-membrane layer has theoretically been estimated on the basis of this model. Some constructions of membrane modules with the separation of the near-membrane layer have been proposed. Experiments have shown that the proposed method allows the concentrate to be enriched in the continuous-flow module by 9–10%, which is much higher than for the traditional concentrating process. The calculated concentration coefficients are in good agreement with experimental values.

Key words: ultrafiltration, concentrating, intensification, concentration polarization, rejection coefficient, concentration coefficient.

INTRODUCTION

The development of simple and economical methods for the separation, purification, and concentrating of liquid media is one of the most important problem in the food industry and, especially, in the dairy industry. Membrane technologies, which have a number of advantages in comparison with traditional separation methods, are especially noteworthy [1, 2]. This explains a profound interest in membrane processes, to which a considerable number of theoretical and experimental studies have been devoted.

However, membrane methods have some disadvantages reducing the efficiency of the process. The most essential of them is the formation of the diffusion boundary layer with an increased concentration of rejected substances on the membrane surface (i.e. concentration polarization), which promotes the formation of a gel layer hindering the removal of a solvent.

The weakening of concentration polarization is a traditional way of increasing the efficiency of membrane equipment [3]. It is attained via the turbulization of a flow with mechanical turbulizers [4–7] or gas sparging [9–13] or via the physical effect on a flow with mechanical vibrations [14–16], ultrasound [17–20], or an imposed electrical field [21]. All these methods lead to additional expenditures, complicate the structure of an apparatus, degrade the quality of a processed product, and increase its cost.

In this work, we consider the possibility of the intensification of ultrafiltration concentrating by the separation of the near-membrane part of a solution flow

as a resulting product. It comprises the diffusion boundary layer, the concentration in which is appreciably higher than in the major part of a flow (flow middle). This enables the obtaining of a highly concentrated product at lower energy consumption, since a solution flows in the laminar regime.

The objective of our work is to perform the theoretical and experimental analysis of the efficiency of the separation of the near-membrane layer, to estimate the effect of geometrical and regime parameters, and to describe the technical implementation of the proposed idea.

OBJECTS AND METHODS OF STUDY

In the theoretical part of our work, we consider the mathematical model of the ultrafiltration concentrating of a high-molecular substance through a tubular membrane with a radius R , with the separation of the near-membrane flow part at the outlet of the membrane channel. In our analysis, we have made the following assumptions:

(1) A solution flows in the laminar regime, and the tangential velocity profile $u(r)$ is determined by the Hagen–Poiseuille equation

$$u(r) = 2U \left(1 - \frac{r^2}{R^2} \right), \quad (1)$$

where r is the radial coordinate counted from the axis of the membrane channel, and U is the average velocity of a solution flow;

(2)The physical properties of a solution are constant and independent of the concentration of a high-molecular substance;

(3)The concentration of a high-molecular substance in the flow middle outside the diffusion layer is constant and equal to c_0 ;

(4)The thickness of the diffusion layer is much smaller than the radius of a membrane;

(5)The selectivity of a membrane with respect to the a filtered high-molecular substance is characterized by a constant rejection coefficient

$$\sigma = 1 - \frac{c_{per}}{c_{ret}}, \quad (2)$$

where c_{per} is the concentration of a high-molecular substance in the permeate (the solution that has been passed through a membrane), and c_{ret} is the concentration of a high-molecular substance in the retentate (the solution rejected by a membrane) immediately near the surface of a membrane; and

(6)The possible decrease of the efficiency of a membrane is due to the formation of a gel layer on its surface, and the formation of a gel begins, when a certain solution concentration c_g is attained.

To model the development of polarization, we selected the integral method, which allows us to obtain simple and easily analyzable approximate estimates of the process characteristics.

The experimental studies of the process of concentrating were performed on the setup schematized in Fig. 1.

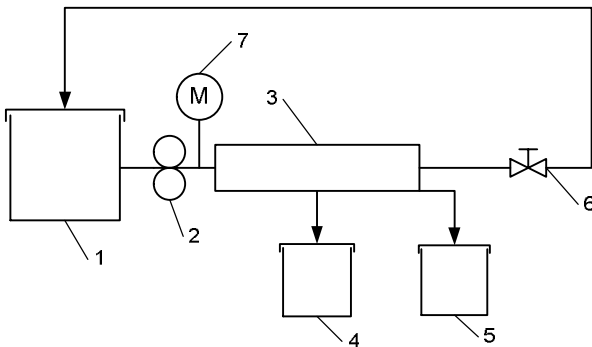


Fig. 1. Laboratory bench scheme: (1) initial solution vessel, (2) pump, (3) membrane module, (4) permeate collection vessel, (5) withdrawn concentrate collection vessel, (6) valve, (7) manometer.

Skim milk and dairy whey with a total solids content of 8.4 and 4%, respectively, were used as objects of experimental study. Tubular ceramic membranes of the two types, namely, aluminum oxide membranes with an average pore size of 20 nm (Mendelev Russian University of Chemical Technology, Moscow) and silicon carbide membranes with an average pore size of 200 nm (“Ceramic Filter” Research and Production Association, Moscow) were applied for concentrating.

THEORETICAL ANALYSIS

1.1. Model of the Development of Concentration Polarization

Since the thickness of the diffusion layer is assumed to be small in comparison with the radius of a membrane, the surface curvature may be neglected. Then the flow of a solution and the mass transfer in the diffusion boundary layer can be described by the equations of a flat boundary layer

$$\begin{cases} \frac{\partial u}{\partial x} + \frac{\partial v}{\partial y} = 0, \\ u \frac{\partial c}{\partial x} + v \frac{\partial c}{\partial y} = D \frac{\partial^2 c}{\partial y^2}, \end{cases} \quad (3)$$

with the boundary conditions

$$\left. \begin{aligned} u &= 0 \\ v &= -J \\ \left(D \frac{\partial c}{\partial y} + \sigma J c \right)_{y=0} &= 0 \end{aligned} \right\} (y=0); \quad (4)$$

$$\left. \begin{aligned} u &\rightarrow U \\ v &\rightarrow 0 \\ c &\rightarrow c_0 \end{aligned} \right\} (y \rightarrow \infty).$$

Here, x and y are the longitudinal coordinate and the coordinate orthogonal to the surface of a membrane ($y=R-r$), respectively, u and v are the longitudinal and transversal components of the velocity vector, c is the concentration of a high-molecular substance, D is the diffusion coefficient of a high-molecular substance, and J is the permeate flux, $m^3/m^2 \cdot s$ (or m/s).

From Eqs. (3) one can obtain

$$\begin{cases} (c - c_0) \left(\frac{\partial u}{\partial x} + \frac{\partial v}{\partial y} \right) = 0, \\ u \frac{\partial (c - c_0)}{\partial x} + v \frac{\partial (c - c_0)}{\partial y} = D \frac{\partial^2 (c - c_0)}{\partial y^2} \end{cases},$$

Summing these two equations and integrating the obtained relationship across the diffusion layer with consideration for boundary conditions (4), one obtains the integral equation

$$\frac{d}{dx} \left[\int_0^\delta u(c - c_0) dy \right] = J [c_0 - (1 - \sigma)c_w]. \quad (5)$$

Here δ is the thickness of the diffusion layer, and the subscript w hereinafter means that the value of the parameter is taken on the surface of a membrane.

To obtain the approximate solution of Eq. (5), the velocity and concentration distributions within the diffusion layer are approximated by the expressions

$$c = c_0 \left[1 + \left(1 - \frac{y}{\delta} \right)^2 \right], \quad u(y) = \frac{4U}{R} y. \quad (6)$$

The linear approximation of the velocity distribution is used in compliance with the assumption about a small thickness of the diffusion layer taking into account Hagen-Poiseuille equation (1).

Using the variables

$$\xi = \frac{1}{16} \frac{x}{R} \cdot \left(\frac{J}{U} \right)^3 \cdot Pe_D^2, \quad \eta = \frac{y}{\delta}, \quad \theta(\xi, \eta) = \frac{c - c_0}{c_0}, \quad p(\xi) = \frac{J\delta}{D}, \quad (7)$$

where $Pe_D = 2UR/D$ is the diffusion Peclet number, and Eq. (6), Eq. (5) may be transformed into the dimensionless form

$$\frac{d}{d\xi} \left[p^2 \theta_w \int_0^1 \eta(1-\eta)^2 d\eta \right] = 1 - (1-\sigma)(1+\theta_w), \quad (8)$$

In terms of variables (7), boundary condition (4) for the concentration on the surface of a membrane takes the form

$$\left(\frac{\partial \theta}{\partial \eta} \right)_w + p\sigma(1+\theta_w) = 0$$

The derivative in this expression is determined from approximate equation (6) written in terms of variables (7). After simple rearrangements, one can obtain

$$\theta_w = \frac{p\sigma}{2 - p\sigma}, \quad (9)$$

Substituting this expression into Eq. (8) and calculating the integral, we finally obtain the following differential equation for the dimensionless thickness of the diffusion layer p :

$$\frac{d}{d\xi} \left[\frac{p^3}{2 - p\sigma} \right] = 12 \frac{2 - p}{2 - p\sigma}, \quad (10)$$

The initial condition for Eq. (10) has the form $p(0) = 0$.

In the case of an ideal membrane ($\sigma = 1$), Eq. (10) can be integrated. As a result, one obtains the cubic equation

$$p^3 + 12\xi \cdot p - 24\xi = 0, \quad (11)$$

the solution of which gives us the following expression for the immediate estimation of the dimensionless diffusion layer thickness:

$$p = \sqrt[3]{4\xi(3 + \sqrt{4\xi + 9})} + \sqrt[3]{4\xi(3 - \sqrt{4\xi + 9})}, \quad (12)$$

The dimensionless concentration of a high-molecular substance on the surface of a membrane is determined from Eq. (9).

In the general case, it is necessary to solve Eq. (10) numerically. The analysis of the solutions obtained at $\sigma = 0.5 \square 0.9$ shows that the distributions of the dimensionless diffusion layer thickness and high-molecular substance concentration can rather precisely be approximated by the formulas

$$p \approx \frac{2\xi^{0.723-0.190\sigma}}{0.098 + 0.122\sigma + \xi^{0.723-0.190\sigma}},$$

$$\theta_w \approx \frac{\sigma \xi^{0.723-0.190\sigma}}{(0.098 + 0.122\sigma) + \xi^{0.723-0.190\sigma} (1-\sigma)}. \quad (13)$$

If the gel forming concentration c_g is known, the corresponding dimensionless concentration θ_g can be found from Eq. (7). From Eq. (13) one obtains the formula for the cross section coordinate (the distance from the leading edge of a membrane), at which the formation of a gel begins:

$$\xi_g = \left[\frac{\theta_g (0.098 + 0.122\sigma)}{\sigma(1+\theta_g) - \theta_g} \right]^{\frac{1}{0.723-0.190\sigma}}, \quad (14)$$

It follows from Eq. (14) that the coordinate of the beginning of gel formation grows with a decrease in the rejection coefficient of a membrane.

1.2. Estimating the Parameters of the Separation of the Near-Membrane Layer

The constructed model for the development of polarization allows of the estimation of the possibility of the intensification of membrane concentrating by withdrawing the solution from the peripheral flow zone adjacent to the surface of a membrane.

To estimate the parameters of the partial withdrawal of the solution from the near-membrane zone, let us divide the flow that moves through a tubular membrane with a radius R , into the two parts, namely, the middle with a radius r^* and the peripheral part (concentrate) that flows through the annular cross section with an inner radius r^* and an outer radius R (Fig. 2). The volumetric concentrate flux through the cross section of the annular zone is

$$Q_{conc} = 2\pi \int_{r^*}^R ru(r) dr, \quad (15)$$

Taking into account Hagen-Poiseuille equation (1), formula (15) can be written as

$$Q_{conc} = 4\pi \cdot U \int_{r^*}^R \left(1 - \frac{r^2}{R^2} \right) \cdot r dr = \pi R^2 U \left[1 - \left(\frac{r^*}{R} \right)^2 \right]^2, \quad (16)$$

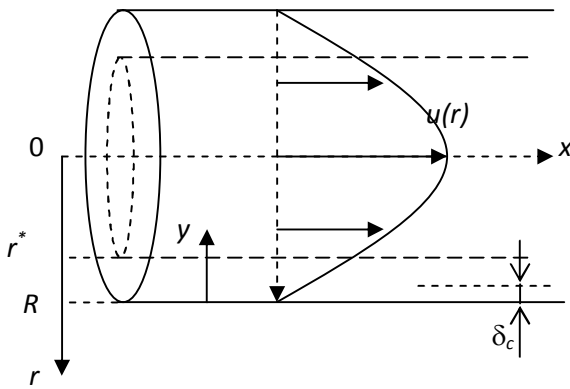


Fig. 2. Separation of the flow of a solution in a tubular membrane.

The mass flux of a dissolved high-molecular substance through the cross section of the annular zone is

$$G_{conc} = 2\pi \int_{r^*}^R u(r) \cdot c(r) \cdot r dr$$

Rearranging this expression into the form

$$G_{conc} = 2\pi \int_{r^*}^R u(r)(c - c_0)r dr + 2\pi \int_{r^*}^R u(r)c_0r dr$$

and taking into account Eq. (15), one obtains

$$G_{conc} = 2\pi \int_{r^*}^R u(c - c_0)r dr + c_0 Q_{conc} \tag{17}$$

Taking into account that the concentration $c = c_0$ everywhere outside the diffusion layer with a thickness δ , this expression can be written as

$$G_{conc} = 2\pi \int_{r^*}^{R-\delta} u(c - c_0)r dr + 2\pi \int_{R-\delta}^R u(c - c_0)r dr + c_0 Q_{conc} = 2\pi \int_{R-\delta}^R u(c - c_0)r dr + c_0 Q_{conc} \tag{18}$$

Taking into consideration that the thickness of the diffusion layer is small, we can assume that $r \approx R$ and neglect the surface curvature. Introducing the variable $y = R - r$, one can write

$$\int_{R-\delta}^R u(c - c_0)r dr = R \int_0^\delta u(c - c_0) dy.$$

Passing to dimensionless variables (7) and taking into account Eq. (6), one obtains in Eq. (18)

$$G_{conc} = c_0 Q_{conc} + 2\pi R \int_0^\delta u(c - c_0) dy = c_0 Q_{conc} + 8\pi U c_0 \delta^2 \int_0^1 \theta \eta d\eta.$$

Taking into account Eqs. (6), (7), and (9), the high-molecular substance mass flux through the cross section of the peripheral annular zone is finally determined by the expression

$$G_{conc} = c_0 Q_{conc} + 2\pi U c_0 \delta^2 \frac{p\sigma}{3(2 - p\sigma)} \tag{19}$$

Dividing this expression by Eqs. (16), one obtains the average concentration of the concentrate withdrawn from the peripheral zone as

$$c_{conc} = c_0 \left[1 + \frac{2p\sigma\delta^2}{3(2 - p\sigma) \left(1 - \frac{r^{*2}}{R^2}\right)^2 R^2} \right], \tag{20}$$

Let us introduce the parameters

$$\left(\frac{r^*}{R}\right)^2 = \Phi < 1, \quad Pe_J = \frac{2JR}{D}, \tag{21}$$

and the dimensionless concentration coefficient K determined as the ratio of the average concentration in the withdrawn peripheral flow part to the initial concentration c_0 . The concentration coefficient is expressed from Eq. (20) with consideration for Eqs. (7) and (21) as

$$K = \frac{c_{conc}}{c_0} = 1 + \frac{8}{3Pe_J^2(1 - \Phi)^2} \left(\frac{p^3\sigma}{2 - p\sigma}\right), \tag{22}$$

The concentration coefficient value allows the estimation of the possibility of obtaining an enriched solution via the separation of its peripheral part.

CONCENTRATE SEPARATION DEVICES

A number of devices have been developed for the technical implementation of the idea of the processed solution withdrawal from the near-membrane zone. One of them [22] is shown in Fig. 3.

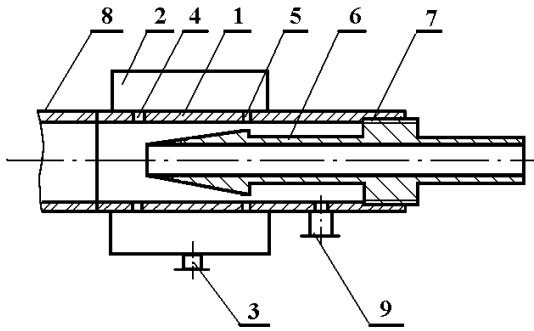


Fig. 3. Device for the separation of the near-membrane layer: (1) housing, (2) shell, (3), (9) fittings, (4), (5) slots, (6) rod, (7) thread, (8) tubular membrane.

The device operates as follows. The initial solution is subjected to filtration, being passed through tubular membrane 8 under pressure. A layer with an increased concentration of dissolved substances is formed near the inner surface of the membrane. The flow enters housing 1 with two annular slots 4 and 5. The pressure created in the first of them is higher than the pressure in the second slot. The pressures are adjusted by displacing the conical tip of hollow rod 6.

The pressure created in shell 2 is lower than the pressure in the cross section of slot 4 (but it is higher than in the cross section of slot 5). As a result, the solution layer part adjacent to the inner housing surface is sucked into the shell and then removed through fitting 3. The remaining flow is divided by the conical tip of the hollow rod into the two parts: the near-wall layer and the middle. The near-wall layer is passed between the rod and the housing and withdrawn through fitting 9. Hence, the concentrate can be withdrawn by the two ways, namely, through fittings 3 and 9.

The middle, in which the concentration of a dissolved high-molecular substance is lower than its concentration in the concentrate, is withdrawn through the central channel of hollow rod 6.

Another device [23], which enables the periodical mechanical cleaning of the membrane surface alongside with the withdrawal of the concentrate, is schematized in Fig. 4.

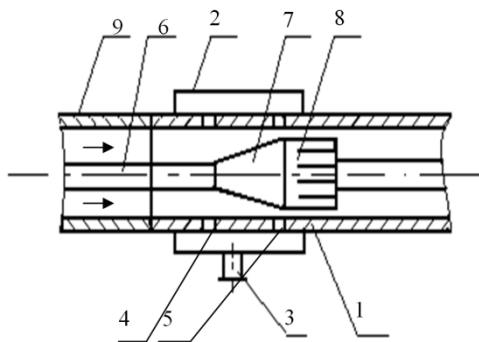


Fig. 4. Membrane module with devices for the withdrawal of the concentrate and the mechanical cleaning of a membrane: (1) housing, (2) shell, (3) fitting, (4), (5) annular slots, (6) guiding rod, (7) cone, (8) cleaning device, (9) tubular ceramic membrane.

The device consists of housing 1, on which shell 2 with fitting 3 for the withdrawal of the concentrate are situated. The housing has two annular slots 4 and 5. Guiding rod 6, on which cone 7 with cleaning device 8 representing a “skirt” of mobile blade scrapers, is enclosed inside the housing. The housing is attached to tubular membrane 9.

The device operates as follows. The initial solution under pressure flows through tubular membrane 9. The flow moves into housing 1 with annular slots 4 and 5. Due to conical attachment 7, the pressure in the region of slot 5 is lower than in the region of slot 4. Due to this factor, the intermediate pressure less than the pressure in the region of slot 4 is maintained inside shell 2. As a result of this, the concentrate layer is sucked from the near-wall flow zone into the shell, from which it is removed through fitting 3, due to the pressure drop between the cross section of slot 4 and shell 2. The process is controlled by adjusting the pressure in shell 2. The middle is passed between the cone and the housing and then withdrawn from the module.

In the course of filtration, the blades of the cleaning device are arranged by the flow of a solution in parallel to it and do not hinder its motion.

To clean the membrane, the direction of the flow should be switched. The cone opening and the cleaning device move along guiding rod 6 and the membrane under the action of the reverse flow of a solution. The cleaning device blades are unfolded and forced against the inner surface of the membrane, thus removing the deposit layer. After the cone has passed along the membrane, the direction of the flow is switched again, and the cone and the cleaning device are returned into the initial position. If necessary, the operation of cleaning is repeated several times.

II. RESULTS AND DISCUSSION

2.1. Theoretical Results

The estimation of the diffusion layer thickness according to Eq. (13) shows that the change of the membrane rejection coefficient has a slight effect on the dimensionless layer thickness p (Fig. 5).

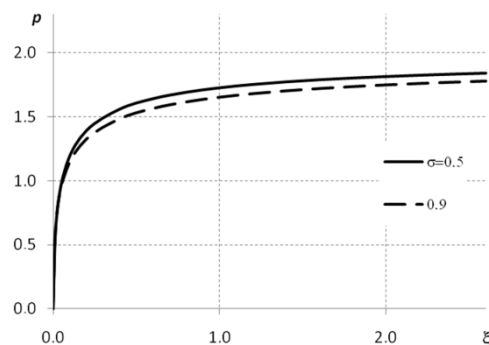


Fig. 5. Effect of the membrane rejection coefficient on the diffusion layer thickness.

At the same time, the change of the rejection coefficient has a considerable effect on the surface solution concentration distribution, which determines the beginning of the gel formation. The change of the

excess dimensionless concentration θ_w along the membrane surface is illustrated in Fig. 6.

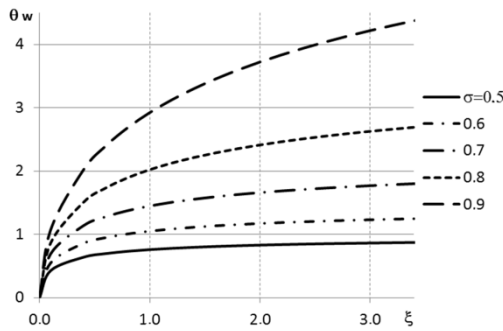


Fig. 6. Effect of the membrane selectivity on the distribution of surface concentrations.

It can be seen that a decrease in the membrane rejection coefficient reduces the surface concentration of a dissolved substance. This in turn delays the formation of a gel.

It should be noted that Eq. (13) implies the existence of the ultimate layer thickness and concentration at increasing membrane length, i.e.,

$$p \xrightarrow[\xi \rightarrow \infty]{} 2, \quad \theta_w \xrightarrow[\xi \rightarrow \infty]{} \frac{\sigma}{1-\sigma}, \quad (23)$$

The ultimate thickness of the diffusion layer and the ultimate concentration of a dissolved substance near the surface of a membrane are determined from these expressions subject to Eq. (7) as

$$\delta_{lim} = \frac{2D}{J}, \quad c_{w lim} = \frac{c_0}{1-\sigma} \quad (24)$$

The knowledge of these parameters allows us to estimate the danger of the fouling of a membrane due to the formation of a gel layer.

To estimate the efficiency of the withdrawal of the concentrate from the near-wall zone of the membrane channel, let us first consider the case of an ideal membrane with a rejection coefficient of 1. In this case, concentration coefficient expression (22) subject to Eq. (11) takes the form

$$K = 1 + \frac{32}{Pe_j^2(1-\Phi)^2} \xi. \quad (25)$$

Taking into account Eqs. (7) and (21), this expression can be written with the use of physical variables as

$$K = 1 + \frac{2}{(1-\Phi)^2} \left(\frac{x J}{R U} \right). \quad (26)$$

From this formula it can be seen that the concentration coefficient grows with an increase in the permeate flux and a decrease in the tangential flow

velocity. It grows as well with an increase in the parameter Φ (i.e., in the volume of the solution withdrawn as a concentrate). Moreover, the concentration coefficient grows linearly along the length of a membrane.

The results of calculating the concentration coefficient in compliance with Eq. (27) are plotted in Fig. 7.

In the case of the nonideal membrane ($\sigma < 1$), the concentration coefficient was calculated by approximate formulas (13). The results shown in Fig. 8 were obtained for the following conditions: membrane channel radius $R=2$ mm; flow velocity $U=0.12$ m/s, permeate flux $J=1.39 \cdot 10^{-6}$ m/s, $\Phi=0.75$, processed medium is skim milk.

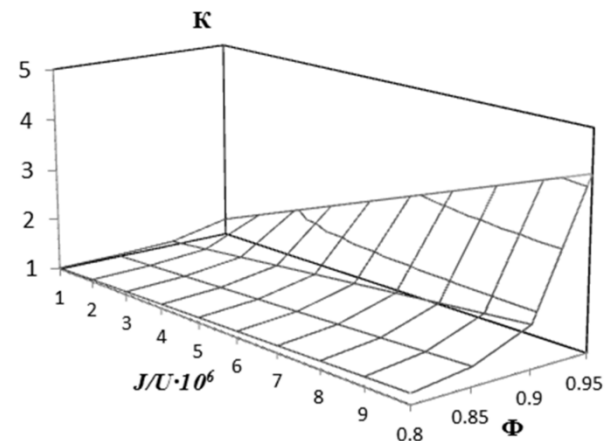


Fig. 7. Concentration coefficient of an ideal membrane for the separation of the near-wall flow part.

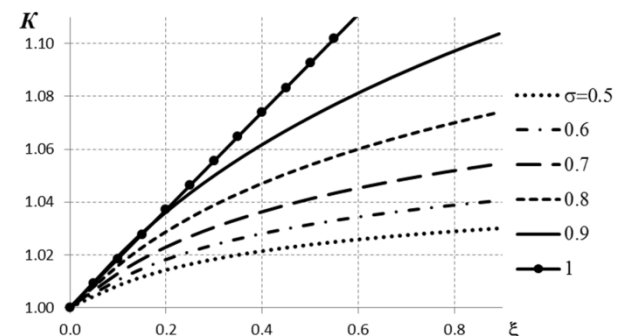


Fig. 8. Effect of the membrane rejection coefficient of the efficiency of concentrating.

As can be seen, the concentration coefficient grows with increasing distance from the leading edge of a membrane. The rate of its growth gradually decreases. It can be seen as well that the separation of the near-wall flow part, for example, at a membrane rejection coefficient of 0.7, allows us to attain a more than 5-% increase in the resulting product concentration in a continuous-flow membrane module with a dimensionless length $\xi=0.8$. This corresponds to the length of a tubular membrane of 0.72 m for the above conditions and the processing of skim milk.

2.2. Results of Experimental Studies

To confirm the possibility of the intensification of concentrating by the separation of the near-wall flow part, we performed some experiments on the concentrating of skim milk with an initial total solids content of 8.4%. A ceramic aluminum oxide membrane with a length of 800 mm, an inner diameter of 4 mm and an average pore diameter of 20 nm was used. The concentrate was separated using the device shown in Fig. 3.

The total solids contents in the concentrate obtained at different intensities of its withdrawal through fittings 3 and 9 (Fig. 3) are plotted in Fig. 9. The withdrawal intensities are given in l/h per 1 m² of the membrane surface.

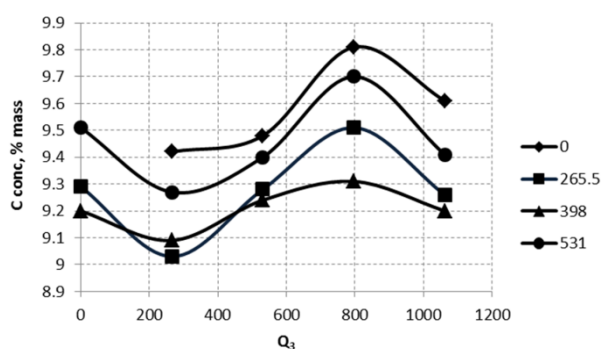


Fig. 9. Total solids content in the concentrate of skim milk ($p=0.2$ MPa, $Re \approx 2300$).

The analysis of the given values shows that the total solids content in the concentrate lies within a range of 9.0–9.8% at different ratios of the intensities of its withdrawal through the fittings, thus corresponding to the concentration coefficient of 1.07–1.17. On the whole, this agrees with the estimates obtained with the model described above (Fig. 8).

We have also performed some experiments on the concentrating of skim milk ($c_0 = 8.4\%$) and dairy whey ($c_0 = 4.8\%$) using ceramic membranes of the two types: membranes with a pore size of 20 nm (Mendelev Russian University of Chemical Technology, Moscow) and membranes with a pore size of 200 nm (“Ceramic Filter” Research and Production Association, Moscow). The concentrate was separated using the device shown in Fig. 4. The results are plotted in Fig. 10.

As one can see from Fig. 10, the separate withdrawal of the solution from the outlet of the membrane module in these experiments also leads to an appreciable increase in the total solids content of the concentrate in comparison with the initial solution. The highest concentration coefficient is 1.21 for skim milk and 1.17 for whey.

The total solids content of the concentrate decreases with increasing concentrate withdrawal intensity. This

agrees with the modeling results. According to Eqs. (16) and (21), an increase in the amount of the withdrawn concentrate corresponds to a decrease in the parameter Φ . According to Eq. (22), this results in a decrease in the concentrate concentration coefficient.

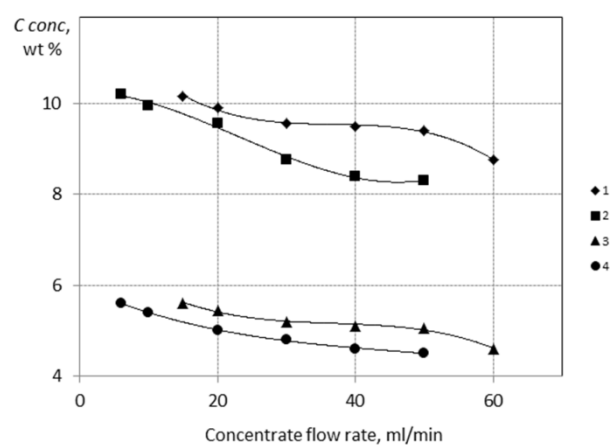


Fig. 10. Total solids content in the concentrate: (1), (3) on the membrane with 200-nm pores, (2), (4) on the membrane with 20-nm pores, (1), (2) the medium is skim milk, and (3), (4) the medium is dairy whey ($p = 0.15$ MPa, $t = 20^\circ\text{C}$, $Re \approx 500$).

As one can see from Fig. 10, the use of the membranes with greater pores (consequently, with a lower rejection coefficient) turned out to be more efficient from the viewpoint of increasing the concentration of the resulting product for both skim milk and dairy whey. This paradoxical result may be explained relying on the modeling results. Under all other conditions being equal, an increase in the pore size leads to the growth of the permeate flux due to a decrease in the hydraulic resistance of a membrane. Meanwhile, as one can see, for example, from Eq. (27), an increase in the permeate flux leads to the growth of the concentration coefficient. It may be supposed that the effect of the permeate flux change on the efficiency of concentrating has proven to be much more considerable in this case than the effect of the rejection coefficient of a membrane.

CONCLUSIONS

The obtained results indicate that the separation of the near-wall flow part in the membrane concentrating with the use of tubular membrane modules allow us to increase the concentration of the resulting product. This effect is attained even in the case of membranes with the partial rejection of a dissolved substance. This opens up the opportunity for intensifying the membrane processes of the processing of dairy raw materials.

REFERENCES

- Brans, G., Schroën, C.G.P.H., van der Sman, R.G.M., and Boom, R.M., Membrane fractionation of milk: state of the art and challenges, *Journal of Membrane Science*, 2005, vol. 243, pp. 263–272.
- Van Reis, R. and Zydney, A., Bioprocess membrane technology, *Journal of Membrane Science*, 2007, vol. 297, pp. 16–50.

3. Wakeman, R.J. and Williams, C.J., Additional techniques to improve microfiltration, *Separation and Purification Technology*, 2002, vol. 26, pp. 3□18.
4. Krstić, D.M., Tekić, M.N., Carić, M.D., and Milanović, S.D., Static turbulence promoter in cross-flow microfiltration of skim milk, *Desalination*, 2004, vol. 163, pp. 297□309.
5. Pal, S., Bharihoke, R., Chakraborty, S., Ghatak, S.K., De, S., and DasGupta, S., An experimental and theoretical analysis of turbulence promoter assisted ultrafiltration of synthetic fruit juice, *Separation and Purification Technology*, 2008, vol. 62, pp. 659□667.
6. Popović, S. and Tekić, M.N., Twisted tapes as turbulence promoters in the microfiltration of milk, *Journal of Membrane Science*, 2011, vol. 384, pp. 97□106.
7. Zhou, N. and Agwu Nnanna, A.G., Investigation of hybrid spring-membrane system for fouling control, *Desalination*, 2011, vol. 276, pp. 117□127.
8. Popović, S., Jovičević, D., Muhadinović, M., Milanović, S., and Tekić, M.N., Intensification of microfiltration using a blade-type turbulence promoter, *Journal of Membrane Science*, 2012, vol. 425□426, pp. 113□120.
9. Taha, T. and Cui, Z.F., CFD modelling of gas-sparged ultrafiltration in tubular membranes, *Journal of Membrane Science*, 2002, vol. 210, pp. 13□27.
10. Mercier-Bonin, M., Gésan-Guizieu, G., and Fonade, C., Application of gas/liquid two-phase flows during crossflow microfiltration of skimmed milk under constant transmembrane pressure conditions, *Journal of Membrane Science*, 2003, vol. 218, pp. 93□105.
11. Psoch, C. and Schiewer, S., Dimensionless numbers for the analysis of air sparging aimed to reduce fouling in tubular membranes of a membrane bioreactor, *Desalination*, 2006, vol. 197, pp. 9□22.
12. Cheng, T.-W. and Li, L.-N., Gas-sparging cross-flow ultrafiltration in flat-plate membrane module: Effects of channel height and membrane inclination, *Separation and Purification Technology*, 2007, vol. 55, pp. 50□55.
13. Qaisrani, T.M. and Samhabe, W.M., Impact of gas bubbling and backflushing on fouling control and membrane cleaning, *Desalination*, 2010, vol. 266, pp. 154□161.
14. Akoum, O.A.I., Jaffrin, M.Y., Ding, L., Paullier, P., and Vanhoutte, C., An hydrodynamic investigation of microfiltration and ultrafiltration in a vibrating membrane module, *Journal of Membrane Science*, 2002, vol. 197, pp. 37–52.
15. Akoum, O., Jaffrin, M.J., and Ding, L.-H., Concentration of total milk proteins by high shear ultrafiltration in a vibrating membrane module, *Journal of Membrane Science*, 2005, vol. 247, pp. 211□220.
16. Gomaa, H.G. and Rao, S., Analysis of flux enhancement at oscillating flat surface membranes, *Journal of Membrane Science*, 2011, vol. 374, pp. 59□66.
17. Kobayashi, T., Chai, X., and Fujii, N., Ultrasound enhanced cross-flow membrane filtration, *Separation and Purification Technology*, 1999, vol. 17, pp. 31□40.
18. Muthukumar, S., Kentish, S.E., Ashokkumar, M., and Stevens, J.W., Mechanisms for the ultrasonic enhancement of dairy whey ultrafiltration, *Journal of Membrane Science*, 2005, vol. 258, pp. 106□114.
19. Kyllönen, H.M., Pirkonen, P., and Nyström, M., Membrane filtration enhanced by ultrasound: a review, *Desalination*, 2005, vol. 181, pp. 319□335.
20. Cai, M., Zhao, S., and Liang, H., Mechanisms for the enhancement of ultrafiltration and membrane cleaning by different ultrasonic frequencies, *Desalination*, 2010, vol. 263, pp. 133□138.
21. Sarkar, B., Pal, S., Ghosh, T.B., De, S., and DasGupta, S., A study of electric field enhanced ultrafiltration of synthetic fruit juice and optical quantification of gel deposition, *Journal of Membrane Science*, 2008, vol. 311, pp. 112□120.
22. RF Patent 2181619, 2000.
23. RF Patent 2234360, 2004.



UDC 664.95.022.39 +613.25
DOI 10.12737/1561

ENRICHED PROTEIN PRODUCTS OF MARINE ORIGIN LIKE THE NEW COMPONENTS OF THE DIET FOR PEOPLE WITH PHYSICAL LOAD

T. K. Kalenik¹, M. V. Kravchenko¹, V. V. Grishchenko¹, Shi Yanguo², and V. A. Lyakh¹

¹ School of Biomedicine, Far Eastern Federal University
690950, Vladivostok, Russia, e-mail: zarco@list.ru

² Key Laboratory of Food Science and Engineering, College of Food Engineering, Harbin University of Commerce,
138 Tonda str., district Daoli, 150076, Harbin, China

(Received March 06, 2013; Accepted in revised form May 28, 2013)

Abstract: The possibility of the use of the native and enzyme modified shrimp biomass (*Pandalus borealis*) for the development of functional foods that compensate for the lack of protein in people engaged in various sports (cyclic, speed-strength, competitive, complex coordination, technically complex, and combat sports) is scientifically substantiated and experimentally confirmed.

For the first time, the technology is developed for the production of combined high-protein structured food systems (pate) using the native and enzyme modified shrimp biomass.

Organoleptic, physico-chemical, and microbiological indicators of quality of high-protein structured food systems (pate) have been analyzed.

In order to prove the biological effect and activity, amino acid and fatty acid comparative compositions of the native and enzyme modified shrimp biomass for the development of functional sport food products have been investigated.

For the first time, fatty acid compositions of pate with and without the addition of an antioxidant have been examined. The storability of these products has been analyzed.

The purpose of the paper is the development of the technology for the production of combined high-protein structured food systems (pate) using the native and enzyme modified shrimp biomass and the comparative analysis of their biological value.

Keywords: native shrimp biomass, enzyme modified shrimp biomass, functional product, sports nutrition, proteins, amino acids, northern shrimp, soy peptides, polyunsaturated fatty acids

INTRODUCTION

According to forecasts of the global supply of the population of the Earth with protein substances in this century the protein balance in products can only be achieved by the combination of vegetable and animal proteins [1].

In this regard, research on expansion of the range of safe and quality food products based on marine fauna and terrestrial plant material has become increasingly important [2].

The Far East is rich in biological resources of plant and animal origin. Northern shrimp (*Pandalus borealis*) which is common in the north of the Far East, the Sea of Japan, and the Gulf of Peter the Great, one of the most accessible for the population of the Far East, is considered as raw material for the production of functional foods. It is the species of cold-water shrimp. This is a small but most valuable species since it contains many useful substances (antioxidant, astaxanthin vitamins, enzymes and hormones, calcium, potassium, magnesium, manganese, copper, molybdenum, phosphorus, iron, amino acids leucine, lysine, aspartic and glutamic acids, and glycine). It was

taken as a basis for the development of the shrimp biomass [3].

According to the Institute of Nutrition of the Russian Academy of Medical Sciences, soy protein is easily digestible, high-value, reasonably balanced in terms of amino acid composition, comparable in biological value with the protein of milk, fish, and beef. The soybean and derived products occupy a special place among legumes because of the high content of valuable protein (up to 40% or more) and fat (20% or more). It is the most common legume in the world.

The importance of the source of soy protein should be noted, since various soy products (soy flour, soy concentrate, and isolated soybean protein) have a different coefficient of digestibility. They are unequal in their medical and biological properties which is also associated with various manufacturing methods. Only soy protein products manufactured with the most modern technology, i.e., by aqueous extraction, have the highest digestibility coefficient and retain most of the natural properties of soy. On average soybean seeds contain about 35% of protein, while isolated soy proteins (isolates) contain up to 90% of protein. In this

context, *isolated* denotes *highly purified protein derived from soybeans* [4].

The reason for the increased use of the shrimp biomass and soy peptides in the production of high-protein functional foods is the unique amino acid composition of shrimp biomass and soy protein, complementarity of soy proteins with muscle proteins which increases the overall biological value of the protein composition of the finished product, neutral flavor characteristics of soy proteins and their compatibility with various types of raw materials in product formulas [5].

These properties make it possible to introduce protein ingredients in formulas of high-protein foods and obtain end products that are not inferior to traditional products in terms of the biological value and most importantly to efficiently use expensive raw materials of animal origin [6]. Products developed with the addition of soy protein are more affordable to the mass consumer in terms of price and make it possible to partially cover the deficit of the protein in the diet [7, 8].

High-protein diet is necessary for people involved in strength sports (cyclic, speed-strength, competitive, complex coordination, technically complex, and combat sports) [9, 10].

The course of food containing protein can be assigned when physical activity is an integral part in maintaining muscle mass and in stimulating muscle hypertrophy, ensuring proper recovery after physical exercises, and maintaining optimal immune function of the human body [11, 12].

SUBJECTS AND METHODS OF RESEARCH

The following subjects of research were used in this paper

1. Fresh-frozen northern shrimp (*Pandalus borealis*).
2. Soybean peptides from the Soybean National Center, Changchun, China.
3. Pate with the native shrimp biomass "Naslazhdenie."
4. Pate with the enzyme-modified shrimp biomass "Bodrost'."

Materials

1) A high concentration of bioflavonoid complex Flavio, TU 9197-030-026999613-2007.

2) Fresh-frozen northern shrimp (*Pandalus borealis*), GOST (State Standard) 20845-2002 Frozen shrimp. Specifications.

3) Fresh food garden carrots for retail, GOST (State Standard) R 51782-2001 Fresh food garden carrots for retail. Specifications.

4) Fresh food pumpkins, GOST (State Standard) 7975-68 Fresh food pumpkins. Specifications.

5) Cream butter, GOST (State Standard) R 52969-2008 Butter. Specifications.

6) Whey dairy, GOST (State Standard) R 53438-2009 Whey dairy. Specifications.

7) Food common salt, GOST (State Standard) R 51574-2000 Food Common Salt. Specifications.

8) Soy peptides, GOST (State Standard) 17109-88 Soy. Requirements for purchases and deliveries.

Methods

1. Determination of the fatty acids content. The fatty acid content was determined by the Folch method [13].

2. Determination of the amino acids content. The amino acid content was determined using the Moore method [14].

3. Determination of the protein content. The total protein content was determined by the Lowry method [15].

Research experimental work was carried out in the laboratories of the Department of Biotechnology of Products from Animal Raw Materials and Functional Foods at the School of Biomedicine of the Far Eastern Federal University.

An original taste of the shrimp is determined by the composition of amino acids, minerals, lipid fraction, and nucleotides. The main contribution is made by free amino acids, i.e., alanine, arginine, glutamic acid, and glycine which give a distinctive sweet taste to shrimp meat. Table 1 shows the amino acid composition of raw northern shrimp (*Pandalus borealis*).

Table 1. Amino acid composition of raw northern shrimp (*Pandalus borealis*), g/100 g of protein [16]

Indicators	Amino acids content
Essential amino acids	
Valine	5.19
Phenylalanine	4.91
Methionine	1.21
Isoleucine	4.69
Leucine	7.26
Threonine	3.88
Lysine	7.84
Sum	31.98
Nonessential amino acids	
Aspartic acid	9.3
Serine	4.29
Glutamic acid	10.76
Proline	5.07
Glycine	12.96
Alanine	9.48
Cystine	0.43
Tyrosine	2.24
Histidine	2.02
Arginine	8.47
Sum	64.82

From Table 1, basic acids with comparable content can be identified. Among essential amino acids there are leucine and lysine. Among nonessential amino acids there are aspartic and glutamic acids as well as glycine.

The only vegetable protein featuring a unique amino acid composition and equivalent to proteins of animal origin in this regard is soy protein. Soy protein is the most digestible vegetable protein, and in terms of nutritional value it is identical to the proteins of meat, fish, milk, and eggs.

Table 2 shows the amino acid composition of soy protein.

In accordance with the data presented in Table 2, it can be concluded that the basic amino acids, whose content exceeds the content of the other amino acids, are leucine and lysine (among essential amino acids) and

glutamic and aspartic acids (among nonessential amino acids).

Table 2. Amino acid composition of soy protein, g/100 g of protein

Indicators	Content	
Essential amino acids		
Isoleucine	1.81	0.66
Leucine	2.67	1.95
Methionine	0.52	-
Threonine	1.39	0.84
Phenylalanine	1.61	0.87
Valine	2.09	0.84
Lysine	2.09	1.24
Sum	26.91	12.8
Nonessential amino acids		
Serine	2.07	1.12
Glutamic acid	6.05	4.23
Proline	1.86	0.96
Glycine	1.42	0.79
Alanine	1.47	0.80
Citrulline	-	0.26
Aspartic acid	4.4	2.12
Cysteine	0.55	0.06
Tyrosine	1.06	0.60
Ornithine	-	0.08
Sum	18.98	10.72
Total	45.89	23.52

The process flow diagram for the production of the native biomass comprises the following steps: thawing, blanching, cooling, cutting, homogenization, preparation of cans, packing, packaging, labeling, and storage.

Fresh-frozen shrimp are subjected to blanching at 100°C for 4 minutes in a low (4%) saline solution. Before lowering the shrimp in the boiler the water is boiled. After that it should boil again (not later than after 2–3 minutes). Boiled shrimp are taken out and immediately cooled in the refrigerator at 0°C for 10–15 min. Next, boiled shrimp are cut, rinsed, and homogenized for 3 minutes.

The enzyme-modified shrimp biomass is produced by the hydrolysis of the frozen northern shrimp (*Pandalus borealis*) using chymotrypsin.

Chymotrypsin cleaves peptide bonds which are formed by carboxyl groups of aromatic amino acids. Furthermore, bonds formed by leucine, valine, methionine, and asparagine can be hydrolyzed with chymotrypsin.

Chymotrypsin hydrolysis is carried out at 37°C in an alkaline medium (pH 8.0–8.6). The ratio of enzyme to protein is 1:100 (weight ratio). In the case of the prolonged hydrolysis the enzyme is added to the substrate in two or three portions. The nature of the buffer used for the hydrolysis depends on the nature of the subsequent operation. In separation of hydrolyzate peptides by chromatographic and electrophoretic techniques on paper or on a thin layer it is convenient to use “volatile” buffers such as 0.5% solution of NH₄HCO₃ (pH 8.2). In hydrolysis with chymotrypsin relatively small peptides are obtained.

The process flow diagram for the production of the enzyme-modified shrimp biomass comprises the following steps: thawing, blanching, cooling, cutting, homogenization, enzymatic hydrolysis, preparation of cans, packing, packaging, labeling, and storage.

We have developed six samples for the research. For the manufacture of pate the native or enzyme-modified shrimp biomass, which is the main source of proteins (18.3%), was used as the main raw material. For the long-term storage the antioxidant Flavio was used.

Types of samples are given in Table 3.

Table 3. Samples

Sample number	Specification
Sample 1	Native shrimp biomass
Sample 2	Native shrimp biomass + antioxidant
Sample 3	Native shrimp biomass + soy peptides
Sample 4	Native shrimp biomass + soy peptides + antioxidant
Sample 5	Enzyme-modified shrimp biomass + soy peptides
Sample 6	Enzyme-modified shrimp biomass + soy peptides + antioxidant

In order to prepare the pate mass, vegetable products, carrots and pumpkin which contain a large amount of β -carotene (3–9 mg) were added to the main raw materials. Whey and soy peptides have been used that enhance the nutritional value of the product and butter which makes it possible to give a specific taste and aroma to the finished product.

Table 4. Amino acid composition of shrimp, g/100 g of protein

Indicators	Native shrimp biomass	Enzyme-modified shrimp biomass
	Content	
Essential amino acids		
Methionine	0.08	0.55
Isoleucine	2.65	2.28
Leucine	5.50	7.98
Valine	3.11	2.59
Phenylalanine	2.03	2.62
Lysine	5.15	7.62
Threonine	4.07	3.64
Sum	22.59	25.38
Nonessential amino acids		
Taurine	0.90	0.25
Aspartic	4.02	7.53
Serine	3.36	3.42
Glutamic	8.59	13.85
Oxoproline	0.49	0.14
Proline	2.22	3.02
Glycine	4.17	7.00
Alanine	3.26	4.12
Citrulline	0.77	4.42
Cysteine	0.15	0.27
Tyrosine	1.62	2.26
Ornithine	0.67	7.78
Histidine	1.38	1.45
Arginine	3.21	3.66
Sum	34.81	56.87
Total	57.4	82.25

The content of amino acids in the native and enzyme-modified shrimp biomasses was analyzed. The results are shown in Table 4.

According to the data presented in Table 4, it can be concluded that in terms of the total protein content the enzyme-modified shrimp biomass exceeds the native one. But it is also important to note that the content of aspartic and glutamic amino acids as well as leucine and glycine necessary for a human body is greater than the content of other amino acids.

Based on the guidelines of the Russian Academy of Medical Sciences and the National Standard for Functional Foods we have calculated the highest content of amino acids that are most important for human life.

The calculation of glutamic acid. If the protein content in 100 g of shrimp is known, it is possible to calculate the protein content of 50 g of shrimp, x :

$$x = \frac{18 \times 50}{100} = 9 \text{ g of protein} \quad (1)$$

Given that in the formula 100 g of pate includes 1 g of soy peptides, the total amount of protein will be 10 g.

Knowing that 100 g of protein contain 11.85 g of glutamic amino acids, we define the amount of glutamic amino acid in 9 g protein of shrimp, β :

$$\beta = \frac{9 \times 11.85}{100} = 1.25 \text{ g of glutamic acid} \quad (2)$$

The content of the glutamic amino acid in 1 g of soy peptides is 0.04 g. Let us find the total amount of glutamic amino acid in 100 g of pate, γ :

$$\gamma = 1.25 + 0.04 = 1.29 \text{ g of glutamic acid} \quad (3)$$

The recommended daily requirement of glutamic acid is 13.6 g.

Let us determine the percentage of the daily requirement of glutamic acid, δ :

$$\delta = \frac{1.29 \times 100\%}{13.6} = 9.6\% \quad (4)$$

Knowing that 100 grams of protein contain 6.62 g of lysine, we determine the amount of lysine in 9 g of the shrimp protein.

$$\beta_1 = \frac{9 \times 6.62}{100} = 0.69 \text{ g of lysine} \quad (5)$$

The lysine content in 1 g of soy peptides is 0.012 g. Let us find the total lysine content in 100 grams of pate

$$\gamma_1 = 0.69 + 0.012 = 0.702 \text{ g of lysine} \quad (6)$$

The recommended daily requirement lysine is 4.1 g. Determine the percentage of the daily requirement.

$$\delta_1 = \frac{0.702 \times 100\%}{4.1} = 17.12\%, \quad (7)$$

Knowing that 100 grams of protein contain 7.08 g of leucine, we determine the amount of leucine in 9 g protein shrimp.

$$\beta_2 = \frac{9 \times 7.98}{100} = 0.72 \text{ g of leucine} \quad (8)$$

The leucine content in 1 g of soy peptides is 0.02 g. Let us find the total amount of leucine in 100 g of pate

$$\gamma_2 = 0.72 + 0.02 = 0.74 \text{ g of leucine} \quad (9)$$

The recommended daily requirement of leucine is 4.6 g. Determine the percentage of the daily requirement of leucine.

$$\delta_2 = \frac{0.74 \times 100\%}{4.6} = 16.1\% \quad (10)$$

Figure 1 shows the comparison scale of the recommended daily requirement and the percentage of the daily requirement.

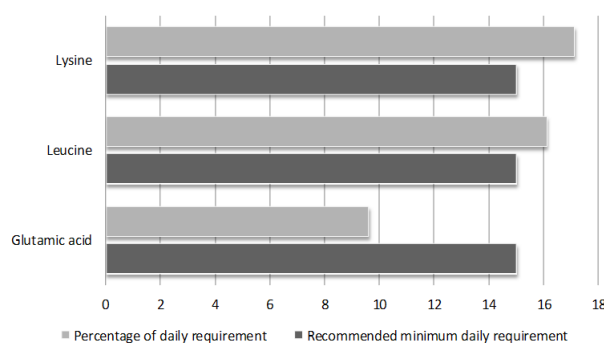


Fig. 1. The comparison scale of the recommended daily requirement and the percentage of the daily requirement.

The results of determining the percentage of the daily requirement show that as a result of the use of this high protein structured system the human body receives the daily requirement of leucine and lysine in accordance with the recommendations of the FAO/WHO. The content of glutamic acid is much lower than the recommended amount of daily requirement.

Based on the above calculations of the greatest amino acid content high-protein structured systems (pate "Nalazhdenie" and "Bodorst") are enriched functional food obtained by adding one or more physiologically functional food ingredients in conventional food products in order to prevent or correct the existing in humans nutrient deficiency, since the amount of functional food ingredients of vegetable and (or) animal raw material in one portion of the product is more than 15% of the daily requirement.

The investigation has been conducted on the content of fatty acids in the pate. Table 5 shows the fatty acid composition of pate with the native shrimp biomass without the addition of an antioxidant (Sample 1 is the nonhydrolyzed shrimp biomass) and antioxidant (Sample 2 is the hydrolyzed biomass of shrimp + antioxidant).

According to the results shown in Table 5, it can be concluded that the fatty acid composition of the Sample 1 without the addition of an antioxidant is higher than in the Sample 2. But some fatty acids contain slightly less

of fatty acids. These are caprylic acid, oleic acid, lauric acid, stearic acid, and arachidonic acid.

Table 5. Fatty acid composition of pate, g/100 g of the product

Acid	Formula	Sample 1	Sample 2
		Content	
Saturated fatty acids			
Myristic	C _{14:0}	5.4	4.85
Palmitic	C _{16:0}	34.32	30.02
Stearic	C _{18:0}	4.12	4.69
Caprylic	C _{8:0}	0.24	0.25
Lauric	C _{12:0}	6.08	6.81
Decanoic	C _{10:0}	2.5	0.6
Pentadecanoic	C _{15:0}	0.27	0.23
Amount		52.93	47.45
Unsaturated fatty acids			
Palmitoleic	C _{16:1}	0.48	0.44
Oleic	C _{18:1}	26.66	27.32
Sum		27.14	27.76
Polyunsaturated fatty acids			
Linoleic	C _{18:2}	14.93	14.53
Linolenic	C _{18:3}	5.22	3.77
Arachidonic	C _{20:4}	0.37	0.55
Eicosapentaenoic	C _{20:5}	0.22	0.22
Sum		20.74	19.07
Total		99.81	94.28

RESULTS AND DISCUSSION

1) The technology for obtaining the native shrimp biomass (*Pandalus borealis*) has been developed. The main operations are thawing, blanching, cooling, cutting, homogenization, preparation of cans, packing, packaging, labeling, and storage.

2) The biotechnology for obtaining the enzyme-modified shrimp biomass (*Pandalus borealis*) has been developed. The basic operations include thawing, blanching, cooling, cutting, homogenization, enzymatic hydrolysis, preparation of cans, packing, packaging, labeling, and storage.

3) Formulas of high-protein combined pates have been developed. Their main components are the native or enzyme-modified shrimp biomass, 50%, and soy peptides, 0.1%.

4) The analysis of the fatty acid composition have shown that the content of unsaturated fatty acids exceeds the amount of saturated acids by 26%.

5) The determination of the composition of protein and amino acids of the shrimp biomass have shown that the content of protein of the enzyme-modified shrimp biomass is higher than that of the native one. However, it is also important to note that asparagine and glutamic acids, leucine and glycine necessary for the human body predominate compared to the other amino acids.

The developed products are functionally orientated since the content of essential amino acids such as leucine and lysine in relation to the daily requirement is more than 15%.

REFERENCES

1. Kalenik, T.K. and Samchenko, O.N., Razrabotka myasorastitel'nykh pashtetov dlya zdorovogo pitaniya (Development of meat-vegetable pate for a healthy diet), *Tekhnika i tekhnologiya pishchevykh proizvodstv (Technique and technology of food production)*, 2012, vol. 1, no. 24, pp. 120–124.
2. Kalenik, T.K., Dotsenko, S.M., Kupchak, D.V., and Lyubimova, O.I., Kombinirovannyye produkty dlya zdorovogo pitaniya (Combination products for a healthy diet), *Pishchevaya promyshlennost' (Food industry)*, 2012, no. 7, pp. 65–67.
3. Lyakh, V.A., Fedyanina, L.N., and Smertina, E.S., Perspektivnye biologicheski aktivnye dobavki morskogo proiskhozhdeniya dlya proizvodstva khlebobulochnykh izdelii funktsional'noy napravlenosti (Prospective dietary supplements of marine origin for the production of functional bakery products), *Tekhnicheskiye nauki - ot teorii k praktike (Engineering – From Theory to Practice)*, 2012, no. 12, pp. 76–80.
4. Kalenik, T.K., Aleshkov, A.V., and Okara, A.I., Geneticheski modifitsirovannyye ingredienty v produktakh pitaniya: regional'nyi aspekt (Genetically modified ingredients in food: a regional aspect), *Tikhookeanskii meditsinskii zhurnal (Pacific Medical Journal)*, 2009, no. 1, pp. 63–64.
5. Kalenik, T.K., Dotsenko, S.M., and Kupchak, D.V., Obosnovanie podkhodov k razrabotke tekhnologii myasorastitel'nykh kompozitsii dlya sozdaniya vesovykh pashtetov funktsional'noi napravlenosti (Justification of approaches to the development of the technology of meat-vegetable compositions for the production of functional weight pates), *Vestnik Krasnoyarskogo gosudarstvennogo agrarnogo universiteta (Bulletin of the Krasnoyarsk State Agricultural University)*, 2012, no. 10, pp. 188–192.
6. Li, X., Li, D., Schmidt, I., Grishchenko, V.V., and Kalenik, T.K., Antioxidative properties of hydrated ethanol extracts from tartary buckwheat grains as affected by the changes of rutin and quercetin during preparations, *Journal of Medicinal Plants Research*, 2011, vol. 5, no. 4, pp. 572–578.
7. Kalenik, T.K., Alder, L.P., and Chernysheva, A.N., Vliyanie biotekhnologicheskoi modifikatsii soi na ee belkovyye komponenty (Effect of the soybean biotech modification on its protein components), *Khreneniye i pererabotka sel'khozsyrya (Storage and processing of agricultural raw materials)*, 2009, no. 2, pp. 71–74.
8. Kalenik, T.K., Aleshkov, A.V., and Okara, A.I., Geneticheski modifitsirovannyye ingredienty v produktakh pitaniya: regional'nyi aspekt (Genetically modified ingredients in food: a regional aspect), *Tikhookeanskii meditsinskii zhurnal (Pacific Medical Journal)*, 2009, no. 1, pp. 63–64.
9. Aranson, M.V., *Pitanie dlya sportsmenov (Sports Nutrition)*, Moscow: Physical Culture and Sports, 2001.
10. Maughan, R.J., *Carbohydrate-Electrolyte Solutions during Prolonged Exercise. Perspectives in Exercise Science and Sports Science. Ergogenics: the Enhancement of Sport Performance*, Maughan, R.J., Lamb, D.R., and Williams, M.H., Eds., Carmel, CA: Benchmark Press, 1991, vol. 4, pp. 35–85.

11.Grishchenko, V.V., Pishchevye produkty zhivotnogo proiskhozhdeniya v profilaktike vozdeystviya ioniziruyushchego izlucheniya (Food products of animal origin in the prevention of exposure to ionizing radiation), *Achievements in the life sciences*, 2012, no. 5, pp. 115–120.

12.Grishchenko, V.V., Lyakh, V.A., Kravchenko, M.V., and Bubnov, Yu.E., Perspektiva primeneniya gidrobiontov zhivotnogo proiskhozhdeniya sovместno s zernovymi kul'turami dlya sozdaniya produktov funktsional'noi napravlenosti (Prospects of the use of hydrobionts of animal origin with cereals for the development of functional foods), *Tekhnicheskiye nauki - ot teorii k praktike (Engineering – from Theory to Practice)*, 2013, no. 17-2, pp. 82–86.

13.Folch, J., Less, M., and Stanley, G.M.S., A simple method for the isolation and purification of total lipids from animal tissues, *Journal of Biological Chemistry*, 1957, vol. 226, no. 1, pp. 497–502.

14.Moore, S. and Stein, W.H., Chromatographic determination of amino acids by the use of automatic recording equipment, *Methods in Enzymology*, 1963, vol. 6, pp. 819–830.

15.Lowry, O.H., Rosenbrough, N.I., Farr, A.U., and Randall, R.J., Protein measurement with Folin phenol reagent, *Journal of Biological Chemistry*, 1951, vol.193, no. 1, pp. 265–275.

16.Paulov, Yu.V., Levankov, S.V., and Shvidskaya, Z.P., Tekhnokhimicheskaya kharakteristika i tekhnologicheskiye osobennosti perspektivnykh vidov okhotomorskikh krevetok (Technical-chemical characterization and technological features of promising types of Okhotsk Sea shrimp), *Izvestiya TINRO (TINRO bulletin)*, 2005, vol. 140, pp. 290–301.



UDC 637.146.613.26
DOI 10.12737/1562

HEALTHY FOOD PRODUCTS WITH PROBIOTIC AND PREBIOTIC PROPERTIES

E. I. Reshetnik¹ and E. A. Utochkina²

¹ Far East State Agrarian University, Blagoveshchensk, Amur Region, Russia
e-mail: Soia-28yandex.ru

² Amur State Medical Academy, Blagoveshchensk, Amur Region, Russia
e-mail: elenautochkinamail.ru

(Received February 27, 2013; Accepted in revised form April 25, 2013)

Abstract: In this paper the results of the study of the structure and properties of arabinogalactan extracted from Dahurian larch as well as its influence on the formation of fermented milk products are presented. The optimum application rate of arabinogalactan in a composite mixture is determined. The choice of the starter culture for the production of a functional fermented milk product is justified.

Keywords: functional food products, probiotic, prebiotic, arabinogalactan, milk, soy-based food

INTRODUCTION

In recent years, the implementation of the healthy food policy has been one of the important trends in health maintenance, disease prevention, restoration of disturbed functions of the body, and active human longevity. Food is the most powerful factor influencing the human body state. It affects all systems and organs continuously throughout life [1].

Food is a source of energy and substances necessary for growth, development, and other human vital processes. Food products should improve metabolism and body's resistance to adverse environmental effects as well as to have physiological, revitalizing, and preventive effects on the human body [2].

An important role in maintaining health and human performance is played by the adequate and regular supply of the body with all the nutrients [3, 4]. Thus it is necessary to take into account that the total number of incoming biologically assimilable nutrients should not exceed the daily physiological need of a healthy person since it can be accompanied by undesirable side effects.

As part of the development of the optimum nutrition concept a new branch of science was formed, i.e., the functional food. It includes the development of theoretical bases of production, sale, and consumption of functional foods.

Functional foods are conventionally divided into main groups with respect to specifics of the production process: conventional foods containing a significant amount of the native physiologically functional ingredient, products with technologically reduced harmful components, and products enriched with prebiotics and probiotics, antioxidants and vitamins, micronutrients and flavonoids, minerals and other substances essential to the human body [5].

A current area of research is the development of technologies for manufacturing fermented milk products with probiotic properties [6]. It is believed that at the beginning of the XXI century dairy products with

probiotic cultures will occupy half of the existing market of chemical drugs and thereby solve the problem of prevention and treatment of many human diseases [7, 8, 9].

The use of probiotics based on live microorganisms from the normal human microflora is an important element of the concept of healthy nutrition of the population and one of the most effective ways to prevent human gastrointestinal tract disorders and treat thereby developing disorders of digestive, immune, and endocrine systems [10, 11].

The possibility of application of probiotics in dairy products is determined by the availability of milk, its low cost, multicomponent composition, possibility of modification, and easy fractionation [12]. In introducing probiotic bacteria (before or after souring), it is necessary to take into account that their viability is a valid unit of measurement of the probiotic activity. Therefore, the content of bifidobacteria in probiotic products should be standardized [13].

In the fermentation of raw milk the focus should be made on the selection of strain of starter microflora. Poor development of bifidobacteria in milk is associated with oxygen dissolved in it, so the co-culture of bifidobacteria with lactic acid bacteria has a number of advantages. Lactobacilli bind oxygen dissolved in milk and thus create anaerobic conditions favorable for the growth of bifidobacteria.

Numerous studies [14, 15] found that dairy products fermented with probiotic bifidobacteria and lactobacilli stimulate the immune system and protective functions of the body and supply a number of essential amino acids and B vitamins. Their ability to reduce the level of urea and cholesterol in the blood as well as anticarcinogenic and antimutagenic activities which perform protective and detoxifying functions were found. Bifidobacteria contribute to the absorption of lactose [15].

According to researchers [16], the mechanism of stimulation of growth of normal microflora of

gastrointestinal tract with probiotics consists in inhibiting the growth of pathogens, immunocompetent cell activation, stimulation of growth of the endogenous microflora resulting from the production of vitamins and other growth promoting factors, neutralizing toxins, and change of microbial metabolism that manifests itself in the increase or decrease of enzyme activity. Because of such properties of probiotic cultures as the survival rate and proliferation in the human intestine, the viability in passing through the gastrointestinal tract, the metabolic activity, and the ability to provide therapeutic effects [17], they are an essential component of functional foods.

In developing dairy products containing bifidobacteria a great role in correction and activation of the habitat of bifidobacteria and lactobacilli is played by prebiotics. Numerous studies have pointed out that prebiotics stimulate the growth of the "right" microorganisms, i.e., bifidobacteria and lactobacilli. Thus, the research on the development of domestic functional prebiotic products is promising and relevant [18, 19].

Prebiotics include nondigestible food ingredients that improve health by selective stimulation of growth and metabolic activity of bacteria living in the colon. Prebiotics are not susceptible to hydrolysis by human digestive enzymes. They are not absorbed in the upper digestive tract. They are selective substrate for the growth and metabolic activity of beneficial microorganisms [3].

Prebiotic properties are most pronounced in fructose oligosaccharides, inulin, galacto-oligosaccharides, lactulose, and lactitol. Prebiotics are found in dairy products, corn flakes, cereals, bread, onions, field chicory, garlic, beans, peas, artichokes, asparagus, bananas, and many other products. Lactulose [20, 21] and gum arabic are generally accepted prebiotics.

In recent years, the food additive Fibregum has become increasingly popular. Fibregum is the exudate of acacia which is a glycoprotein whose macromolecules consist of protein core and arabinogalactan side chains. Because of the combination of technical characteristics and nutritional properties, Fibregum is recommended for use in the manufacture of various food products. Dietary fibers of Fibregum can stimulate the growth of beneficial bacteria and promote the formation of short chain fatty acids that have a beneficial effect on the physiology of the human body [22, 23].

When producing dihydroquercetin from larch, a significant amount of biologically active substances can be obtained as a byproduct. One such biologically active substance is arabinogalactan.

From the middle of the last century domestic and foreign scientists have been studying its structure and properties. Arabinogalactan is found in immunomodulating herbs (*Echinacea purpurea*, *Baptisia tinctoria*, *Angelica acutiloba*, and *Curcuma longa*), but the study of the arabinogalactan extracted from larch is of the greatest interest, since it constitutes a significant part of its biomass. The heartwood of some species of larch comprises up to 35% of arabinogalactan [24].

In recent years, the study of the biological activity of arabinogalactan has been intensified. The difference of arabinogalactan from many polysaccharides has been reported in terms of physico-chemical properties such as low viscosity of concentrated aqueous solutions, high solubility in water, resistance to acid environment, thermal and hydrolytic stability, and good dispersing ability [25]. It was found that arabinogalactan has a significant membranotropic and antimicrobial action against certain bacteria as well as immunomodulating property [26, 27] and antimutagenic activity [27].

The prebiotic ability is of particular interest in studying the properties of arabinogalactan. The results of studies of foreign and domestic scientists show the effect of larch arabinogalactan as a nutrient medium for Lactobacilli and Bifidobacteria since it is a fermentable fiber.

Arabinogalactan serves as food to beneficial symbiotic bacteria in the colon. In turn it helps to reduce the growth of pathogenic bacteria [24, 28, 30, 29, 30].

Over the past few years because of its multifunction properties arabinogalactan has been aggressively introduced in the production of dietary supplements and foods. Thanks to the dispersing ability it is relevant to use arabinogalactan in the development of formulas of yogurt, juices, pastries, confectionery, powdered milk, and other foods rich in mineral supplements and vitamin complexes.

Arabinogalactan mixes well with all kinds of food and does not affect the organoleptic properties of the finished product. It is a source of dietary fiber and has a positive impact on the gastrointestinal tract. It can be recommended as a nutraceutical or functional food supplement in the human diet [31].

Based on the above, studies were carried out in order to assess the possibility of using arabinogalactan extracted from the larch as a functional ingredient adding probiotic and prebiotic properties, improving traditional technologies, intensifying the process of fermentation of soy milk mixture, improving physical, chemical, and organoleptic properties, and microbiological parameters of the fermented milk product.

SUBJECT AND METHODS OF RESEARCH

The whole experiment cycle consists of a number of interrelated steps.

At different stages of work there were the following objects of study: composite blend (skim milk and soy-based food) in the ratio of 70:30, arabinogalactan extracted from larch, which according to TU 9325-008-706-921-52-08 is produced and sold under the trade mark "Lavitol-arabinogalactan" at ZAO Ametis, Blagoveshensk, Amur region, Russia, the starter culture composition YF-L811 (*Streptococcus thermophilus*, *Lactobacillus delbrueckii* subsp. *bulgaricus*) and BB-12 (*Bifidobacterium lactis*) in the ratio of 1:1.

At the first stage of the experiment, the structure and properties of arabinogalactan extracted from larch were investigated.

At the second stage, the effect of the arabinogalactan portion on the dynamics of the acid formation of the clot in the fermentation of the composite mixture was

determined. Syneresis properties, effective viscosity, and microbiological properties of the final clot with respect to the portion of arabinogalactan in the mixture were considered. The technological stage of introduction of arabinogalactan in the product was defined.

At the third stage, the effect of the portion of arabinogalactan on the product storability was investigated.

In carrying out the experimental part, the complex of generally accepted and standard research methods was used including chemical, physical, microbiological, biochemical, and rheological methods.

RESULTS AND DISCUSSION

Arabinogalactan is the main part of intracellular wood polysaccharides that performs protective functions and contains bioactive nutrients.

The structure of arabinogalactan has been studied by infrared spectroscopy. Infrared spectra of arabinogalactan are shown in Fig. 1.

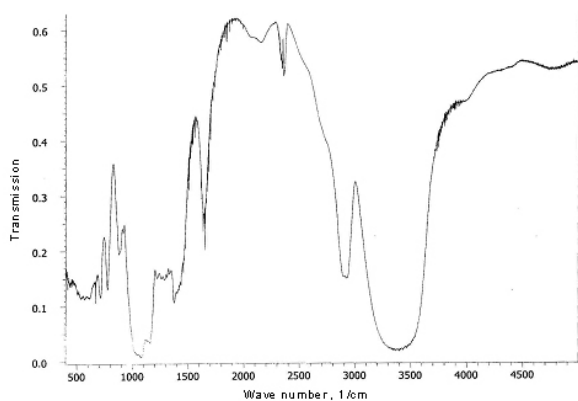


Fig. 1. The IR-spectrum of arabinogalactan.

In the IR spectrum of arabinogalactan there were intense absorption bands characteristic of deformation vibrations of cycles (716 cm^{-1} , 781 cm^{-1} , 884 cm^{-1} , 1085 cm^{-1} , 1162 cm^{-1}).

The carbonyl group has significant absorption bands at 1647 cm^{-1} . Absorption bands characteristic of stretching vibrations of C-O manifest themselves in bands 1085 cm^{-1} and 1162 cm^{-1} . Vibrations of hydroxyl groups are in the area of 2913 cm^{-1} . Broad peaks are characteristic of associated hydroxyl groups 3385 cm^{-1} .

In terms of organoleptic parameters arabinogalactan is an amorphous pale cream dry powder with a light almost impalpable pine smell and faint sweet flavor.

In the course of work the effect of the portion of arabinogalactan extracted from the larch on the formation of qualitative properties of the fermented milk product was investigated, in particular on the dynamics of titratable acidity, effective viscosity, syneresis, organoleptic, and microbiological properties of clot samples. The technological stage of introduction of arabinogalactan in the product was defined.

In the experiment, five samples of the composite mixture (skimmed milk and soy-based food in the ratio of 70:30) enriched with arabinogalactan in an amount of

0.5 to 2.5% were used. The sample of the mixture without arabinogalactan served as the control.

The mixture was fermented with the starter culture composition YF-L811 (*Streptococcus thermophilus*, *Lactobacillus delbrueckii* subsp. *bulgaricus*) and BB-12 (*Bifidobacterium lactis*) in the ratio of 1:1.

The effect of arabinogalactan on the organoleptic characteristics of the product was examined at various stages of the technological process.

The experiment showed that in the introduction of arabinogalactan in the mixture before the heat treatment, the sample of the clot had a sour-milk taste, was moderately sweet, white colored with cream tint, uniform throughout the mass, smoothly consistent, and moderately viscous and sticky. In the introduction of arabinogalactan in the mixture before fermentation, the clot was obtained which was characterized by a loose consistency with a significant separation of serum. In the introduction of arabinogalactan in the product after fermentation an extensive destruction of the clot takes place. Thus, it is recommended to introduce arabinogalactan in the mixture before heat treatment.

During the fermentation the dynamics of the acid formation of clots depending on the portion of arabinogalactan was investigated. The fermentation was carried out at a temperature of $(40 \pm 2)\text{ }^{\circ}\text{C}$ for 6 hours. The titratable acidity was determined at intervals of 1 hour. The results are presented in Fig. 2.

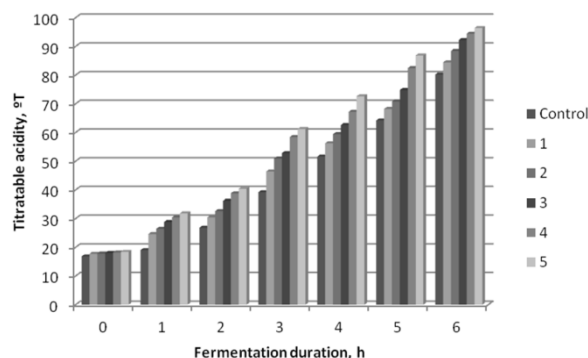


Fig. 2. The titratable acidity of the clot depending on the portion of arabinogalactan: control is without arabinogalactan, 0.5% (1), 1.0% (2), 1.5% (3), 2.0% (4), and 2.5% (5).

The analysis of the obtained data suggests that as a result of introduction of arabinogalactan in the composite mixture the fermentation time is greatly reduced. It can be associated with an increase in dry matter content in the mixture and the stimulating effect of the introduced polysaccharide on the microflora of starter cultures. It was found that if the portion of arabinogalactan is 0.5, 1.0, 1.5, 2.0, and 2.5% the titratable acidity of samples increases intensively by 4.5%, 11.3%, 17.0%, 20.1%, and 23.0%, respectively, compared to the control sample.

The effect of the portion of arabinogalactan on the number of viable microbial cells in the resulting sour-milk clot was investigated. The results are shown Table 1.

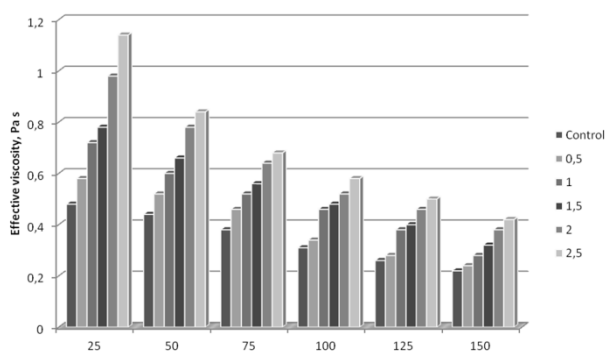
Table 1. The effect of the arabinogalactan portion on the number of viable microbial cells

Portion of arabinogalactan	Bacterial culture type		
	Streptococcus thermophilus	bacillus delbrueckii subsp. bulgaricus	Bifidobacterium lactis
0.5	$8 \cdot 10^7$	$6 \cdot 10^7$	$6 \cdot 10^7$
1.0	$4 \cdot 10^8$	$8 \cdot 10^7$	$2 \cdot 10^8$
1.5	$3 \cdot 10^9$	$4 \cdot 10^8$	$6 \cdot 10^8$
2.0	$5 \cdot 10^9$	$6 \cdot 10^8$	$8 \cdot 10^8$
2.5	$7 \cdot 10^9$	$7 \cdot 10^8$	$9 \cdot 10^8$
Control	$3 \cdot 10^7$	$5 \cdot 10^6$	$2 \cdot 10^7$

The analysis of table data shows that the introduction of a portion of arabinogalactan up to 1.5% leads to an increase in the number of viable microbial cells in the product compared to the control sample. However, it should be noted that the introduction of 2.0 and 2.5% of arabinogalactan had no significant impact on the increase in the number of viable microbial cells. This is possibly associated with a sufficient accumulation of lactic acid and other metabolic products and the high density of the bacterial population of microorganisms.

The structure of the clot is formed in souring and depends on various factors. In particular, it depends on used raw materials and a kind of starter cultures as well as on the introduced various food components. In this connection, the effect of the introduced portion of arabinogalactan on the effective viscosity of investigated clots at different shear rate was examined. The control sample is without arabinogalactan.

The nature of the change of the effective viscosity of the product depending on the amount of introduced arabinogalactan is presented in Fig. 3.

**Fig. 3. The dependence of the effective viscosity on the shear rate in the fermented milk product with different portions of arabinogalactan:**

0.5% (1), 1.0% (2), 1.5% (3), 2.0% (4), and 2.5% (5), control is without arabinogalactan.

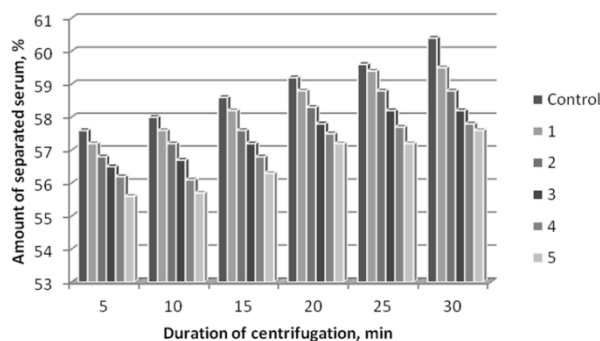
It was found that with the increasing portion of arabinogalactan in the samples structural and mechanical properties are modified, the viscosity increases in proportion to the increase in the content of arabinogalactan. In the mixture which does not contain arabinogalactan (control sample) the clot was less viscous. It is noted that in the case of the mass concentration of arabinogalactan of 2.0 and 2.5% the

consistency of the clot was excessively viscous. The product with a mass fraction of 1.5% arabinogalactan had the most appropriate viscosity.

In the finished samples syneresis properties of the clots have been examined. The results of these studies are presented in Fig. 4.

The results of the experiment revealed the ambiguous dependence of syneresis properties of clots on the portion of arabinogalactan introduced into a mixture. With the increasing portion of polysaccharide in the product the decrease in the syneresis ability of clots by 1.2, 1.4, 1.6, 1.7, and 1.8 times was observed respectively as compared with the control sample. It confirms water-binding properties of arabinogalactan.

The analysis of organoleptic characteristics of the analyzed samples indicates that the introduction of arabinogalactan has no effect on the taste and smell of the product. All the obtained clots had high quality organoleptic characteristics, i.e., they had taste and smell of sour milk, the soy component was almost not felt, the color was white with a cream tint, they were uniform throughout the mass.

**Fig. 4. The syneresis ability of clots depending on the arabinogalactan portion:**

control, 0.5% (1), 1.0% (2), 1.5% (3), 2.0% (4), and 2.5% (5) of the mixture weight.

The biological value is an important indicator characterizing the quality of dairy products. It is determined by the presence of complex nutrients in the product.

In order to determine the biological value of the obtained soy-milk-based product enriched with arabinogalactan, its amino acid composition has been analyzed. It makes it possible to assess its biological value with a greater degree of correctness. The amino acid composition of the product is shown in Fig. 5.

The biological value of dairy products was also assessed by the amino-acid score. The calculation results of amino-acid score of essential amino acids are given in Table 2.

The results have indicated that the analyzed dairy product based on soy-milk mixture enriched with arabinogalactan extracted from Dahurian larch has a high biological value.

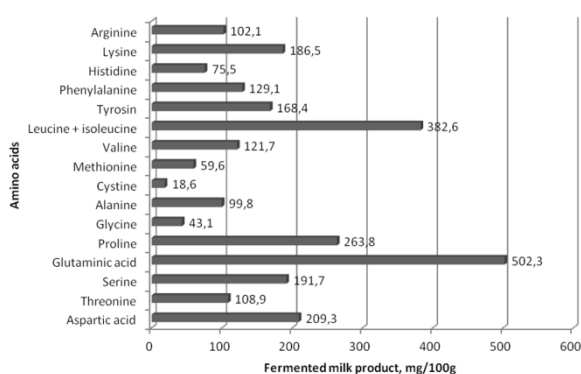


Fig. 5. The amino acid composition of the fermented milk product

According to the calculation results the amino-acid score of essential amino acids, i.e., leucine, isoleucine, threonine, and phenylalanine + tyrosine, exceeds 100%. It has been noted that the limiting amino acids are methionine + cystine (84.5%) and valine (92.1%).

Table 2. The composition of essential amino acids and amino-acid score of the fermented milk product in comparison with the recommendations of the FAO/WHO

Amino acid	FAO/WHO g/100 g of protein	Fermented milk product	
		g/100 g of protein	Score. %
Valine	5.0	4.60	92.1
Leucine	4.0	5.78	144.6
Isoleucine	7.0	10.12	145.0
Lysine	5.5	7.05	128.3
Methionine + cystine	3.5	2.96	84.5
Threonine	4.0	4.12	103.0
Phenylalanine + tyrosine	6.0	11.06	184.4

The production of functional foods with extended shelf-life is an important and promising direction in the food industry.

The storability manifests itself in the immutability of sensory, chemical, and physical properties throughout the storage life of the product [32, 33]. The quality of the finished product greatly depends on the variability of its basic constituents such as proteins, carbohydrates, and, in the first place, lipids which are oxidized when processed and stored.

The design of new functional foods should include careful planning and testing of the shelf life of the finished product. A comprehensive approach to this problem involves the analysis of the composition of the product, technological process parameters, packaging,

environmental factors, chemical and biochemical reactions, and the types of microorganisms present [34].

The antioxidant activity of natural products is one of the important indicators that determine their biological value.

Arabinogalactan is a polysaccharide with a wide range of useful properties, but there is almost no data on its antioxidant activity in literature.

Based on the above, the effect of the introduction of the portion of arabinogalactan on the storability of the fermented milk product was investigated.

When storing prepackaged in plastic five samples of products containing different portions of the introduced arabinogalactan, at $(40 \pm 2)^\circ\text{C}$ the change in the number of viable cells of lactic acid bacteria and bifidobacteria were observed for 10 days.

The number of viable microbial cells was determined on second, fourth, sixth, eighth, and tenth day of storage. The sample without arabinogalactan served as a control one.

The results showed that in the samples with arabinogalactan during the storage for two, four, six, eight, and ten days the number of viable cells of bifidobacteria maintained at the desired level ($5 \cdot 10^8$, $3 \cdot 10^8$, $1 \cdot 10^8$, $7 \cdot 10^7$, $3 \cdot 10^7$ CFU/cm³) and corresponded to microbiological requirements on the eighth day of storage, which was not the case for the control sample in which on the sixth, eighth, and tenth day of storage the quantitative indicator of bifidobacteria content was $1 \cdot 10^6$, $8 \cdot 10^5$, $2 \cdot 10^5$ CFU/cm³.

CONCLUSIONS

The obtained results suggest that arabinogalactan extracted from Dahurian larch has a stimulating effect on bifidobacteria and lactobacilli. It is proved that its introduction makes it possible to obtain a product with a high number of viable cells of the probiotic microflora in the final product.

The use of arabinogalactan intensifies the fermentation of the composite mixture (skimmed milk and soy-based food in the ratio of 70:30) which accordingly reduces the production cycle of the product.

The application rate of 1.5% arabinogalactan in the composite mixture has been found. It is recommended to introduce arabinogalactan in the composite mixture before its pasteurization which makes it possible to obtain a product with high physical-chemical, rheological, and organoleptic characteristics.

The expediency of the use of arabinogalactan in the production of dairy products is proved.

Summing up the above, we can conclude that the study of the enrichment of food with components with prebiotic properties is relevant in the field of technology of production of functional foods.

REFERENCES

1. Ashirova, N.N., Bychkova, E.S., Vasyukova, A.N., et al., *Realizatsiya kontseptsii zdorovogo pitaniya naseleniya: sostoyanie i perspektivy: monografiya* (The Implementation of the Concept of a Healthy Nutrition of Population: Status and Prospects: Monograph), Novosibirsk: NGTU, 2012.

2. Azolkina, L.N. and Solov'eva, N.I., Problemy proizvodstva molochnykh produktov (Production problems of dairy products), *Polzunovskii almanakh (Polzunovskii almanac)*, 2005, no. 1, pp. 5–9.
3. Shenderov, B.A., Sovremennoe sostoyanie i perspektivy razvitiya kontseptsii "Funktional'noye pitanie" (Current state and prospects of development of the concept of functional food), *Pishchevaya promyshlennost' (Food industry)*, 2003, no. 5, pp. 4–7.
4. Shenderov, B.A., *Funktional'noye pitanie i yego rol' v profilaktike metabolicheskogo sindroma (Functional Food and its Role in the Prevention of Metabolic Syndrome)*, Moscow: DeLi print, 2008.
5. Roberfroid, M.B., Global view on functional foods: European perspectives, *British Journal of Nutrition*, 2002, vol. 88, no. 2, 133–138.
6. Tikhomirov, N.A., Sovremennoe sostoyanie i perspektivy razvitiya produktov funktsional'nogo naznacheniya (Current state and prospects of development of functional food products), *Molochnaya promyshlennost' (Dairy industry)*, 2009, no. 7, pp. 5–8.
7. Anan'eva, N.V., Ganina, V.I., Nefedova, N.V., and Gabril'yan, G.R., Primenenie immobilizovannykh form probioticheskikh bakterii v proizvodstve molochnykh produktov (The use of immobilized forms of probiotic bacteria in the production of dairy products), *Molochnaya promyshlennost' (Dairy industry)*, 2006, no. 11, pp. 46–47.
8. Arai, S., Global view on functional foods: Asian perspectives, *British Journal of Nutrition*, 2002, vol. 88, no. 2, 139–143.
9. Milner, J.A., Functional foods and health: a US perspective, *British Journal of Nutrition*, 2002, vol. 88, no. 2, pp. 151–158.
10. Gavrilova, N.B., Pas'ko, O.V., Kanya, I.P., et al., *Nauchnyye i prakticheskiye aspekty tekhnologii proizvodstva molochno-rastitel'nykh produktov: monografiya (Scientific and Practical Aspects of the Production Technology of Dairy-Vegetable Products: monograph)* Omsk: OmGAU, 2006.
11. Yarkina, Ya.A., Bakkontsentrat bifidobakteriy i bakteriy *Lactobacillus casei* (Bacterial concentration of bifidobacteria and bacteria *Lactobacillus casei*), *Molochnaya promyshlennost' (Dairy industry)*, 2005, no. 2, pp. 34–35.
12. Ostroumov, L.A., Popov, A.M., Postolova, A.M., and Kuprina, I.K., Funktsional'nye produkty na osnove moloka i ego proizvodnykh (Functional foods based on milk and its derivatives), *Molochnaya promyshlennost' (Dairy industry)*, 2003, no. 9, pp. 21–22.
13. Semenikhina, V.F. and Begunova, A.V., Tekhnologicheskie aspekty ispol'zovaniya bifidobakterii dlya kislomolochnykh produktov (Technological aspects of the use of bifidobacteria for dairy products), *Molochnaya promyshlennost' (Dairy industry)*, 2009, no. 12, pp. 9–11.
14. Reshetnik, E.I., Maksimiyuk, V.A., and Utochkina, E.A., *Nauchnoe obosnovanie tekhnologii fermentirovannykh molochnykh produktov na osnove biotekhnologicheskikh sistem: monografiya (Scientific Substantiation of the Technology of Fermented Dairy Products based on Biotechnological Systems: Monograph)*, Blagoveshchensk: DalGAU, 2012.
15. Shenderov, B.A., *Funktional'noye pitanie i yego rol' v profilaktike metabolicheskogo sindroma (Functional Food and its Role in the Prevention of Metabolic Syndrome)*, Moscow: DeLi print, 2008.
16. Korovina, N.A., Zakharova, I.N., Malova, N.E., and Skuin', I.N., Rol' prebiotikov i probiotikov v funktsional'nom pitanii detei (The role of prebiotics and probiotics in functional food for children), *Lechashchiy vrach (Attending physician)*, 2005, no. 2, pp. 17–23.
17. Pasko, O.V., *Nauchnye osnovy tekhnologii produktov dlya spetsial'nogo pitaniya: monografiya (Scientific Bases of Technology of Products for Special Nutrition: Monograph)*, Omsk: Omsk Institute of Business and Law, 2005.
18. Zobkova, Z.S., Funktsional'nye tsel'nomolochnye produkty (Functional whole-milk products), *Molochnaya promyshlennost' (Dairy industry)*, 2006, no. 4, pp. 68–70.
19. Shenderov, B.A., Probiotiki, prebiotiki i simbiotiki. Obshchiye i izbrannyye razdely problemy (Probiotics, prebiotics and synbiotics. General and selected aspects of the problem), *Pishchevye ingredienty. Syr'ye i dobavki (Food ingredients. Raw materials and supplements)*, 2005, no. 2, pp. 23–26.
20. Ostroumov, L.A. and Gavrilov, G.B., Sposoby polucheniya i ispol'zovaniya laktulozy (Methods for obtaining and use of lactulose), *Molochnaya promyshlennost' (Dairy industry)*, 2006, no. 3, p. 52.
21. Ryabtseva, S.A., *Technologiya laktulozy (Lactulose Technology)*, Moscow: DeLi print, 2003.
22. Tokayev, E.S., Fibregam – pishchevoi ingredient novogo pokoleniya (Fibregam – a new generation food ingredient), *Pishchevye ingredienty. Syr'ye i dobavki (Food ingredients. Raw materials and supplements)*, 2006, no. 1, pp. 32–35.
23. Cherbut, C., Michel, C., Raison, V., Kravtchenko, T., and Severine, M., Acacia gum is a bifidogenic dietary fibre with high digestive tolerance in healthy humans, *Microbial Ecology in Health and Disease*, 2003, vol. 15, pp. 43–50.
24. Reshetnik, E.I. and Utochkina, E.A., *Prakticheskiye aspekty proektirovaniya funktsional'nykh produktov pitaniya: monografiya (Practical Aspects of the Design of Functional Foods: Monograph)*, Blagoveshchensk: DalGAU, 2012.
25. Reshetnik, E.I., Utochkina, E.A., and Maksimiyuk, V.A., Kislomolochnyi produkt s arabinogalaktanom (Fermented milk product with arabinogalactan), *Molochnaya promyshlennost' (Dairy industry)*, 2011, no. 11, pp. 56–57.

26. Dubrovin, V.I., Medvedeva, S.A., Aleksandrova, G.P., et al., Immunomoduliruyushchiye svoystva arabinogalaktana listvenitsy sibirskoy (*Larix sibirica* L.) (Immunomodulatory properties of arabinogalactan of Siberian larch (*Larix sibirica* L.)), *Farmatsiya (Pharmacy)*, 2001, no. 5, pp. 26–27.
27. Belicova, A., Ebringer, L., Krajcovic, J., Hromadkova, Z., and Ebringerova, A., Antimutagenic effect of heteroxilans, arabinogalactans, pectins and mannans in the euglena assay, *World Journal of Microbiology and Biotechnology*, 2001, vol. 17, no. 3, pp. 293–299.
28. Grieshop, S.M., Flickinger, E.A., and Eahey, G.C., Oral administration of Arabinogalactan affects immune status and fecal microbial populations in dogs, *Journal of Nutrition*, 2002, vol. 132, no. 3, pp. 478–482.
29. Robinson, R.R., Causey, J., and Slavin, J.L., *Nutritional Benefits of Larch Arabinogalactan*, McCleary, B.V. and Prosky, L., Eds., Oxford, UK: Blackwell Science, 2001, pp. 443–451.
30. Robinson, R.R., Feirtag, J., and Slavin, J.L., Effects of dietary arabinogalactan on gastrointestinal and blood parameters in healthy human subjects, *Journal of the American College of Nutrition*, 2001, vol. 20, no. 4, pp. 279–285.
31. Medvedeva, E.N., Babkin, V.A., and Ostroukhova, V.A., Arabinogalaktan listvenitsy – svoystva i perspektivy ispol'zovaniya (obzor) (Larch arabinogalactan—properties and prospects for the use (review)), *Khimiya rastitel'nogo syr'ya (Chemistry of plant raw materials)*, 2003, no. 1, pp. 27–37.
32. Gavrilova, N.B., *Biotekhnologiya kombinirovannykh molochnykh produktov: monografiya* (Biotechnology of Combined Dairy Products: Monograph), Omsk: Variant–Sibir', 2004.
33. Gavrilova, N.B., Vokorina, E.N., Zhdaneeva, N.P., and Simonova, K.M., *Sovremennyye aspekty tekhnologii molochnykh i molokosoderzhashchikh produktov s prolongirovannymi srokami khraneniya* (Modern Aspects of Technology for Milk and Dairy Products with a Prolonged Shelf Life), Omsk: Varinat–Sibir', 2007.
34. Utochkina, E.A. and Reshetnik, E.I., Vliyaniye arabinogalaktana na mikrobiologicheskie pokazateli i khranimosposobnost' kislomolochnogo produkta (Effect of arabinogalactan on microbiological and storability of fermented milk products), *Tekhnika i tekhnologiya pishchevykh proizvodstv (Technique and technology of food production)*, no. 4, pp. 72–75.



UDC 663.8:628.19
DOI 10.12737/1563

THE IMPACT OF PRIORITY WATER CONTAMINANTS ON THE STABILITY OF THE MAIN COMPONENTS OF NECTARS

T. A. Krasnova and I. V. Timoshchuk

Kemerovo Institute of Food Science and Technology,
bul'v. Stroitelei 47, Kemerovo, 650056 Russia
phone:/Fax: 8 (3842)-39-00-61, e-mail: ecolog1528@yandex.ru

(Received February 19, 2013; Accepted in revised form August 01, 2013)

Abstract: This paper presents the results of a study on the impact of organic impurities contained in water (phenol, chlorophenol, chloroform, formaldehyde, and acetaldehyde) on the stability of nectar components: sucrose, citric acid, vitamins A and C, and B group vitamins.

A reduction in the concentrations of the main components of nectars and priority contaminants, except for chloroform, has been established.

The mechanism of interaction of sucrose, citric acid, and vitamins contained in nectars with phenol, chlorophenol, chloroform, formaldehyde, and acetaldehyde has been substantiated theoretically.

Key words: nectar, sugar, citric acid, vitamins, water, phenol, chlorophenol, chloroform, formaldehyde, acetaldehyde.

INTRODUCTION

At present, nectars, as opposed to juices, are becoming popular soft drinks with the Russian public in terms of price affordability. Having a variety of flavors, nectars are not only a pleasant way of refreshment and thirst quenching but also a source of vitamins and other essential nutrients. In accordance with GOST R 51398-99 and the AIJN Code of Practice (European Association of the Industry of Juices and Nectars), nectars are defined as drinks obtained by the addition of water and sugar to fruit juice, concentrated fruit juice, or purée from edible parts of fresh fruits. Citric or ascorbic acid may be added. The minimum fruit juice content in nectars should be 25--50%, depending on the type of berries or fruits.

Presently, water from the central water supply system is predominantly used in the production of nectars. The quality of such water determines the consumer appeal of finished soft drinks: flavor, taste, color stability, etc.

Kemerovo oblast forms a large territorial production unit within the Russian Federation. Hence, in addition to natural organic substances, water supply sources contain anthropogenic organic impurities from industrial wastewater. According to the Kemerovo Oblast Sanitary and Epidemiological Center, in 2011, 30.5% of water samples from the Kuzbass central water supply system did not comply with the hygienic standards in terms of sanitary and chemical indices, including 33.9% of water samples from surface water bodies and 29.8% from underground water bodies. The phenol concentration constantly exceeds the MAC values in many Kuzbass

surface and underground water bodies. According to the State Environmental Protection Committee for Kemerovo Oblast, random samples taken from the Tom' River during snowmelt show phenol concentrations exceeding 30 MAC [1]. In natural waters, the content of humic substances responsible for the formation of organic halogen compounds is 10--50 mg/dm³ [2].

Water treatment plants act as barriers against organic substances only to a slight extent; moreover, water treatment yields more dangerous toxic agents than the initial substances. The application of chlorine for decontamination during water treatment results in the formation of such by-products as chlorophenol and chloroform; in the same way, the application of ozone results in the formation of formaldehyde and acetaldehyde [3--5]. As a result of experimental studies, we have found out a two- to five-times exceedance of the MAC values of the above organic impurities in random water samples taken in spring and summer. When concentrations of these contaminants in water exceed the MAC values, they exert toxic, allergenic, mutagenic, and carcinogenic effects on humans [6--9]. In addition to their toxic effect, the organic impurities found in water can interact with the main components of soft drinks, degrading their quality. Thus, studies on the impact of priority organic contaminants periodically present in water on the quality of nectars during their production and storage are relevant and timely.

In this work, we will study the impact of priority organic contaminants periodically present in water (phenol, chlorophenol, chloroform, formaldehyde, and acetaldehyde) on the quality attributes of nectars (the

contents of sucrose, citric acid, vitamins A and C, and B group vitamins) during their production and storage.

OBJECTS AND METHODS OF RESEARCH

The objects of research were water solutions containing organic contaminants (chloroform, phenol, chlorophenol, formaldehyde, and acetaldehyde) with added sucrose and citric acid. The sucrose concentration in the test samples was taken at 110 mg/kg according to GOST R 53396-09. The citric acid concentration was taken at 5 mg/l according to the Fruit Juice Regulations. For a reliable assessment of the impact of organic impurities on the stability of the nectar components, the concentration of organic contaminants in the systems under investigation was taken at 10 MAC values; sucrose and citric acid water solutions without any harmful impurities were used as reference standards. The sucrose content in the samples was measured using refractometry; the content of citric acid, phenol, formaldehyde, chlorophenol, and acetaldehyde was measured using molecular absorption spectroscopy; and the chloroform content was measured using gas-liquid partition chromatography.

Given the volatility of some organic contaminants and the duration of the study of nectar components stability after selection of the next sample for the analysis, the source samples were stored in sealed vessels in a dark place.

The objects of research also included nectars (apple, blackcurrant, raspberry, sea-buckthorn, and chokeberry) made with water without organic impurities and with water containing phenol, chlorophenol, chloroform, formaldehyde, and acetaldehyde. Changes in the color intensity of nectars during their production and storage were studied using molecular absorption spectroscopy; the vitamin content was measured using capillary electrophoresis [10, 11].

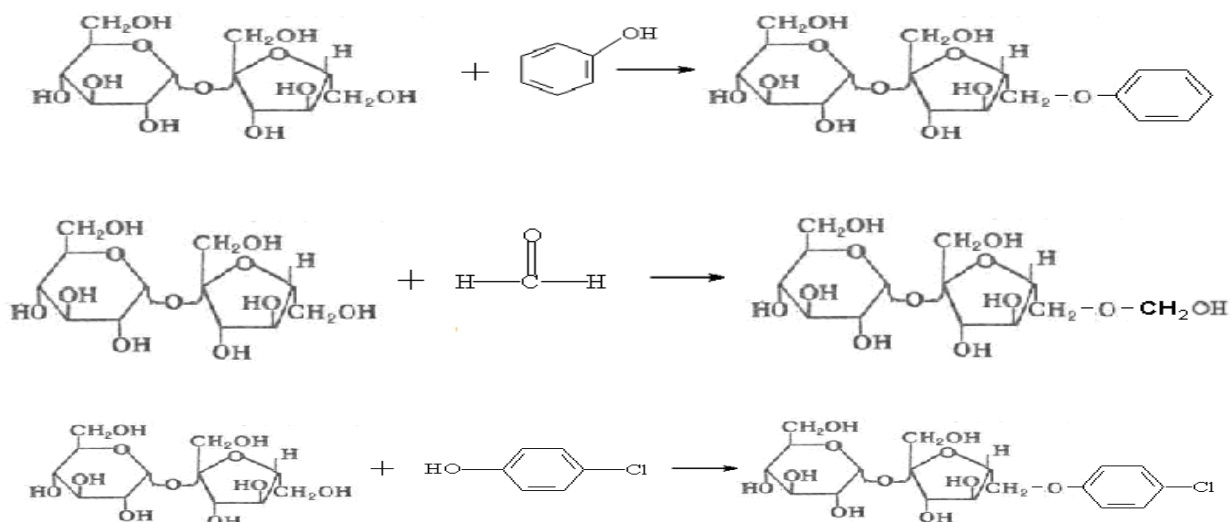


Fig. 1. Chemical reaction of contaminants and sucrose.

The chemical reaction of organic impurities and sucrose is verified empirically by the respective reduction of phenol, chlorophenol, formaldehyde, and acetaldehyde in the presence of sucrose (Fig. 2).

Changes in all indicators were observed until reaching a constant concentration of the test components in drinks and solutions.

RESULTS AND DISCUSSION

Sucrose (C₁₂H₂₂O₁₁) is one of the main components of nectars. Considering chemical properties of sucrose and the organic contaminants under investigation, there is a probability that their chemical interaction will occur.

It has been established that all organic contaminants except for chloroform interact with sucrose, as follows from the chemical equations (Fig. 1). The reaction of sucrose and formaldehyde was the most active, while the reaction of sucrose and chlorophenol was the least active (Table 1).

Table 1. Variation in the sucrose content in the samples under investigation during storage, %

Number of days of storage	Water solution without organic impurities	Water solution containing chloroform	Water solution containing phenol	Water solution containing chlorophenol	Water solution containing formaldehyde	Water solution containing acetaldehyde
1	100	100	100	100	100	100
3	100	100	85	90	61	85
6	100	100	82	85	55	74
8	100	100	71	83	40	63
14	100	100	66	70	35	56
20	100	100	65	68	30	56

Citric acid (C₆H₈O₇ · H₂O) is often used as an acidity regulator in the production of nectars since it has a milder flavor compared to other edible acids and does not irritate the mucosae of the gastrointestinal tract.

There is a probability of interaction between citric acid and organic components. During the interaction, the content of citric acid may decrease, whereas its overconsumption may grow. Since citric acid is an expensive component, its wastage is undesirable. Therefore, it is appropriate to study the impact of organic impurities (phenol, chlorophenol, chloroform, formaldehyde, and acetaldehyde) on the stability of citric acid in the water used for nectar production.

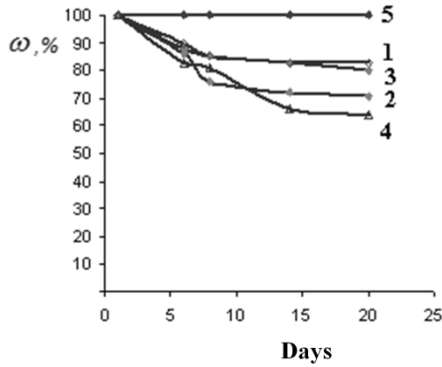


Fig. 2. Variations in (1) acetaldehyde, (2) phenol, (3) formaldehyde, (4) chlorophenol, and (5) chloroform contents in water containing sucrose over time.

The experimental data suggest that the citric acid content decreases in the presence of all of the organic contaminants except for chloroform (Table 2).

Table 2. Variation in the citric acid content in the samples under investigation during storage, %

Number of storage days	Water solution without organic impurities	Water solution containing chloroform	Water solution containing phenol	Water solution containing chlorophenol	Water solution containing formaldehyde	Water solution containing acetaldehyde
1	100	100	100	100	100	100
6	100	100	81	100	90	98
8	100	100	75	100	76	95
12	100	100	63	93	60	87
18	100	100	53	83	54	83
20	100	100	53	63	53	70

Chemical reactions between citric acid and priority water contaminants are given in Fig. 3.

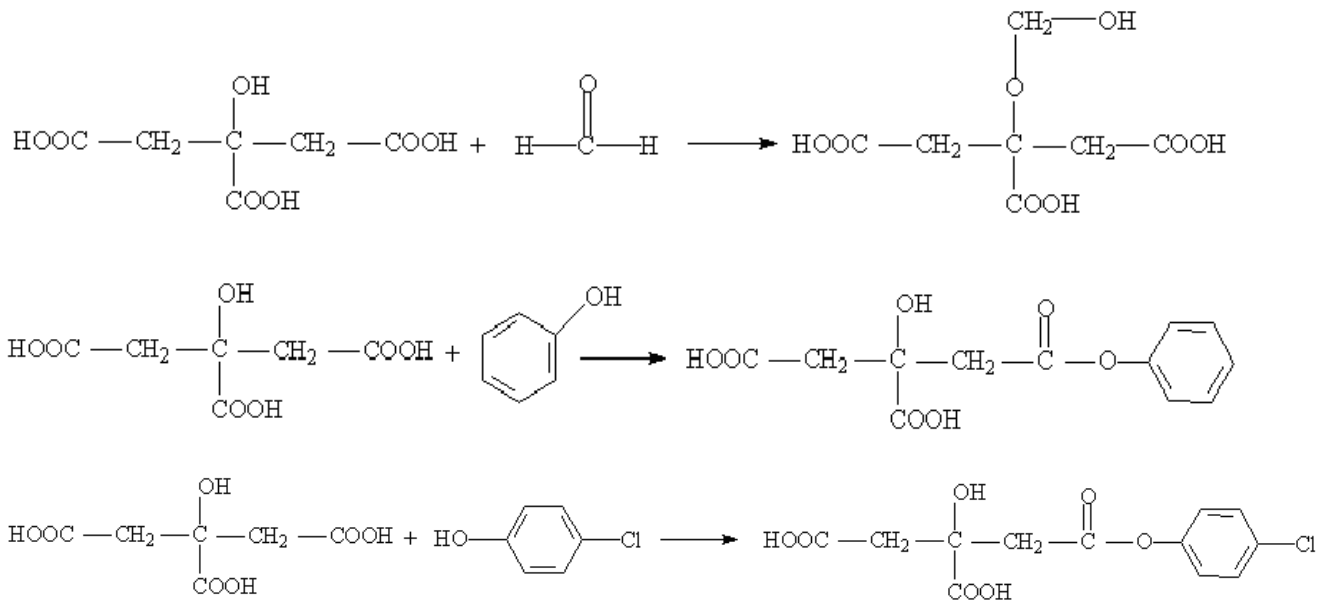


Fig. 3. Chemical reaction between the contaminants and citric acid.

The chemical reaction of organic impurities and citric acid is verified empirically by the respective reduction of phenol, chlorophenol, formaldehyde, and acetaldehyde in water containing citric acid over time, as is shown in Fig. 4.

Berries and fruits used in nectars contain substances that determine their color. The colors of all berries and fruits are largely determined by coloring substances, such as flavonoids (anthocyanins) and carotenoids. Flavonoids produce red, blue, and purple pigmentation

in fruits, while carotenoids produce yellow-to-orange colors. The content of the components that provide fruits and berries with colors is given in Table 3. It appeared appropriate to study the impact of organic contaminants on the color stability of nectars.

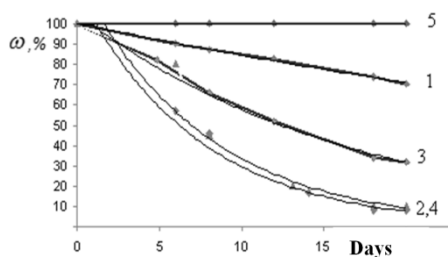


Fig. 4. Variations in (1) acetaldehyde, (2) phenol, (3) formaldehyde, (4) chlorophenol, and (5) chloroform contents in water containing citric acid over time.

Berries and fruits used in nectars contain substances that determine their color. The colors of all berries and fruits are largely determined by coloring substances, such as flavonoids (anthocyanins) and carotenoids. Flavonoids produce red, blue, and purple pigmentation in fruits, while carotenoids produce yellow-to-orange colors. The content of the components that provide fruits and berries with colors is given in Table 3. It appeared appropriate to study the impact of organic contaminants on the color stability of nectars.

Table 3. Content of components providing berries and fruits with color, mg/100 g

Substance	Flavonoids (anthocyanins, catechines, leucoanthocyanins), mg	Carotene (provitamin A), mg
Sea-buckthorn	800–1.000	11
Chokeberry	250–600	0.5
Raspberry	600–1.300	1
Apple	300–600	1.1–15

No variation in the color intensity in nectars produced from all sorts of berries in the presence of chloroform was detected during the entire research period (Figs. 5–8).

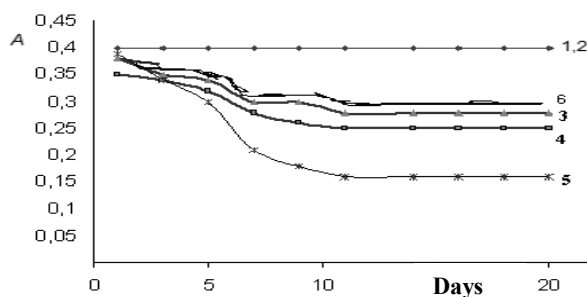


Fig. 5. Variations in the color of apple nectar over time made with (1) water without organic impurities and with water solutions containing (2) chloroform, (3) formaldehyde, (4) phenol, (5) chlorophenol, and (6) acetaldehyde.

The least color fading occurs in raspberry nectar in the presence of chlorophenol and in apple, chokeberry, and sea-buckthorn nectars in the presence of acetaldehyde; the most color fading occurs in raspberry nectar in the presence of formaldehyde; in sea-

buckthorn and chokeberry nectars in the presence of phenol; and in apple nectar in the presence chlorophenol.

It is obvious that chemical properties of the coloring substances and organic contaminants predetermined the possibility of their interaction, as is shown by the example of carotenoids (Fig. 9).

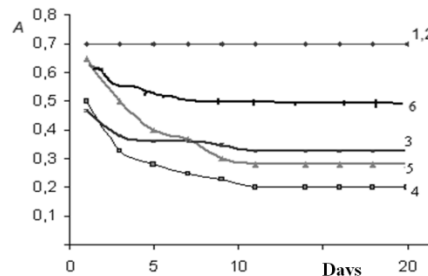


Fig. 6. Variations in the color of chokeberry nectar made with (1) water without organic impurities and with water solutions containing (2) chloroform, (3) formaldehyde, (4) phenol, (5) chlorophenol, and (6) acetaldehyde.

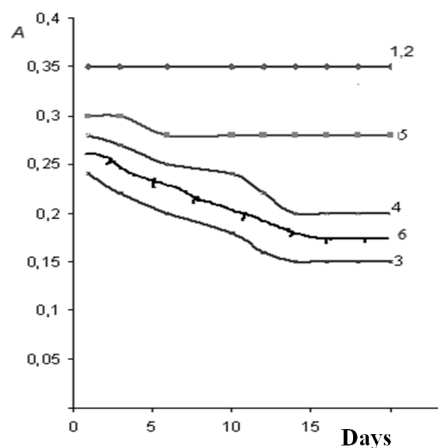


Fig. 7. Variations in the color of raspberry nectar made with (1) water without organic impurities and with water solutions containing (2) chloroform, (3) formaldehyde, (4) phenol, (5) chlorophenol, and (6) acetaldehyde.

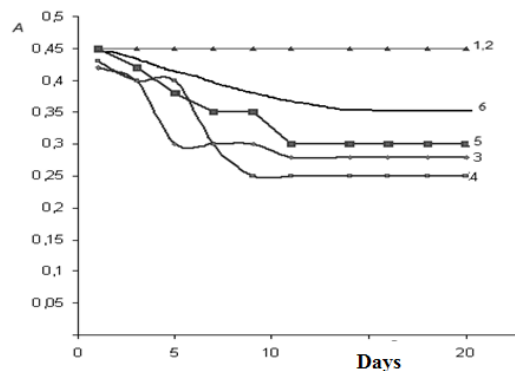


Fig. 8. Variations in the color of sea-buckthorn nectar made with (1) water without organic impurities and with water solutions containing (2) chloroform, (3) formaldehyde, (4) phenol, (5) chlorophenol, and (6) acetaldehyde.

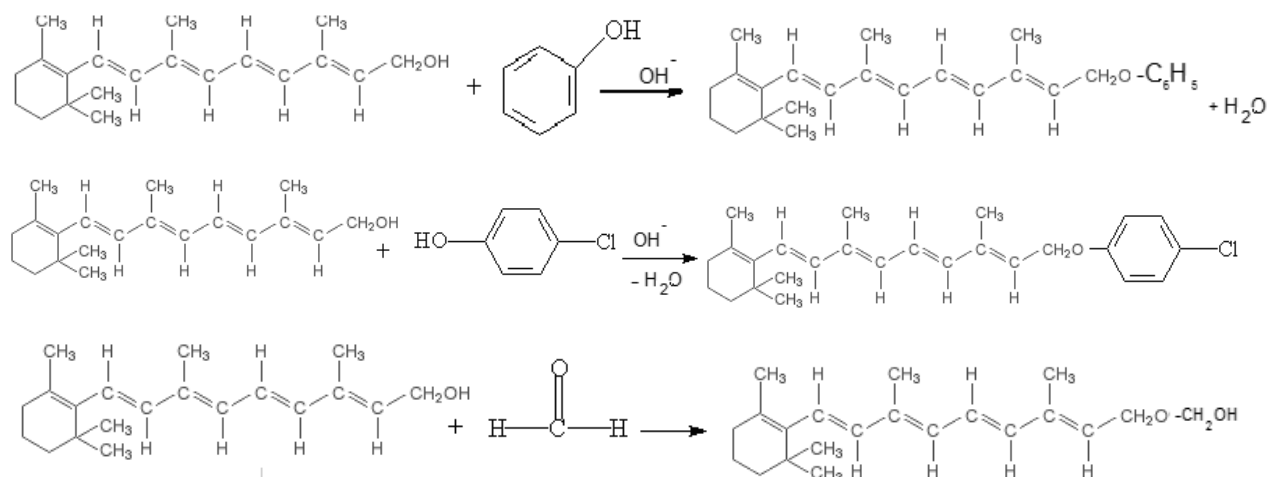


Fig. 9. Chemical reaction of carotenoids and priority contaminants contained in water.

Vitamins contained in nectars are organic compounds of different chemical nature, which can lead to their interaction with organic impurities contained in water. The content of individual vitamins in the nectar samples under investigation is shown in Table 4.

Table 4. Vitamin content in the nectar samples under investigation, mg/100 g

Vitamins, mg/100 g	Apple	Black-currant	Rasp-berry	Choke-berry	Sea-buckthorn
C	33.2	26.6	21.5	22.1	54.7
B ₃	0.03	0.02	0.009	0.055	0.06
B ₆	-	0.04	-	-	0.065
B ₉	-	-	0.037	0.062	-
B ₅	-	-	0.009	0.023	-
B ₂	0.03	-	-	0.0021	-
B ₁	-	-	-	0.05	0.05

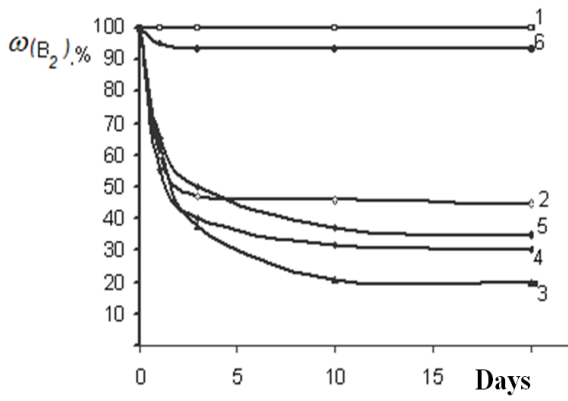
Over the research period, the vitamin B₂ reduction in apple nectar was 80% in the presence of formaldehyde in water, 75% in the presence of chlorophenol, 65% in the presence of acetaldehyde, and 60% in the presence of phenol. The vitamin B₃ reduction was 40% in the presence of phenol, 47% in the presence of formaldehyde, 33% in the presence of chlorophenol, and 27% in the presence of acetaldehyde. The vitamin C reduction was 50% in the presence of phenol, 44% in the presence of formaldehyde, 35% in the presence of chlorophenol,; and 25% in the presence of acetaldehyde (Fig. 10).

In blackcurrant nectar, vitamin B₃ was reduced by 45% in the presence of acetaldehyde in water, by 40% in the presence of phenol, by 30% in the presence of chlorophenol, and by 25% in the presence of formaldehyde. Vitamin B₆ was decomposed almost by 100% due to its small initial concentration in the presence of phenol and acetaldehyde, by 95% in the presence of formaldehyde, ; and by 90 % in the presence of chlorophenol. Vitamin C was reduced by 38% in the presence of chlorophenol, by 30% in the presence of phenol, by 25% in the presence of formaldehyde, and by 20% in the presence of acetaldehyde (Fig. 11).

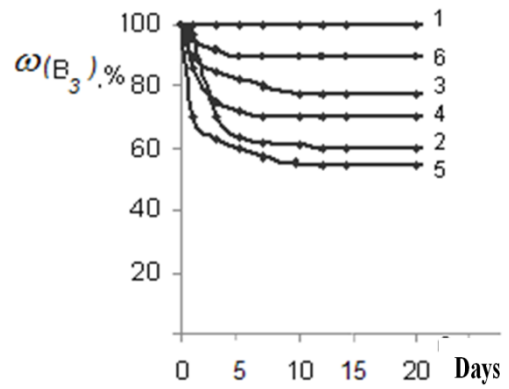
In raspberry nectar, vitamin B₃ was reduced by 40% in the presence of acetaldehyde in water, by 30% in the presence of formaldehyde and phenol, and by 20% in the presence of chlorophenol, . Vitamin C was reduced by 40% in the presence of chlorophenol, by 35% in the presence of phenol, by 30% in the presence of formaldehyde, and by 25% in the presence of acetaldehyde. Vitamin B₅ was reduced by 40% in the presence of phenol, by 35% in the presence of acetaldehyde, and by 35% in the presence of formaldehyde and chlorophenol. Vitamin B₉ in the presence of all water contaminants was reduced by 20–28% (Fig. 12).

In chokeberry nectar, the vitamin B₃ content was reduced by 35% in the presence of phenol and formaldehyde, by 40% in the presence of phenol, by 55% in the presence of chlorophenol, and by 65% in the presence of acetaldehyde. Vitamin B₉ was decomposed by 40% in the presence of phenol, by 50% in the presence of formaldehyde, and by 60% in the presence of chlorophenol and acetaldehyde. Vitamin B₅ was reduced by 25% in the presence of acetaldehyde, by 58% in the presence of formaldehyde, by 70% in the presence of phenol, and by 80% in the presence of chlorophenol (Fig. 13).

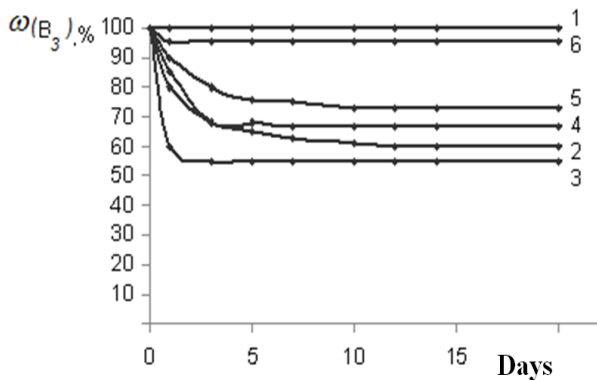
In sea-buckthorn nectar, vitamin B₁ was reduced by 60% in the presence of formaldehyde in water, by 45% in the presence of phenol, by 40% in the presence of acetaldehyde, and by 35% in the presence of chlorophenol. Vitamin B₃ was reduced by 95% in the presence of chlorophenol, by 90% in the presence of formaldehyde, by 87% in the presence of acetaldehyde, and by 50% in the presence of phenol. Vitamin C was reduced by 60% in the presence of acetaldehyde, by 55% in the presence of formaldehyde, by 44% in the presence of chlorophenol, and by 34% in the presence of phenol (Fig. 14).



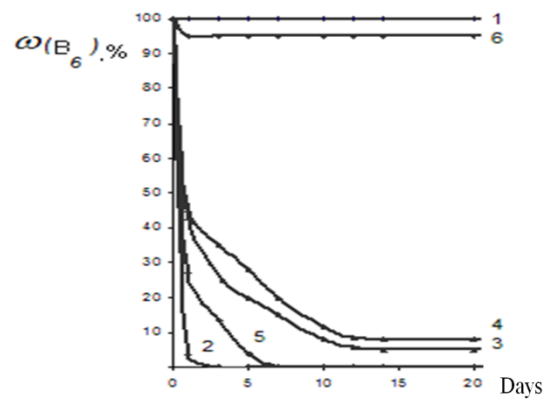
a)



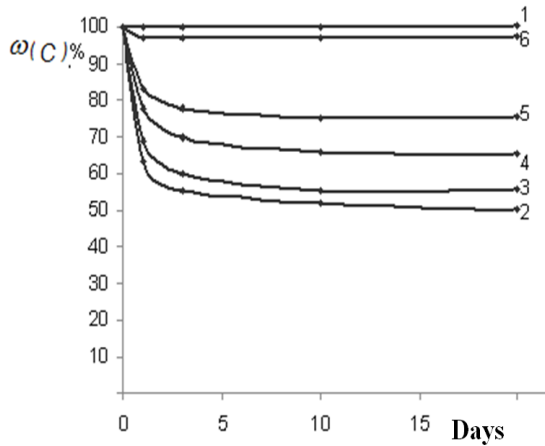
a)



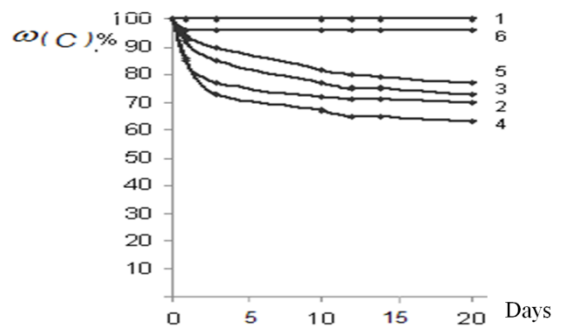
b)



b)



c)



c)

Fig. 10. Vitamins B₂, B₃, and C contents in apple nectar made with (1) water without organic impurities and with water solutions containing (2) phenol, (3) formaldehyde, (4) chlorophenol, (5) acetaldehyde, and (6) chloroform.

Fig. 11. Vitamins B₃, B₆, and C content in blackcurrant nectar made with (1) water without organic impurities and with water solutions containing (2) phenol, (3) formaldehyde, (4) chlorophenol, (5) acetaldehyde, and (6) chloroform.

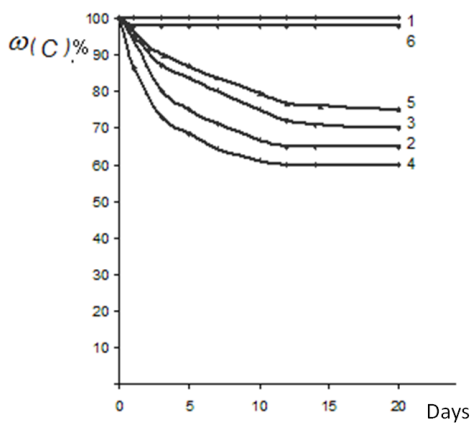
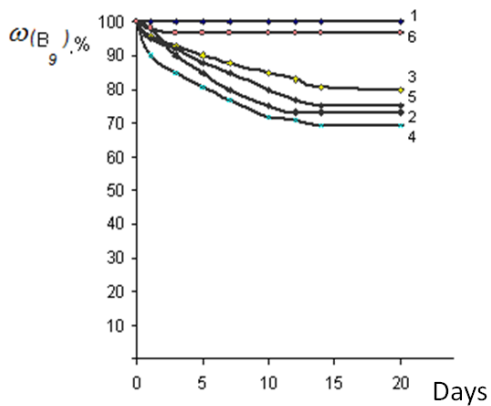
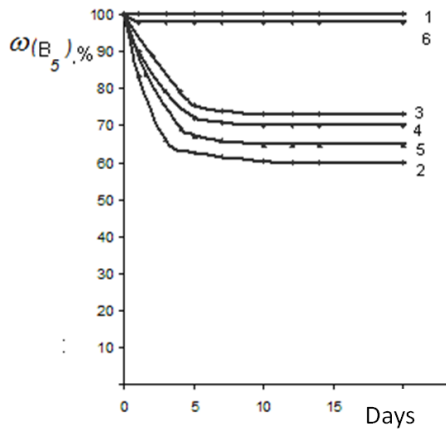
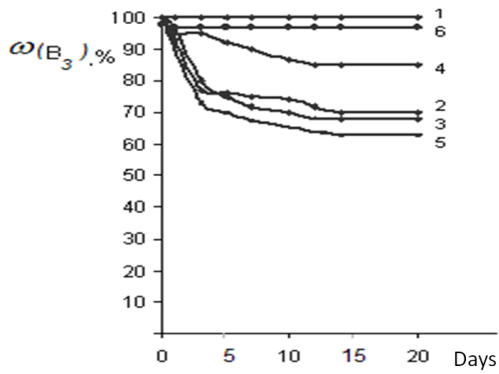


Fig. 12. Vitamins B₃, B₅, B₉, and C content in raspberry nectar made with (1) water without organic impurities and with water solutions containing (2) phenol, (3) formaldehyde, (4) chlorophenol, (5) acetaldehyde, and (6) chloroform.

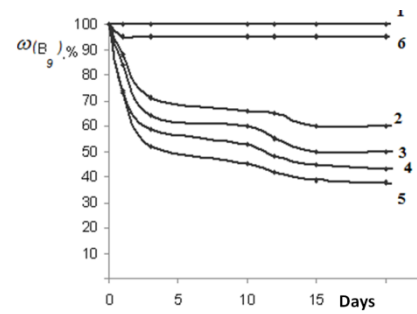
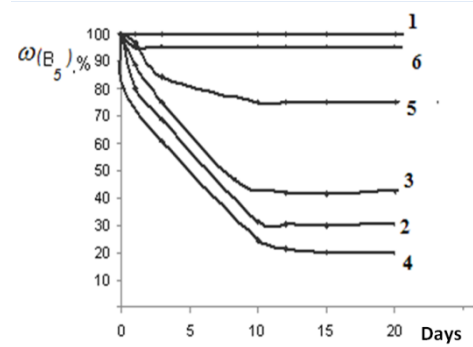
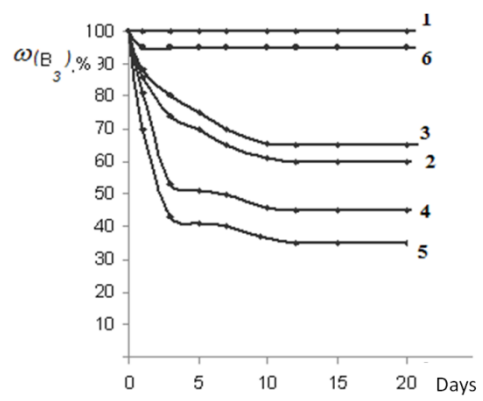
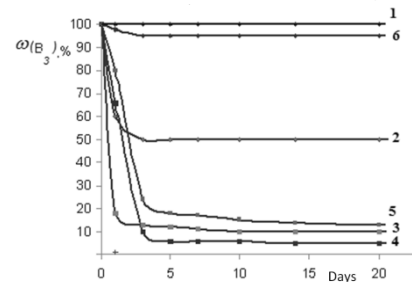
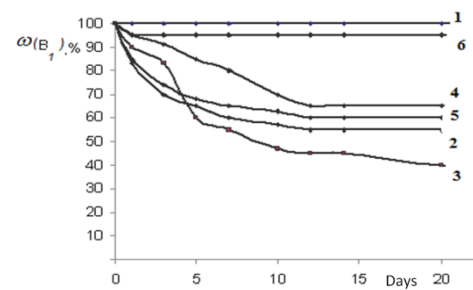
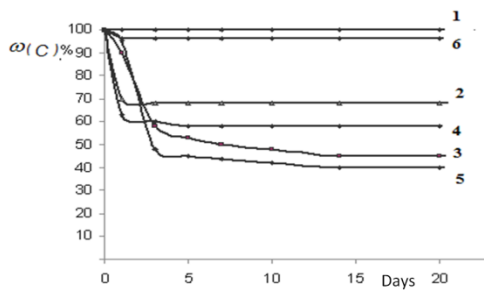


Fig. 13. Vitamins B₃, B₅, B₉ contents in chokeberry nectar made with (1) water without organic impurities and with water solutions containing (2) phenol, (3) formaldehyde, (4) chlorophenol, (5) acetaldehyde, and (6) chloroform.





water solutions containing (2) phenol, (3) formaldehyde, (4) chlorophenol, (5) acetaldehyde, and (6) chloroform.

Variation in the vitamin content in nectars in the presence of chloroform was not shown over the entire period of research. The chemical reaction of priority contaminants (phenol, formaldehyde, acetaldehyde, and chlorophenol) contained in the water used for the production of nectars and vitamins is verified by the following chemical equations (Figs. 15--21):

Fig. 14. Vitamins B₁, B₃, C content in sea-buckthorn nectar made with (1) water without organic impurities and with

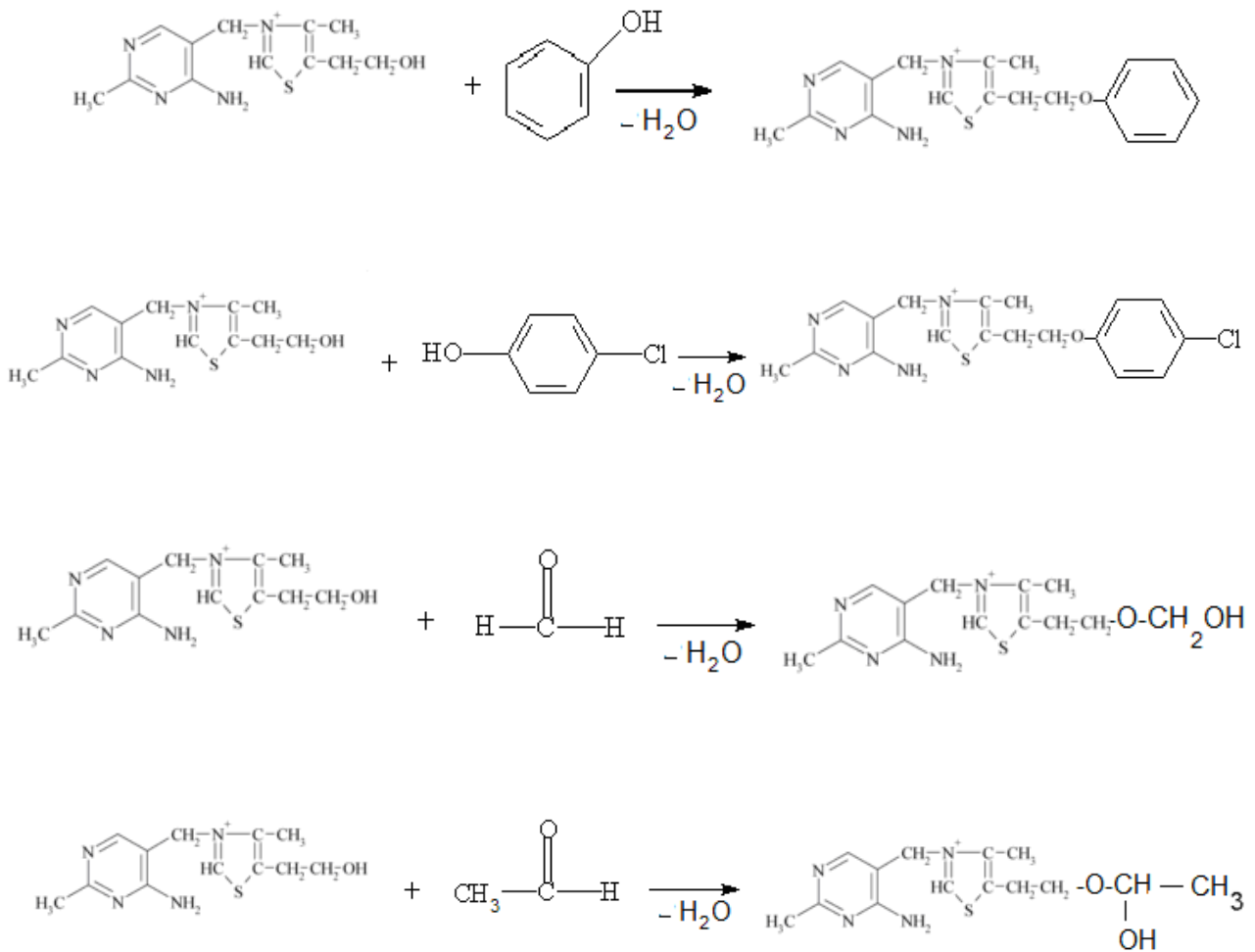
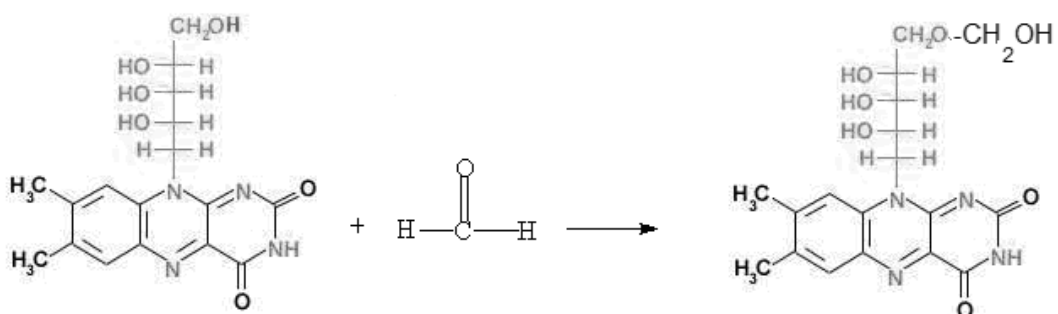


Fig. 15. Chemical reaction of vitamin B₁ and priority contaminants contained in water.



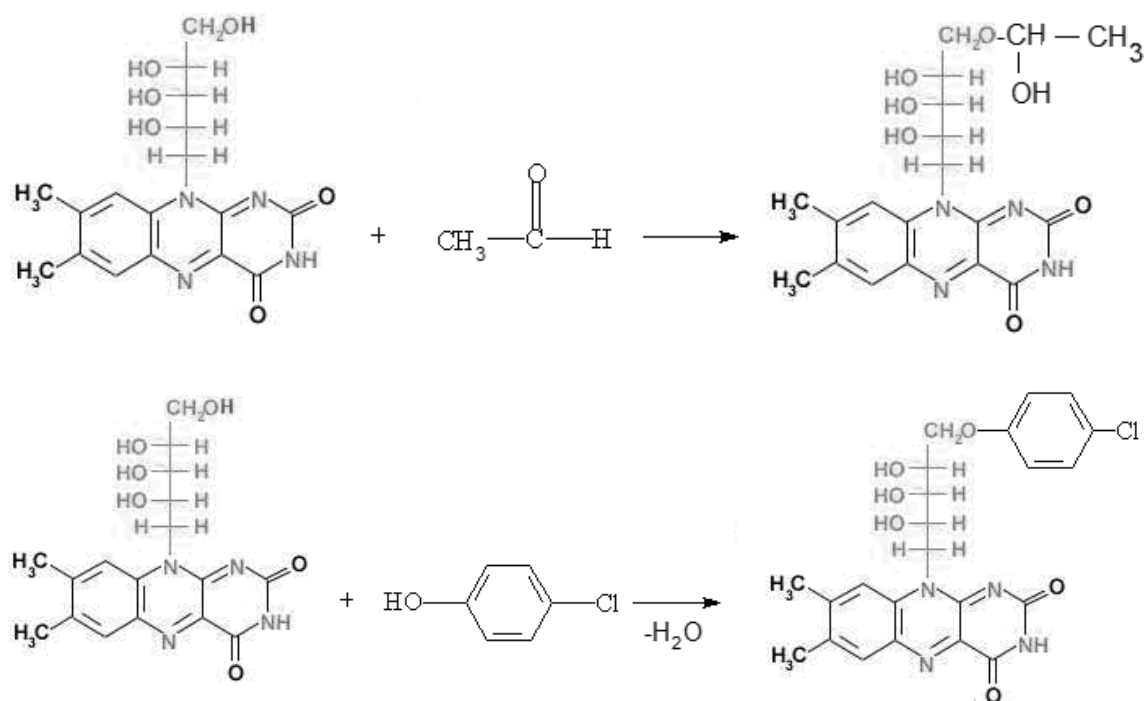


Fig. 16. Chemical reaction of vitamin B₂ and priority contaminants contained in water.

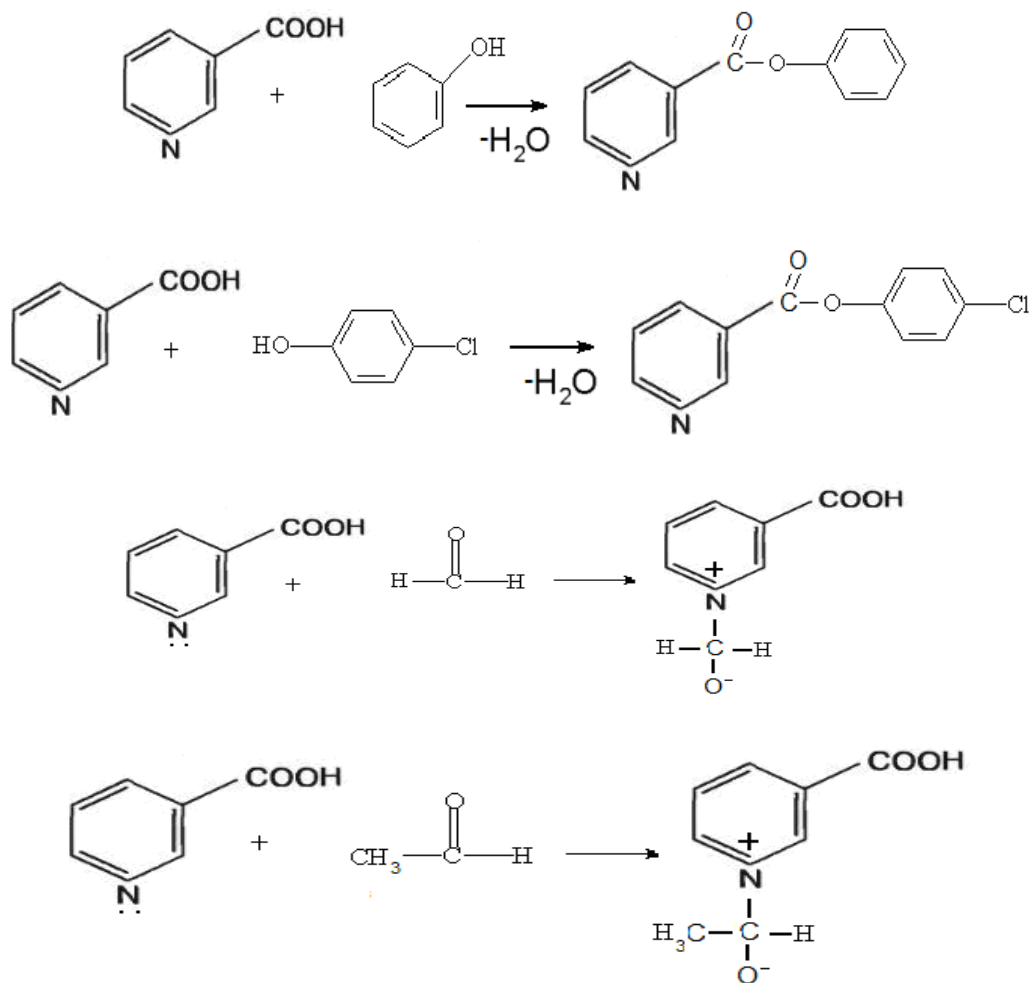


Fig. 17. Chemical reaction of vitamin B₃ and priority contaminants contained in water.

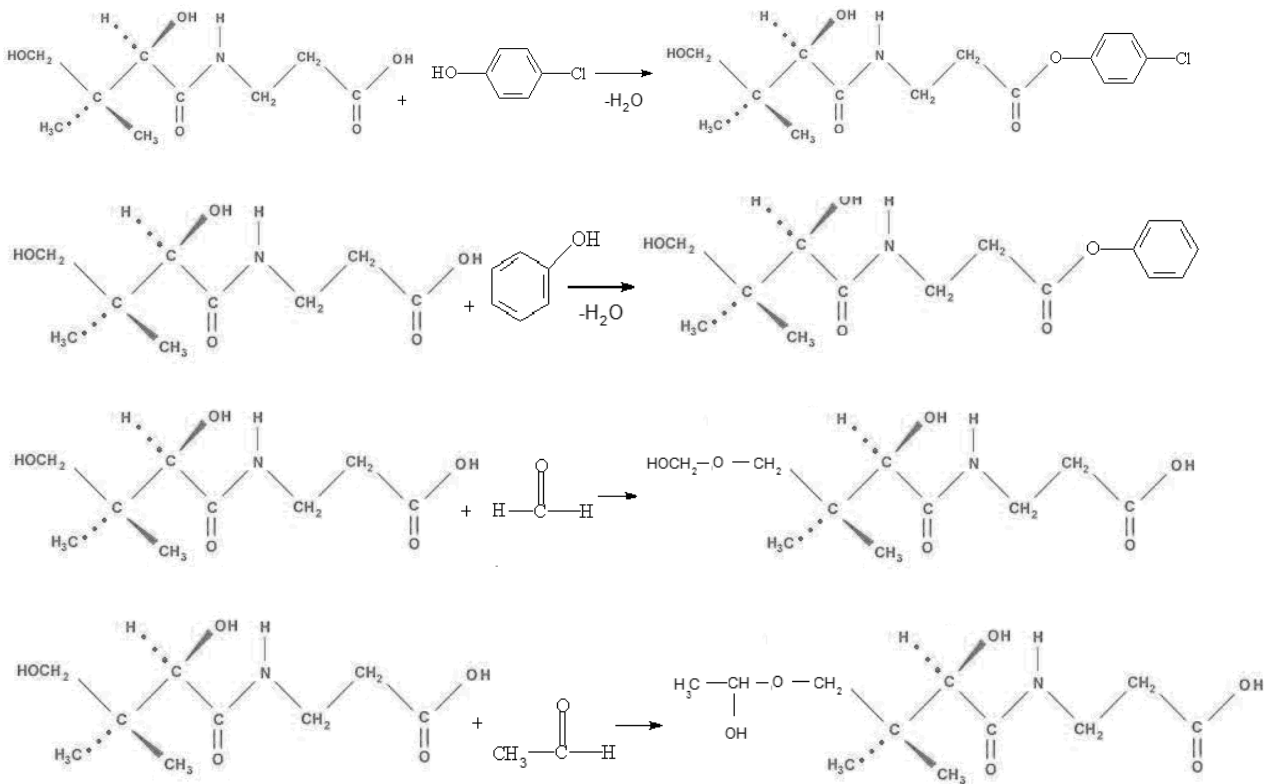
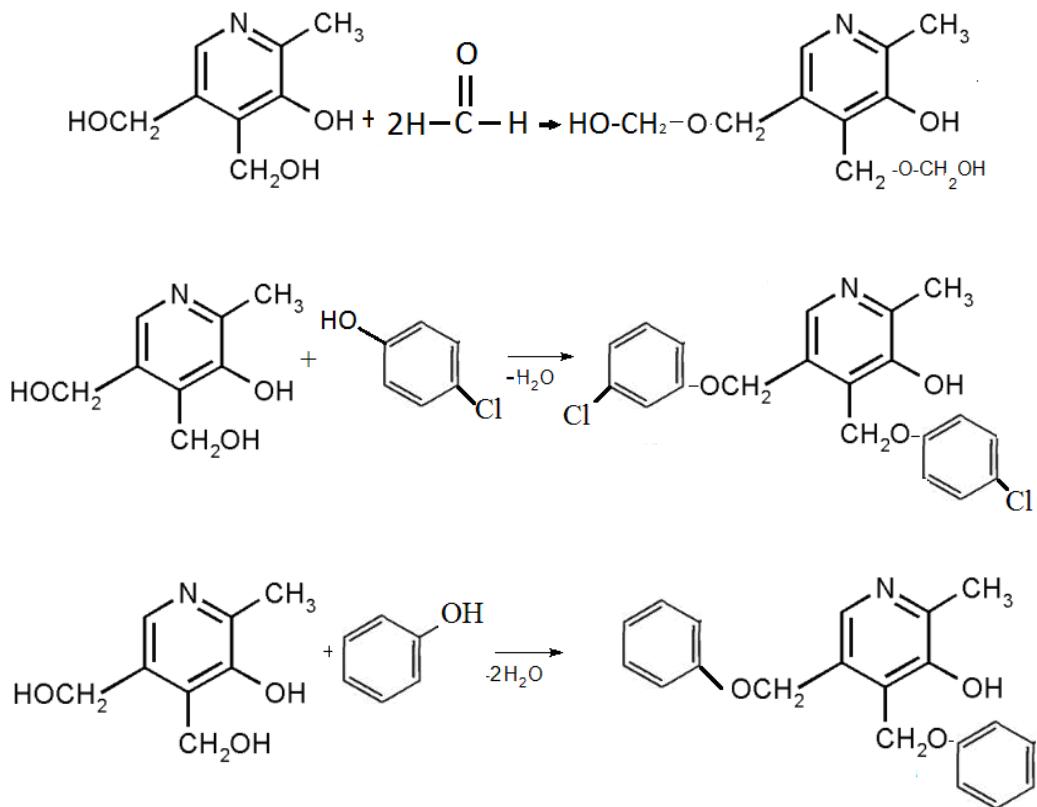
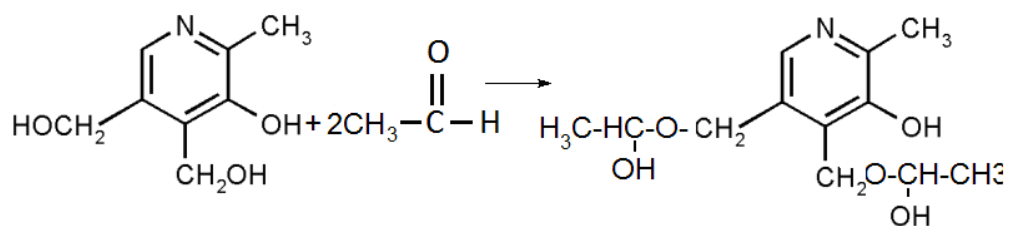
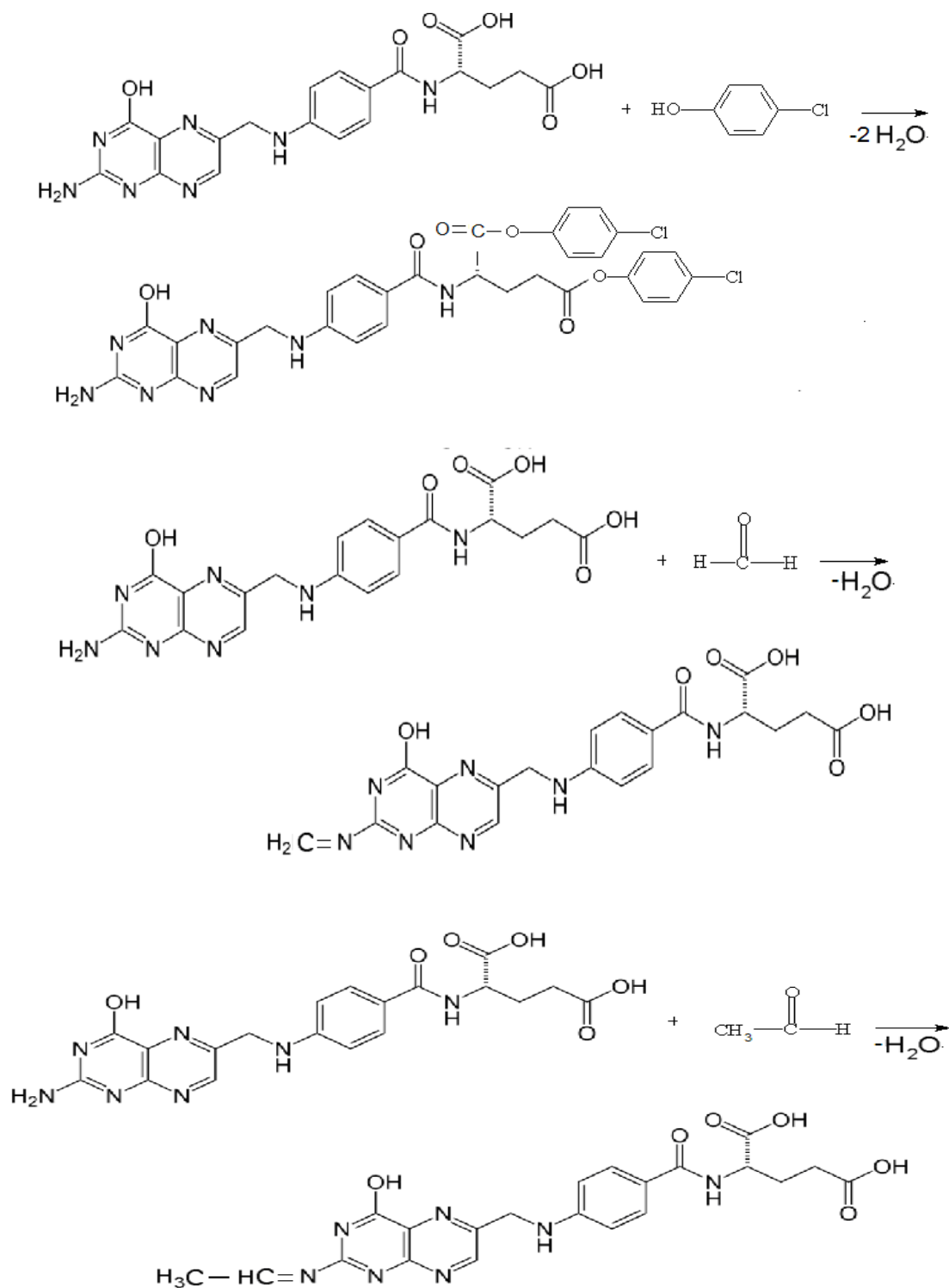


Fig. 18. Chemical reaction of vitamin B₅ and priority contaminants contained in water.



Fig. 19. Chemical reaction of vitamin B₆ and priority contaminants contained in water.Fig. 20. Chemical reaction of vitamin B₉ and priority contaminants contained in water.

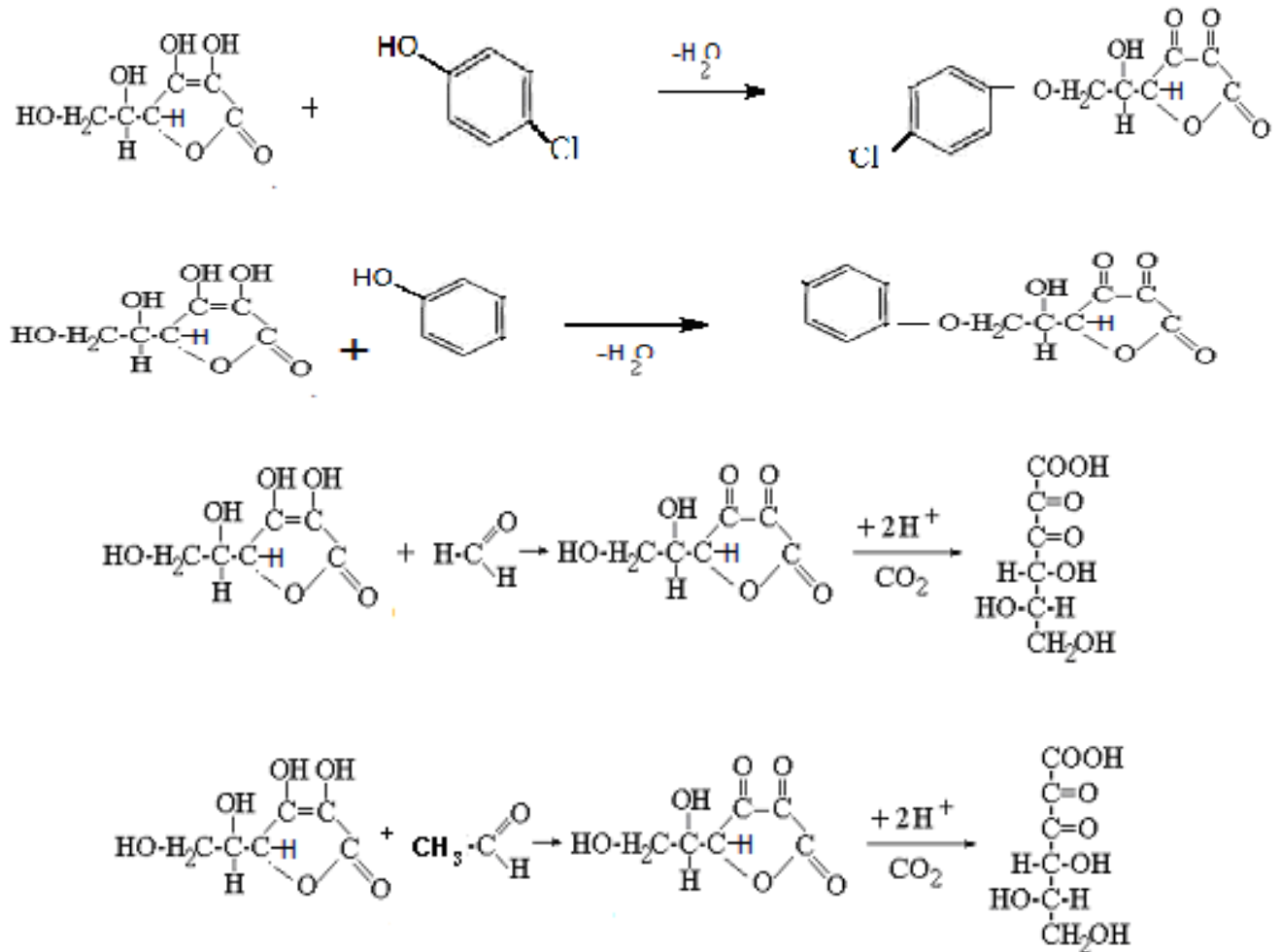


Fig. 21. Chemical reaction of vitamin C and priority contaminants contained in water.

The study of the changes in the organic contaminant concentrations has shown that a relation can be traced between the reduction of the vitamin concentrations and their molecular weights and the molecular weights of the priority water contaminants.

The research results show that formaldehyde, acetaldehyde, chlorophenol, and phenol have a considerable impact on the color stability and

preservation of nectar components, such as sugar, citric acid, ascorbic acid (vitamin C), provitamin A (carotene), and B group vitamins by interacting with them and degrading the quality attributes of nectars. Therefore, the water used in nectar production must undergo additional decontamination to remove organic impurities using, for instance, adsorption on activate carbon.

REFERENCES

1. Materialy k gosudarstvennomu dokladu "O sostoyanii i okhrane okruzhayushchei sredy Kemerovskoi oblasti v 2011" (Materials to the State Report "On Environmental Condition and Protection in Kemerovo Region in 2011). <http://gosdoklad.kuzbasseco.ru/2011/>
2. Nikoladze, G.I., *Podgotovka vody dlya pit'evogo i promyshlennogo vodosnabzheniya* (Water Treatment for Potable and Industrial Water Supply), Moscow: Vysshaya Shkola, 1984.
3. Slavinskaya, G.V., Vliyanie khlorirovaniya na kachestvo pit'evoi vody (Impact of water chlorination on the quality of drinking water), *Khimiya i tekhnologiya vody (Water chemistry and technology)*, 1991, vol. 12, no. 11, pp. 1013--1022.
4. Sato, T., Yamamori, H., and Matsuda, H., Estimation of safety of ozonation and chlorination of a water purification plant, *Water Science and Technology*, 1992, vol. 26, no. 9, pp. 2385--2388.
5. Warming to ozone, *Water and Waste Treatment*, 1992, no. 4, pp. 12--16.
6. Neale, P., Antony, A., and Bartkow, M., Bioanalytical assessment of the formation of disinfection byproducts in a drinking water treatment plant. *Environmental Science and Technology*, 2012, vol. 46, no. 18, pp. 10317--10325.

7. Itoh, S., Gordon, B., and Callan, P., Regulations and perspectives on disinfection by-products: importance of estimating overall toxicity, *Journal of Water Supply: Research and Technology---Aqua*, 2011, vol. 60, no. 5, pp. 261--274.
8. Jeong, C., Wagner, E., and Siebert, V., Occurrence and toxicity of disinfection byproducts in European drinking water in relation with the HIWATE epidemiology study, *Environmental Science and Technology*, 2012, vol. 46, no. 21, pp. 12120--12128.
9. Grushko, Y.M., *Vrednye organicheskie soedineniya v promyshlennykh stochnykh vodakh: Spravochnik* (Harmful organic compounds in industrial wastewaters: Reference Book), Leningrad: Khimiya, 1982.
10. Zhao, D., Lu, M., and Cai, Z., Separation and determination of vitamins and essential amino acids in health drinks by CE-LIF with simultaneous derivatization, *Electrophoresis*, 2012, vol. 33, pp. 2424--2432.
11. Dziomba, S., Kowalski, P., and Baczek, T., Field-amplified sample stacking-sweeping of vitamins B determination in capillary electrophoresis. *Journal of Chromatography*, 2012, vol. 1267, pp. 224--230.



UDC 637.146.3:634.74

DOI 10.12737/1564

IDENTIFICATION OF THE ORIGIN OF SEA BUCKTHORN OIL OF THE ALTAI KRAI BY DIFFERENTIAL SCANNING CALORIMETRY

S. N. Khabarov¹, A. L. Vereshchagin², Yu. G. Gur'yanov²,
N. V. Goremykina², and N. V. Bychin²

¹Lisavenko Research Institute of Horticulture for Siberia, Siberian Branch,
Russian Academy of Agricultural Sciences, Zmeinogorskii trakt 49, Barnaul, 656045 Russia
Fax: (3852) 68-50-17, Tel.: (3852) 68-49-68, e-mail: niilisavenko@hotmail.ru, val@bti.secna.ru

²Biysk Institute of Technology, Polzunov Altai State Technical University,
str. Trofimova 27, Biysk-05, Altai krai, 659305 Russia
e-mail: val@bti.secna.ru

(Received February 21, 2013; Accepted in revised form March 19, 2013)

Abstract: The composition of lipids derived by extraction with Freon 22 and enzymatic hydrolysis from berries, berry shells, and seeds of the Chuy sea buckthorn cultivar has been studied. The fatty acid composition and acid and peroxide values of the samples have been analyzed; the differential scanning calorimetry (DSC) melting curves have been examined. The DSC method has been found to be appropriate for determining the origin of raw materials and the production method for sea buckthorn oil.

Keywords: sea buckthorn oil, the Altai Territory, production method, differential scanning calorimetry

1. INTRODUCTION

Sea buckthorn berries are rich in vitamins, carotenoids, flavonoids, proteins, antioxidants, amino acids, fatty acids, and phytosterols [1]. The most valuable component of sea buckthorn berries is their oil. The oil from the sea buckthorn pulp and seeds is characterized by a high content of lipids, including tocopherols, tocotrienols, carotenoids, and ω -3 and ω -6 polyunsaturated fatty acids [2, 3]. The composition of the sea buckthorn seeds and pulp varies in accordance with the subspecies, cultivar, soil and climate conditions, origin, cultivation activities, harvesting time, and extraction method [3]. The aim of this study is to explore the possibility of identifying samples of sea buckthorn oil derived from different parts of sea buckthorn berries by differential scanning calorimetry (DSC).

2. MATERIALS AND METHODS

2.1 Berries

Berries of the Chuy sea buckthorn cultivar harvested on commercial plantations of the Lisavenko Research Institute of Horticulture for Siberia of the Russian Academy of Agricultural Sciences in 2012 were used.

Samples of sea buckthorn oil extracted with difluorochloromethane (Freon 22) from the crushed pulp (prepared by juicing the berries), the kernel (seed), and the berry shells and oil samples prepared by the enzymatic method were studied.

2.2. Sample Preparation

The extraction of sea buckthorn oil was conducted in an extractor for 8 h with the subsequent removal of Freon 22.

The Protosubtilin and CelloLux-A enzymes in a ratio of 1 : 1 were used to derive oil by enzymatic hydrolysis.

2.3. Study of Melting Process

The melting of the samples was studied by DSC using a DSC-60 instrument (Shimadzu, Japan). The weighed portion was 10.0 ± 0.5 mg. The measuring cell was cooled with liquid nitrogen to a temperature of -100°C . The experiments were conducted in a temperature range of -100°C to 50°C at a heating rate of $10^\circ\text{C}/\text{min}$. The experiments were conducted in a nitrogen environment at a gas flow rate of $40\text{ cm}^3/\text{min}$. The α -quartz was used to bring the system into the state of equilibrium. The instrument was calibrated against indium ($T_{\text{melt}} = 156.6^\circ\text{C}$, $\Delta H_f = 28.71\text{ J/g}$). The calculated data were obtained using the DSC-60 software.

2.4. Determination of Fatty Acid Composition

The fatty acid composition of the oil samples was determined by gas chromatography (GC). The oil samples were converted to their methyl esters and analyzed on a Kristallyuks 4000 gas chromatograph using a flame ionization detector, a 50 m x 0.25 mm FFAP capillary column, and helium as a carrier gas (Hewlett-Packard, Palo Alto, CA). The thermostat temperature was programmed as follows: from 60°C (an isothermal mode for 1 min) to 190°C at a rate of $20^\circ\text{C}/\text{min}$ and an isothermal period of 30 min at 190°C . The temperature of the injector and the detector was 250°C .

2.5. Determination of Peroxide and Acid Values

The peroxide and acid values of the samples were determined by standard methods [5, 6].

2.6. Statistical Analysis

All the studies were conducted at least twice. The measurement results were processed by the analysis of variance.

3. RESULTS

3.1. Fatty Acid Composition

The fatty acid composition of the prepared oil samples is shown in Table 1.

Table 1. Fatty acid composition of the oil samples (a measurement error of 2–6%)

Species, cultivar	Fatty acids								Refer- ence
	14:0	16:0	16:1	18:0	18:1 oleic	18:1 vaccenic	18:2	18:3	
	from berry pulp and shells								
Hippophae rhamnoides	0.5	28.4	50.3	0.6	11.3	not detected	1.3	1.3	7
Hippophae rhamnoides	0.6	35.8	45.6	0.5	0.8	not detected	0.8	0.5	7
Hippophae rhamnoides	0.4	33.8	46.4	1.0	13.4	not detected	5.4	1.3	7
Hippophae salicifolia	0.3	29	32.9	2.9	17.6	not detected	16.1	0.6	7
Hippophae tibetana	1.1	25.7	32.1	0.5	26.0	not detected	9.3	5.2	7
Chuy	0.5	35.1	35.3	1.2	4.3	5.8	11.3	0.9	***
Quebec	-	35.3	40.1	0.8	3.2	6.5	10.6	0.9	4
carpatica	0.46	39.1	26.7	0.8	20.8	6.4	4.6	0.90	8
from seeds									
Chuy	0.3	11.0	5.5	2.2	15.1	not detected	35.1	25.6	***
quebec	- n.o.	8.0	2.8	3.1	13.1	2.2	32.4	37.2	4
carpatica	0.24	12.4	0.36	2.9	16.7	1.5	33.7	31.8	8
from berry shells									
Chuy	0.87	36.6	34.5	1.27	5.8	5.1	12.1	0.9	***
prepared by enzymatic hydrolysis									
Chuy	0.52	34.3	33.7	1.8	5.1	5.7	14.2	1.4	***
Jutland, Germany	0.3	33.0	34.2	0.3	28.4	not detected	3.3	1.0	9
Canada, Quebec	0.4	36.1	39.4	0.8	2.9	6.2	10.8	0.9	10
from whole berries									
carpatica	0.59	36.2	24.6	0.9	22.3	6.2	6.2	2.7	8

^aTrace, ≤0.1%.

*Total amount of oleic and vaccenic acids.

**Arachidonic and behenic acids are also detected.

***The data obtained by the authors.

These data suggest the following.

–The composition of the oil samples prepared from the pulp, shells, and seeds of Chuy sea buckthorn berries is most similar to the composition of the samples of oil produced in the province of Quebec (Canada).

–The composition of the oil derived from berry shells is close to the composition of the pulp oil.

–The composition of the oil sample prepared by enzymatic hydrolysis is similar to the composition of the analogous Canadian sample and significantly differs from the German sample.

3.2. Differential Scanning Calorimetry

The melting curve of the seed oil is shown in Fig. 1.

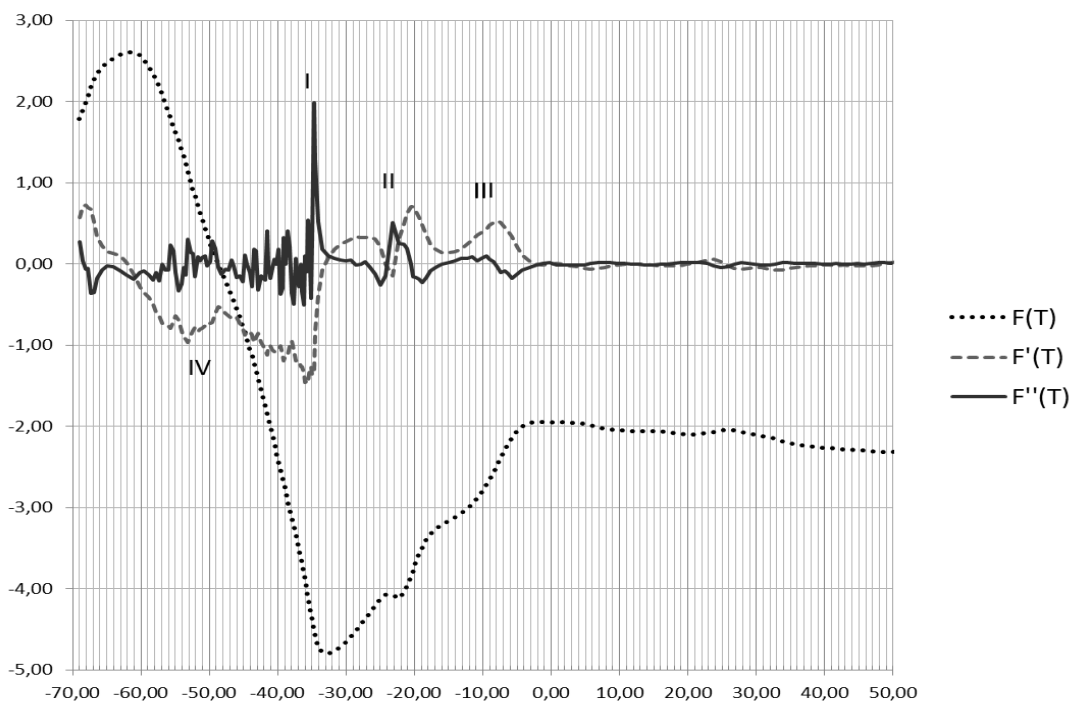


Fig. 1. Melting curve of the Chuy sea buckthorn seed oil.

These data suggest that the melting curve of the seed oil is a superposition of four overlapping peaks.

The characteristics of their total peak are listed below.

Peak position, °C	-33.5 ± 0.4
Endoeffect onset temperature, °C	-39.9 ± 0.4
Finishing melting temperature, °C	-12.0 ± 0.3
Melting heat, J/g	57.0 ± 1.5

The first-derivative analysis makes it possible to determine the peak positions of four endoeffects of melting of triglycerides at -54°C , -32°C , -19°C , and -8°C .

The melting curve of the oil from the berry shells is shown in Fig. 2.

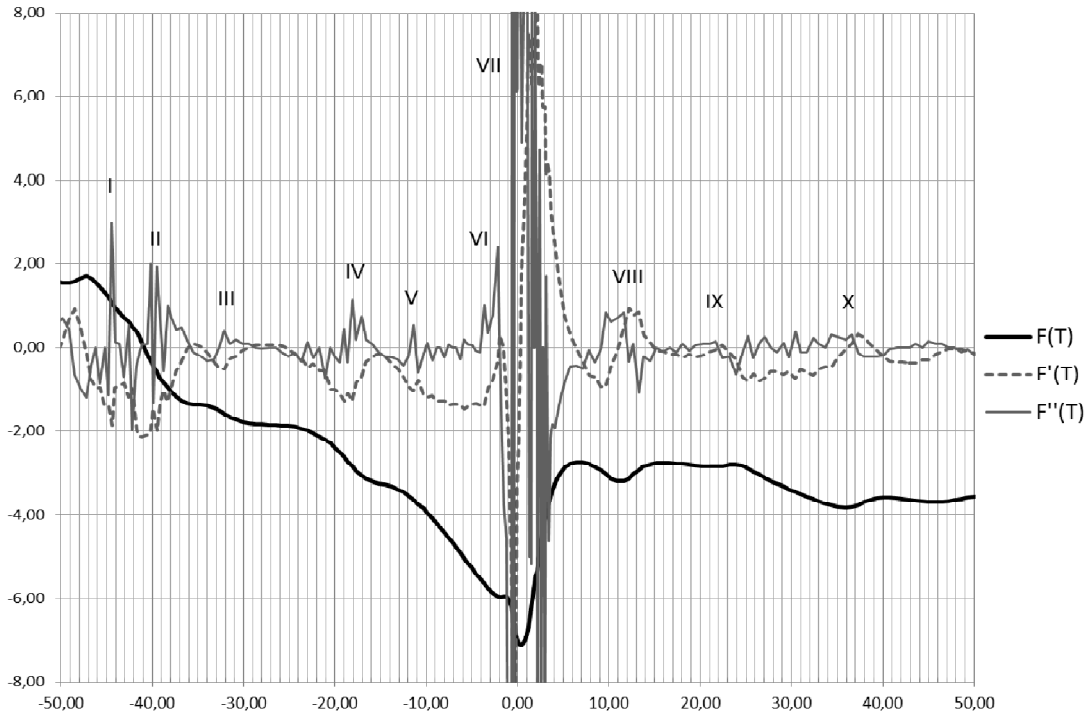


Fig. 2. Melting curve of the oil derived from Chuy sea buckthorn berry shells.

Unlike the previous sample, the melting curve of the oil derived from sea buckthorn berry shells is a superposition of at least ten peaks.

The data on five of them that could be identified with the data processing program are shown in Table 2.

However, the first-derivative analysis of the melting curve reveals two additional peaks in a range of -30 to -45°C , which should be apparently attributed to the melting of triglycerides of unsaturated acids. The peak position exhibits a divergence of 2–4 deg, which requires a unified approach to the method of analysis of these complex melting curves.

The melting curve of the oil sample prepared by enzymatic hydrolysis is shown in Fig. 3.

The melting curve of this sample is a superposition of four overlapping peaks. Their parameters are listed in Table 3.

The melting curve of the sea buckthorn oil extracted with Freon is also a superposition of four overlapping peaks (Fig. 4).

Table 2. Parameters of the melting curve of the oil derived from sea buckthorn berry shells

Peak	Parameter	Values
I	Peak position, °C	-24.9 ± 0.4
	Endoeffect onset temperature, °C	-37.9 ± 0.4
	Finishing melting temperature, °C	-21.3 ± 0.4
	Melting heat, J/g	2.8 ± 0.2
II	Peak position, °C	-22.2 ± 0.4
	Endoeffect onset temperature, °C	-21.9 ± 0.4
	Finishing melting temperature, °C	-15.1 ± 0.4
	Melting heat, J/g	0.8 ± 0.1
III	Peak position, °C	0.7 ± 0.4
	Endoeffect onset temperature, °C	-2.5 ± 0.4
	Finishing melting temperature, °C	4.0 ± 0.4
	Melting heat, J/g	21.9 ± 1.4
IV	Peak position, °C	11.5 ± 0.4
	Endoeffect onset temperature, °C	8.3 ± 0.4
	Finishing melting temperature, °C	14.0 ± 0.4
	Melting heat, J/g	0.9 ± 0.1
V	Peak position, °C	39.9 ± 0.4
	Endoeffect onset temperature, °C	19.6 ± 0.4
	Finishing melting temperature, °C	42.5 ± 0.4
	Melting heat, J/g	2.6 ± 0.2

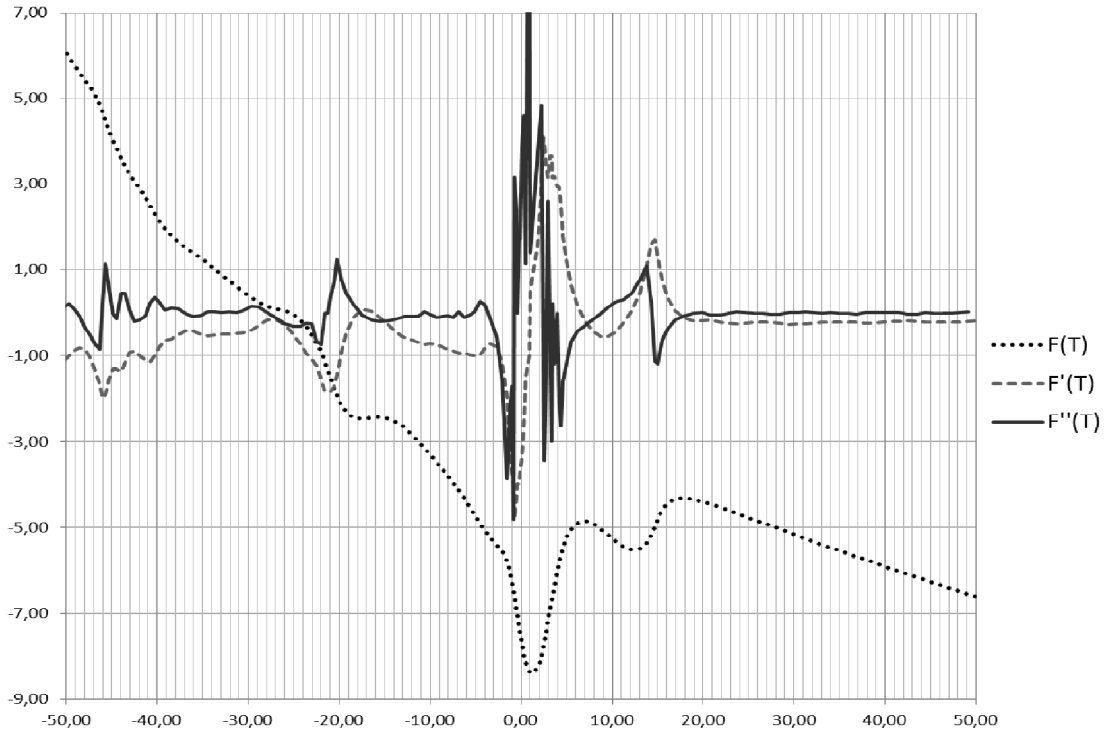


Fig. 3. Melting curve of the oil derived by enzymatic hydrolysis.

Table 3. Parameters of the melting curve of the sea buckthorn oil derived by enzymatic hydrolysis

Peak	Parameter	Value
I	Peak position, °C	-19.8 ± 0.4
	Endoeffect onset temperature, °C	-23.3 ± 0.4
	Finishing melting temperature, °C	-15.0 ± 0.4
	Melting heat, J/g	2.6 ± 0.4
II+III	Peak position, °C	1.2 ± 0.4
	Endoeffect onset temperature, °C	-1.5 ± 0.4
	Finishing melting temperature, °C	5.0 ± 0.4
	Melting heat, J/g	11.7 ± 0.8
IV	Peak position, °C	12.8 ± 0.4
	Endoeffect onset temperature, °C	7.5 ± 0.4
	Finishing melting temperature, °C	16.0 ± 0.4
	Melting heat, J/g	2.9 ± 0.2

These data suggest that the melting curve is a superposition of four overlapping peaks. Their parameters are listed in Table 4.

Table 4. Parameters of the melting curve of the sea buckthorn pulp oil extracted with Freon

Peak	Parameter	Value
I	Peak position, °C	-19.6 ± 0.4
	Endoeffect onset temperature, °C	-24.0 ± 0.4
	Finishing melting temperature, °C	-15.3 ± 0.4
	Melting heat, J/g	3.6 ± 0.4
II+III	Peak position, °C	-1.0 ± 0.4
	Endoeffect onset temperature, °C	-4.4 ± 0.4
	Finishing melting temperature, °C	3.7 ± 0.4
	Melting heat, J/g	16.7 ± 0.8
IV	Peak position, °C	11.3 ± 0.4
	Endoeffect onset temperature, °C	6.9 ± 0.4
	Finishing melting temperature, °C	15.1 ± 0.4
	Melting heat, J/g	3.5 ± 0.4

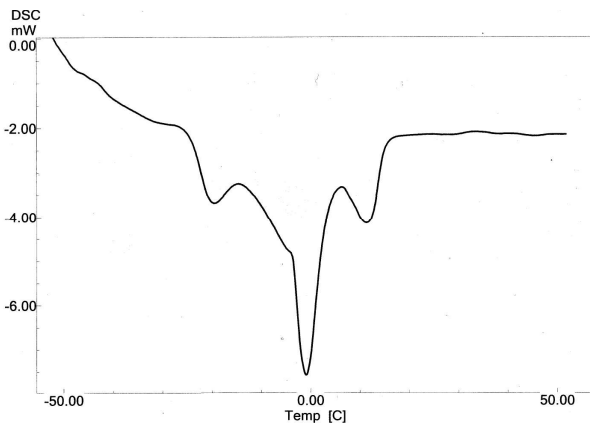


Fig. 4. Melting curve of the oil extracted with Freon.

It should also be noted that the total heat of melting of the oil samples is 17 to 57 J/g, which is comparable to the data for vegetable oils [10].

3.3. Acid and Peroxide Values

The acid and peroxide values of the oil samples are listed in Table 5.

Table 5. Acid and peroxide values of the sea buckthorn oil samples

Oil sample	Acid value, mg KOH/1 g of oil	Peroxide value, ½ O ₂ mmol/kg
extracted with Freon 22	12.05	0.7
from berry shells	6.85	4.8
from seeds	7.2	4.4
enzymatic hydrolysis	2.6	0.5
from dried berries [3]	-	1.8–4.0; 5.4 ± 0.3; 3.0 ± 1.9

According to the set of parameters, the oil sample prepared by enzymatic hydrolysis is the most promising for use in cosmetic formulations.

4. DISCUSSION

The above data suggests that the oil derived from Chuy sea buckthorn berries has a similar qualitative composition and peroxide value as the oil from other subspecies of sea buckthorn.

Differences in the fatty acid composition lead to differences in the melting curves: four to ten peaks were recorded for the studied samples. An assumption of the nature of these endothermic effects was made only by the Canadian authors in [4]. Table 6 shows a comparison of the DSC data on the melting peak temperatures of our and Canadian samples.

The data suggest that the samples mostly exhibit three minima corresponding to the melting of three triglycerides or their complexes. With allowance for the melting point of even-numbered fatty acids and the triglycerides formed by them, these acids can be arranged in the following series with respect to increasing melting point: linolenic > linoleic > palmitoleic > oleic > myristic > palmitic > stearic.

Taking into account that the mass fraction of a number of acids is negligible and they cannot be shown as a separate peak in the melting curve and given the fact that they are isostructural with homologs, the following three groups of triglycerides can be

distinguished: a high-temperature group composed of C18:0, C16:0, and C14:0 acids; a medium-temperature group consisting of C16:1 and C18:1; and a low-temperature comprising C18:2 and C18:3. However, if we take into account that the melting point of pure triglycerides of the saturated acid series is significantly higher (e.g., stearic acid triglyceride is melted at 75°C), then we can conclude that the DSC curves describe the melting process of multicomponent eutectic mixtures, as described for milk fat [12, 13], rather than individual triglycerides.

Table 6. Parameters of the melting curves of the oil samples

Sample	Endoeffect peak temperature, °C for the peak				
	I	II	III	IV	V
seeds	-33.5				
berry shells	-24.9	-22.2	0.7	11.5	39.9
enzymatic	-25.8	1.2		12.8	
extracted with Freon 22		-19.6	-1.0	11.3	
[3]	-22.5		-4.0	10.0	
[11]	-24.4		-4.1	10.7	

Note also that none of the samples contain water; therefore, the extensive endothermic effect in the region of 0°C is not attributed to the melting of ice.

Taking into account that the fatty acid composition of sea buckthorn oil depends not only on the cultivar, geographical location, climatic conditions, and cultivation activities, the derived melting curves are individual and can be used to determine the composition of the feedstock for the production of sea buckthorn oil in the Altai Territory and in the used extraction technology.

REFERENCES

- Koshelev, Yu.A. and Ageeva, L.D., *Oblepikha: Monografiya* (Sea Buckthorn: A Monograph), Biysk: Nauchno-Issled. Tsent, Biysk Gos. Pedag. Univ., 2004.
- Bal, L.M., Meda, V., Naik, S.N., and Satya, S., Sea buckthorn berries: A potential source of valuable nutrients for nutraceuticals and cosmeceuticals, *Food Research International*, 2011, vol. 44, no. 7, pp. 1718–1727.
- Larmo, P., *The Health Effects of Sea Buckthorn Berries and Oil*, Turku: Univ. Turku, 2011.
- Gutierrez, L.-F., Ratti, C., and Belkacemi, K., Effects of drying method on the extraction yields and quality of oils from Quebec sea buckthorn (*Hippophae rhamnoides L.*) seeds and pulp, *Food Chemistry*, 2008, vol. 106, pp. 896–904.
- AOCS Official Method Cd 8b-90: Acid Value, 2011.
- AOCS Official Method Cd 8–53: Peroxide Value–Acetic Acid–Chloroform Method, 2011.
- Ranjith, A., Kumar, K.S., Venugopalan, V.V., Arumughan, C., Sawhney, R.C., and Singh, V., Fatty acids, tocopherols, and carotenoids in pulp oil of three sea buckthorn species (*Hippophae rhamnoides*, *H. salicifolia*, and *H. tibetana*) grown in the Indian Himalayas, *Journal of American Oil Chemists Society*, 2006, vol. 83, no. 4, pp. 359–364.
- Dulf, F.V., Fatty acids in berry lipids of six sea buckthorn (*Hippophae rhamnoides L.*, subspecies *carpatica*) cultivars grown in Romania, *Chemistry Central Journal*, 2012, vol. 6, no. 9, pp. 106–118.
- Mörsel, J.-T. and Steen, S., Analysis and identification of sea buckthorn oil of different origin, *Proc. 1st Int. Conf. on Seabuckthorn*, Berlin, 2003, pp. 8–10.
- Tan, C.P. and Che Man, Y.B., Comparative differential scanning calorimetric analysis of vegetable oils: I. Effects of heating rate variation, *Phytochemical Analysis*, 2002, vol. 13, no. 1, pp. 129–141.

11. Gutierrez, L.F., Extraction et caractéristiques des huiles de l'argousier (*Hippophaë rhamnoides L.*). Une étude des effets de la méthode de déshydratation des fruits sur le rendement d'extraction et la qualité des huiles, *Thesis*, Quebec: University Laval, 2007, pp. 87–97.

12. Metin, S. and Hartel, R.W., Crystallization of fats and oils, in *Bailey's Industrial Oil and Fat Products*, Shahidi, F., Ed., New York: Wiley, 2005, vol. 1, 6th ed., pp. 45–76.

13. Sato, K. and Ueno, S., Polymorphism in fats and oils, in *Bailey's Industrial Oil and Fat Products*, Shahidi, F., Ed., New York: Wiley, 2005, vol. 1, 6th ed., pp. 77–120.



UDC 657:663.5
DOI 10.12737/1565

A METHODOLOGY FOR IMPLEMENTING A CURRENT COST MANAGEMENT SYSTEM AT PROCESSING COMPANIES OF THE DISTILLING INDUSTRY: THE CASE OF THE MARIINSK DISTILLING PLANT

V.P. Zotov, E.A. Zhidkova, and N.S. Alekseeva

Kemerovo Institute of Food Science and Technology,
bul'v. Stroitelei 47, Kemerovo, 650056 Russia
phone:/Fax: 8 (3842)- 39-68-60, e-mail ekonomika-kemtipp@yandex.ru

(Received August 01, 2013; Accepted in revised form August 20, 2013)

Abstract: Methods of controlling current costs in the processing industry are discussed. A description is given of cost and profit management techniques based on the concept of financial responsibility centers. An algorithm is provided to consistently develop financial responsibility centers, determine the scope of their competence, and thus achieve an effective functioning of the system. A method is described which is based on direct costing and is used to determine the financial safety margin of a processing company. The implementation of advanced direct costing in the context of financial responsibility centers allows one to analyze the structure of fixed and variable costs, marginal income, and profits for the whole company and, thus, improve the cost management and financial performance.

Keywords: current cost management, financial responsibility centers, direct costing.

INTRODUCTION

Important elements in the analysis of a company's activities and financial performance are (a) product cost analysis and (b) cost-effectiveness analysis in terms of identifying products with a low value of this indicator. There should be a methodology enabling a cost management system based on the analysis of the structure of fixed and variable costs and the marginal income, determination of responsibility centers, and development of indicators for each center. The methodology aims to identify responsibility centers and analyze and control costs for each center and, as a consequence, for the whole company.

SUBJECT AND METHODS OF RESEARCH

OOO Mariinskii Spirtovyi Kombinat (Mariinsk Distilling Plant; hereinafter referred to as the distilling plant), the largest company in the alcohol market of Kemerovo oblast, is the longest-standing enterprise in the industry in Siberia and the Far East. The plant was put into operation in 1937 and occupies a land plot of 38.1 ha.

In August 1993 the company was incorporated. The authorized share capital is 252 978 rubles; the controlling stake is owned by the state and is part of the federal state unitary enterprise FGUP Rossirtprom.

The distilling plant is a diversified enterprise employing 830 people. The main products are ethyl alcohol, dried fodder yeast, food additive carbon dioxide, etc.

The company's first priority is the production and

supply of ethyl alcohol of the following varieties: highly refined, "Extra", "De Luxe", "Alpha", and "Denatured".

The production capacity of the distilling plant is 3 558 355 dal of alcohol, 9882 t of carbon dioxide, and 7875.1 t of fodder yeast per year.

The company was ranked first among the leading Russian alcohol producers in 2009 and 2010 in the rating of the National Alcohol Association of Russia.

The financial and economic activities of the distilling plant in the last three years include current, investment, and financial operations. The analysis is based on comparing the distilling plant with peer companies and leading businesses in the industry. It is complicated to conduct an objective analysis of business activities due to a high level of privacy and the lack of analytical information on the activities of the competitors.

The annual alcohol production capacity was used to 67.3% in 2008, 96.1% in 2009, and 100% in 2010. There is a tendency for the production of the main product – food-grade ethyl alcohol – to grow: 2 262 000 dal in 2008, 3 421 000 dal in 2009, and 4 607 000 dal in 2010.

In 2010 the shipping volume increased by 167.9% compared to 2008 and by 82.5 % compared to 2009 and was 2997 million rubles with the excise duty and VAT and 1394 million rubles without the excise duty and VAT [1].

The plant's production capacity is used to 96.1%. The costs of production and sales were 1361 million rubles in 2010 to exceed the 2009 level by 747 million

rubles.

The higher costs resulted from the increased production and higher prices for raw materials and services, which in turn leads to an increase in costs per unit of output.

RESULTS AND DISCUSSION

Business management issues arising from the operation of a company can be summarized in three groups:

- Implementation of cost management processes.
- Development of an effective product range policy.
- Managerial decision-making.

Addressing the first group of issues requires a large amount of time and data to implement the cost management processes. The data obtained from the analysis of this group of issues provide an information base to address the other tasks.

Cost management is necessarily a continuous process; therefore, the key to addressing the cost management issues is to tie costs to their place of origin, i.e., cost centers. The need to control costs and final financial results on the basis of estimated figures is dictated by the isolation of financial responsibility centers that are to be subordinate to the heads of structural subdivisions of the company.

Responsibility center management is one of the subsystems ensuring the in-house management. This subsystem helps evaluate the contribution of each unit to the final results of the company, decentralize the cost management system, and monitor the formation of costs at all levels of management. All this significantly increases the cost-effectiveness of management.

In the context of the distilling plant, the financial responsibility center is a main shop or a structural unit that is engaged in operations with the ultimate aim to optimize profits and is responsible to senior management for the implementation of the set objectives and keeping the costs within the established limits.

The aim of a management system based on financial responsibility centers is to increase the efficiency of management of company units by summarizing data on the costs and performance of each responsibility center so that a deviation can be attributed to a particular manager. The main principle of this type of management is that each responsibility center is only responsible for those costs and (or) revenues and, in a broader sense, only for those indicators that must and can be controlled by its managers during a certain period [2].

The distribution of revenues and expenses, as well as control over costs or financial performance only, between the company's structural units that are objects of managerial accounting ensures a correctly arranged financial structure, which would allow one to see how and where profits are generated, reported, and distributed and ensure the monitoring of expenses and revenues.

We propose a procedure to develop an effective management system based on financial responsibility centers at the distilling plant. The procedure is based on a stepwise implementation of the system. When forming

the financial responsibility centers, for the system to function effectively, we need to define the scope of competence and demarcate the areas of responsibility of the centers. This will help collect more reliable information about the company's revenues and expenses. Defining the main areas of economic activity, such as the company's organizational structure, is the first, decisive step in building a management system.

Studying the company's production activity to define technological accountability centers is a necessary step in collecting information on incurred costs. It includes the distribution of the main areas of economic activity by business unit and identification of auxiliary units that do not manufacture the key products. The analysis of the accountability of costs, revenues, profits, and investment by business unit and the identification of controllable items determine the borderline between financial responsibility centers and define their status.

An important step is to define the rules of interaction (including the list of reporting and planning documents and the range of indicators characterizing the performance and regulating the rights and responsibilities) between the various financial responsibility centers within the company and between individual centers and the senior management.

Setting a cost limit (with respect to material, financial, and labor costs) for the company for a specific output in each financial responsibility center is a key point in the company's cost management system. The final stage of any well-functioning system should be a motivation system focused on compliance with the approved cost limit to establish a direct dependence between spending, performance, and the outcome.

Table 1 presents a classification of financial responsibility centers by a number of criteria.

Table 1. Classification of financial responsibility centers

Classification criteria	Types of responsibility centers
In-house management objectives	Operational / Strategic
Management level	Company / Company departments and services / Individual business units/ Workshop / Team
Scope of competence and responsibilities	Cost centers Revenue centers Profit centers Investment centers Management and control centers
Tasks and functions of the center	Primary / Auxiliary
Degree of resemblance to the place of origin of costs	Resembling / Nonresembling
Place in the responsibility center hierarchy	One-type horizontal / Many-type horizontal / Pyramidal
Relations with the in-house management system	Analytical / Self-supporting

Financial responsibility centers are accountable for the costs and results that are directly dependent on their scope of competence. The centers' activities should be reflected and presented in the accounts by means of double-entry to ensure the comparability of costs and results for each center.

Figure 1 shows a cost management procedure for a manufacturing company.

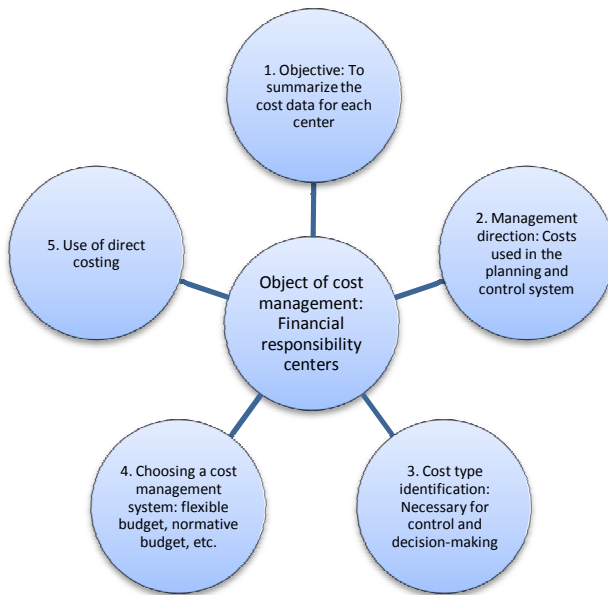


Fig. 1. Cost management procedure based on financial responsibility centers.

At the distilling plant, financial responsibility centers are identified on the basis of their tasks and functions:

(1) The main responsibility centers are involved in the direct manufacture of goods, performance of works, and provision of services to consumers. Their costs are included directly in the product costs. These centers comprise an alcohol shop, fodder yeast shop, enzyme shop, and carbon dioxide shop.

(2) The auxiliary responsibility centers exist to serve the main ones. Their costs are first spread over the main responsibility centers and then included (as part of the main centers' total costs) in the product costs.

An analysis of the existing financial responsibility centers at the distilling plant shows that they are singled out using the widespread criterion of the scope of competence and responsibility:

(1) Main and auxiliary shops, the foremen of which are responsible for costs only.

(2) The commercial service, which is responsible for the revenues from sales of products and services and for the cost of sales.

Currently, there are no profit-, investment-, or management/control-based responsibility centers at the distilling plant. As a result, it is impossible to evaluate the performance of these centers, and they bear no responsibility for the financial results of their activities.

The principle whereby individual costs are included in the product costs by means of distribution between product items may not allow for their monitoring and control because the production cycle may consist of

several different processing steps, with a specific person being responsible for each step. Therefore, the data on product costs is insufficient to determine exactly how costs are distributed between individual production units (responsibility centers). This problem is solved by tying costs and revenues to the actions of specific individuals who are responsible for spending the respective funds. This approach to cost management is only possible when cost planning is based on financial responsibility centers (FRCs).

The underlying idea of FRC-based cost management is the separation of competences, i.e., employees' responsibilities for costs and revenues.

FRC-based cost management aims at maintaining the cost allocation and marginal income determination scheme for each FRC. To this end, costs and sales revenues need to be accounted to the corresponding FRCs, and those costs that can be directly attributed to a given FRC should be accounted to this center without using indirect distribution methods. As a rule, a number of marginal incomes (full and partial) are specified in the course of variable and direct fixed cost accounting. In Table 2 we consider the determination of the full and partial marginal incomes, depending on whether variable and direct fixed costs are included in the product costs.

Table 2. Scheme for the inclusion of variable and direct fixed costs in the product costs and determination of full and partial marginal incomes for individual financial responsibility centers (FRCs) in advanced direct costing

Cost centers	Costs included in the product costs at each level	Marginal income
Team	Variable costs	Full
Shop	Variable costs plus specific direct fixed costs included in the product	Partial (1)
Individual production units (FRCs)	Variable costs plus specific direct fixed costs included in the product range	Partial (2)
Company	All costs	Profit

To illustrate the above, we discuss the organization of FRC-based cost management at the distilling plant as of May 2011 (Table 3). To this end, we single out three FRCs and determine the corresponding proportions of variable costs and the marginal income from variable costs in sales revenues.

The marginal loss of the main production processes is 3.046 million rubles, and the marginal loss of the FRCs is 4.367 million rubles. The development of a methodology for FRC-based cost management, classification of costs, and selection of planning and control methods for managerial decision-making is the key to the effective management of the company's profits.

Profit management through the organization of FRCs affects the functioning of in-house services and business units that ensure the development and implementation of managerial decisions on certain aspects of profit generation, distribution, and use and are responsible for the results of these decisions.

Table 3. Organization of cost management based on advanced direct costing at the distilling plant

Indicator	FRC total		Financial responsibility centers					
			Alcohol shop		Fodder yeast shop		Carbon dioxide shop	
	Total, thousand rubles	%	Total, thousand rubles	%	Total, thousand rubles	%	Total, thousand rubles	%
Sales revenues	102 100	100.00	92 100	100.00	8 500	100.00	1 500	100.00
Cost of basic materials, raw materials, and components	52 022.5		46 260		5 700		62.5	
Direct labor costs	1 317.5		720		490		107.5	
Fringe benefit expenses	354.1		208.8		142.1		3.1	
Cost of fuel and electric power	15 056		13 800		1 100		156	
Cost of maintenance and repair of machinery and equipment	1 291		1 050		207.9		33.1	
Total variable costs	70 041.3	68.60	62 039	67.36	7 640.0	89.88	362.2	24.15
Marginal income from variable costs	32 058.7	31.40	30 061	32.64	860.0	10.12	1 137.8	75.85
Direct fixed costs of main production processes	35 105	34.38	33 750	36.64	1 200	14.12	155	10.33
Marginal income of main production processes	-3 046.3	-2.98	-3 689	-4.00	-340.0	-4.00	982.8	65.52
Direct costs of FRCs	1 320.6	1.00		0.00		0.00		
Total fixed costs	36 425.6	35.68		0.00		0.00		
Marginal income of FRCs	-4 366.9	-4.28		0.00		0.00		

The reason for the application of FRC-based profit management technologies is that the company is interested in forecasting and achieving an optimal return, performance, and profitability both of FRCs and the enterprise as a whole.

It is recommended to identify the following stages in FRC-based profit management:

(1) Analysis of the functioning of business units and their impact on the generation and use of profit.

(2) Identification of the main types of FRCs among the company's business units.

(3) Development of a system of rights, responsibilities, and liabilities of the heads of the units identified as FRCs.

(4) Development of operating and capital budgets to communicate them to the FRCs.

(5) Monitoring of the FRCs' performance on their tasks through the analysis of reports to determine the causes of deviations.

The key points of profit management within a FRC are considered in Table 4.

The calculation of profit and breakeven point is preceded by an analysis of marginal income using advanced direct costing, which is conducted for each FRC.

Advanced direct costing allows one to infer about the profitability and sustainability of production and predict the changes in the company's revenues and profitability, depending on the volume of production and sales, prices, and variable and fixed costs. The implementation of this method in the context of FRCs allows one to analyze the structure of fixed and variable costs, marginal income, and profits for the whole company and, therefore, improve the cost management system and financial performance.

Table 4. Features of the FRC-based profit management technology

Feature	Content
Profit management objective	Ensuring profit maximization in the current and future periods
Methodological tools of profit management	Marginal analysis based on advanced direct costing Marginal income Relative income Production leverage Breakeven point Financial safety zone
Development of a flexible budget	Provision of forecast data for different output levels within activities
Control and analysis of deviations	For materials For labor For overheads For gross profit

Table 5 presents the estimates of economic indicators made by direct costing, which help determine the breakeven point in volume and value terms, the level of sustainability, and the financial performance of FRCs.

The analysis of deviations is aimed at comparing the total actual costs to the total normative costs for each operation of a FRC for a period in order to control costs. The deviations for each FRC are determined for each element and must be analyzed in accordance with the prices and resource amounts. The results are used to develop an optimal production program taking into account the features of the industry.

Table 5. System of economic indicators used in advanced direct costing at the distilling plant

Indicators	Formula	FRC	Financial responsibility centers		
			Alcohol shop	Fodder yeast shop	Carbon dioxide shop
Revenues (R), thousand rubles		102 100	92 100	8 500	1 500
Variable costs (VC), thousand rubles		70 041.3	62 038.8	7 640.0	362.5
Marginal income (MI), thousand rubles	$MI=R-VC$	32 058.7	30 061.2	860.0	1 137.5
Relative income (RI), %	$RI = MI/R \times 100$	31.40	32.64	10.12	75.83
Fixed costs (FC), thousand rubles		36 425.6	33 750.0	1 200.0	0
Profit per shop (P), thousand rubles	$P = MI-FC$	-4 366.9	-3 688.8	-340.0	982.5
Leverage (L)	$L = MI / P$	-7.34	-8.15	-2.53	1.16
Sustainability level (SL)	$SL = FC / MI$	1.14	1.12	1.40	0.14
Breakeven point (BEP), thousand rubles	$BEP = FC / RI$	1 160.0	1 034.0	118.6	2.0
Marginal income per unit (MI_{unit}), rubles	$MI_{unit} = MI / Output$		66.80	860.00	4 550.00
Breakeven point (BEP), units	$BEP = FC / MI_{unit}$		505 239.52	1 395.35	34.07

The development of an optimal production program is an essential part of cost management since this production plan determines the costs. If a company produces several types of products, it is important to pay attention to planning the product range.

The breakeven point depends on the size of the fixed and variable costs per unit of output, which suggests a reasonable selection of the best selling price and managerial decision.

The proposed key points of the cost management system used at processing companies of the distilling industry are based on the principles of advanced direct costing, a popular accounting method in the world. The main feature of this method is that direct fixed costs of production and sales are included, as well as variable costs, into the product costs [3].

An important advantage of the system is the possibility of a detailed and qualitative study of the relationship between the output, costs, and marginal

income and the profit as a result of economic activity.

The analysis of the relationship of the output, costs, and profits is the most important feature of advanced direct costing because one can analyze not only profit but also marginal income, the values of which are derived from those of revenues and expenses. Direct costing helps understand the relationship between the product price, output, direct costs per unit of output, total fixed costs, and mixed costs.

The analysis based on direct costing helps trace the relationship between such important characteristics as costs, output, and profit; it is a key factor in much of the decisions-making process, including on the determination of output and product range.

In Table 6 we consider the performance indicators of the distilling plant, which were calculated from the major indicators such as the output in physical terms and the costs grouped into fixed and variable costs by type of alcohol produced.

Table 6. Performance indicators of the distilling plant calculated by advanced direct costing

Calculated performance indicators	Alcohol			
	De Luxe	Raw	Highly refined	Total
Actual output, thousand dal (q)	100 000	300 000	50 000	450 000
Selling price per one dal, rubles (P)	260.00	180.00	242.00	205.00
Actual revenue, thousand rubles (Q)	26 000	54 000	12 100	92 100
Variable costs, thousand rubles (V)	14 386.4	40 459.2	7 193.2	62 038.8
Fixed costs, thousand rubles (Z)	7 500	22 500	3 750	33 750
Total costs, thousand rubles (F)	21 886.4	62 959.2	10 943.2	95 788.8
Marginal income, thousand rubles ($X = Q-V$)	11 613.6	13 540.8	4 906.8	30 061.2
Profit, thousand rubles (Q-F)	4 113.6	-8 959.2	1 156.8	-3 688.8

If the managers of the distilling plant made decisions within a management system based on total cost, the company would have to exclude all its products from the product range because the loss from alcohol production would be 3 688 800 rubles.

If we use advanced direct costing, the company would have only one unprofitable product – raw alcohol (the amount of loss is 8 959 200 rubles) and the other types of alcohol would have a positive financial result.

We now calculate the rate of variable costs per 1 dal alcohol produced by type and write equations for the total costs that include fixed costs, output in physical

terms, and the variable cost rate per unit of output by type (q is the output):

De Luxe alcohol: $7 500 000 + 143.86 q$;

raw alcohol: $22 500 000 + 134.86 q$;

and highly refined alcohol: $3 750 000 + 143.86 q$.

These formulas are used to calculate the breakeven points for each type of alcohol, which will allow us to evaluate the financial safety margin for each product type and for all the products taken together

The critical (threshold) volume of sales of De Luxe alcohol is:

$$Q_{cr \text{ De Luxe}} = (7 500 000 \times 26 000 000) / 11 613 600 =$$

1 679 0659.2 rubles.

The critical volume of production of the said type of alcohol ($q_{cr De Luxe}$) is:

$$q_{cr De Luxe} = 16\,790\,659.2 / 260 = 64\,579.5 \text{ dal.}$$

Similar calculations for the other types of alcohol are given in Table 7.

Table 7. Threshold revenues, threshold volume of sales, and financial safety margin of alcohol production

Product type	Financial sustainability indicators		
	Threshold revenues, rubles	Threshold volume of sales, thousand dal	Financial safety margin, rubles
De Luxe alcohol	16 790 659.2	64 579.5	9 209 340.8
Raw alcohol	89 728 819.6	498 493.4	-35 728 819.6
Highly refined alcohol	9 247 371.0	38 212.3	2 852 629.0

Not all of the above types of alcohol have sufficiently high profit margins and improve the company's financial sustainability. Thus, it would be recommended to exclude raw alcohol from the company's production plan, or the sales department should consider increasing its selling price.

The total financial safety margin for the three types of alcohol is: $9\,209\,340.8 + (-35\,728\,819.6) + 2\,852\,629.0 = -23\,666\,849.8$ rubles.

Effective organization of cost management bears a considerable potential to improve the company's financial sustainability. Isolating individual elements of variable and fixed costs in the total cost can help identify the key areas to reduce the costs [4].

We believe that the division of the company into self-standing cost centers brings the following benefits:

(1) Collecting high-quality real information on product costs.

(2) Collecting real data to draw the company's budget.

(3) Evaluating the activities of each cost center from in terms of efficiency and in connection to specific processes and individuals who are in charge of these centers.

In our view, a cost management system based on the organization of cost centers allows one to implement the following principles:

– Knowledge: at what cost center (responsibility center) and in what amounts the company's resources are spent.

– Prediction: at what cost center and in what amounts additional funding may be required given a change in the sales forecast.

– Competence: to ensure the maximum return on the use of all types of resources.

The use of the proposed method, i.e., FRC-based cost management, as well as advanced direct costing based on the system of marginal income, allows one to collect detailed information about the costs and revenues for each responsibility center. Moreover, the analysis helps identify the areas where deviations occur most frequently and the types of products with low profit margins. The core of this approach is the analysis of the structure of fixed and variable costs, marginal income, and profit for the whole company. In turn, the forecasting of performance and profitability in response to changes in the output, product prices, and variable or fixed costs makes it possible to strengthen the financial condition of the company, take more effective business development decisions, and improve the production processes of Russian companies [5].

To ensure the controllability of costs, it is highly important to attribute (in planning and accounting) to individual centers only the costs that are largely under control of the head of the corresponding responsibility center.

If the management of the distilling plant used the total-cost system in their decision-making, all the company's products should be excluded from the product range as unprofitable. However, the use of advanced direct costing leads us to conclude that there is only one loss-making product.

Therefore, the results of our study, which is based on the case of a processing plant of the distilling industry, suggest the need to improve the system of current cost management. All the processes taking place in the company should be evaluated in terms of the costs associated with them.

REFERENCES

1. Alekseeva, N.S. and Zotov, V.P., Improvement of current cost management at companies of the agroindustrial complex (the case of Kemerovo oblast), *Cand. Sci. (Econ.) Dissertation*.
2. Kondrakov, N.P., *Bukhgalterskii (finansovyi, upravlencheskii) uchet: uchebnik* (Accounting (General, Financial, and Managerial): Tutorial), Moscow: Prospekt, 2012.
3. Shim, J.K. and Siegel, J.G., *Modern Cost Management and Analysis*, New York: Barron's, 1992.
4. Garrison, R.H., Noreen, E.W., and Brewer, P.C., *Managerial Accounting*, 12th ed., Boston: McGraw-Hill/Irwin, 2008.
5. Horngren, C.T., Datar, S.M., and Foster, G., *Cost Accounting: A Managerial Emphasis*, Prentice Hall, 2007.